Tephra in lake sediments: an unambiguous geochronological marker?

Jane E. Boygle

Submitted in accordance with the requirements
for the degree of Doctor of Philosophy

The University of Edinburgh
Department of Geography

December 1994

UNIVERSITY OF EDINBURGH

ABSTRACT OF THESIS (Regulation 3.5.10)

Name of Candidate Jane Elizabeth Boygle

Address Department of Geography, Drummond Street, Edinburgh, EH8 9XP

Degree PhD *Date* 31st October 1994

Title of Thesis Tephra in lake sediments: an unambiguous geochronological marker?

No. of words in the main text of Thesis 40,000

This thesis has three aims: (1) to construct tephrochronologies on large and small scales at sites in Sweden and Iceland; (2) to assess the effects of erosional and depositional processes on the nature and distribution of tephra in the sedimentological record; (3) to use these case studies to propose a model of the deposition of tephra in lakes.

The Swedish Timescale based on the annually laminated sediments (varves) has recently been linked to the present. To test the chronology, traces of volcanic glass (tephra) from five historical eruptions of Icelandic volcanoes were sought within relevant sections of the varve deposits. Difficulties in isolating and identifying tephra to define isochrones in distal deposits led to the adoption of an integrated catchment and lake basin sampling strategy to assess the processes which affect the temporal and spatial distribution of tephra in lakes. A detailed tephrochronology of Svínavatn, a lake in northern Iceland, was constructed by identifying and correlating 95 tephra deposits from five lake cores and twelve profiles situated in the lowland peats, hillslopes and delta areas of the catchment. The tephra record from each site was highly variable due to both uneven fallout of the tephra following the eruption, and later reworking of the deposits in the lake and the catchment.

The environmental changes of Svínavatn and its catchment were reconstructed using tephra as a geomorphological tracer. The peats and soils of the catchment were stable throughout most of the Holocene until the deposition of Hekla 3 (2800 yBP). Repeating layers of reworked Hekla and Katla tephra after this period at several terrestrial and lacustrine sites reflect increasing episodic instability of the catchment and the effects of this disturbance on the lake record. Until the arrival of Norse settlers in the 9th century, much of this disturbance was linked to climate and vegetation changes around the catchment. Significant, but temporally discrete, secondary inputs of H3 and H4 (3800 yBP) into the lake occur several thousand years after the original airfall.

The assumption that a tephra layer in a lake deposit is an unambiguous geochronological marker is questioned. Processes such as sediment focussing in lake basins, piping and bog bursts in peat bogs, and erosion and redeposition due to hillslope processes in soil profiles produce a more complicated picture of the tephra record than is fully appreciated. A model outlining the processes affecting tephra deposition and the characteristics of the layers provides guidelines for future identification of tephra isochrones in lakes.

PGS/ABST/88

Declaration of originality

I hereby certify that this thesis has been composed by me and is based upon my own work.

Signed:

Date: 24th May 1995

Acknowledgements

I gratefully acknowledge the financial assistance of the Natural Environmental Research Council through PhD Studentship Grant GT4/90/GS/38. Additional support for fieldwork came from The Leverhulme Trust, the Carnegie Trust for the Universities of Scotland, and the US NSF (Arctic Social Science, Arctic Systems Science and Global Change Program).

Whilst working on my PhD at Edinburgh I have enjoyed the company of many supportive and encouraging colleagues, as well as two enthusiastic supervisors! Firstly, I'd like to thank Professor David Sugden and Dr Andy Dugmore for watching over me. Their expertise has been invaluable in keeping me on the straight and narrow. The postgraduate and ex-postgraduate community at Edinburgh deserve a huge kiss, especially the small, yet select group which helped me in the dark hours before dawn! Thanks team! I've enjoyed the intellectual and social company of Malcolm Murray, Anthony Newton, Bob McCulloch, Mary McCulloch, Loretta Lees, Debbie Greene, Mike Bentley, Herm Cockburn, Andy Kerr, Sheila Paul, Marianne Broadgate, Camilla Erskine, Neil Glasser, Dave Robinson, Nick Spedding, Kirsty Duncan, Lisa Denomme and Alun Hubbard - not a bad list! In addition, the Geography Department wouldn't be the same without the cheery hellooos from Anna, Lena and Sue in the morning as I check my pigeon hole.

Fieldwork in Iceland enabled me to make many friends, and I'd like to thank them for their warmth and hospitality, especially Kristján Siggtryggsson, Guðriður Árnarsdóttir, and Kate Levett. Guðrún Larsen at the Science Institute in Reykjavík helped me a great deal with the interpretation of the geochemical data - many thanks to her.

Dr Peter Hill and Dr Stuart Kearns in the Geology Department, Edinburgh University have provided valuable support and expertise during my hours on Tiddles the electron probe. Mr Graeme Tulloch at the British Geological Survey in Edinburgh allowed me access to the NERC X-ray facility. Finally, thank you to all the kind folk in reprographics and computing at the Geography Department for the time and help they've given me.

Table of Contents

List of Figures

List of Tables

CHAPTER ONE: Tephra in lake sediments

1.1 Aims and specific objectives

The overall aim is to study the deposition of tephra in lake sediments. More specifically, the aim is to link the Swedish varve sequences with the Icelandic tephra chronologies. There are five specific objectives:

1) to find and identify historical tephras in the Swedish varve chronology.

2) to determine experimentally the physical characteristics of tephra that influence its depositional behaviour in lake sediments.

3) to study Icelandic lake sediments in an area with a well-developed tephra stratigraphy to understand the sedimentation processes involved.

4) to explain the presence of primary fallout layers and secondary redeposited layers in such lake sediments, and,

5) to propose a model of sediment redistribution in catchment and lake sediments to indicate appropriate practice and possible pitfalls.

1.2 Introduction and background to the research

In order to understand the sensitivity of any environmental system, there is a need to determine accurate rates of change in climatic, vegetational and geomorphological studies. Securely dated sedimentary sequences have two particularly important applications: firstly, for the linkage of modern process studies to the long-term environmental records within depositional sequences; and secondly, for the reconstruction of past environments through the proxy data sources in the sediment. To achieve these aims, clearly identifiable and dated marker horizons are advantageous. It is particularly important if such markers provide unequivocal links between different parts of the environmental system, for example between the slopes of a catchment and a lake basin. On a geological timescale, tephra falls are instantaneous events, cover wide areas and so have the potential to provide such markers. Other dating techniques have either technical or spatial limitations when linking sedimentary records in different environments. For example, radiocarbon

dating is not applicable in organic-poor lake sediments or loess, dendrochronological records are not available in many areas in the world, and laminated sediments are difficult to link with terrestrial records.

Tephras are formed by all explosive volcanism and are common world-wide and through geological time. Tephrochronology was seen by Þórarinsson (1944), working in Iceland, as a geochronological tool. Layers of volcanic ash provide well-dated isochrones in all environments, terrestrial and lacustrine if securely identified and linked to an established tephrochronology. Most studies have concentrated on developing the postglacial eruption history of Icelandic volcanoes (Larsen, 1981, 1984), dating archaeological sites (Þórarinsson, 1967, 1981; Hermanns-Auðardóttir, 1991) and providing a known datum in a series of vegetational and glacial histories (Dugmore, 1989; Dugmore and Sugden, 1991; Norðdahl and Haflidason, 1992). These studies are particularly viable in Iceland since many tephra deposits are readily visible to the eye, and the rate of soil accumulation throughout the island is high enough to separate temporally close eruptions. Further afield, microscopic layers of glass shards have been identified in peat (Persson, 1967a, 1967b, 1971; Dugmore, 1989; Mangerud *et al.*, 1984) and ocean cores (Long and Morton, 1987), providing useful dating and correlation between sites. The dating provided by tephra layers is not absolute, i.e. precise in historical time; however it is an accurate dating technique of correlating proxy records at a variety of sites.

Correlations across lacustrine and terrestrial sedimentary environments can be achieved by identifying and constructing tephrochronologies. The dating framework is more powerful when tephra layers occur in conjunction with dated laminated sediments, which may provide historical dates for the tephra. Annually laminated sediments (varves) are discrete layers representing a yearly addition of material to a water body. Varves can be widespread and relatively easily correlated, especially when there are distinct stratigraphic horizons within cores (Kristiansson, 1982, 1986; Strömberg, 1985, 1989; Cato, 1985). The nature of the varved deposit is related to inflow and lake conditions, especially bathymetry and stratification (Gilbert and

Shaw, 1981; Sundborg, 1992), catchment vegetation characteristics and lake productivity (Renberg *et al.*, 1984; Almquist *et al.*, 1992), and residence time of suspended sediment in the lake (Ashley, 1975). To understand the nature of the material, environmental processes and mechanisms producing varves, Sundborg (1992) suggests analysing "synchronously deposited sediments from different localities". Varves are assumed to be synchronous across a lake floor (De Geer, 1940). However, this is not known with certainty and therefore volcanic ash provides an important test because an isochronous horizon may be followed across lake sediments.

An important goal is therefore to link established tephrochronologies and varve chronologies. The Holocene tephra record in Iceland is one of the most detailed and best studied in the world, whilst the varve chronology in Sweden (the Swedish Timescale) covers ca. 13ka and has been linked to the present day to provide calendar year dates for the sediments. The connection to the present is assumed accurate to within an estimated error margin of +35/-205 varve years for the 12,500 years long chronology (Cato, 1985, 1987). These errors may have been caused by processes within the lake basin such as turbidite erosion or freak floods (see De Geer, 1940). Several independent checks indicate divergence from established time scales. Björck *et al.* (1987), using magnetostratigraphy to compare radiocarbon dates and varve years, found a significant difference of approximately 500-600 varve years during the period 10,500-10,200 ^{14}C BP. Brunnberg and Miller (1990), examining macro and micro fossils from the late-glacial clays around Stockholm, found that the radiocarbon dating of the shells did not match the varve dates. This may be due to poor dating because of using shells, but possible inaccuracies in the varve chronology are indicated by the presence of shallow water diatoms in an area of supposed deep water (130m above present sea level).

To provide precise geochronological frameworks, the accuracy of the varve chronology must be assessed. One method is to investigate the presence of historic tephras known to have fallen in Sweden. Persson (1971) identified ashes from the

Öraefajökull eruption in AD 1362, Hekla in AD 1104 and AD 1947, and Askja in AD 1875 in Swedish peat bogs. The presence of these tephras is substantiated by historical records. Mohn's (1877) map of the ashfall from the Askja in 1875 is probably the first isopach map of tephra. In addition, microscopic glass shards from the eruption of Öraefajökull in AD 1362 have been identified in the Greenland ice cap (Palais *et al.*, 1991). Þórarinsson (1958) showed that the eruption cloud moved eastwards from Iceland and, if so, then it is likely to have reached Scandinavia.

The isopach maps in Iceland constructed for the settlement layer or "Landnam ash" from the eruption of Vatnaöldur in the Veidivötn fissure swarm in AD~900 also indicate that the prevailing winds at the time may have deposited the tephra in Scandinavia (Larsen, 1984). This view is supported by evidence from tephra layers in the Faeroes (Waagstein and Jóhansen, 1968) The presence of any or all these tephras in the varve sequences in the Swedish Timescale would provide a calibration of the varves and a link between terrestrial and lacustrine sites in both Scandinavia and Iceland. Identification of Vatnaöldur AD~900 (Landnamslag) would securely anchor the first 1093 years of the varve chronology. Any errors apparent in this section could be used to determine the magnitude of errors in earlier sections, and therefore provide a better estimate of error margins than is presently available.

A calibrated varve chronology could also provide calendar dates for important prehistoric eruptions, if these tephra layers were found in the varve record. Several ashes of pre-Landnam age are of great interest in Quaternary dating studies. These ashes have approximate radiocarbon dates but lack precision. Of most interest are the mid-Holocene tephra layers Hekla 3 and Hekla 4, and the tephra from the North Atlantic Ash Zone 1 (NAAZO) dated at around 10,600 BP.

Two of the most important prehistoric tephras are Hekla 3 (2800 BP) and Hekla 4 (3800 BP). Due to the size of the eruptions microscopic traces can be found as far afield as Scotland (Dugmore, 1989), Northern Ireland (Pilcher and Hall, 1992) and Scandinavia (Persson, 1971). Most related research has been into the linkage to

proxy records of climatic and vegetational systems and the controversial question of the possible environmental and cultural impacts of volcanism. The size of the dust veils from each eruption may have been great enough to affect the annual growth rings of the Irish bog oaks (Baillie and Munro, 1988). Volcanic impact may have contributed to the decline in *Pinus sylvestris* pollen in northern Scotland ca. 3800 BP (Gear and Huntley, 1991; Blackford *et al.*, 1992). The effects of the eruptions have also been used to explain the phases of apparently abrupt abandonment of marginal archaeological sites in upland Britain (Burgess, 1989).

The major problem with these tephras is that the radiocarbon dating is too coarse in resolution effectively to link to the tree-ring and varve chronologies. A connection to calendar years is vital. This is claimed by Baillie and Munro (1988) in the Irish bog oak chronology. However this suggested link has no firm evidence as it is not certain if the perturbation in the tree-ring record has been caused by volcanic activity, or, if it is volcanic in origin, which volcano is responsible. Hekla 3 and H4 are known to have fallen in Scandinavia (Persson, 1971) but have so far only been found in the peat bogs. These discoveries suggest that a link between the varve and tephra chronologies has the potential to test numerous hypotheses regarding other dating techniques such as dendrochronology and radiocarbon. The linkage might also aid analysis of human settlement during the Holocene.

Older prehistoric tephra deposits also require secure dating. A large amount of research has focused on the termination of the last ice age, and the rapidity of the last glacial/interglacial transition with all the implications this has for humans, climate, oceans and vegetation. The NAAZO tephras are the result of increased explosive volcanism around 10,800-9000 BP during the biostratigraphically defined Late glacial Younger Dryas cold period (Mangerud *et al.*, 1984).

Several problems exist regarding the tephras, however. The problem in the ocean cores is that it is impossible clearly to distinguish, date, and identify all the different eruptions due to low sedimentation rates and bioturbation of the sediments

(Mangerud *et al.*, 1984; Morton, 1987; Kvamme *et al.*, 1989). Two distinct tephras have been recognised, namely the Vedde ash (10600 BP) and the Saksunarvatn ash (9000 BP), but there are several more such as I-THOL-1 and I-THOL-2 (Mangerud *et al.*, 1984; Kvamme *et al.*, 1989).

Terrestrial records provide a better resolution than ocean sediments. However there are few good undisturbed sites available for the Late-glacial period due to severe environmental disturbance. There have been two recent breakthroughs. Torfadalsvatn, a small lake in the Skagi peninsula northern Iceland, has apparently sufficient a resolution to distinguish and radiocarbon date five NAAZO tephras (Björck *et al.*, 1992). These results correlate with the dates for the Skógar tephra from central north Iceland, which has been identified as the Vedde ash (Norðdahl and Haflidason, 1992). However, the tephra stratigraphy at Torfadalsvatn includes tephra-rich strata which could be discounted because they appear to be reworked. No substantial evidence is given in support of this assumption and the record from Torfadalsvatn remains ambiguous.

The fundamental methodological assumptions behind both tephra deposition and lake sedimentology must be assessed before linking the two geochronologies in northern Iceland. The processes which create the sedimentary record are of vital importance in geochronology, since lack of understanding of depositional processes allows spurious connections to be maintained. Any well known dating framework can become self-enforcing if later evidence is made to fit the chronology and there are no independent tests (Watkins, 1971; Oldfield, 1977). Dates from many techniques may also cluster around an apparently important event. This is the "suck in and smear" effect whereby a well dated event in the tree ring chronology "attracts" inaccurately dated events in other time scales. An example of such an effect is the way possible H3 ashes have been correlated with Santorini (Baillie,1989).

The main assumption when using tephra as a marker horizon is that ash is deposited instantaneously over all types of environment. However, equal amounts are not

deposited. Despite several studies examining the thickness of the deposit with distance from the volcano, few studies concentrate on the smaller scale differences between thicknesses of tephra in various sedimentary environments. Processes such as focusing in lake basins, bioturbation in peat bogs creating dispersed horizons, and erosion and redeposition due to hillslope processes in soil profiles may produce a more complicated picture of the tephra record than is fully appreciated.

There are implications for using a tephra layer for long distance correlation and dating especially if it cannot be fully established that it is the original airfall and that it may have been reworked. Björck *et al.*, (1992) have put forward several criteria to distinguish airfall tephra from redeposited material. These are:

a) Sharp lower boundaries
b) Compact zone of greater than 95% volcanic particles
c) Well defined geochemical composition
d) Constant grain size

These criteria are arbitrary and not based on empirical work. Therefore, it may be possible to misinterpret layers of tephra in lake sediments by assuming that they represent the original airfall input when they simply reflect internal lake processes. Lake basins, despite possessing an equal or higher resolution than most other sedimentary environments and being more accessible than deep sea cores, are affected by processes that may affect the nature and distribution of tephra in the sediments. For example, in calm deep lakes, tephra or any allochthonous material may settle through the water column and settle out with a "sharp lower boundary". Due to sorting of particles there will be a concentration of types of material and size. It is necessary to use integrated catchment and lake basin studies to understand the complete tephra stratigraphy of the area.

There is also the possibility of using tephra as a "tracer" to attack several problems in studies of lake sedimentology (Oldfield, 1977). Firstly, sedimentation patterns in lakes are difficult to determine without dense sampling strategies. Lake basins can be divided into areas of net erosion, transport and accumulation (Håkanson and

Jansson, 1983). To map this distribution, multiple cores have to be taken. Few studies however have the time or resources to do this, and reliance is placed on one or two cores analysed in detail. The main problem is the difficulty of distinguishing the source of the sediment, especially if the geology of the catchment is homogenous. One study has tackled this question by examining the deposition of mine waste from a point source in Loe Pool, Cornwall (O'Sullivan *et al.*, 1982). The advantage of a tephra stratigraphical approach is that, using profiles from the catchment area, it is possible to identify areas of disturbance in the sediments and therefore past processes. For instance, repeating tephra layers or missing layers indicate erosional and depositional processes acting in the past. Incomplete profiles may point to large scale mass movement or river action, dependent on geomorphic setting.

Secondly, sediment focusing within the lake basins may affect core correlation unless there is a very clear identifiable horizon throughout the lake bottom sediments (Oldfield, 1977; Oldfield *et al.*, 1985; Downing and Rath, 1988). Tephra layers within lake sediments are ideal marker horizons especially if they are historical, or securely radiocarbon dated.

Thirdly, it is difficult to separate the sources of lacustrine sediment, whether derived from outside the lake proper or from aquatic solution through biological uptake, chemical sorption or precipitation. Tephra, however, is an allochthonous input. It has to have come from the air and catchment. In this respect it provides an important tool for distinguishing other allochthonous and autochthonous sediments. For instance, research into the ecology of Þingvallavatn and Mývatn, Iceland indicates that increased amounts of nutrients into the lake (in this case via a tephra fall) cause accelerated biogenic production and therefore increased sedimentation rates, an important point when sedimentation rates from cores are used to indicate erosion from the catchment (Einarsson, 1982; Haflidason *et al.*, 1992).

Fourthly, it is difficult to distinguish the amount of material redeposited into the lake from the catchment. Several studies have used lake basins to calculate sediment

yields and sediment delivery ratios. These are of more value than accumulation rates which are affected by minerogenic influx, bathymetry and internal production (Foster *et al.*, 1988). However, these types of studies need secure dating and correlation as well as a means of identifying sediment sourcing and budgeting. Tephra layers are an ideal means of tackling the problem.

1.3 Thesis structure and research strategy

The general objectives of the thesis are: firstly, to construct tephrochronologies in lake sediments in Sweden and Iceland; secondly, to assess the effects of erosional and depositional processes on the nature and distribution of tephra in the lake sediments and; thirdly, to propose a model of sediment redistribution in lake sediments and catchments.

The thesis structure is outlined in Figure 1.1. Chapters 2 and 3 are concerned with an initial search for Icelandic tephra in the Swedish varve chronology. Chapter 2 reviews varve studies and the current state of the Swedish Timescale, assessing the limitations to knowledge of processes vital to making the appropriate linkage between tephra and varves. Chapter 3 discusses the laboratory studies of tephra characteristics that are fundamental in determining its behaviour in the lake system. The results of the first chapters indicate the importance of assessing both lake processes and tephra characteristics which may cause variation in the spatial and temporal distribution of tephra in the sedimentary record. As a result, the remaining chapters concentrate on refining understanding of lake-catchment systems. Chapter 4 describes the field site in northern Iceland and discusses the field and laboratory methods employed in the study. Chapter 5 describes the tephrostratigraphy, whilst Chapter 6 examines the possible mechanisms causing the variations in tephra distribution. A model is introduced which is used to represent the processes occurring in the catchment and resulting tephra stratigraphy in the lake sediments. Chapter 7 concludes with a discussion of the wider implications of the study and its relevance for future work on the varve chronology of Sweden.

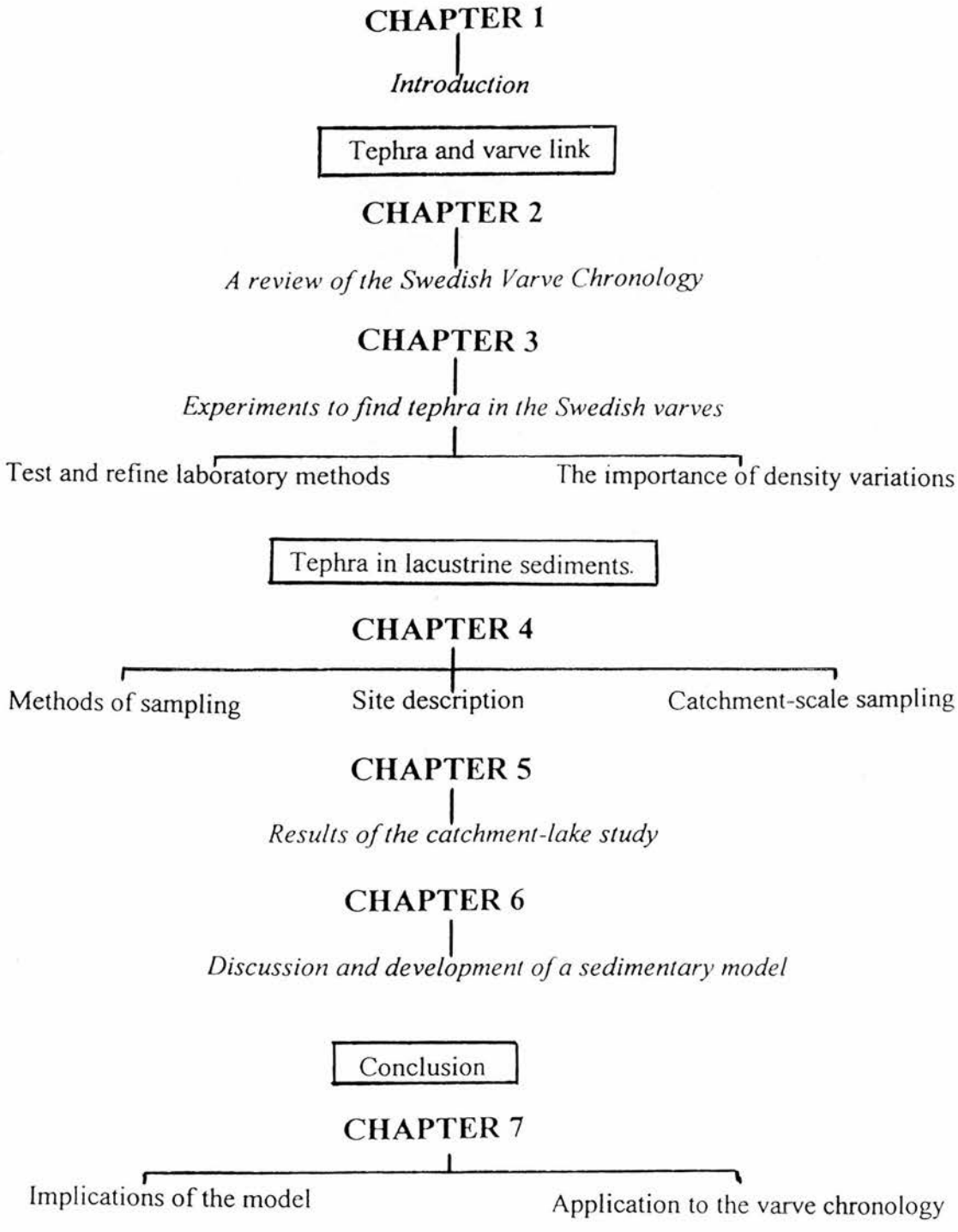

Figure 1.1 Thesis Structure

CHAPTER TWO: The Swedish varve chronology - a review

2.1 Introduction

The aim of this section is to review the nature and formation of Swedish varves and their role in geochronology with special reference to the history and problems of the Swedish Timescale. The Swedish glacial and non-glacial varves provide a year by year chronology since the end of the last glaciation with a detailed record of environmental change. The geochemical and sedimentary information from diatoms, shells, salt concentrations, colour and structure contained in each layer has great potential for regional environmental reconstruction.

The term "varve" (Swedish "varv") was introduced by De Geer (1912) to describe "rhythmic accumulations of sand, silt and clay" (Tauber, 1970). A classic glacial varve consists of two layers or laminations associated with the annual cycle of glacier melting. There is, however, some terminological confusion. Renberg (1981a) points out that several terms for the sedimentary deposit already exist in the literature such as varve, annual band, seasonal rhythmite, annual lamination and a couplet of laminae. He advocates the definition of a varve as "sediment deposited in the course of one year" thereby including the possibility of several laminae within one annual unit. O'Sullivan (1983) believes that this is too broad and prefers the use of the term "non-glacial" in order to avoid confusion with the classic glacial varves. In this review the terms "varve" and "annual lamination" are interchangeable, whilst lamination simply describes the sedimentary structure.

Large areas of Sweden which were part of the Baltic Ice Lake during the Late-glacial have thick deposits of varved clay. De Geer was able to construct a chronology, tracing the retreat of the ice margin using the principle that varves "ought to transgrediate in said direction (of ice recession) like tiles on a roof" (De Geer, 1940). The uppermost varve in one core sequence would therefore be the same age as the lowest varve in a neighbouring core closer to the ice margin. This simple concept

disguises the complex and diverse nature of these sediments. Several hydrological processes may produce similar characteristic sedimentary structures, therefore a thorough understanding of the depositional environment involved in classic glacial varve chronologies requires information from studies of the processes of varve formation in recent environments (Sturm, 1979).

Varved sediments have increasingly been found in a variety of non-glaciolacustrine areas so that the original role of varves as a geochronological tool (De Geer, 1940) has been supplemented by their use in different environmental reconstructions. Insights into the processes of formation have in turn helped to indicate the possible areas of error in any constructed chronology. De Geer's ultimate goal of correlating varve sequences throughout the world obscured the important small-scale investigations needed to give the Swedish Timescale precision (Kristiansson, 1986). The consequent lack of confidence and interest in varve chronologies outside the Nordic countries stemmed from errors in the early connections.

Several of these uncertainties were known to De Geer (1940) and attempts were made to minimise spurious correlations by careful measurement and continuous revision. In this way the Swedish varve chronology remains essentially reliable. The latest revisions (part of the IGCP Project 253 started in 1975) have strengthened the chronology considerably and a new connection with the present has been made (Cato, 1985, 1987). This major advance has far reaching implications for both the chronology of deglaciation and studies of environmental change.

2.2 Varve Location

Annually-laminated sediments or varves have been found in a wide range of marine, estuarine and lacustrine environments (O'Sullivan, 1983). This is in part due to developments in coring techniques, especially freezing samplers (Huttenen and Meriläinen, 1978; Wright Jnr, 1980; Renberg, 1981b). Laminated sediments are more common than previously thought. O'Sullivan (1983), however, points out that

the distribution of present sites reflects merely the distance from major palaeolimnological research centres and there are many gaps to be filled.

There are also several varve chronologies which require thorough re-investigation. For example Caldenius (1932) correlated varved clays in Patagonia with the Swedish Timescale, but there has been little subsequent research in this area despite the potential for understanding Quaternary glaciations in the southern hemisphere. Antevs (1925, 1951), another co-worker of De Geer in the days of global "teleconnection", constructed a Canadian Timescale ("Timiskaming"). The complicated dynamics of the Laurentide ice sheet, however, make even short distance correlations difficult (Tauber, 1970).

2.3 Formation of laminated sediments

Recent research has focused on varve processes. There are several important conditions governing the formation of varves in either marine, estuarine or lacustrine environments.

2.3.1 Material in suspension

The formation of varves depends on the existence of suspended matter within the water column (De Geer, 1912; Sauramo, 1923; Kuenen, 1951). The variations in sediment quantity and quality during a year reflect seasonal and other environmental changes (O'Sullivan, 1983). If there is no change in the supply of sediment at any period during a year, laminated sediments are unlikely to form.

Five different sources are considered to be responsible for the supply of suspended matter to a depositional basin; these are allochthonous inputs (from rivers and the atmosphere), autochthonous inputs, and sediment from processes occurring within the lake (resuspension and upwelling) (see Figure 2.1). Sediment in suspension and in bed traction in streams is probably the most important source material in glacial lakes. Other inputs from the atmosphere, hydrochemical precipitation and biogenic activity, upwelling from groundwater, and resuspension from bottom currents are of

relatively greater or lesser importance in other types of environments. The relationship between these different components has been generalised as a model by Sturm (1979) and is valid for all basins.

$$S_{DEP} = (S_{RIV} + S_{AIR} + S_{AUT} + S_{RES} + S_{UPD}) - S_{EXT}$$

where S_{DEP} is deposition in a basin, S_{RIV} is influx by rivers, avalanches etc., S_{AIR} is atmospheric input, S_{AUT} is autochthonous material from biogenic activity, chemical precipitation, S_{RES} is resuspended material, S_{UPD} is sediment from groundwater etc., and S_{EXT} is extinction by outflow.

Oligotrophic (nutrient poor) alpine lake basins will have suspended matter nearly exclusively from river tributaries, whilst more eutrophic lakes (nutrient rich) will have a larger autochthonous input due to bioproduction.

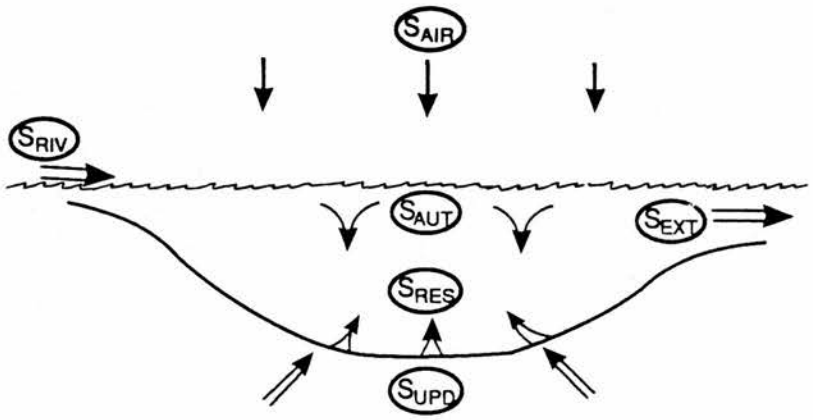

Where DEP - deposition in basin
RIV - influx by rivers, subaerial slumps, avalanches etc.
AIR - atmospheric input by wind, rain etc.
AUT - autochthonous material (bioproduction, chemical precipitation etc.)
RES - resuspended material (bottom currents, subaqueous slumps etc.)
UPD - influx by updwelling of material (groundwater, subaqueous slumps etc.)
EXT - extinction by outflow

Figure 2.1 Model of hypothetical sources of suspended sediment in a depositional basin (*source:* Sturm, 1979).

2.3.2 Basin morphometry

The depositional basin should have a particular morphometry for the preservation of undisturbed, laminated sediments. Lake basins should be flat-bottomed and deep enough to prevent mixing of the water column and sediments by winds (O'Sullivan, 1983). Other favourable characteristics include a bedrock basin, a small drainage area and an absence of significant inflow (Saarnisto 1986). There are two main types of basins in which laminated sediments are known to form: Small lakes less than 1km in length with an area of less than 20ha and a depth of greater than 15m, and isolated deep basins in very large lakes (Saarnisto, 1986). It is difficult to list exact dimensions as several variables such as fetch, bottom currents and trophic status combine with basin morphometry to aid or inhibit the formation of laminated sediments.

2.3.3 Lake water stratification

The preservation of varved sediments is aided by a strong seasonal semi-permanent stratification of the water column, which reduces the effects of turbulence and therefore mixing. Figure 2.2 shows the layering of lake water during seasonal stratification. The upper layer of water (the epilimnion) is separated from the lower hypolimnion by the thermocline (a layer with a pronounced temperature gradient). This structure is destroyed during overturning of the lake water and mixing occurs. Lakes can be classified in terms of mixing (mixis). In monomictic lakes a thermal stratification exists only in one season of the year (summer). In dimictic lakes mixing takes place twice, namely in the spring and autumn. Mixing is prevented by thermal stratification in summer and by ice cover in winter. Meromictic lakes are a special kind of lake where the water column never mixes completely in any season due to the chemical stratification of the deepest water layer.

Associated with stratification is the absence or scarcity of oxygen in profundal waters (anoxia) for certain periods in the year. This inhibits the activities of bottom-dwelling (benthic) organisms, therefore reducing the effects of bioturbation and

favouring preservation of any laminated sediments. However, anoxia is not an essential condition for well-preserved sediments. Varved sediments from Sweden

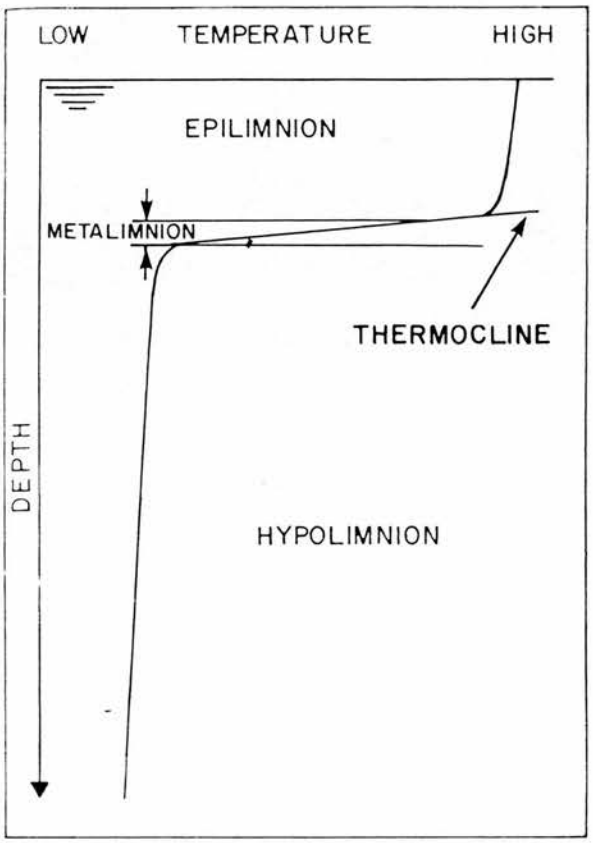

Figure 2.2 Thermal regions of lake waters (*source:* Drewry, 1986).

are mainly from dimictic lakes (two turnovers during a year) in which oxygen is relatively abundant even in the deepest water (Renberg, 1981a). These lakes, however, are mainly oligotrophic and therefore biological production is minimal. Ludlam (1979) found that productive lakes may also yield varved sediments if the influx of material is greater than the rate of mixing by organisms.

O'Sullivan (1983) has summarised all the processes leading to the formation and deposition of annually laminated sediments in freshwater lakes (Figure 2.3). Different types of lamination will be deposited depending on the strength of the lake circulation and the seasonal supply of sediment. The diagram shows that the only situation where laminated sediments are not produced is in a well-mixed, non-

thermally stratified lake. Varves in estuarine and marine environments will be affected by processes different from those in freshwater lakes. For example, the production of laminated sediments in marine areas requires seasonal density stratification which prevents salinity-induced flocculation of clay particles (Stevens, 1985). Flocculation would prevent the formation of well-defined annual laminations.

2.4 Composition and structure

O'Sullivan (1983) classifies varves into four main groups. Laminations of autochthonous sediment can be produced by the interaction of the climate and internal lake processes to form either ferrigenous, calcareous or biogenic varves. On the other hand, allochthonous material may be more prevalent and produce clastic varves (Figure 2.3).

2.4.1 Ferrogenic laminations

In non-calcareous lakes, dark and pale laminations may be caused by changes in the solubility of Fe species due to reduced or oxidising environments (Anthony, 1977). Renberg (1981a), studying dimictic lakes in northern Sweden, found that sediments coloured light brown by iron hydroxides were deposited during the spring and autumn overturns. During anoxic conditions in the summer and winter the sediment was stained black by iron sulphide. Consequently, a varve consisted of four laminae, two light and two dark, with the visual appearance depending on the redox potential and the duration of the aerobic and anaerobic periods.

Dickman (1979) argued that the dark laminae in all non-glacial varves reflect the mass mortality of anaerobic bacteria during the autumn overturn. The pale laminae in varves formed in iron-rich lakes may not therefore represent the period of circulation but the winter, spring and summer. He also believed that two or more dark laminae are impossible in one year, even though there may be partial oxygenation of the water column in both spring and autumn. This is because the low density of anaerobic bacteria during the spring would be unlikely to produce enough

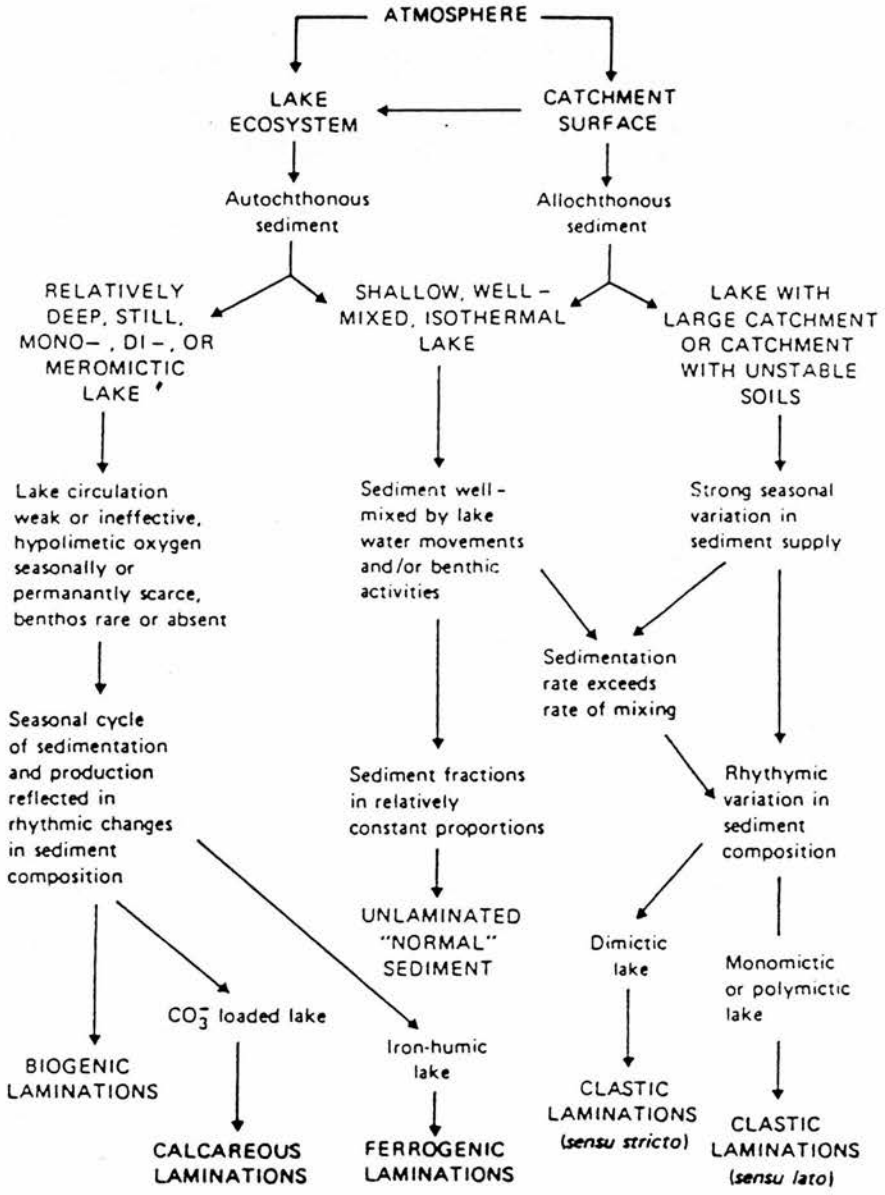

Figure 2.3 Processes and relationships leading to the formation and deposition of annually-laminated sediments in freshwater lakes (*source:* O'Sullivan, 1983).

biomass for a separate dark layer. There is currently no consensus regarding varve processes in iron-rich lakes.

2.4.2 Calcareous laminations

In carbonate lakes layers of calcite ($CaCO_3$) represent the growing season. Higher pH values due to increased algal uptake of atmospheric CO_2 may encourage CO_3^- saturation. This was found to be the case in the Zurichsee, Switzerland (Kelts and Hsü, 1978). On the other hand, Brunskill (1969) found CO_3^- saturation in Fayetteville Green Lake, New York, was controlled mainly by rising temperatures. Whichever is the case, carbonate lakes may have calcareous layers followed by darker bands of organic and inorganic detritus, the latter formed in autumn, winter and spring. Pollen and diatom studies in Canada support these conclusions as pollen from species flowering in late spring and summer were embedded in the calcite layer (Tippett, 1964).

2.4.3 Biogenic laminations

According to Renberg (1981a) biogenic varves from a dimictic lake in northern Sweden consist of a well developed spring layer of mineral grains, a layer of biological material such as algal remains and pollen deposited in late spring, summer and autumn, and finally a thin organic winter layer. The winter layer is usually formed under ice by the simple vertical settling of particles by Stoke's Law, especially in the absence of underflow activity. Ludlam (1976, 1979) found that varves in several Massachusetts lakes were composed mainly of diatom fustules. This was due to seasonal changes in algal productivity and/or seasonal breakdown of the stratified water column. Increasing productivity of a lake may initiate varve formation by providing a seasonal source of autochthonous sediment as organisms die (Ludlam, 1976). As time goes on and increasing productivity decreases the level of bottom water anoxia, the disturbance of the laminations will decrease as fewer organisms can survive in the sediments.

2.4.4 Clastic laminations

Laminations formed mainly from allochthonous matter often arise in oligotrophic lakes where other sources of suspended matter are minute (Figure 2.4). Sturm (1979) modelled oligotrophic lakes with mainly clastic sedimentation, varying both the input of suspended matter and the degree of stratification. A classical varve couplet is formed only when suspended matter is introduced to a lake by discontinuous influx during the period of stratification. This is illustrated in case 7 in Figure 2.5. Here, coarser particles start settling immediately, depositing a basal graded bed of sand and silt. The bulk of the clay particles, being trapped during stratification within the water column, will only start settling after the seasonal overturn. This causes the deposition of a distinct non-gradational clay lamina on top of a previously formed coarser layer.

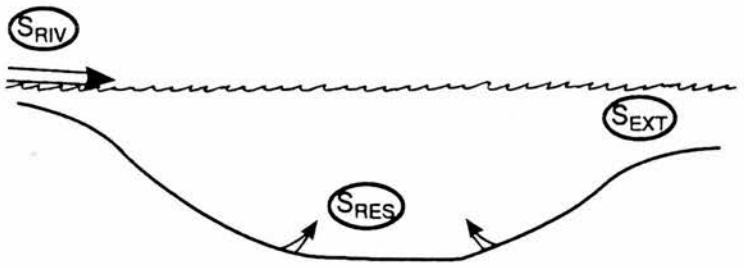

Where RIV - influx by rivers, subaerial slumps, avalanches etc.
RES - resuspended material (bottom currents, subaqueous slumps etc.)
EXT - extinction by outflow

Figure 2.4 Sources of suspended matter in an alpine oligotrophic lake (*source:* Sturm, 1979).

These characteristic laminations may also form in eutrophic lakes. However, in such conditions, the varves are likely to be far more complex due to contemporaneous autochthonous sediment production.

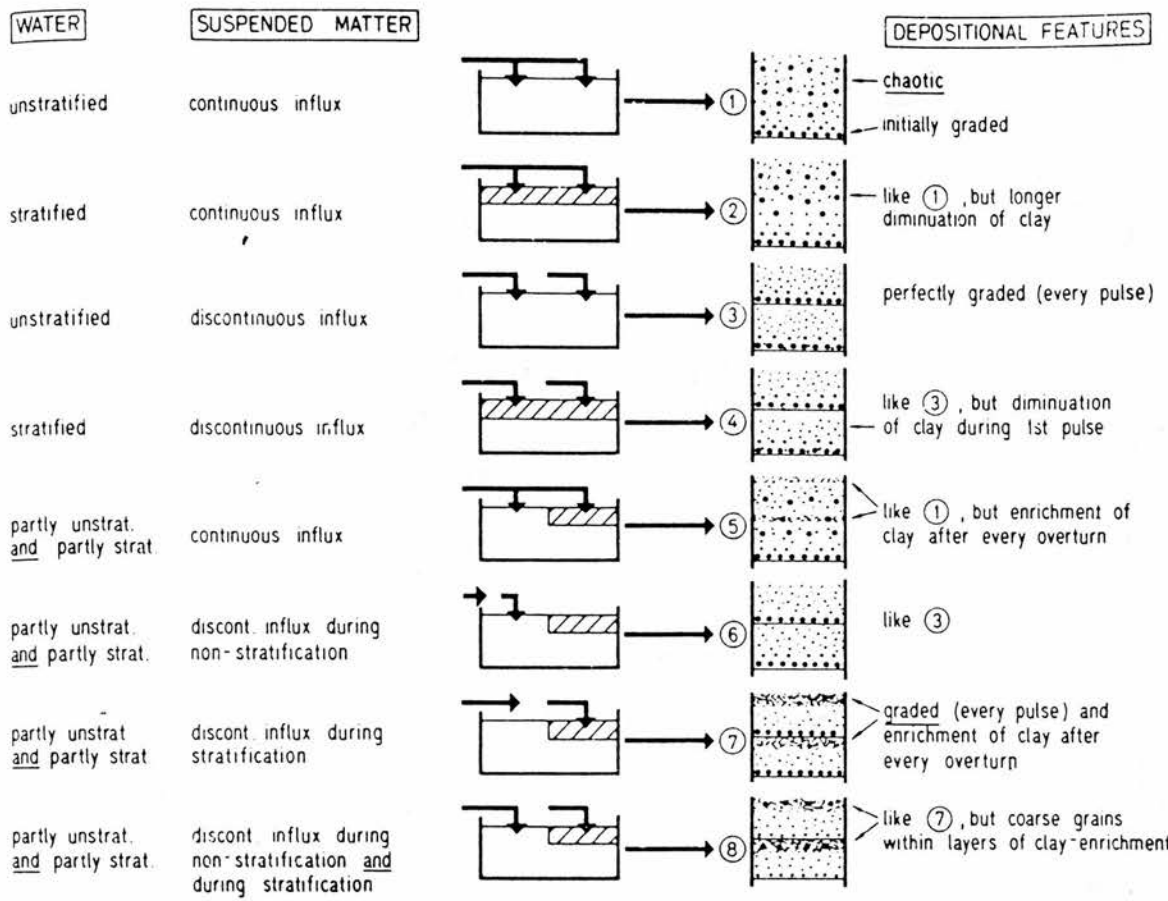

Figure 2.5 Idealised sedimentary features as a result of two hydrological parameters (stratification of the water column and influx of suspended matter) in an oligotrophic lake with clastic deposition. (Heavy dots for sand, light dots for silt, light dashes for clay) (*source*: Sturm, 1979).

2.5 Environmental applications of varves and other laminated sediments

The type of sediment found within a varve sequence yields a greater amount of information than most other palaeoenvironmental records. A principal chronological strength of varves for the Quaternary scientist is that deposits which may have accumulated over centuries, or even millennia, have readily identifiable annual units. Given this degree of precision, there are five main uses of laminated sediments: climatic change; vegetation history; sediment influx; monitoring of contemporary environmental processes; and geochronological studies. A fuller review of recent work can be found in O'Sullivan (1983) and Saarnisto (1986).

2.5.1 Climatic change

The information obtained from varves depends upon the type of lamination present, so that varves which are primarily autochthonous in origin (ferrigenous, calcareous and biogenic) may be expected to record the influence of climate upon internal lake processes. The formation of clastic laminations may be related to some external factor such as runoff (O'Sullivan 1983).

Renberg and Segerström (1981) related the organic and inorganic content of varves from Kässjön, north central Sweden to Holocene climatic changes. The peaks of organic matter just after 3000 BC and between 0 BC and AD 1000 may be a record of climatic optima.

One example of climatic change recorded by varve sediments comes from Lake Van in Turkey where the depth of the summer epilimnion represents the upper limit of contemporary varve formation (Degens and Kurtman, 1978). In shallower waters annual laminations are not presently formed. Consequently the presence in deep water cores of non-laminated sequences may be indicative of lower lake levels in the past.

2.5.2 Vegetation history

The rates of change and stability of vegetation may be studied in great detail due to the very precise chronology available for the pollen diagrams (O'Sullivan, 1983). Varved sediments also give precise estimates of the rate at which taxa recorded in the pollen diagrams invade closed plant communities (Davis, 1976). This is of great importance when the role of fire is considered in studies of regeneration (Swain, 1973).

2.5.3 Calculation of sediment influx

Annually laminated sediments are particularly well suited for making rapid inter-core correlations especially where there are prominent marker horizons. A chronology of rates of erosion and an analysis of patterns of sedimentation can then be made. For example, O'Sullivan *et al.* (1982) used multiple coring of the sediments of Loe Pool, Devon to find that sedimentation has been concentrated since AD 1938 in four main localities, and that there was an increase in the rate of deposition during the 1930s due to tin mining in the area.

2.5.4 Monitoring of contemporary environmental processes

The varves of very recent years are heavily affected by the activities of industrialised societies especially by heavy metal pollution (O'Sullivan, 1983). Renberg and Segerström (1981) used the annually laminated sediments of Gråsastjärn, a lake in northern Sweden to study levels of lead in the region since AD 1980.

Other types of pollution which can be monitored include the increase in phosphorus and nitrogen which lead to eutrophication of lakes, for example Huttenen and Tolonen (1977) in Lake Lovojärvi, Finland.

2.5.5 Geochronological studies

The varve chronology implies distinct, readily-visible, yearly units of sediment. Theoretically, it is possible to use varve counts to calibrate other dating techniques in much the same way as tree ring chronologies have been used to complement

radiocarbon dating. So important is this aspect, that it is crucial to investigate the chronology in detail.

2.6 The Swedish Varve Chronology

The Swedish Timescale based on the varve chronology was introduced by De Geer (1912, 1940) to construct the rate of retreat and pattern of deglaciation of the Scandinavian ice sheet. The last ice advance consisted mainly of a lobe extending into the southern half of the Baltic. Once this lobe disappeared, the ice sheet retreated in an "almost unidirectional way" (Tauber, 1970).

Ice recession was associated with large inland lakes into which rhythmic accumulations of clays were laid down. These formed the basis of a varve chronology of 12,500 years from Skåne in the south of Sweden to the Ångermanälven river in the north (see Figure 2.7). De Geer (1912, 1940) examined distal varves as these were less likely to contain local irregularities. He divided his timescale into the earlier part of the late-glacial (De Geer's "gothi-glacial") corresponding to the ice recession through southern Sweden to Stockholm, and the later part ("fini-glacial") from Stockholm to the rivers Indalsälven and Ångermanälven. The end of the Scandinavian glaciation and the start of post-glacial varve deposition was represented by a thick varve at Döviken in the Indalsälven valley caused by the drainage of an ice-dammed lake . This drainage varve, known as the zero year, is therefore an arbitrary point and not necessarily synchronous across a region nor even in the Indalsälven valley itself (Strömberg, 1989).

To connect the Indalsälven glacial varves with the post-glacial, De Geer correlated his series at Vikbäcken, south of the Indalsälven with Lidén's Sand series from the Ångermanälven (Figure 2.7). Strömberg (1989) regards this correlation as essentially correct after re-examination of the cores and stratigraphic diagrams. This is despite the distance between the two sites (~50 km). De Geer obtained a date for the Döviken varve via tentative correlations with the Vikbacken series. Several revisions

(Järnefors, 1963; Hörnsten, 1964) and new correlations (Borrell and Offerberg, 1955) between the two valleys give a date of 6923 BC for the Döviken zero year, but suspicions that several connections were poor prompted further revisions and an IGCP Project was initiated to establish a firm connection to the present. Further difficulties in dating the zero year arise from errors in previous revisions. For instance the zero year varve has been correlated with three different equivalents in Lidén's series, namely varve number 425 (Borrel and Offerberg, 1955; Bergström, 1968), varve 426 (Fromm 1985), varve 426 or 427 (Järnefors 1963) and varve 427 (Fözö, 1980; Cato, 1987) The most recent research indicates that varve 427 is the most likely candidate for the zero year (Strömberg, 1989).

2.7 Errors in the Swedish Varve Chronology

In view of the errors involved in both De Geer's chronology and subsequent research, it is important to examine the inherent assumptions within the varve chronology.

The first assumption is that the coarse laminations of varves are deposited by bottom currents in proglacial lakes. This means that the meltwater would have to be slightly denser than the lake water or else it would spread as plumes or turbidity overflows. In the latter case, there would be a simple weak grading of silts and clays as particles settle according to Stoke's Law rather than a couplet. Another problem is that in lakes with pronounced bottom currents there may be erosion due to the descent of turbidites, the bulk of suspended material and some bedload being transferred directly to distant, deeper parts of the lake basin (Drewry, 1986). Most workers support the concept of "bottom currents" (Kuenen, 1951). One study of laminated sediments in the Walensee Switzerland indicates the complexity of underflows (Lambert and Hsü, 1979). Current meters were used to study the occurrence of turbidity underflows and their relationship to flood stages of tributary rivers (especially the Linth). Underflows were found, but only during years with major rainstorms when the floodwater was denser than the lakewater. During the dry years there were no silt-bearing underflows, only overflows carrying clay and the finest

particles to the lake. Floods on the Linth are not regular annual events, leading the authors to conclude that the varves present were not formed annually.

A second assumption is that the underflows owe their origin to the annual melting of glaciers. Results from the Walensee (above) indicate that this is not always the case and that drier, colder years may not produce significant underflows. To ensure the annual nature of recent varves, cores and sediment harvest traps have been used (Cato, 1985). This procedure cannot be applied to Late-glacial sediments and so doubts as to whether all varved deposits are really annual remain in the Swedish Timescale, especially in the Skåne area (Fromm, 1970). On the other hand, during a phase of rapid deglaciation there could be greater melting than from a glacier in equilibrium and strong underflows would deposit silt annually.

Other rhythms can be found within varves, for example, diurnal varves occurring in former ice proximal situations in Blekinge, southern Sweden (Ringberg, 1984). The Blekinge varves consist of couplets of thin winter clay layers and thick (~1m) summer silt layers. The summer layers have around 45 distinct bands of silt and sand indicating daily melting. Exceptional events such as jökulhaups may also affect any annual pattern in the record (Drewry, 1986).

Given the assumptions outlined above, Fromm (1970) identified three errors in the Timescale: The link to the present; problems of correlation between sites; extra and missing varves. Twenty years on, several of these uncertainties have been re-investigated and the chronology updated (Lundqvist, 1987). It is useful to reexamine these developments in the light of recent studies of present day varve processes.

2.7.1 The connection to the present

The greatest advance in the establishment of a reliable timescale was the link to the present day in the varve series from the Ångermanälven valley in northern Sweden (Cato, 1985, 1987). The postglacial varves in the Ångermanälven series are fluvial varves with the seasonal variations in river flooding provide the mechanism for

annual rhythmic accumulation of deltaic sediments. Continued land elevation since the last glaciation has caused the estuary delta to be displaced eastwards into the Baltic, resulting in a series of overlapping delta facies.

The potential of the Ångermanälven sediments for geochronology was first established by Lidén (1913) who constructed a postglacial varve chronology ending with the youngest varve 7522, an old delta plain, at Prästmon. Lidén estimated the depth of water above the former delta to have been 2-5 metres, the same depth as is associated with the formation of the present delta. An examination of the exposed silty delta deposits and the varves below them enabled Lidén to construct a graph of the land elevation of the area. This calculation was used to deduce a time span of 980 years between the formation of the youngest varve (10.2m above present sea level) and the present (AD 1900). The hypothesis of a continued rate of land elevation of 1.25 cm/yr up to the present, resulting in a date for the Prästmon delta of AD 920, was apparently supported by historical evidence. A mediaeval ruin nearby pointed to a water level of 8 metres around AD 1300, whilst two historically dateable shorelines and a map from 1701 substantiated the calculation.

Subsequent investigations of water marks, however, reveal a rate of uplift of approximately 0.8-0.85 cm/yr, therefore slower than Lidén's estimations (Bergsten, 1954). This implies an extension of the gap between historical time and the youngest varve of about 200 years (Fromm, 1970). This extended gap is confirmed by examination of varves deposited up to the present day (AD 1980) in the non-tidal estuary of the Ångermanälven. Here, Cato (1985) found that 1345 varves were deposited during the period between Lidén's youngest varve 7255 and AD 1900. This means that 365 years should be added to the original estimate of 980 years.

The error in Lidén's connection is responsible for the largest uncertainty in the Swedish timescale. All dating of Swedish varves in historical times is based on this approximate calculation. Furthermore, Lidén's work was used to obtain a date of 6923 BC for De Geer's zero varve at Döviken by backcounting from AD 920. The

new connection with the present now dates the zero year at 7288 BC. Given that there may still be errors in defining varve limits, Cato (1987) estimates the length of postglacial time up to the present (1986) as 9273 $^{+10}/_{-180}$ varves, excluding the zero year.

This result has major consequences for the dates obtained for other geological and archaeological events which were based on the original Swedish Timescale. For instance the deglaciation pattern in central Sweden and timing of the stages of the Baltic Ice Lake (Björk and Digerfeldt, 1989) can now be dated in calendar years and a true assessment of the difference between ^{14}C dates and varve dates can be made. However, cautious of past criticisms, varve chronologists have concentrated on tightening up the accuracy of the Timescale as a whole before major revisions of correlated events take place.

2.7.2 Errors in varve measurements and core correlations

De Geer (1940) pointed out the many types of physical and observational errors possible (Table 2.1). These he argued, must be minimised by a careful examination of the sediments otherwise "omission...would introduce often quite irrelevant and local variations which have nothing to do with the climatical curve". The best way of avoiding such errors is to make several measurements in the same region in order to establish the local varve facies as a background for further comparison (Fromm, 1970; Strömberg, 1989).

De Geer's graphical method of presenting connections between the varves (Figure 2.6) is still reliable, as it depends on the coincidence of thickness maxima and minima as well as the general configuration of the graphs. The confidence placed in the varve profiles depends on the distance between localities. A general agreement between short profiles is acceptable as the possible chronological range is limited to a few years. Over longer distances, however, the range may amount to hundreds of years, and within these wide limits purely accidental similarities may appear. Many of the early varve diagrams cannot be used due to the combining of several short

profiles from an area into one long composite diagram (Kristiansson, 1986). Resampling has been necessary to overcome these difficulties.

Physical errors

A *Primary facies from:*

Changed distance of receding river mouth.

Changed current direction.

Bottom topography.

Extra-marginal river erosion.

Littoral erosion.

Ice-dam draining.

Ice-river capturing.

B *Secondary facies from:*

Sliding of many or single varves.

Disturbance by icebergs.

Ice-raft deposition.

Deposition of esker-talus

Shrinkage by leaching.

Observational errors from:

Deceptive bands, simulating winter layers.

Overseen, indistinct layers.

Overseen small faults.

Joints between measuring strips.

Measurements on sloping or uneven sections.

Extra thin varves

Table 2.1 Sources of error in varve counting (*source*: De Geer 1940, Geochronologia Suecica Principles. Kungliga Svenska Vetenskapsakademiens Handlingar 18:6: Almqvist and Wiksells.)

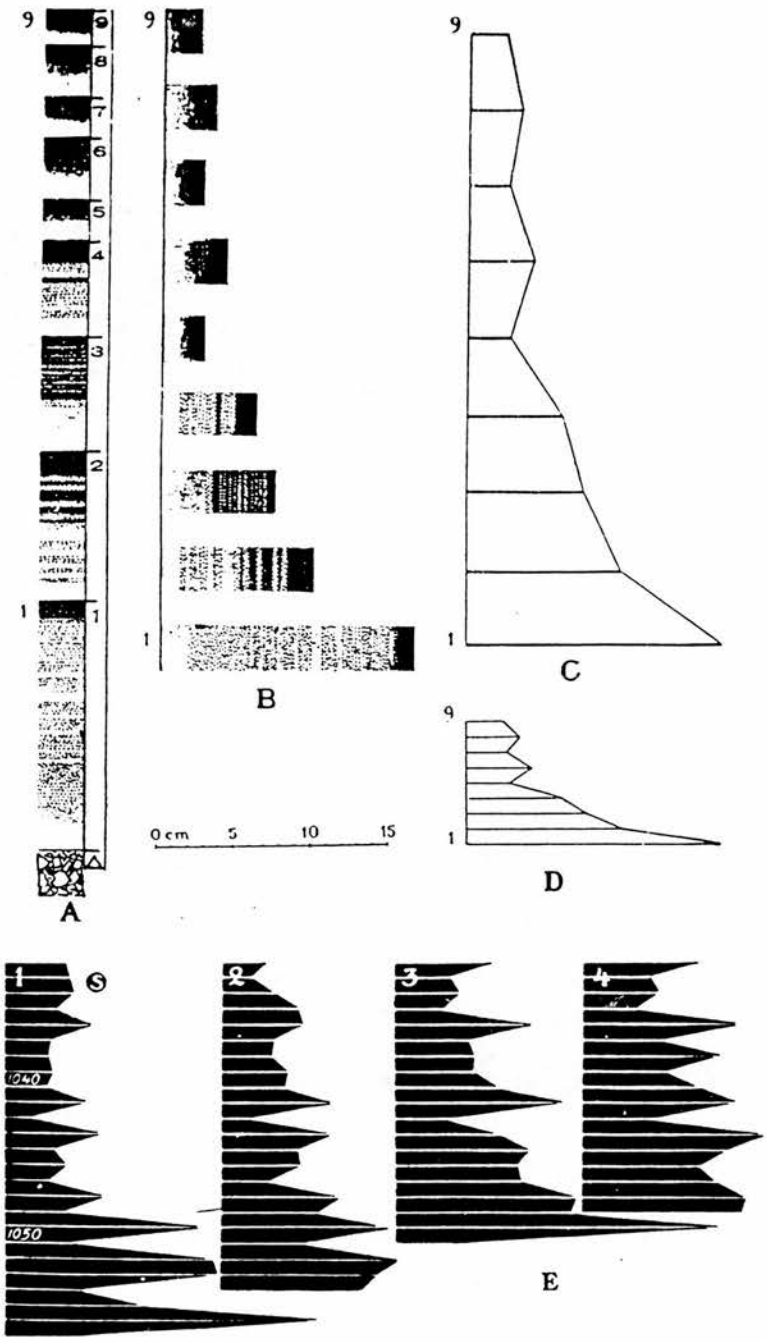

Figure 2.6 Schematic view of varves measured and turned into a graph. **A**-varve thickness marked on paper; **B**-varves turned sideways; **C**-varves represented each by a single line, tops combined into a curve; **D**-graph compressed with distance between the year lines of half a cm; **E**-first varve connections displaying ice recession (*source*: De Geer 1940)

The extent of De Geer's chronology and the major revisions are shown in Figure 2.7. The south-eastern section has been strengthened via new sites and correlations (Perhans, 1981; Ringberg and Rudmark, 1985; Kristiansson, 1986). Connections with the present and the new date of the zero year however (7288 BC Cato, 1985) depend on the good correlations across the Middle Swedish End Moraine Zone (Brunnberg pers. comm.; Perhans pers.comm.). The section north of Stockholm contains several weak points notably near Gävle (Lundqvist, 1975) where clay varves are thin and variations in thickness are small. Errors also occur in the Stockholm/Uppsala sections where the clay varves were laid down in brackish water from the Yoldia Sea stage of the Baltic. As discussed above, flocculation of clays in saline waters gives rise to indistinct varve boundaries making reliable correlations difficult unless several measurements are taken. Reliance on connecting sections by matching thick (proximal) varves can therefore be dangerous. Strömberg (1989) believes that the difficulties encountered by Järnefors (1963) when constructing a chronology for Stockholm to Uppsala were due to his accidentally matching non-synchronous drainage varves. Errors can be avoided by taking intermediate varve measurements (Strömberg, 1989). Problems during the actual counting of laminations may be solved by applying techniques from dendrochronology (Saarnisto, 1986).

2.7.3 The suppression or duplication of annual deposits

As mentioned above, irregular flows may affect the varve count. The sudden drainage of ice lakes may result in an "extra" varve. For instance, varve number -48 (that is 48 years before the zero year) is found in most cores from the Indalsälven valley but is missing from Ångermanälven sections (Strömberg, 1989). This is best explained as due to a local drainage event in the Indalsälven valley. Several of the varve diagrams from the revisions of Järnefors (1963), Hörnsten (1964) and Bergström (1968) have had to be cut and moved by one varve year to compensate. High water discharges from ice lakes which create thick drainage varves may also

erode laminations below. This is easily identified in large, open clay sections. Correlation is more difficult if interpretation is based only on cores (Strömberg, 1989).

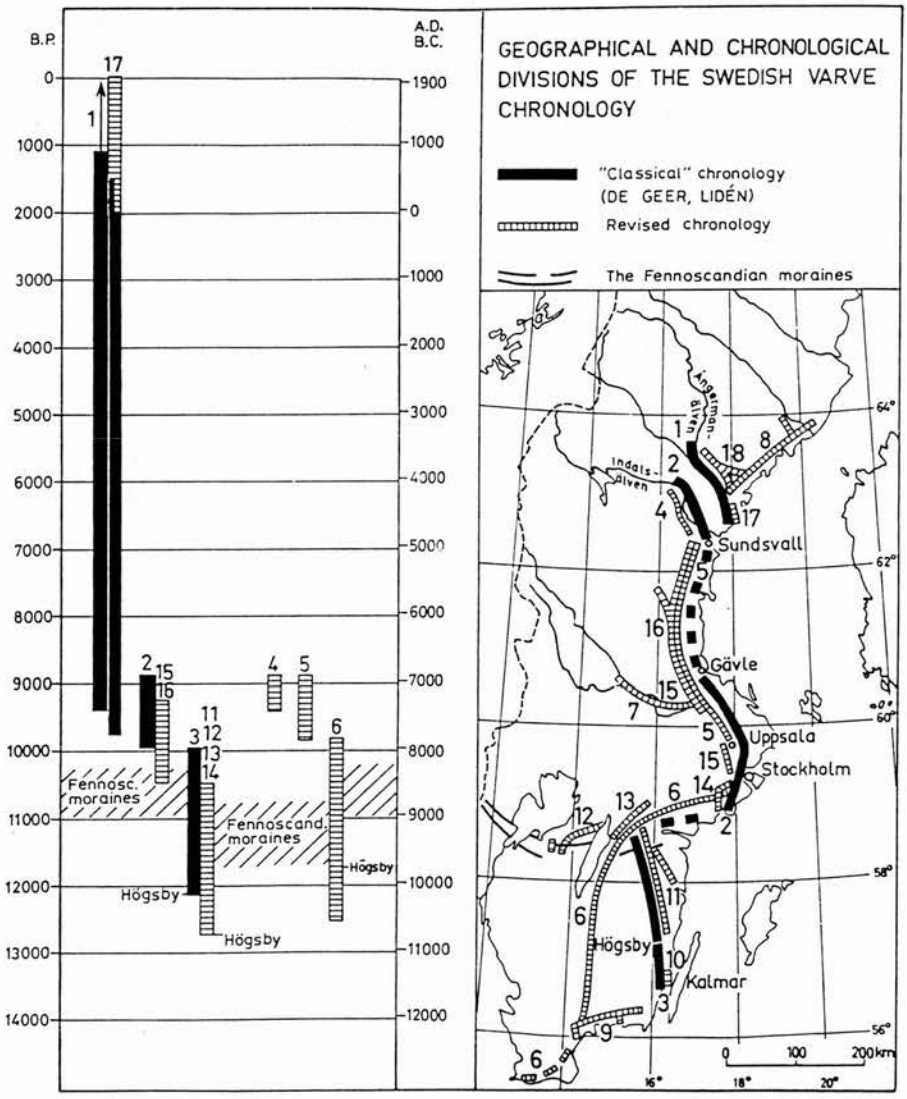

Figure 2.7 The Swedish Timescale. **1** - Lidén, 1913; **2** - De Geer, 1940; **3** - De Geer, unpublished; **4** - Borell and Offerberg, 1955; **5** - Järnefors, 1963; **6** - Nilsson 1968; **7** - Fromm, 1964; **8** - Hörnsten 1964 and Bergström, 1968; **9** - Ringberg, 1979, and Ringberg and Rudmark, 1985; **10** - Rudmark, 1975; **11** - Kristiansson, 1986; **12** -

Caldenius, 1944; **13** - Perhans, unpublished; **14** - Brunnberg, unpublished; **15** - Strömberg, 1989; **16** - Forssmark, unpublished; **17** - Cato, 1987; **18** - Fözö, 1980. (*source*: Strömberg, 1985, modified from Fromm, 1970).

The deposition of post-glacial varves which depend upon precipitation rather than insolation creates another problem. Secondary autumn flows associated with floods sometimes occur and create two varves, whilst low flows suppress varves. Lidén's work (1913) along the Ångermanälven consistently neglected years with low flows and, with suppression of varves rather than duplication being the norm, Fromm (1970) estimates a possible error of +1% of Lidén's postglacial timescale (i.e. +75 years).

The annual nature of the varves needs to be ascertained as some laminations may be longer than one year (Simola and Tolonen, 1981; Saarnisto, 1986; Lemmen *et al.*, 1988). Other rhythms may also be apparent within thick proximal varves, such as diurnal laminations (Ringberg, 1984). Cato (1985, 1987) was able to determine the annual nature of the recent varves in the Ångermanälven by using sediment traps and correlating maximum daily mean discharge during spring floods and the corresponding varve thickness. However, it is more difficult to establish such a relationship for the late-glacial varves.

2.7.4 The Present Chronology

The corrections made by the IGCP 253 revisions have minimised the number of errors of the type above. Estimates of the limits of accuracy by each researcher (Table 2.2) add up to an overall error margin of $^{+85}/_{-260}$. It is important to note that, even with these clear sources of error, the record has an accuracy matched only by tree rings.

	Section of the chronology	Error
Cato (1987)	Ångermanälven valley	$^{+10}/_{-180}$
Strömberg (1989)	Stockholm-Sundsvall	$^{+25}/_{-25}$
Kristiansson (1986)	Högsby-Norrköping	$^{+10}/_{-10}$
Ringberg and Rudmark (1985)	Karlskrona-Kalmar	$^{+40}/_{-45}$

Table 2.2 Estimates of the margin of error in the Swedish Timescale

A new exciting way of refining the record still further may be the use of Icelandic volcanic ash (tephra) which provides isochronous horizons across all depositional environments. The instantaneous deposition of ash means a tightly constrained date for the sediment and facilitates correlation from site to site. The correct identification of tephra of a known historical age may make the varve chronology more reliable since it provides a check for the annual nature of the sediments. The presence of a known tephra within different varve sequences would provide proof of both age and correct correlation. The prospect of long distance correlation of varve series provides an opportunity for including varve chronologies from areas of Sweden previously regarded as floating. Furthermore, the correlation with different depositional environments such as the peat bogs investigated by Persson (1971) could provide new insights into environmental changes since the last glaciation.

The role of tephra as a tracer throughout the sedimentary record could be developed to study the processes of varve formation. The nature and pattern of ash preservation within a varve indicate the effects of many sedimentological processes such as catchment erosion, bioturbation, and seasonal variations in sediment (Thompson *et al.*, 1986). Information provided by these types of studies used in conjunction with theoretical models such as Sturm's structure model (1979) could improve our understanding of the depositional environment of the Swedish varves.

2.8 Conclusion

The Swedish varve chronology has an important role to play in the reconstruction of the Quaternary environmental record of Northern Europe. The annual layering of sediment allows a detailed history to be constructed, especially rates of ice recession. It is not only the measurement of time which is important, but also the clues to the palaeoenvironment.

The picture provided by a chronology must also be assessed in the light of the information available from presently forming laminated sediments. Applications of varve chronologies are wide-ranging. However, all research must take into account the uncertainties by checking and rechecking the inherent assumptions within the technique. The annual nature of the sediments is a crucial factor to check. The distribution of sediments within depositional basins is also extremely complicated, indicating that a full description of the whole sedimentological setting of each core must be undertaken in order to prevent confusing interpretations.

The errors indicated by Fromm (1970) may be impossible to correct for, but they have been minimised sufficiently for the Swedish Timescale to be reasonably accurate. The greatest advance has been in the linking of the chronology to the present (Cato 1985, 1987). There is now a detailed history of ice retreat and climatic change going back 12,500 years. The major changes in climate associated with the Younger Dryas for example are reflected in the indistinct varved sediments deposited in brackish water. Correlation during this period with more accurate and established records such as the polar ice cores and tree ring chronologies is now possible.

3.1 Introduction

The aim of this chapter is to detail the attempts to find Icelandic tephra in the Swedish varves. More specifically the investigation attempts to test the accuracy of the link of the varve chronology to the present with its inherent assumption that the varves are annual.

This chapter concentrates on the laboratory investigations undertaken to establish a link between Iceland and Sweden. The approach to the research can be summarised as a problem-solving procedure whereby results from each step lead to the next. Five historical Icelandic tephras are known to have fallen over Scandinavia and may have been deposited in the varve chronology from northern Sweden. The aim was to try and find these tephras in the appropriate varve sequences. A specific objective was to test the hypothesis that a tephra fall in lake deposits can be identified as a clear layer with a tail of decreasing concentration in younger sediments, or whether the tephra is washed in over subsequent years.

Attempts to locate the correct varve series and identify the glass shards included the use of heavy liquid separation techniques. Such techniques have been used routinely elsewhere in sedimentology, petrology and palaeoecology but their use in fine tephra studies produced new challenges. Problems arose because the fine particles of tephra and the viscous nature of the heavy liquid meant that retrieval of samples and effective cleaning was difficult. Modifications to the standard procedure for extraction were developed and used on all samples. The sections below discuss many of the aspects of these changes. The difficulty of finding tephra of a size and quantity to analyse and identify prompted further investigations into the properties of tephra and the processes of deposition.

3.2 Ashfalls in Sweden

Following the pioneering work of Þórarinsson (1944) in constructing a tephrochronology for Iceland, several workers have attempted correlations with the Icelandic record or constructed regional chronologies. Most of this research concentrated on visible tephra layers in soils and lake cores, while Persson (1967a, 1967b, 1971) extended the technique to include microscopic layers of glass in Scandinavian peat bogs. A preliminary Swedish tephrochronology was constructed from several lines of evidence. It is known that tephra from Iceland reached Sweden, Norway and Finland in historical times. Indeed the first tephra fallout to be mapped (Figure 3.1) made clear the importance of the prevailing winds in depositing tephra over Scandinavia.

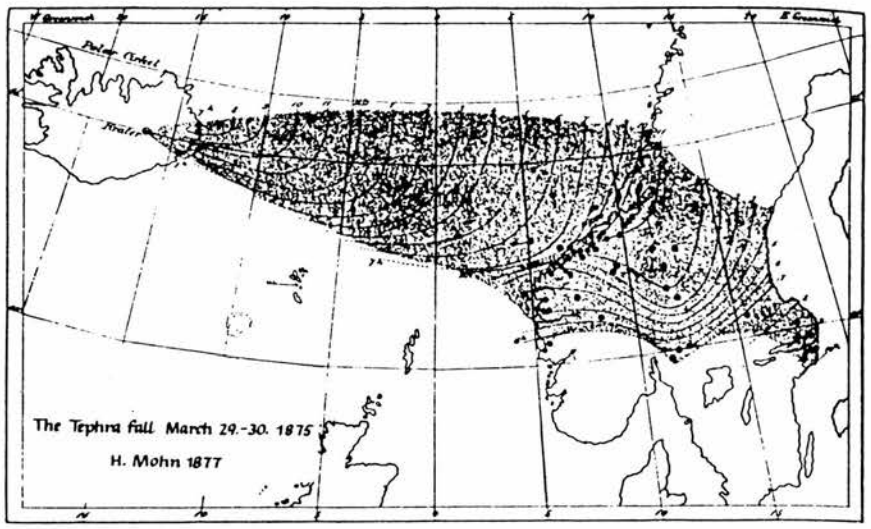

Figure 3.1 The tephra sector of the Askja eruption in AD 1875. The broken lines are isochrones (GMT) for the beginning of the tephra fall (*source:* Mohn, 1877).

The ashfall from the eruption of Hekla in 1947 was also measured. Previous historical eruptions such as from Hekla in AD 1845 and AD 1510 have also been mentioned in records from the Faroes and Norway, although there were no equivalent reports from Sweden and Finland (Þórarinsson, 1944). Another method for predicting possible tephra layers comes from extending the mapped isopach range of known eruptions in Iceland. In this way Þórarinsson's (1958) work on the eruption of

Öraefajökull in 1362 indicating an east-south-east fallout direction was used by Persson to identify glass shards from that eruption in the peatlands of Sweden, Norway and the Faroes (Persson, 1971).

From Persson's work, the following tephras were identified by refractive indices, morphology, grain size of the glass particles and radiocarbon dating of the peat sediments: Askja 1875, Öraefajökull 1362, Hekla 1104 and 1947, Vatnaöldur AD~900, and the important mid-Holocene Hekla tephras H3 and H4. No analysis of the geochemistry of the glass shards was undertaken despite the problems apparent when relying on refractive indices for identification, such as the state of hydration of the glass shards (v.d.Bogaard and Schmincke, 1985). In addition, there is greater variation in silica content within one tephra layer than between different tephras. Several correlations between peat bogs were made by comparing grain sizes from site to site. For example, approximately 70% of glass shards from Öraefajökull AD 1362 are under 30μm. The tephra layers were dated by radiocarbon using samples obtained from layers of peat immediately below the layer with the highest concentration of ash particles. The research presented here attempts to find in the varve record from northern Sweden all the historical tephras listed above. This section of the Swedish Timescale however does not extend back to the mid-Holocene and so it was not possible to look for ash from Hekla 3 and Hekla 4.

3.3 Geochemical analysis of tephra deposits

3.3.1 The electron probe microanalysis (EPMA) technique

The most common and effective analytical tool to determine the geochemical composition of volcanic glass is the electron microprobe (Westgate and Gorton, 1981; Larsen, 1981). This technique has major advantages over bulk analysis methods such as X-ray fluorescence (XRF) since it can be used where there is limited material available. Electron probe microanalysis is grain-discrete and therefore it is possible to target parts of a glass shard which have not undergone alteration or contain vesicles or microphenocrysts (Dugmore, 1989; Hunt and Hill; 1993). The

ability to choose fresh faces reduces the factors which yield poor analysis totals and means that EPMA can produce precise and accurate geochemical data.

The use of EPMA in petrology is widespread but its use in tephrochronology is relatively recent. An electron microprobe operates by detecting X-rays produced when a sample is bombarded by an electron beam. The composition of the sample, automatically calculated as X-ray energy, is unique to each element, and X-ray intensity is proportional to the amount of that element (Hunt and Hill, 1993). The fact that tephra requires more sensitive operating conditions than stable minerals and crystals means that each operator has to determine the optimum conditions to achieve precision and accuracy. This has led to a lively debate on how to standardise operating procedures so that results from different groups are comparable (Froggatt, 1992; Hunt and Hill, 1993).

The controversy centres mainly around two related areas; data normalisation and presentation, and the inclusion of sodium in the published results. Firstly, due to the presence of water and highly mobile elements in volcanic glass, it is often difficult to achieve totals of 100%. For this reason some workers publish results with low totals of ~90% (Kvamme *et al.*, 1989), others set the level of acceptance higher at >95% (Dugmore *et al.*, 1992), whilst others automatically normalise to 100% (Bennett *et al.*, 1992). Hunt and Hill (1993) argue against INQUA recommendations for accepting totals around 90% (Froggatt, 1992) since this high a water content is probably linked to glass alteration and poor point selection. They define a minimum cut off boundary of 95%. They also recommend the publication of data tables to allow other workers to apply their own statistical and correlative techniques to the data. Normalisation of published data to 100% effectively prevents any comparison by outside workers, hides low totals and extends geochemical fields. In this thesis analyses below 95% total have been discarded and the data presented have not been normalised. Ninety-five percent is considered acceptable because trace elements and minor constituents such as phosphorous are not measured and a hydrated glass may

contain ~3% water without a physical disintegration of the polymer. Comparison of results is achieved graphically using binary and tertiary plots.

The second area of debate centres around the mobility of sodium and potassium during analysis. Sodium is a difficult element to analyse but is often diagnostic especially for rhyolitic tephra. It is therefore not practical to omit sodium totals from analyses. Problems during analysis lie in the relationship between sodium loss and the intensity and duration of the electron beam. In other words, the longer a sample is exposed to a strong electron beam, the greater will be the sodium mobilisation during analysis. (Dugmore *et al.*, 1992; Hunt and Hill 1993).

Although the abundance of sodium may be accurately estimated by measurement early in the analysis, loss of Na during the remaining time will artificially elevate the apparent concentration of elements measured later, in particular silica. The simplest way to achieve accuracy is to use a low current beam and monitor the mobility of each element during analysis. A low beam current however affects the precision and therefore a balance has to be struck between high precision (high counts per element) and accuracy (minimum sodium mobility). All the geochemistry presented in this thesis was determined on an electron microprobe at Edinburgh University (Cambridge Instruments Microscan V) which effectively preserves precision and accuracy by using a current of 15 nA, a 10 second counting time, 20 kV accelerating voltage and Wavelength Dispersive Spectrometry (WDS). Wavelength dispersive systems operate by measuring elements sequentially and therefore allow monitoring of each element through time. The beam diameter was about 8μm.

The Microscan V has two spectrometers measuring two elements at a time beginning with sodium and potassium. Sodium is measured again during the next ten second count so it is possible to see how much has been lost due to mobilisation. The remaining major elements in order of analysis are Magnesium, Manganese, Titanium, Iron, Calcium, Aluminium, and Silica. To reduce sodium migration and destruction

of the glass shards by the electron beam, the beam was blanked whilst the two spectrometers moved to the next paired peak position.

3.3.2 Reproducibility of geochemical results

The operating parameters used in this study follow the guidelines outlined by Dugmore (1989), Dugmore *et al.,* (1992) and Hunt and Hill (1993). The optimum machine settings are determined at the start of each day's analysis by running standards of known composition (pure elements, oxides and silica compounds). The stability of the electron beam is then determined by analysing another standard of known composition (an andradite) immediately after analysing the standards and every half hour interval thereafter. Totals for the andradite reading of 97%±0.5% throughout the day indicate beam stability and therefore reproducibility of the results.

3.4 Annual varves in the Ångermanälven River valley

The section of the Swedish Timescale corresponding with historical times is found in the estuary of the Ångermanälven River (Cato, 1985, 1987 see Figure 2.7). The annual nature of the varves was tested before coring took place as part of an International Geological Correlation Programme (number 24). This was achieved by taking X-radiographs of two cores drilled at a four year interval. The X-rays revealed four new couplets in the younger core confirming that varves are currently being formed in the estuary. To test whether this had been the case for a longer period of time, varve thicknesses were correlated with records of the maximum daily mean discharge during spring floods, and with the annual sediment transport for the period 1909-1978. A high correlation coefficient (0.8) for several cores indicates the annual nature of the varves and the close relationship of discharge to varve thickness. The major aim of the programme was to link the new subaquatic cores with the supra-aquatic record constructed by Lidén (1913). This was achieved by matching overlapping cores along the estuary and shorelines (Figure 3.2) by means of varve thickness. The characteristics of the couplets were also examined to aid correlation, such as the variations in the grain size of the fine-grained and coarse-grained layers of the couplet. Each varve from the estuary consists of a fine silt-clayey upper

section deposited in calm summer-winter conditions, and a lower section of coarse silt-fine sand deposited during high water periods in the spring. The Swedish Timescale is now apparently securely anchored to the present, and each numbered varve corresponds to an actual calendar year.

3.5 Experimental procedure

3.5.1 Sampling

The Ångermanälven varve series is the only section of the Swedish Timescale which could incorporate Icelandic tephras. Therefore the original varved cores from the Ångermanälven site were sampled at the Swedish Geological Survey (S.G.U.) in Uppsala with the kind permission of Dr Ingemar Cato. Each core spanning the time of the five historic eruptions mentioned by Persson (1971) was first identified and then the individual varve from the eruption year was sampled. Table 3.1 lists all the eruptions, varve dates and codes, and the sampling interval for each tephra. For example four cores from the Ångermanälven non-tidal estuary span the time of the eruption of Hekla in 1947, namely gravity cores 2, 3, and 8 (see Figure 3.2). The varves are relatively thick and so single annual samples could be taken. The equivalent varve date for AD 1947 is 8915 and the range of varves sampled is 5 (varves 8917-8913). This recent part of the section can be assumed to be accurate and so fewer samples were needed. Confirmation of this accuracy was the fact that a paper mill along the river in 1945 gave the sediment from this section a unique smell

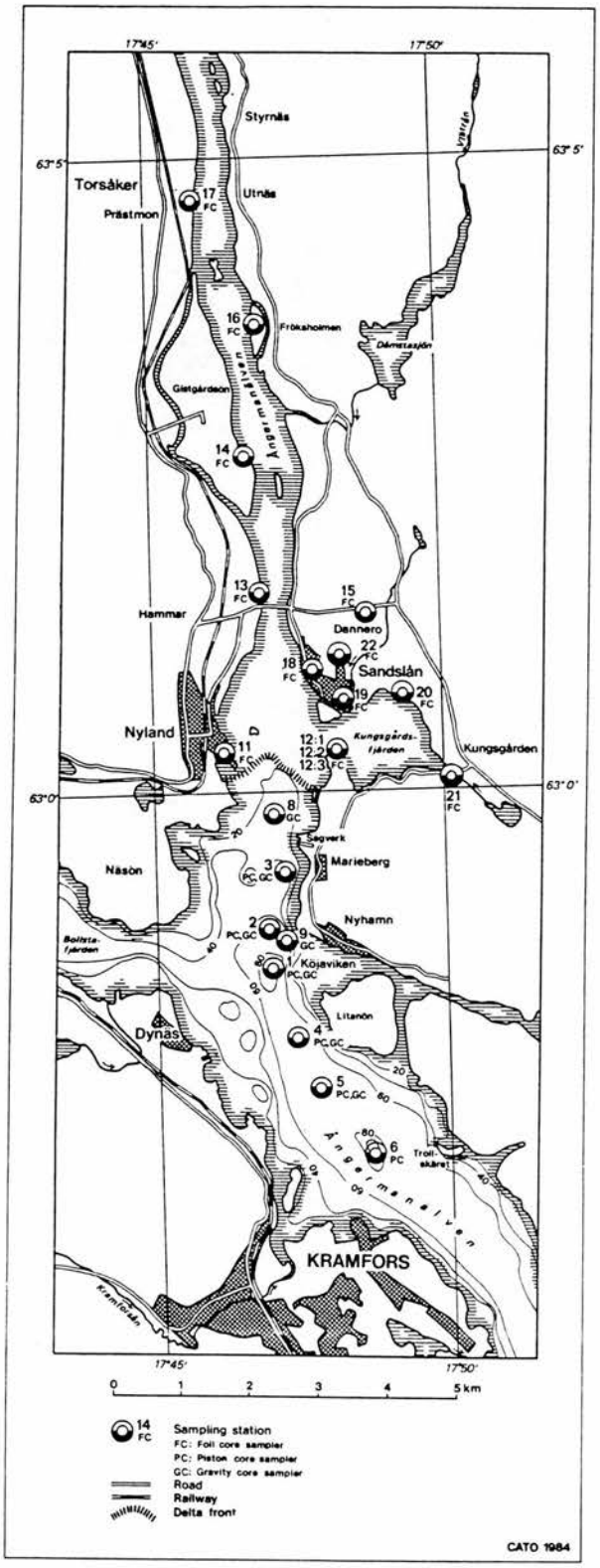

Figure 3.2 Map showing the locations of the sub-aquatic and the supra-aquatic coring sites along the Ångermanälven. (*source:* Cato, 1987, S.G.U. Series Ca 68).

when opened in the lab! For the older tephra deposits, five individual varves (i.e. five years) either side were also sampled for analysis. This was to ensure the correct year/varve was included in the analysis and therefore account for any errors in the varve counting.

Where the varves were thin and difficult to sample individually (i.e. the older sections), multiple groups of 3-5 varves were taken. For example Table 3.1 shows that three cores spanned the time of the eruption of Vatnaöldur around AD 900. The varves from coring sites at Kungsgårdsfjärden and Dannero (foil cores 12:3 and 15) were thin and multiple samples were taken over a wide range (39-45) years. The third core, from the site at Gistgårdsön, contained thick varves which could be sampled individually making it possible to determine an exact varve date for any tephra found in the sediment. The varves were sampled with a small spatula and carefully placed in clearly labelled individual containers. Further analysis was undertaken at Edinburgh.

Due to the amount of material, the samples had to be treated before searching for tephra. The usual methods of extracting tephra from its matrix are digestion techniques (sulphuric acid or hydrogen peroxide - see Persson, 1971; Dugmore, 1989). However the varves of the Ångermanälven river valley are clastic i.e. they contain little or no organic material, and so density separation was carried out on the samples to extract any volcanic glass shards present.

Eruption	varve no.	sample range	multiple/single sample	core code	Site name	lat/long
Hekla 1947	8915	8917-8913 (5)	single	GC2	Ångermanälven non-tidal estuary	62°58'55"/17°47'00"
				GC3	"	62°59'21"/17°47'17"
				GC8	"	62°59'50"/17°47'06"
				GC9	"	62°58'08"/17°47'18"
Askja 1875	8842	8847-8837 (11)	single	PC2a	"	62°58'55"/17°47'00"
				PC3Bf	"	62°59'21"/17°47'17
				PC6upp	"	62°57'07"/17°48'17"
Öraefajökull 1362	8329	8336-8322 (15)	multiple (5)	PC2Bb	"	62°58'55"/17°47'00"
				PC6Bc	"	62°57'07"/17°48'17"
		8334-8324 (11)	single	FC12:3G	Kungsgårdsfjärden	63°00'20"/17°48'11"
				FC22B	Pershem	63°01'05"/17°48'14"
Hekla 1104	8071	8093-8059 (35)	multiple (5)	PC2Bc	Ångermanälven non-tidal estuary	62°58'55"/17°47'00"
		8078-8064 (15)	multiple (5)	FC12:3J	Kungsgårdsfjärden	63°00'20"/17°48'11"
		8084-8066 (15)	multiple	FC15C	Dannero	63°01'22"/17°48'46"
		8076-8066 (11)	multiple	FC22G	Persham	63°01'05"/17°48'14"
Vatnaöldur ~900	7867	7889-7845 (45)	multiple (5)	FC12:3J	Kungsgårdsfjärden	63°00'20"/17°48'11"
		7883-7845 (39)	multiple	FC15E	Dannero	63°01'22"/17°48'46"
		7874-7861 (14)	single	FC14upp	Gistgårdsön	63°02'38"/17°46'56"

Notes

PC piston core
GC gravity core
FC foil core
22G, 12:3J core number and subsection
Multiple (5) multiple sample of 5 varves

Table 3.1 Table showing the sampled sections of the Swedish varve chronology and equivalent year of tephra fall.

3.5.2 Heavy liquid separation

The most commonly used heavy liquids for separating heavy and light mineral fractions are the halogenated hydrocarbons such as tetrabromoethane (TBE - acetylene tetrabromide $C_3H_2Br_4$ specific gravity 2.96 at 20°C) and bromoform (tribromomethane $CHBr_3$ specific gravity 2.89 at 20°C). Density adjustments are made with alcohol or acetone until the required specific gravity is reached (Gregory and Johnston, 1987). Although commonly used and relatively inexpensive, the heavy liquids and organic solvents are toxic and potentially carcinogenic. For this reason a non-toxic alternative was used for the varve research.

Sodium polytungstate ($3Na_2WO_4.9WO_3.H_2O$) has two major advantages as well as non-toxicity. It is reusable and has a wider range of working densities than the halogenated hydrocarbons (i.e. 1-3.1 g/cm³). Distilled water is all that is required to adjust densities and clean samples (Callaghan, 1987). Another important aspect is that it is not necessary to remove organic material from the sample before density separation. The only important aspect when using sodium polytungstate is that there must be no soluble compounds, especially calcium ions. If they are present then insoluble calcium tungstate ($CaWO_4$) is produced (Gregory and Johnston, 1987; Callaghan, 1987; Krukowski, 1988). These difficulties can be avoided by simply using distilled water for density control, frequent washing of samples and equipment, and by using plastic (polypropylene and polyethylene) containers for separation.

Figure 3.3 shows the laboratory equipment needed for heavy liquid separation. All the containers which come into contact with the sodium polytungstate are polypropylene to prevent dried salts becoming cemented to the surface. The sample is continually stirred by a plastic rod to break up any aggregates and to permit settling. The heavy liquid is made up to the required density by adding quantities of distilled water to the manufacturer's specification. A useful starting point is 84/16 salt/water ratio to produce a density of 2.65 g/cm³. Care must be taken to add the

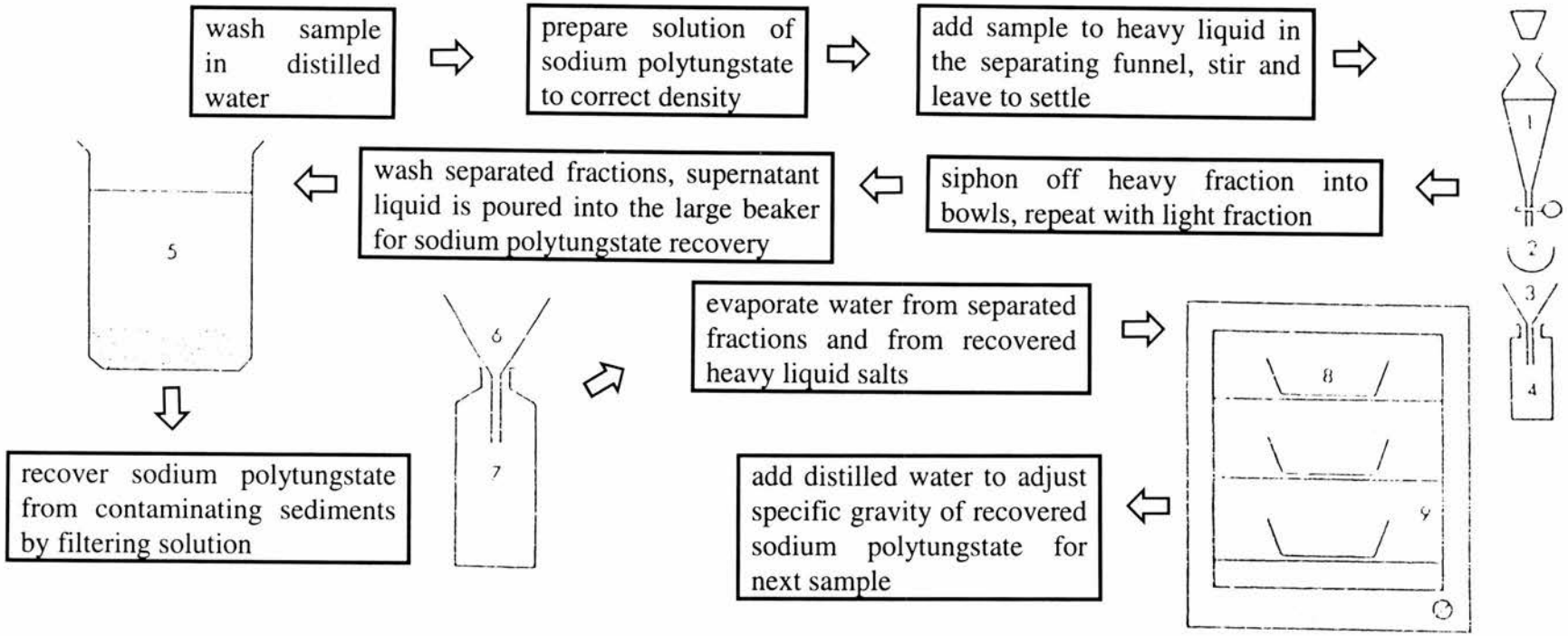

Figure 3.3 Laboratory equipment methods for heavy liquid separation of tephra from lake sediments using sodium polytungstate. Simple apparatus for separation are: 1) separation funnels with stoppers; 2) small dishes for collecting heavy fraction; 3) funnels and filter papers for recovering sodium polytungstate; 4) beaker for heavy liquid solution collection; 5) large beaker for washing equipment and discarded supernatant liquid for sodium polytungstate recovery; 6) funnel and filter paper for filtering washings; 7) beaker to collect filtered washings; 8) nalgene heat resistant dishes for evaporating washings and samples to dryness; 9) oven with exhaust fan.

heavy liquid salts *to* the water rather than vice versa, otherwise an unmixable cement is produced!

3.5.3 Preparation and initial tests

Initial tests were made to determine how efficiently tephra could be extracted and concentrated from varves using heavy liquid separation techniques. Five samples of glacial clay varves from Svalbard (supplied by Dr A Dugmore) were used as an experimental sample group rather than risk the loss of the Swedish varves. The Svalbard varves were spiked with a known quantity of tephra from Hekla 3 and placed in the heavy liquid solution. Tephra from H3 was chosen to highlight any future experimental contamination of the Swedish samples as the sodium polytungstate was subsequently used many times. Tephra from Hekla 3 (dated at 2800 yBP) would not be found naturally in the historical section of the Swedish Timescale and therefore the presence of H3 glass shards would indicate laboratory contamination.

Following the method outlined in Figure 3.3, the varves from Svalbard were cleaned thoroughly before being added to the heavy liquid solution. Previous research using sodium polytungstate indicates that simple washing with distilled water is sufficient to remove all soluble compounds, such as calcium ions, which may have adverse effects on the solution (Gregory and Johnston, 1987; Callaghan, 1987; Krukowski, 1988). It is also possible to wash the sample in ethylenediamine tetraacètic acid for added security against the production of insoluble calcium tungstate. The cleaned Svalbard varves were added to a solution with a density of 2.4 g/cm^3. This value was chosen for the experiment as most New Zealand and US tephrochronologists work at this density for tephra extraction (Carl Swishur pers comm.). Several problems with the technique as described in the literature came to light during the final runs. It was impractical simply to swill the sample and decant the supernatant, as the fines containing the tephra component had not settled sufficiently. Filtering the sample

after a period of standing in distilled water was eventually employed to overcome the problem of losing tephra. However, tephra was observed to stick within the fibres of the filter paper along with the very fine clays. Initially immersion in water and ultrasounding of the filters was attempted to extract the trapped material but this simply increased the amount of water which had to be removed later from the sample. Finally it was decided to ash the filter papers in a furnace at 375°C. This upper temperature was chosen so as to avoid melting and recrystallising glass shards and possibly affecting the chemistry by mobilising the volatiles. The ashed residue from the filter papers was added to the bulk of the cleaned varve sediment and placed in heavy liquid solution. The mixture was stirred vigorously and left to settle, after which both fractions were drawn off and cleaned thoroughly with distilled water.

The method proved successful and 90% of the spiked tephra was retrieved from the Svalbard varves. The method also revealed the steps in the process where the tephra was most likely to be lost.

3.5.4 Experiment I: density separation

The Swedish varves corresponding to the eruption of Askja in AD 1875 were the first samples to be analysed, since these recent sections of the varve chronology could be expected to be accurate and thus the probability of sampling the correct varve was high. As it was known that the size of glass shards reaching Sweden was about 30μm (Persson, 1971), a longer time was given for gravitational settling in the distilled water, and the supernatant was carefully filtered to ensure that no tephra particles were lost.

Eleven varves from piston core 2a (refer to Table 3.1 above) spanning the AD 1875 eruption (varve date 8842) were cleaned in distilled water. Material floated on the meniscus of the distilled water for a long period whilst rinsing. A sample of this material was pipetted onto a microscope slide and examined for tephra. Glass shards are relatively easy to identify under an optical microscope as they are isotropic in transmitted light. One small (4μm), platy glass shard was found in the varve sample

corresponding to AD 1875, which was kept separate from the rest of the sample and it was hoped that a greater number of larger more analysable shards could be found. The frothy, light material floating in the varves above and below varve 8842 was examined as well. A shard of similar size and shape was found in the varve of the following year (varve no. 8843).

The presence of glass shards in some of the samples from PC2a was encouraging. Therefore, after cleaning and preparation, the varves from this core section and from PC3Bf and PC6upp were added to heavy liquid of density 2.4 g/cm^3. The 33 samples were left to separate into light and heavy fractions. After rinsing, examination revealed no tephra in the main body of any of the varves.

An unsuccessful attempt was made to identify the glass shards found in PC2a during the cleaning stage of the experiment. However, this procedure depends on successfully extracting a glass shard from the optical microscope slide and creating a thin-section for electron probe microanalysis. This technique is difficult and the probability of producing a clean surface for analysis on one grain is very low. Moreover, the geochemical data for a single glass shard is not sufficient to allow identification of the eruption producing the tephra. It is necessary to have a greater abundance of material to characterise the tephra, especially if several phases of the eruption are present in the deposit.

The results from this initial attempt to extract tephra from Swedish varves can be summarised; firstly, two grains were found floating but nothing was found in the main body of the sample, and secondly the tephra present has a very low density. The low density of the retrieved glass shards indicates that using a cut-off point of density 2.4g/cm^3 during separation merely includes more varve material rather than separates out the tephra fraction. It was decided to try and refine the method of tephra extraction. The following section details an experiment to find the range of density of glass shards for an efficient method of searching varves.

3.5.5 Experiment II: range of density

The heavy liquid solution was made up to a density of 2.65 g/cm^3 as outlined above. This value was chosen as a starting solution since it is unlikely that any glass shard would have as great a density as pure quartz. Therefore at the start of the experiment all the glass would float at the top of the separating funnel.

Crushed pumice from the Öraefajökull eruption in 1362 was used to determine the density range of glass shards. Pumice has the advantage over samples of tephra in that it is mainly vitric in composition containing very small amounts of lithics and crystals. This is important as it is the vitric component of volcanic eruptions which carry as far as Sweden (Persson, 1971) and therefore the experimental results would not be biased by the inclusion of heavier fractions from the tephra sample.

The crushed pumice was placed in the separating funnel with the heavy liquid solution and stirred vigorously to break up any aggregates. The mixture was allowed to settle to ensure that all glass shards did indeed float at the top. Distilled water was added slowly by pipette until some of the tephra was seen to fall through the column of liquid. This mixture was again stirred and left to settle for 24 hours to allow the more dense tephra to sink. The tephra which had fallen to the bottom of the separating funnel was drawn off and the density of the liquid was found using a small 1cm^3 density bottle.

Distilled water was again added until more tephra began to sink. The procedure was repeated until the density of the remaining tephra was greater than the density of the liquid so all the sample was retrieved from the solution. This method produced four separate density intervals. A more finely tuned method of adding distilled water to vary the density would have produced more classes. The samples from each stage were washed thoroughly with distilled water to retrieve the sodium polytungstate salts, and bottled for future work.

Table 3.2 reveals interesting results for the exploratory test. Unlike the narrow range of densities for mineral suites (for example, wollastonite $CaSiO_3$ 2.8-3.1 g/cm³), the density of glass shards ranged from 2.45 to 1.18 g/cm³. Therefore the density of the solution at which tephra first began to settle was 2.45 g/cm³ and all of the glass settled only when the density was as low as 1.18 g/cm³.

Mineral	**Specific gravity (g/cm³)**
Olivine $(Mg, Fe)_2SiO_3$	3.3-3.4
Wollastonite $(CaSiO_3$	2.8-3.1
Muscavite $(KAl_2(AlSi_3O_{10})(OH,F)$	2.8-2.9
Plagioclase $(NaALSi_3O_8$-$CaAl_2Si_2O_8)$	2.6-2.8
Quartz (SiO_2)	2.65
Orthoclase $(KAlSi_3O_8)$	2.5-2.6
Volcanic glass (Ö1362)	2.43-1.18 (splits at 2.25 and 1.63)

Table 3.2 Specific gravity ranges for selected minerals and volcanic glass from the eruption of Öraefajökull in AD 1362.

The unexpected results necessitate a further discussion of factors involved in the density variations and settling velocities of glass shards and the assumptions used when searching for distal deposits. There are three factors thought to control the densities at which tephra falls out of an ash cloud: Size, morphology, and chemistry of the vitric, lithic and crystal components. There is a relationship between size of glass shard and distance from source, with the grain size of tephra decreasing systematically with increasing distance from the volcano (Þórarinsson, 1967; Walker *et al.*, 1971; Einarsson, 1986). This observation has been used in relating unknown distal deposits to a proposed source, and in simulating eruptions (Sigurdsson and Carey, 1989). However, computer modelling studies related to the Campanian tephra in the Mediterranean and the recent Mount St Helens tephra indicate that large shards are found beyond their predicted range and very small shards are found near the vent (Cornell *et al.*, 1983). It has been proposed that particle aggregation explains the polymodal grain size distributions found in these tephras, and field evidence in the form of delicate ash clusters supports this view (Sorem, 1982; Carey and Sigurdsson, 1982). The actual mechanism of aggregation is unknown, and functions of moisture, electrostatic attraction or mechanical interlocking have been proposed to explain the fallout pattern in grain size. Therefore if grain size is the controlling factor on

density of the Icelandic tephra then the relationship may be a complicated one with shards of all sizes being found at a distant site like Sweden.

The second factor thought to affect density is the shape of the grain. It has been shown that morphology significantly affects the terminal settling velocity of a particle (Walker *et al.*, 1971; Wilson and Huang, 1979). Vesicle-rich shards will be of a lighter density than more massive shards due to greater interstitial void space. Indeed this characteristic has been used by Carey and Sigurdsson (1982) to argue for a lower bulk density of ash aggregates and therefore explain anomalous fallout patterns in the 1980 Mount St Helens tephra. The morphology of Icelandic tephra has not been examined in distal deposits.

Thirdly the geochemistry of glass shards is thought not to differ with distance from source, but the overall geochemical fingerprinting of the bulk tephra deposit does change due to winnowing and differential settling of lithics and crystals (Randle *et al.*, 1971; Juvigne and Porter, 1985). It is important, therefore, to test whether the assumption that the vitric component remains chemically distinct is true or whether physical characteristics such as size and shape have a more important influence on density. If differences in the geochemistry of glass affect density, then there are implications for long distance correlations of tephra deposits.

A number of experiments were carried out to narrow down which factor (size, shape or chemistry), or combination of factors, has the greatest control over the density of glass shards. This is important for several reasons. Firstly, knowing the average density of glass which reached Scandinavia from Iceland would speed up the extraction process. Secondly, if size or shape is the limiting factor then some knowledge of the appearance of the vitric component will aid identification. For instance, if the least dense component consists of angular non-vesicular shards of the same grain size, then searching the sample is made more efficient. Thirdly, despite some of the assumptions about density built into many eruption fall out models, no experiments on factors controlling density have been carried out.

3.5.6 Experiment III: factors affecting density

The following experiments used the four density-separated samples of Öraefajökull pumice. The geochemistry, size distribution and morphology of each density class were examined with the methods and results outlined below.

3.5.6.1 Geochemical analysis

The geochemistry of samples from each of the four density classes was determined using the electron probe microanalysis (EPMA) technique as outlined in section 3.3.1. Following the procedure outlined in Dugmore *et al.* (1992) and Hunt and Hill (1993), thin grain mounts on slides were produced firstly by frosting the slide surface using grade 600 grit, and then pipetting the sample onto the slide. Roughening the surface of microprobe slides is essential to prevent the sample being lifted from the slide during the grinding process. The tephra was impregnated with epoxy resin (in this case, araldite), mixed thoroughly and allowed to dry. As it is necessary to have flat polished surfaces to prevent absorption of X-rays by scratches in the surface of samples, the slides were carefully ground to a thickness of 75μm and then polished down to successively with 6μm and 1μm diamond pastes. A thin coating of carbon provided the necessary conductivity. The electron probe microanalyser used was a Cambridge Instruments Microscan V a standard wavelength dispersive analytical technique was employed with a voltage of 20 kV and beam current of 15 nA and beam diameter of 5μm.

Corrections were made for counter dead time, atomic number effects, fluorescence and absorptions using a ZAF correction programme based on Sweatman and Long (1969). Machine stability was assessed by reading a standard (in this case andradite) subsequent to the calibration and periodically throughout the analyses of the tephra. Ten shards were selected from each density group and analysed for silica, titanium, aluminium, iron, magnesium, manganese, calcium, sodium, and potassium. The count time was 10 seconds per pair of elements. Any totals under 95% were omitted.

	2.45 g/cm^3	2.25 g/cm^3	1.63 g/cm^3	1.18 g/cm^3
Element	%Oxide (range)	%Oxide (range)	%Oxide (range)	%Oxide (range)
SiO_2	73.67-69.37	73.28-71.30	73.24-70.25	72.29-70.46
TiO_2	0.31-0.23	0.32-0.23	0.34-0.22	0.33-0.23
Al_2O_3	13.16-12.64	13.39-12.55	14.32-12.86	13.38-12.78
FeO	3.28-3.06	3.38-3.04	3.30-2.43	3.21-3.02
MnO	0.14-0.05	0.15-0.07	0.15-0.07	0.13-0.06
MgO	0.04-0.01	0.06-0.01	0.03-0.01	0.03-0.01
CaO	1.08-0.78	1.13-0.90	1.06-0.85	1.06-0.91
NaO_2	5.83-4.89	5.70-5.21	6.69-5.26	5.97-5.34
K_2O	3.52-2.93	3.68-3.24	3.61-2.86	3.52-3.25

Table 3.3 Geochemistry of the four density splits of the Öraefajökull 1362 pumice sample.

The results from the electron probe microanalysis indicate that there is no difference in geochemistry between the four density groups (see Appendix 1 for analysis totals). Table 3.3 highlights the composition of each sample, showing the ranges of the abundances of all the elements analysed. As can be seen from the table the glass has high silica, aluminium and sodium content and low calcium content. A graphic approach is more revealing, therefore, these data were transformed into triangular graphs. Titanium, calcium and iron are good discriminators of Icelandic volcanic systems (Dugmore *et al*, 1992) and therefore all three were standardised to 100% using the formula

$$a = \frac{a}{a+b+c} \times 100$$

where a, b, and c are the percentage abundances of three elements. Figure 3.4 shows the triangular graphs for the elements Fe, Ti and Ca indicating no difference in geochemistry between the four density splits. The conclusion is that geochemistry is not the controlling factor affecting the density of glass shards.

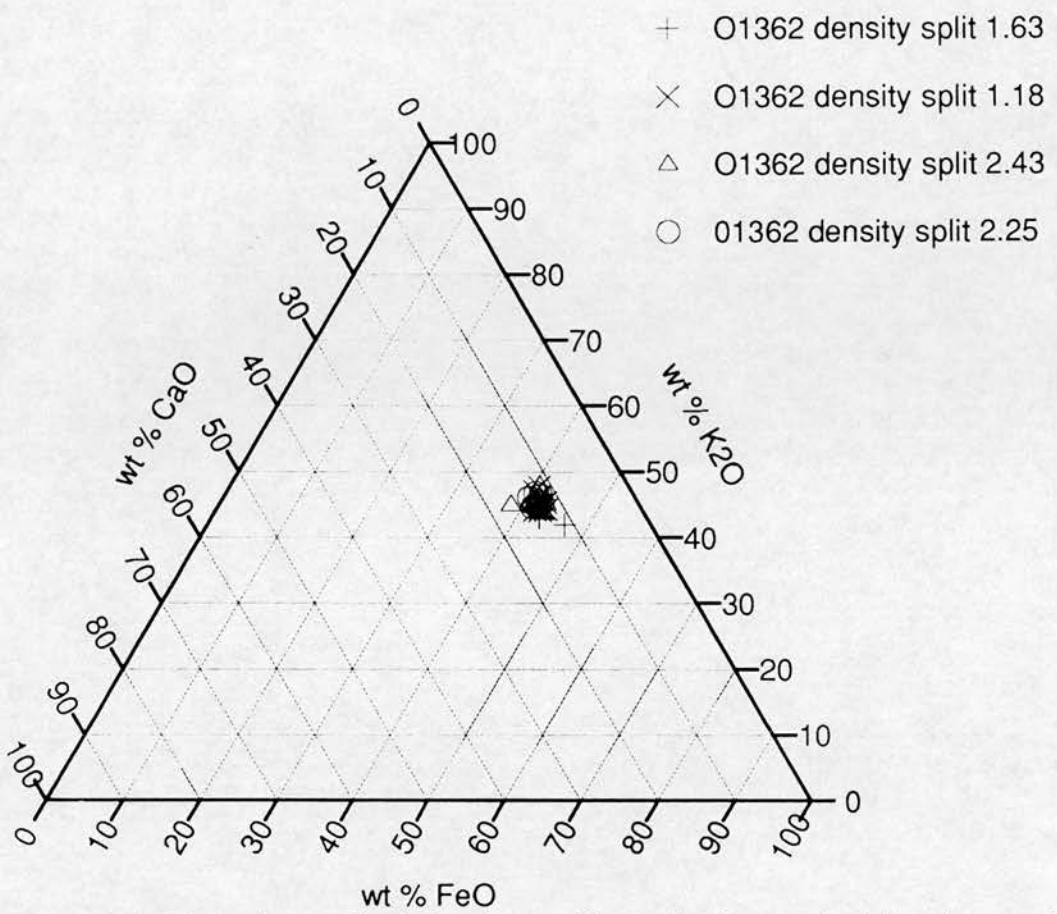

Figure 3.4 Triangular graph of abundance of iron, titanium and calcium in samples from Öraefajökull 1362 pumice.

3.5.6.2 Size

The microprobe slides used for geochemical analysis were cleaned of the coating of carbon and placed on an optical microscope. Photographs of each of the four density classes were taken to determine size and shape characteristics. The size of the shards were measured using the optics grid on the microscope which indicated the great range in shard size within the density groups. For example, large shards of 300μm (long axis) and small shards of ~30μm were found in all four classes. The microphotographs in Figure 3.5 show the size range between all density classes indicating that size is not a factor controlling settling velocity of glass in separation experiments.

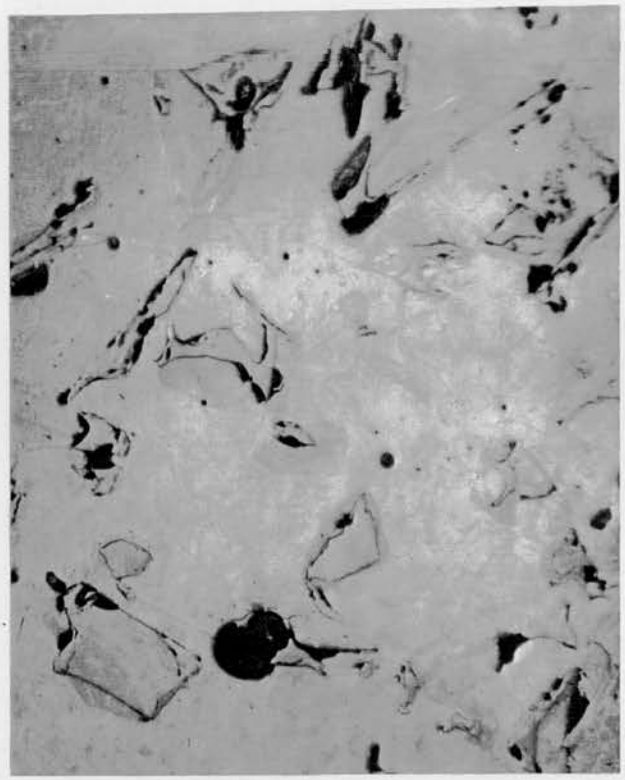

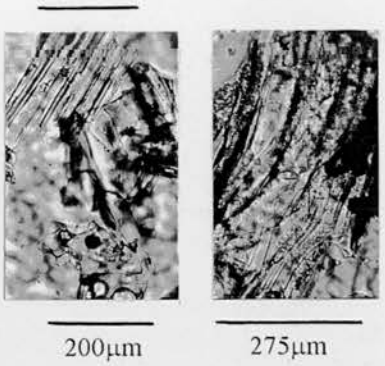

200μm 275μm

2.43 g/cm^3

The photographs show vesicle-poor, massive, and angular shards. The vesicles are both spherical and elongate.

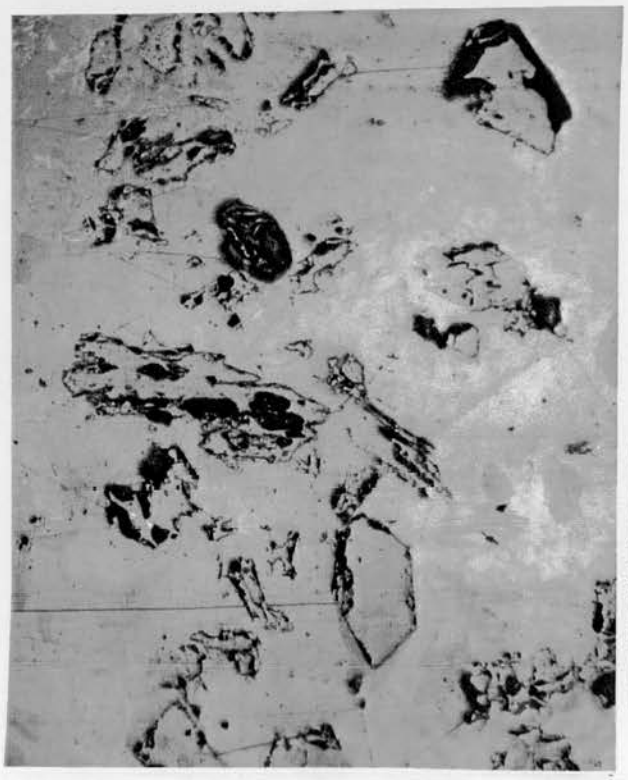

2.25 g/cm^3

The photographs show sub-angular shards with large spherical vesicles.

235μm 200μm

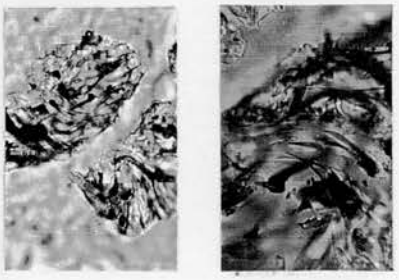

Figure 3.5 Photographs of the four density classes of the Öraefajökull 1362 sample showing size and morphological characteristics. The low magnification photographs (x20) show the microprobe slide surface. The inset pictures are at a higher magnification (x40) to show shard structure more clearly.

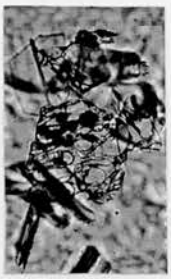

125μm

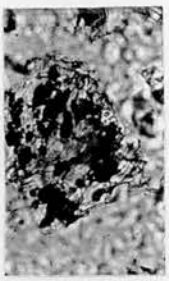

205μm

1.63 g/cm^3

The photographs show a mixture of elongate and sub-angular, platy shards with large vesicles.

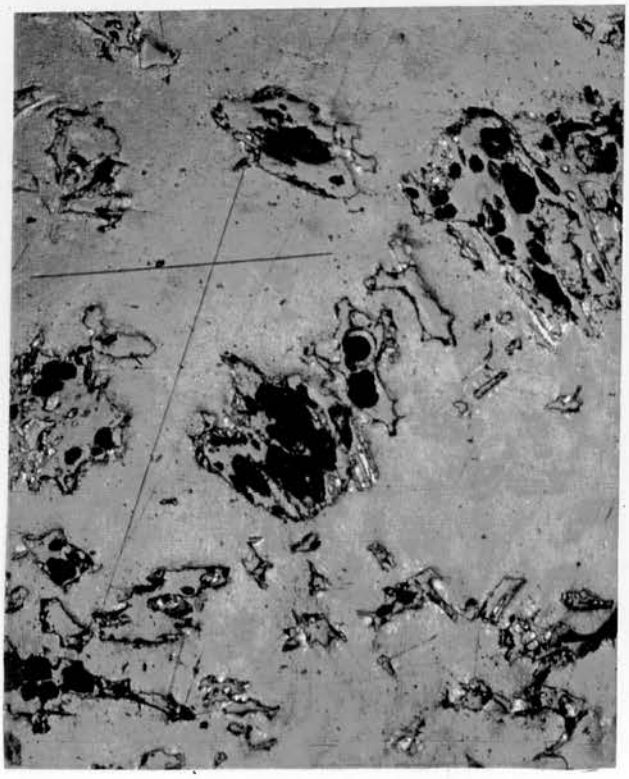

1.18 g/cm^3

Photograph showing sub-rounded, frothy shards with large, spherical vesicles

287μm

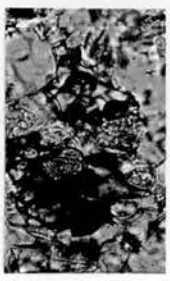

300μm

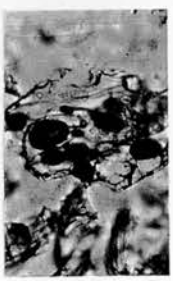

3.5.6.3 Morphology

Figure 3.5 reveals however that morphology is quite different in the high and low density groups. It is difficult and time-consuming to measure morphology unless computerised two-dimensional analysis is employed (Eiríksson and Wigum, 1989). Form parameters used in pebble analysis such as sphericity, elongation and OP (oblate-prolate) index require measurement of the long, intermediate and short axes of samples and provide a quantitative approach to classification. The standard geological classification methods and diagrams for particle shapes (Zingg, 1935; Sneed and Folk, 1958) do not, however, reflect the important variation in tephra grain shape caused by vesicle shape and fluidal structure. For this reason, glass shard form is simply described as vesicle rich or poor, angular or rounded.

There appear to be two types of glass shards in all four samples: vesicle-poor, angular shards; and vesicle-rich, irregular shaped shards. The most dense (2.43 g/cm^3) are particularly massive shards, whilst the lightest group (1.18 g/cm^3) contains mainly frothy glass.

From the above results, density is likely to be dependent on the shape of the glass shards which affects the settling velocity. There are several wider implications:

1) Glass shards have a wide range of densities compared with crystals and lithics. Previous studies using heavy liquids to separate out the glass fraction may have missed or lost a large amount of analysable tephra from the sample. It is necessary therefore to find the range of densities encompassed by tephra in any samples. A simple split at an arbitrary value of 2.4 g/cm^3 may be inappropriate.

2) The homogeneity of the glass chemistry indicates examination of the vitric component of tephra is indeed the most accurate method of correlating distal samples with proximal deposits. Identification of tephra on the basis of mineral assemblages may prove problematic as crystals, with narrow ranges of densities will progressively

fall out with distance from the source vent, and only in proximal deposits will the full mineral assemblage plus vitric and lithic elements be present (Juvigne and Porter, 1985).

3) Studies which estimate distance from the probable source of tephra on the basis of particle aggregate modelling studies may also need re-assessment in the light of this work (Carey and Sigurdsson, 1982). There is no simple relationship between fallout and shard size. Particle aggregates and morphology which is related to them may be more important in determining the characteristics of deposits.

These positive results indicate that in Scandinavia the type of shard to seek (especially for the Öraefajökull 1362 equivalent varves) is a polymodal frothy pumiceous shard. Any tephra more dense than about 2 g/cm^3 would have been deposited nearer Iceland without reaching Scandinavia.

In view of these conclusions, the remaining sections of the varve chronology to be analysed (tephra from Ö1362, H1104 and Vö~900) were treated and separated using sodium polytungstate. All material denser than 2.45 g/cm^3 and lighter the 1.0 g/cm^3 was discarded. The remainder was cleaned and examined for glass shards. The removal of all the heavier quartz and feldspar minerals and the lighter clay minerals made the search for glass shards simpler and more efficient by removing both bulk and grains which have optically similar properties to volcanic glass (i.e. extinction under crossed polars).

The remaining 200 varves were examined but, despite the advances made in refining the separation technique, no glass shards were found in any of the varves sampled. This result may be disappointing for purely chronological reasons but it raises interesting new questions which are followed up in the next section.

3.6 Significance for the tephra-varve link

The absence of analysable tephra in the sampled varves leads to several interpretations. These are:

1) None of the tephra supposed to have reached Scandinavia fell over the catchment of the Ångermanälven in northern Sweden to become incorporated in the fluvial deposits. This is entirely possible. Although 4mm of tephra from Askja is reported to have fallen over Sollefteå in 1875 (Figure 3.1), the raining out of tephra is known to be patchy, especially when associated with a weather front (Þórarinsson, 1967). However Sollefteå is only 25 km from the varve collection site, suggesting that there was a sufficient quantity of tephra available. The peat bogs investigated by Persson (1971) also indicate that tephra fell in the region, for example at Klockamyren near Lake Ann, 150 km west in the Indalsälven river valley. Although the frequency of glass is low, peaks of material lie at 23 cm (radiocarbon dated at AD 1375±65) and 71 cm (1750±75 BC) below the surface. No distinct peak amongst the inorganic material was found in the upper parts of the bog which would suggest the presence of Askja 1875, but this may simply be due to the limits of the technique at the time. On the other hand patchy distribution may be the cause. No definite conclusion can be drawn about the patchy distribution of the tephra and therefore this interpretation cannot be ruled out.

2) The tephra is in the correct varves, but glass shards are on the whole too small to analyse. Again using Persson's data (1971), the apparent grain size of Scandinavian deposits should not be too small to be identified as glass. Another alternative is that, although larger sizes fell, there was selective deposition of very small shards (and possibly only in minute quantities). Larger particles of glass are known to raft laterally on water bodies and obscure the grain size pattern (Þórarinsson, 1979). This does not occur on raised peat bogs, but it may be a problem on other types of bogs with high water tables (Persson, 1971). It may be possible that some mechanism of

deposition operating within the water column of the Ångermanälven is responsible for winnowing the glass shards.

3) Tephra was deposited over the region in sufficient quantity and quality but the varve chronology is wrong i.e. the incorrect section of the chronology was sampled or poor connections were made in the Timescale's construction. This is of course always a possibility. However the connection to the present (Cato 1985, 1987) would have to be highly inaccurate not to incorporate tephras from H1947 and A1875. Several independent checks on the chronology exist such as stage data and pollution from the paper mill. The problem may lie in the sampling interval, for example 11 years spanning Askja 1875 would miss the tephra if the varve counts were out by more than 5 years either way. The sampling interval is only generous if double varves (i.e. freak flood events during a year add another lamination) were common during the late 19th and 20th centuries. However, the correlation of the water discharge records since 1909 (Cato, 1985) would negate this possibility especially as obvious double varves, e.g. AD 1945 (GC2) and AD 1967 (GC491) are accounted for. The same defence cannot be made for the earlier eruptions e.g. Öraefajökull AD 1362, Hekla AD 1104 and Veidivötn AD~900. However, the sampling interval was increased up to 45 years (Table 3.1) to accommodate both the uncertain connection and the narrowness of the varves in some of the cores. The whole postglacial period according to the Swedish Timescale is 9273 years long and the error estimated over the whole of this period is only +10/-180 years. Therefore although the varves in the recent historic period may be a few annual units out, the sampling interval employed was sufficient to contain any error.

4) The varve chronology is correct and tephra fell in the region. However the cores taken along the axis of the Ångermanälven missed the localised deposits of tephra in the sediments. Of course, any sampling interval has the risk that material of interest is missed and the result is unrepresentative. This is a major problem in lake studies as all lakes have zones of deposition, erosion and transport (Håkanson and Jansson, 1983). The piston cores used in the construction of the link to the present were taken

along the deepest axis of a flat-bottomed fjord, a good area for sediment focusing of both varves and tephra to take place. Any tephra incorporated in the bottom deposits may favourably accumulate around varve sites and so localised deposition should not be a problem. The above interpretation assumes that the tephra found in the lake sediments is due to the initial eruption fallout. However, if the tephra fell elsewhere in the catchment and was subsequently transported by rivers, then its presence in the varves may reflect deposition many years after the initial fallout. This may occur due to the erosion or anthropogenic destruction of peat bogs, shifting of tributary rivers and subsequent erosion of banks, or the melting of glaciers and ice caps containing tephra deposits. Searching the entire varve sequence above the eruption is impractical especially as the residence time of tephra in depositional environments such as ice caps and peat bogs can be considerable. In addition, the recently varved sediments of the Ångermanälven are themselves formed from redeposited deltaic sediments originating upstream. Any concentration of glass shards in a particular varve may not indicate direct deposition from an eruption but an erosional event. If this is so, then it is necessary therefore to examine the processes of tephra deposition in lakes and rivers in more detail.

The discussion of the results and the interpretations presented here indicate that a better understanding of tephra deposition and the formation of lake sediments is required in order to assess the linkage between Iceland's tephrochronology and Sweden's varve chronology. The conclusion remains that tephra is present in Sweden, but this study did not provide a link to the lake sediment sequences. An alternative line of enquiry is to investigate the processes involved in varve and tephra deposition in lakes. This is the thrust of the remaining chapters.

4.1 Introduction

The aim of this section of the thesis is to investigate the factors controlling the temporal and spatial distribution of tephra in the sedimentological record of a lake. The specific objective is to answer the questions raised by the results of the laboratory experiments concerning a varve-tephra link. Firstly, assuming tephra has fallen evenly over a region, what is the eventual spatial distribution of the deposit and how long does the change take? It is important to distinguish which transportation processes act upon tephra because they may be the primary control that determines the eventual pattern of the deposit in a lake environment. Secondly, the objective is to identify possible reworked tephra layers in the sedimentary record and determine causal mechanisms. This objective tests the idea that the first major peak of tephra in a lake sediment record is the original airfall, and that a "tail" of decreasing concentration is apparent in younger sections. Thirdly, the objective is to determine which properties, if any, distinguish the original fallout layer from reworked deposits.

4.2 Multiple site correlation

This project tackles these problems by changing the scale of the study in two ways; firstly, by constructing a very detailed catchment-scale correlation using many profiles rather than concentrating on a single idealised profile; and secondly, by increasing the stratigraphic thickness of the tephra deposits. The difficulties involved in finding and identifying microscopic glass shards can be overcome by investigating an area with relatively thick, easily identifiable tephra layers, such as Iceland.

The best way to gain insight into the processes of tephra deposition is to carry out detailed multiple site correlations across both lacustrine and terrestrial records on a catchment scale. This provides a way of distinguishing primary and secondary products, and builds a complete tephrostratigraphy over a small area. Importantly, this strategy allows one to reconstruct events in different parts of the catchment, for

instance hillslopes and delta areas. It also avoids the problem of over-reliance on one site which later turns out not to be representative due to localised geomorphological or sedimentological processes. There are many examples of the problems associated with using a single core from either terrestrial or lacustrine deposits to reconstruct regional environmental histories (Downing and Rath, 1988; Bennett *et al.*, 1992; Edwards and Whittington, 1993); the same is true for tephrostratigraphies. Tephra also has the particular advantage that it may be clearly identified and is geochemically distinguishable in all environments. It is possible therefore to identify disturbance over time in the catchment and establish the effects this has on the spatial and temporal distribution of tephra in the lake record.

Any model of the processes involved and the environmental history reconstructed from a multiple site correlation strategy is essentially locally constrained. However, it is possible to identify the underlying controls and establish principles applicable in other areas. The remainder of the chapter discusses the field site and the sampling strategy behind the approach of multiple correlation techniques.

4.3 Iceland: A natural laboratory-site specifics

Iceland is an ideal location for a catchment study because a good tephrochronology has already been established (Þórarinsson, 1967; Larsen, 1984). A second advantage is that processes such as soil erosion and rock weathering act rapidly on the softer, weaker rocks of Iceland compared with more stable areas such as Scandinavia. The main justification for the choice is the increased temporal resolution in the sediments but an additional advantage is that Iceland acts as an analogue of the rapid changes occurring in northern Europe throughout the Holocene and, later, the Little Ice Age. The fact that there was no human or grazing mammal impact prior to the 9th century AD makes it possible to distinguish natural from anthropogenic changes easily. Although Iceland has the advantage of thicker tephra layers, several parts of the island have such thick deposits that they behave very differently from other sediments. For example, deposits of Hekla 3 around Þórsadalur in southern Iceland

are 8m thick and clearly have no equivalent in the Swedish landscape (Þórarinsson, 1944). A good field site in Iceland must therefore be near enough to volcanic sources to have distinguishable tephra layers so they can be mapped in the field, but far enough away not to be dominated by thick deposits.

A further criteria is a suitably deep lake with a flat-bottomed topography. This is to ensure the presence of undisturbed lake sediment sequences and possible varved/laminated structures. Lakes in present geothermally active regions were not considered as earth tremors and escaping gas bubbles are known to disturb the structure (Haflidason *et al.*, 1992). In addition, a lot of the sediment in these lakes is biogenic rather than clastic and different from lakes in Scandinavia. To make the Icelandic site comparable to the Ångermanälven, sediments had to be mainly minerogenic and the water body nutrient poor. Large areas of northern Iceland are far from the volcanically active rift zone in central Iceland and therefore suitable for this type of study. During a reconnaissance fieldtrip in August 1991 it was found that the majority of named lakes in northern Iceland are shallow (<5m) and exposed to strong winds. Several of the lakes visited had dried up by the late summer thereby restricting choice considerably. However, Svínavatn in Húnavatnssýsla (Figure 4.1) fulfilled all the environmental requirements. Also, it had already been sampled by Thompson *et al.* (1986) and this offered the chance to put a conventional approach into a wider perspective.

4.4 The tephrochronology of northern Iceland

The early work of Þórarinsson (1944, 1958, 1967, 1981), Þórarinsson and Sigvaldason (1972), and Einarsson (1961, 1963) on the peat and soil sections of northern Iceland indicated that, although containing fewer tephra layers than the south, the north has been affected by many large eruptions from the major volcanic systems. Mapping of deposits in the north as well as around the parent volcanoes and fissures enabled Þórarinsson and later workers accurately to date eruptions and indicate the wind direction and changes in chemistry throughout an eruption (Larsen

and Þórarinsson, 1977; Annertz *et al.*, 1985). The published data from these studies indicate that identifiable tephra from eruptions of Hekla, Snaefellsjökull, Katla, and Veiðivötn dating from prehistoric and historical time are present in northern Iceland (Þórarinsson, 1967; Jóhannesson *et al.*, 1981; Larsen, 1984).

4.4.1 Hekla tephras

4.4.1.1 The silicic tephras

The tephra from Hekla can be divided into two distinct groups; the highly silicic tephras produced by large scale plinian eruptions and other intermediate to basic tephras (Larsen and Þórarinsson, 1977). For much of its postglacial history, Hekla has intermittently produced major highly silicic tephra with an initial silica content of 70-74%, decreasing to around 57% towards the end of the eruption. This period of eruptive history lasted from about 7000 BP to the eruption in AD 1104 (H1). During this time particularly large, highly silicic tephra were produced, Hekla 5 (~6600 BP), Hekla 4 (~3800 BP), the Selsund Pumice (~3500 BP), Hekla 3 (~2800 BP) and Hekla 1 (AD 1104). All except the Selsund Pumice are present in northern Iceland, appearing as distinct white layers in the peat sections. Figure 4.1 is a composite diagram of the isopach maps published by Þórarinsson and others for these tephra layers. Also shown on the map are the locations of the sections used to radiocarbon date the tephra layers (Kjartansson *et al.*, 1964).

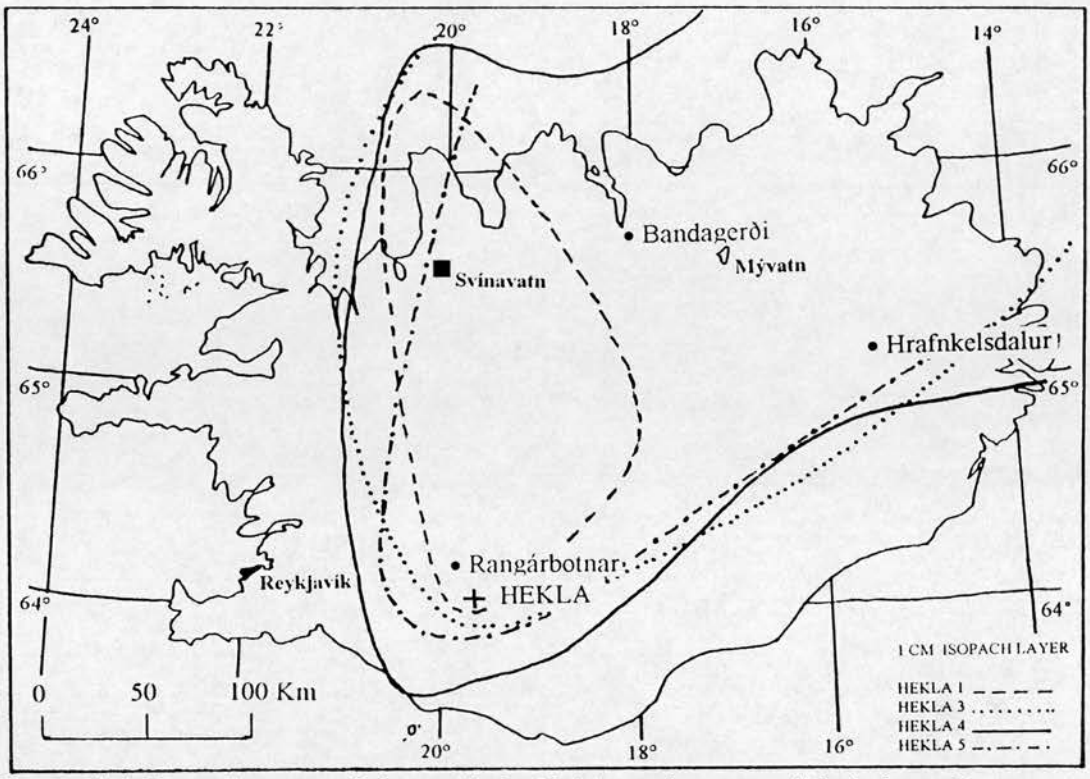

Figure 4.1 Isopach map of four silicic Hekla tephra. (modified from Larsen and Þórarinsson, 1977, *Jökull* 27, 28-46). Three sites used for ^{14}C dating of the tephra layers are indicated (•).

The characteristics of the white tephra layers in the north of Iceland remain the same over a large area. Hekla 5 (6600 BP) has a main axis extending to Mývatn in the NE of Iceland. The thickness of the layer appears to drop off relatively quickly although, according to Larsen and Þórarinsson (1977), it spread over as wide an area as the larger Hekla 4 and Hekla 3 ashes. The silica content of the tephra is around 74%. No significant changes in composition are apparent through the depth of the tephra and it is a light yellowish-grey colour throughout the layer. Hekla 4 (ca. 3800 BP) and Hekla 3 (ca. 2800 BP) are geochemically similar to each other with a range in silica content from 70-74% to around 57% (Annertz *et al.*, 1985). It is calculated that they have almost the same volume (6.7-8.0 km^3 freshly fallen on land) and cover the same areas (Figure 4.1). Changing wind directions during the eruptions resulted in differing geographical distributions of constituent parts of each tephra, therefore the main differences lie in the colour changes and grain size through the layers. In the

north of Iceland H4 has a thick, white lowermost unit of pumice which has two distinct subsets. The lowest sub unit is fine-grained (mean 0.02 mm) white ash and the younger sub unit is relatively coarse grained (mean 4 mm). The three uppermost units of Hekla 4 (greyish-yellow, greyish-brown and brownish black) were deposited towards the west and are missing on the north coast. This also implies that less silicic parts of the tephra are not present at the fieldsite.

Hekla 3 also has distinct colour changes from a white lower unit through greyish-pink to brown and black. In the north of Iceland a continuous record of the geochemical changes is present probably because Hekla 3 was deposited in more stable weather conditions than Hekla 4 (Larsen and Þórarinsson, 1977).

Hekla 1 is also present in the north of the island (Figure 4.1) and is the youngest of the acid tephra layers. Although not as large an eruption as H3 and H4, H1 still covers approximately half of the country (55,000 km^2). The silica content of the tephra is about 70% and it is uniformly white throughout the layer. There was no differentiation in chemical composition during the eruption indicating that the initial phase was highly explosive and short-lived (Þórarinsson, 1967).

The major element geochemistry of the initial plinian phases of the highly silicic Hekla tephras is distinct, although the ranges overlap to some extent. From work by Imsland (1978), Jakobsson (1979) and Larsen (1981) it is possible to differentiate between the different volcanic systems of Iceland, identify the trends within eruptions and to distinguish individual layers. Therefore analysis of the geochemistry of different tephras relates to the volcanic system. Iceland is composed of several active volcanic zones comprised of 29 volcanic systems producing lavas and tephra of basaltic composition (Figure 4.2). Within each system, one or two especially productive centres can be defined which contain all the known acid and intermediate eruption sites of the system. The petrography of each volcanic system is distinct and simple characteristics such as alkali abundance can be used as an effective initial split to determine the source of a tephra.

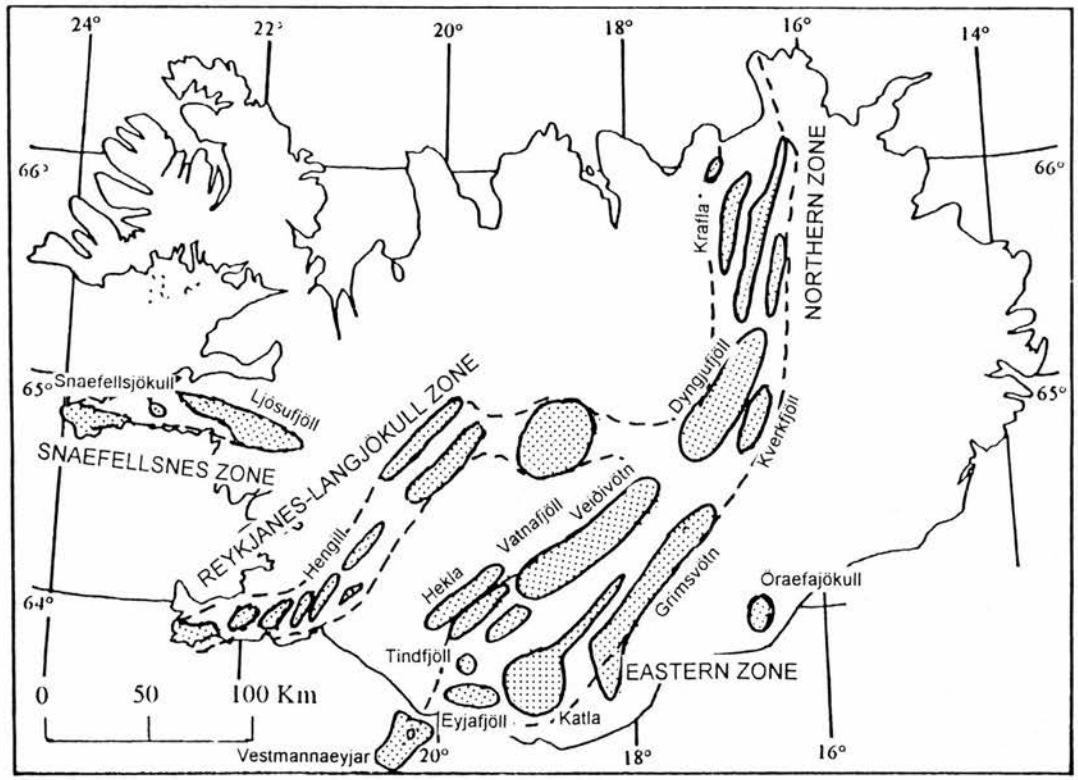

Figure 4.2 The volcanic zones of Iceland divided into the 29 volcanic systems (shaded). (modified from Jakobsson, 1979, *Acta Naturalia Islandica* 26.)

Following identification of the system, individual eruptions can be distinguished by geochemical characteristics. A complete electron probe micro-analysis of each tephra grain provides nine major element variables to compare plus combinations (e.g. Na/K against Ti). Compositional changes in the acid tephras from Hekla are best brought out by the variation in iron and titanium. The bi-plot in Figure 4.3 shows the titanium-iron ratio fields for H1, H3 and H4. The data shown in this diagram are from published sources (Larsen and Þórarinsson, 1977; Dugmore *et al.*, 1992) and from analyses of reference samples kindly supplied by Guðrún Larsen. Hekla 4 has the lowest Fe/Ti ratios forming a discrete cluster in the lower left hand corner of the bi-plot. The initial products of H3 and H1 have greater amounts of iron and overlap significantly. The abundance of Fe and Ti also increase during the course of the eruptions of H3 and H4, producing a trend towards more intermediate glass. According to the data from Larsen and Þórarinsson (1977), only H3 has the full range of geochemistry in the north.

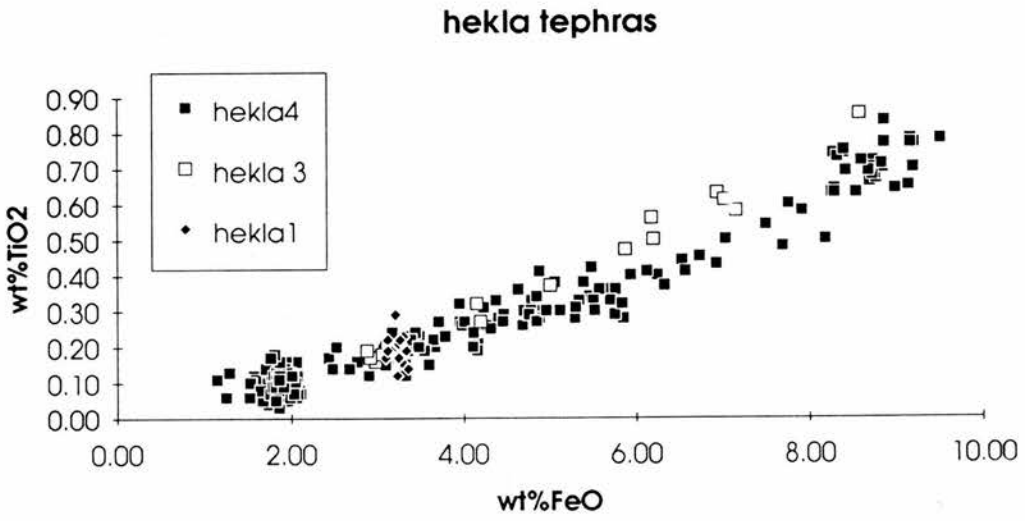

Figure 4.3 Bi-plot of the Fe-Ti ratios for H4, H3 and H1. (*sources*: Larsen and Þórarinsson, 1977, *Jökull* 27, 28-46; Dugmore *et al.*, 1992, *Journal of Quaternary Science* 7, 173-183; reference samples at Edinburgh University Geography Department).

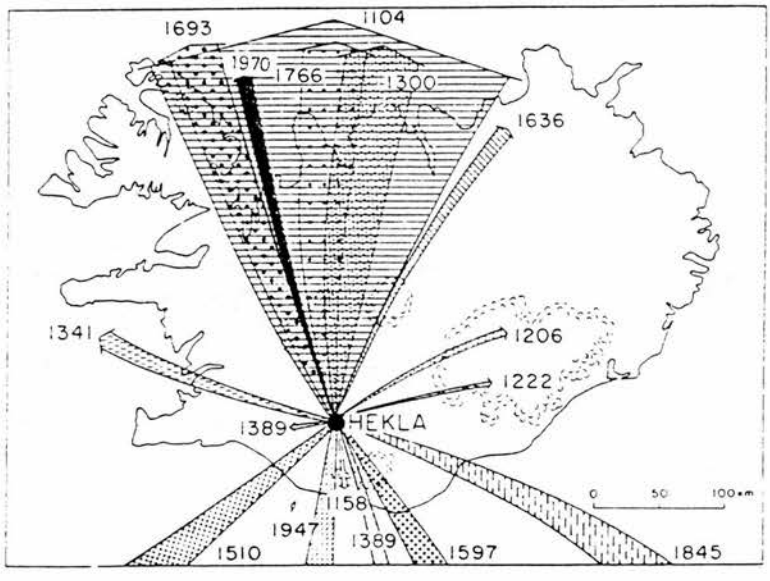

Figure 4.4 Map showing the directions in which tephra was dispersed during the initial phase of each of Hekla's 15 eruptions in historical times. The width of the arrows indicates roughly the relative size of the tephra layers' estimated volume. (*source*: Þórarinsson and Sigvaldason, 1972, *Bulletin Volcanologique* 36, 269-288.)

4.4.1.2 The basaltic tephras

In addition to the prehistoric Hekla layers, the north has also been affected by basaltic andesitic historical Hekla tephras. There have been 18 documented eruptions (excluding H1) since Iceland was first inhabited and 6 are known to have fallen in the north (Figure 4.4), namely eruptions of Hekla in AD 1300, 1636, 1693, 1766, 1970, and 1980. The geochemistry of these historical layers has not been published in detail since the early work of Þórarinsson (1967) and so it is important to use samples from type sites to aid correlation and rely on the stratigraphic relationship to other known tephras. The main discriminant of these tephras, however, is that the silica content varies with the length of the period of repose. For this reason great reliance is placed on the data in Figure 4.5 (Þórarinsson and Sigvaldason, 1972).

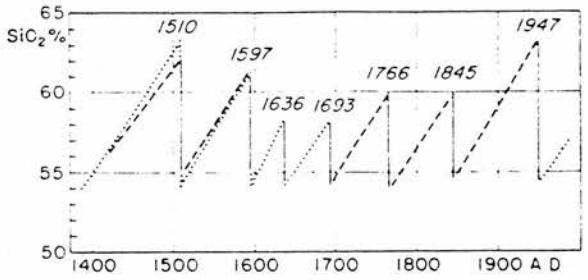

Figure 4.5 The relation between the SiO_2 content of the initial tephra of seven Hekla eruptions and the lengths of the preceding intervals of repose. The continuous and broken lines are based on chemical analyses. The hypothetical dotted lines show the SiO_2 content as a strictly linear function of time. (*source*: Þórarinsson and Sigvaldason, 1972, *Bulletin Volcanologique* 36, 269-288.)

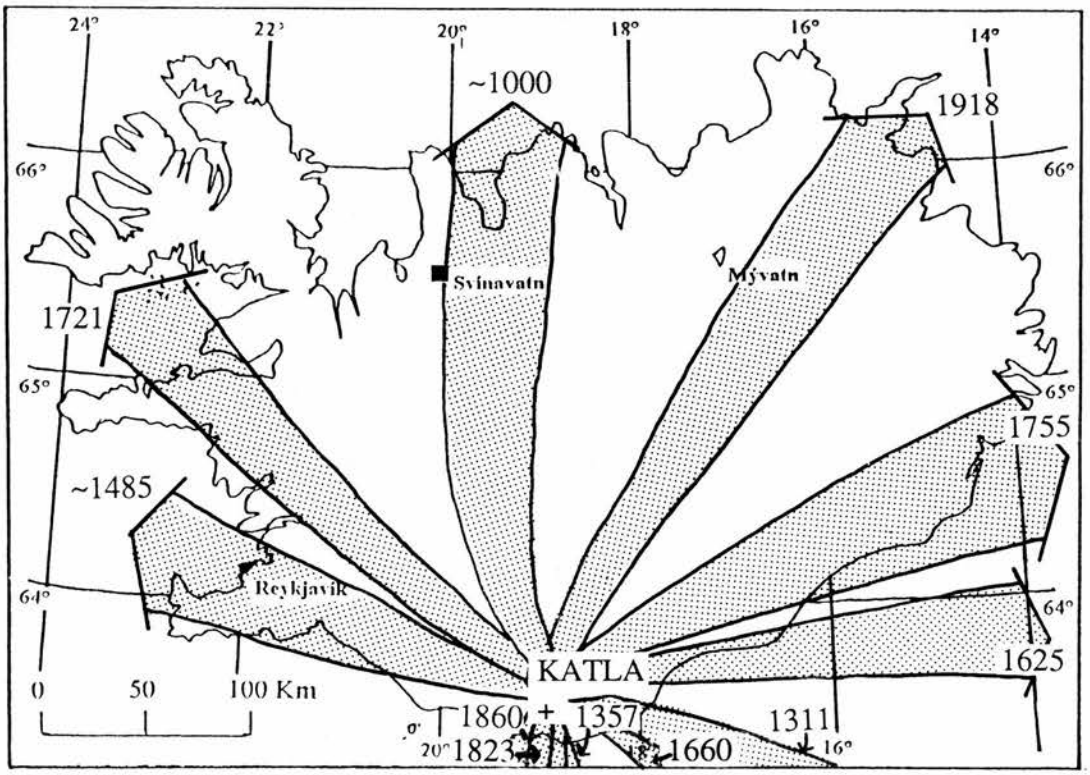

Figure 4.6 Map showing the dispersal directions of tephra from the 17 known historical eruptions of Katla. (*source*: Þórarinsson, 1975, *Árbók Ferdafélags Íslands*, 124-149.)

4.4.2 Katla tephra

The north of Iceland is also affected by eruptions from the Katla volcanic system. According to Þórarinsson there have been 17 eruptions in historical times and an unknown number of prehistoric eruptions. It is difficult, however, to distinguish geochemically the separate eruptions of Katla since the products are of homogeneous composition, being black and basaltic (~48% SiO_2) throughout eruptions. A tephrochronology for the products of Katla relies greatly on stratigraphic relationships and historical documentation. This is difficult in the early settlement period as events which took place then were not described until the 12th century AD. Some dates for eruptions are therefore contentious. For example, a black medium silt to sand size tephra dated to between AD 950 and AD 1050 from the Katla system, may be from an undocumented eruption of Katla in AD 1000 or from an eruption of Eldgjá in AD 934 (Þórarinsson, 1967; Larsen, 1979). Attempts have been made to construct a regional chronology for southern Iceland using records and minor element analysis but no detailed study has been attempted for the north (Larsen, 1979, 1981, 1984). The only published list of Katla tephras is shown in Figure 4.6 which shows that ?K1000/E934 should be present in the north of Iceland. Due to uncertainty regarding the origin and date of this tephra, it is referred to as K-X (Larsen, 1979).

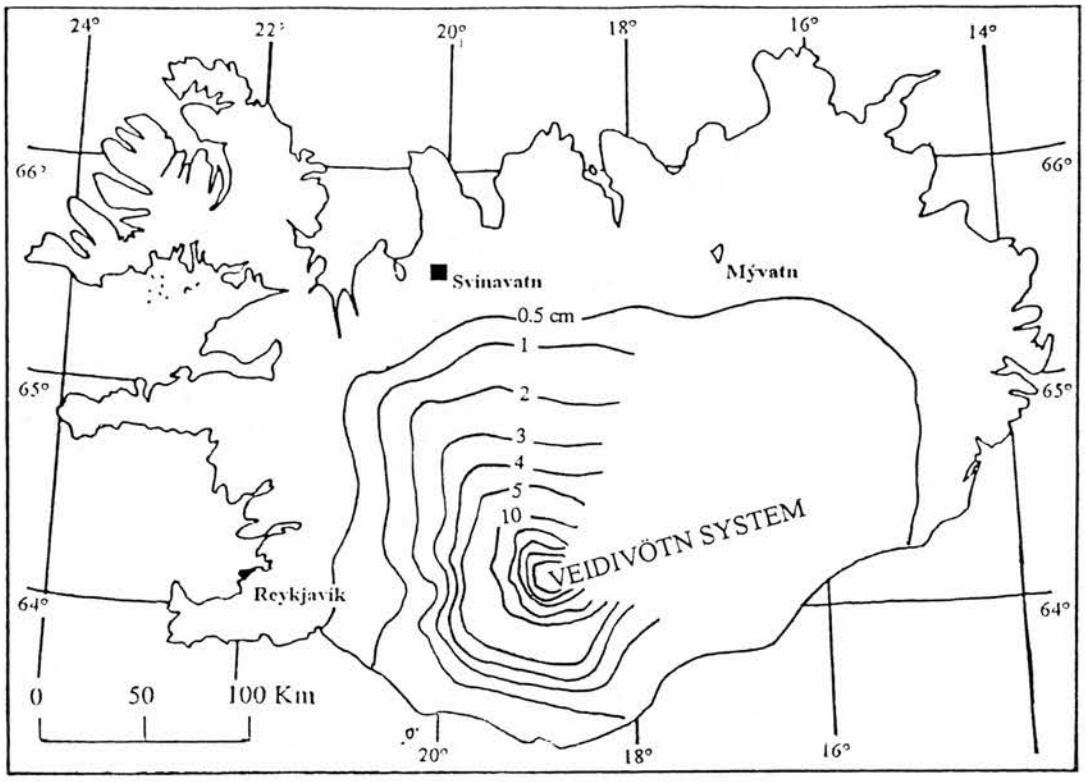

Figure 4.7 Isopach map of the upper basaltic part of the Vatnaöldur eruption AD~900. (modified from: Larsen, 1984, *Journal of Volcanology and Geothermal Research* 22, 33-58).

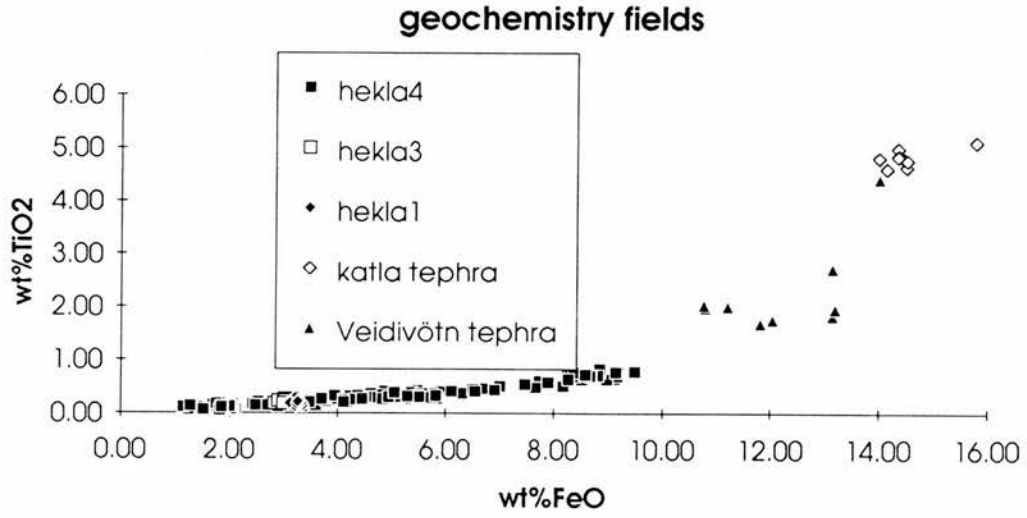

Figure 4.8 Bi-plot of Fe-Ti ratios for the Hekla, Veiðivötn and Katla volcanic systems. (*sources*: Larsen and Þórarinsson, 1977, *Jökull* 27, 28-46; Dugmore *et al.*, 1992, *Journal of Quaternary Science* 7, 173-183; reference samples at Edinburgh University Geography Department).

4.4.3 Veiðivötn tephra

Another basaltic tephra found extensively in Iceland is from the Veidivötn system. This olive green tephra is called the Landnamslag or settlement layer (Layer VIIa+b) and is dated to an eruption in the Vatnaöldur eruptive fissure within the Veidivötn fissure swarm in AD 897-898 (Larsen, 1984). There are two parts to Vö~900; a darker, upper layer with high SiO_2 content deriving from the silicic centre at the south end of the fissure; and a lighter coloured basaltic lower part (Figure 4.7). Titanium and iron are lower in tephra from Veiðivötn and it is possible to distinguish it from Katla products (Figure 4.8). Apart from the Landnam tephra, Veiðivötn is known to have erupted at least twice, a prehistoric eruption dated to 1860+/-100 yBP (Larsen, 1984) and in AD 1477 (Þórarinsson, 1958), but there may have been eruptions every 1000 years (Larsen pers comm).

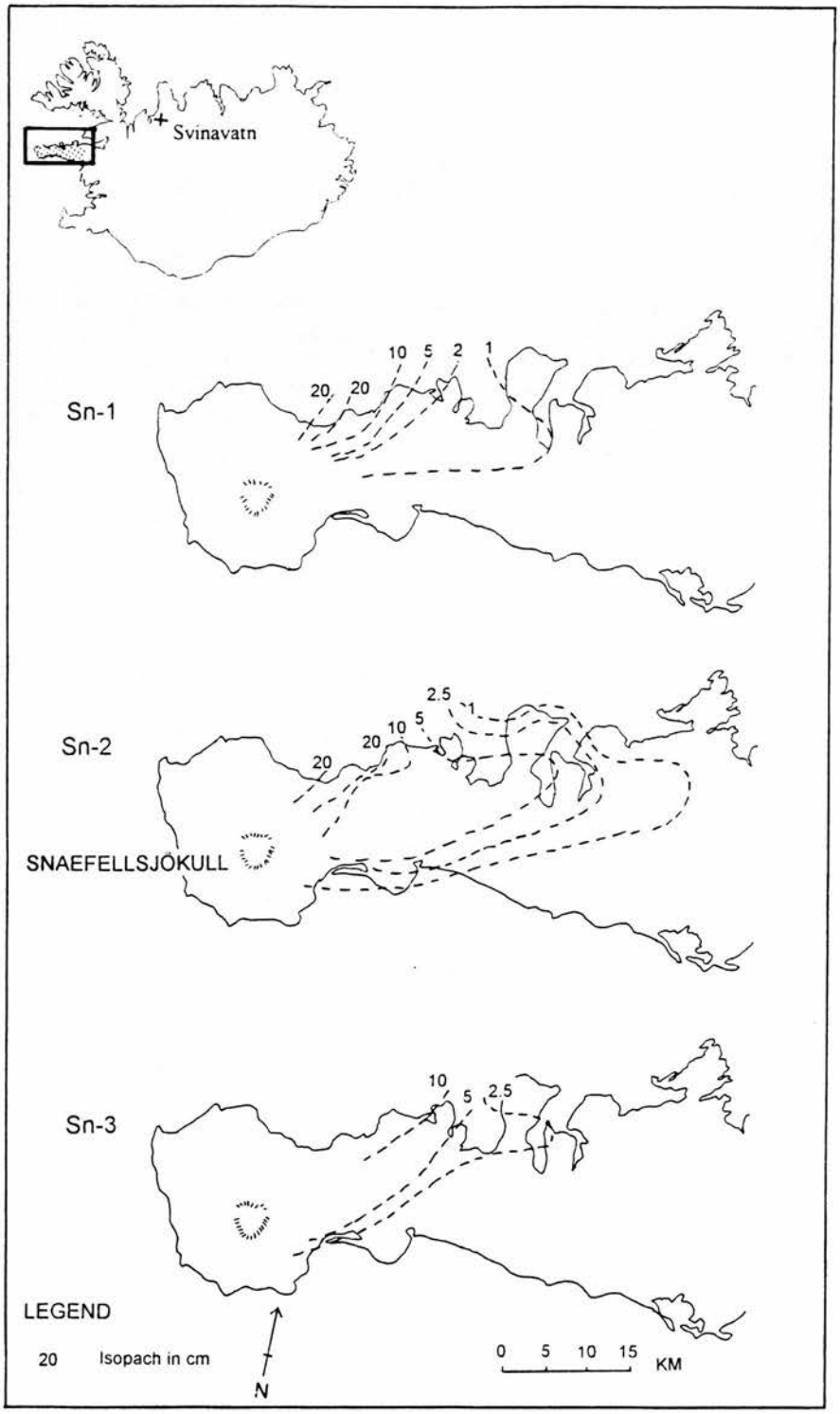

Figure 4.9 The distribution of the three major silicic tephra layers from Snaefellsjökull central volcano. The inset shows the distance of the volcanic system to the fieldsite. (modified from: Jóhannesson *et al*, 1981, *Jökull* 31, 23-31).

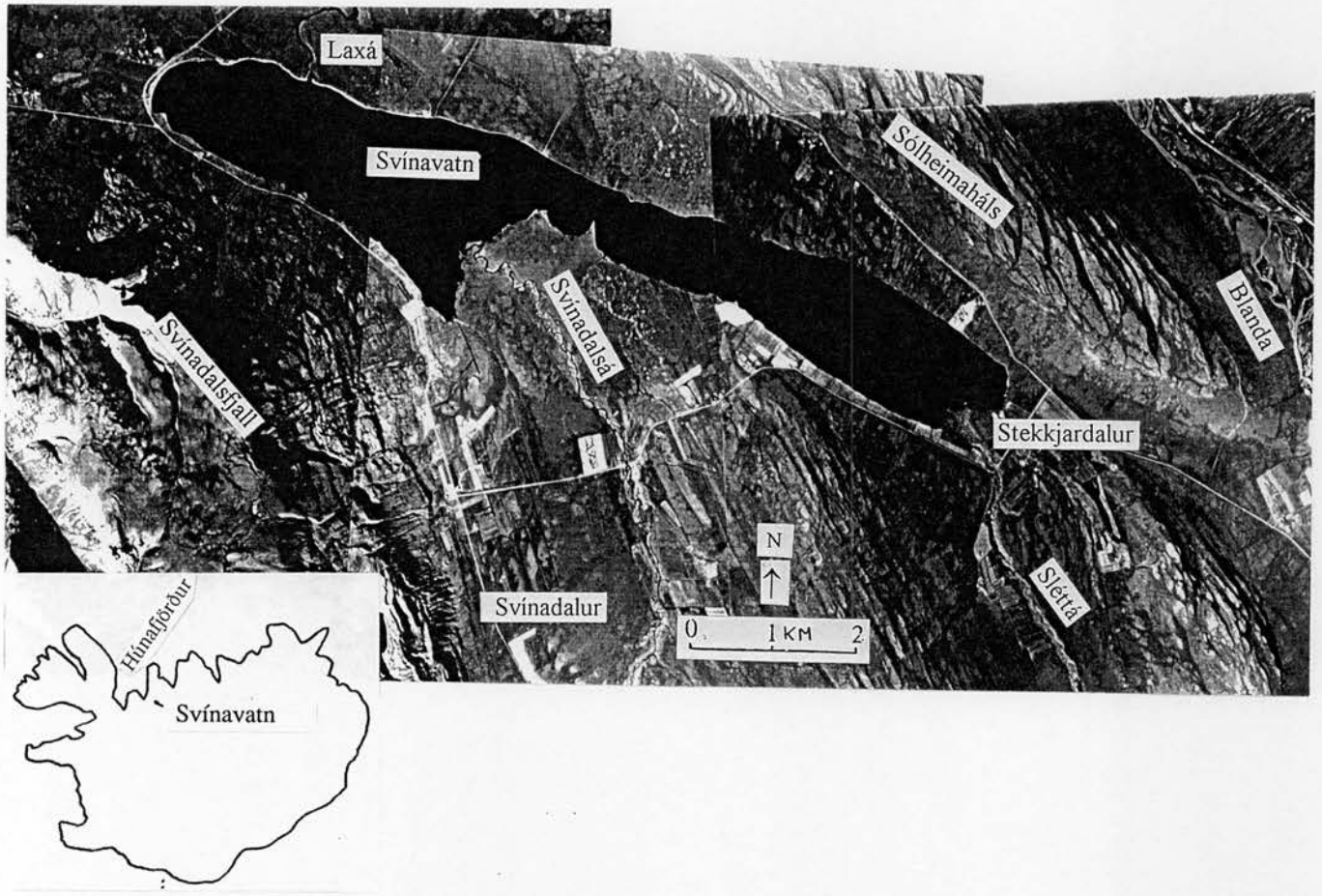

Figure 4.10 Aerial photograph of Svínavatn catchment (taken 3rd September 1984, at a height of 5486 metres). Inset shows location of catchment. (air photographs from Landmaelingar Íslands, Reykjavík).

4.4.4 Snaefellsjökull tephra

In addition to tephra originating from the Southern Volcanic Zone of the main axial ridge, the north may have been affected by activity in the Snaefellsnes Volcanic Zone (see Figure 4.2). The zone consists of three volcanic systems, the most productive of which is the Snaefellsjökull central volcano. Three acidic tephra layers (Sn1-3) have been mapped extensively around the peninsula (Figure 4.9); all three consist of light coloured frothy pumice and ash (Jóhannesson *et al.*, 1981). The eruptions Sn1 and Sn2 have been radiocarbon dated to 1750±150 BP and 3960±100 BP respectively, whilst Sn3 has an estimated age of 7000-9000 BP as it was deposited shortly after the start of soil accumulation following the last glacial (Steinthórsson, 1967). These layers have not been mapped beyond the peninsula but they may be present to the NE (Larsen pers comm). There are significant compositional differences between the alkali olivine basalts of the Snaefellsnes Volcanic Zone and the transitional alkali basalts (TAB) of the Southern Volcanic Zone. According to Imsland (1978) the silicic rocks and tephra of Snaefellsjökull have alkali ratios (Na_2O:K_2O) close to 1 compared with other silicic centres such as Hekla (alkali ratio around 1.5).

In summary, therefore, the fieldsite in northern Iceland is likely to contain a detailed tephrochronology with several tephras from each of the major volcanic systems present and most importantly, the white Hekla tephras. Each layer would also be of optimum thickness to trace in the field.

4.5 Fieldsite description

4.5.1 Catchment physiography

The study site in northern Iceland is a relatively large catchment (229 km^2) composed of the Svínadalur and Stekkjardalur valleys and Svínavatn lake basin (11.72 km^2). The valley is oriented NW-SE with the main outlet, the Laxá river, entering Húnafjörður to the north (Figure 4.10). The two main inlet rivers to Svínavatn (the Sléttá and Svínadalsá) rise in flat-lying highlands (<500m) to the south-east where

several small lakes and peat bogs provide runoff all year round. Flat-topped basaltic mountains south-west of the lake are the main relief features, rising steeply to 973m. The northern edge of the lake is bounded by Sólheimaháls, a low-lying ridge of Plio-Pleistocene extrusive rock (maximum elevation of 348m) which separates Svínadalur from neighbouring Langidalur and the Blanda river. Apart from this ridge the geology of the catchment is Upper Tertiary (>3.1ma) basic and intermediate extrusive rock. The large north-south oriented valleys around the catchment are thought to have been formed by outlet glaciers coming off a large inland ice sheet during glaciations (Kjartansson *et al.*, 1964; Norðdahl, 1991).

4.5.2 Climate of the region

Iceland lies near the Arctic Circle between latitudes 63°23'N and 66°32'N and longitudes 13°30'W and 24°32'W. The island is situated near the border between warm and cold ocean currents and as such is sensitive to changes in the position of this front. At the present day the North Atlantic Drift passes to the south whilst a branch of the cold East Iceland Current flows south along the east coast. This temperature front influences weather and climate considerably. High precipitation levels along the warmer south coast maintain the large ice caps of the south and central districts (Figure 4.11). However, a large rain shadow north of this belt means that the climate of northern and central Iceland is more continental.

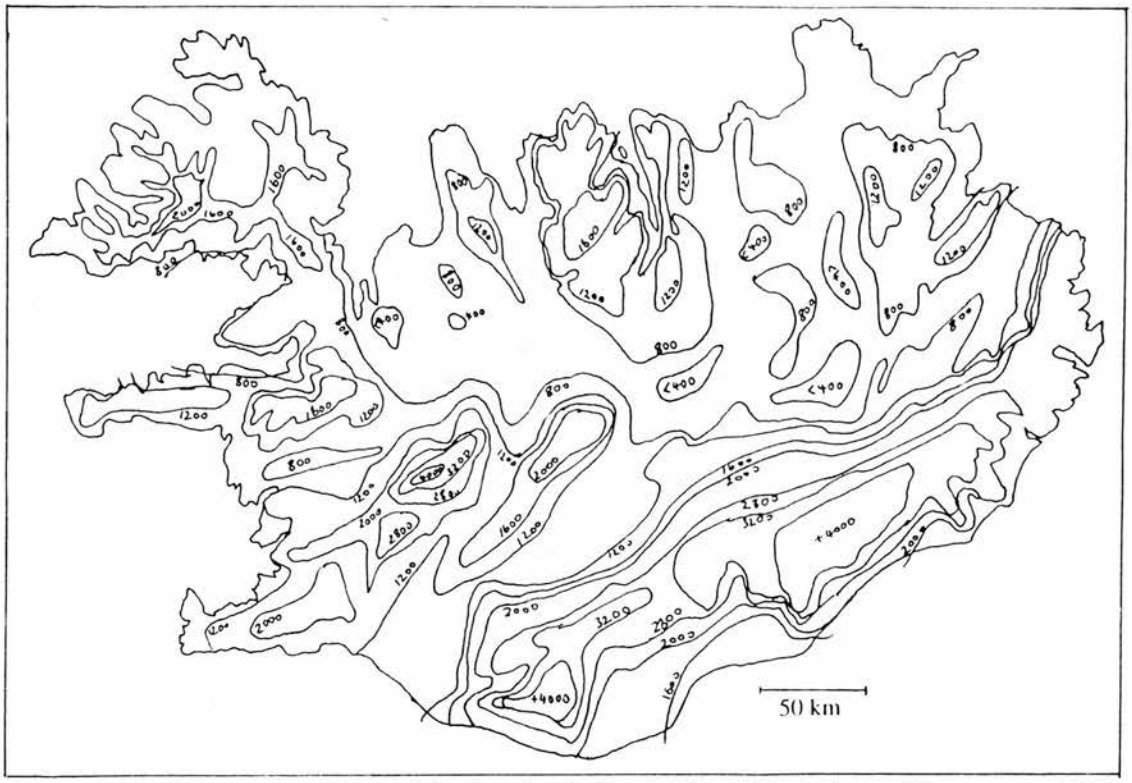

Figure 4.11 Mean annual precipitation in Iceland (simplified from: Einarsson, 1984, *World Survey of Climatology* 15, 673-697.)

The mean annual temperature in northern areas is 3-4°C with August the warmest month and February the coldest. The annual range of temperature around Svínavatn is 12°C (mean January temperature of -3°C, mean July temperature of 9°C (Figure 4.12, Figure 4.13). Climatic data relating to the fieldsite are presented in Table 4.1 (compiled from Einarsson, 1984). The main characteristics of the climate are that precipitation is low for maritime cool temperate climates (around Svínavatn it is only 500 mm), most of which falls in autumn and early winter. The annual number of days with precipitation of more than 0.1 mm is low at around 130-140 days and 66% of days during June to August are dry. The main form of winter precipitation is snow. The tabulated data for Akureyri (50 km east of Svínavatn) show that the first snowfall tends to be in September and the last day of complete snow cover is usually in April, although snowfalls occur as late as May. The weather at each place is greatly affected by local topography, especially wind direction, strength, and insolation levels. Frost is frequent as are thaws. Svínavatn lies therefore in a relatively dry but cool region, comparable with eastern Scandinavia.

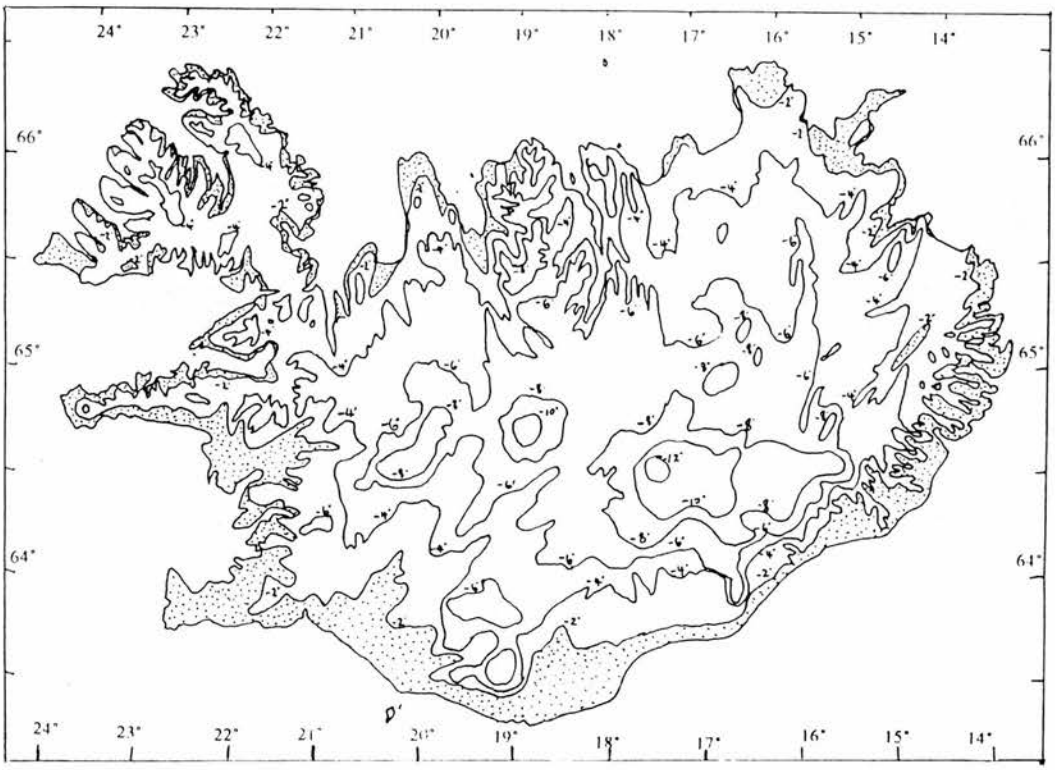

Figure 4.12 Mean temperature for January in Iceland (simplified from: Einarsson, 1984, *World Survey of Climatology* 15, 673-697.)

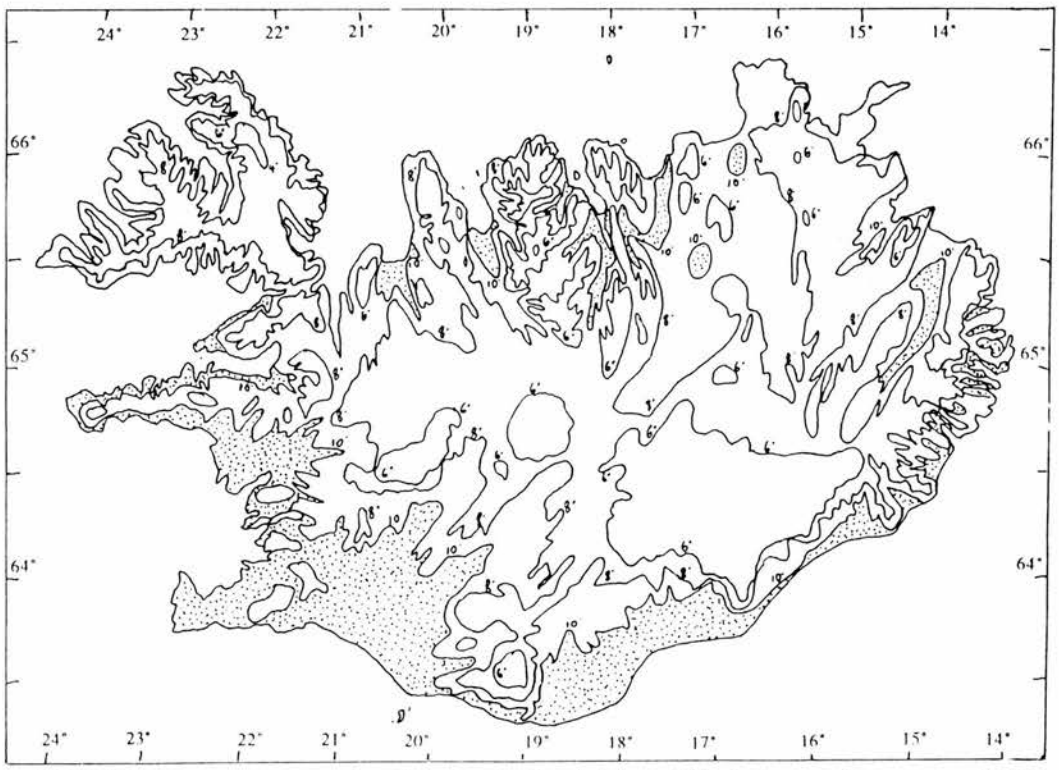

Figure 4.13 Mean temperature for July in Iceland (simplified from: Einarsson, 1984, *World Survey of Climatology* 15, 673-697.)

Temperature data

mean annual temperature (°C)	3-4
annual range of temperature (°C)	12
-mean temperature in January (°C)	-3
-mean temperature in July (°C)	9
warmest month	August
coolest month	February

Frost days data (for Akureyri 1951-1960)

Annual number of days	Last frost-average date	First frost-average date
151	31/5	15/9

Jan	Feb	Mar	Apr	May	Jun	Jul	Aug	Sep	Oct	Nov	Dec
26	22	22	17	8	0.9	-	0.3	2	12	16	25

Precipitation data for Blönduös (1951-1970)

annual precipitation	500 mm
months of greatest precipitation (% of annual rainfall total)	Oct-Mar (50-65%)
annual number of days with precipitation >0.1 mm	130-140 days (low)
monthly number of days with precipitation (Autumn/Winter)	12-16 days
monthly number of days with precipitation (May)	7-10 days
percentage dry days during June-August	66%
snow as a percentage of total precipitation (Nov-Mar)	50-70%
snow cover (% of total cover Oct-Mar)	50-70%

Snow data for Akureyri (1951-1970)

date of first snowfall	25/9
date of last snowfall	27/5
first day of complete snow cover	23/10
last day of complete snow cover	22/4
first day of no snow cover	13/5

Wind information - average direction between NE and SE, but greatly affected by local topography e.g. Akureyri is situated in a N-S fjord.

Table 4.1 Climate statistics for Svínavatn and northern Iceland (compiled from: Einarsson, 1984, *World Survey of Climatology* 15, 673-697).

4.5.3 Soils and vegetation

The soils around the catchment can be classified as aeolian-andic which describes material comprised of tephra and wind blown sediments of various origins such as glacial till and sandar (Arnalds, 1990). This type of andisol commonly mantles glacial till and basalt bedrock over much of Iceland and includes many distinct tephra layers. The characteristics of the soils such as low bulk density, high water retention and weak aggregate strength, make Icelandic soils highly susceptible to erosion, especially where coarse tephra layers provide material for saltation (Guðmundsson, 1978; Arnalds, 1990). Around Svínadalur, soil has been stripped from the highlands (especially on Sólheimaháls) and patterned ground of various forms is apparent. The slopes have a thin regolith near the top which gradually thickens downhill where minerogenic peat interfingers at the bottom of the slope. More organic silt/peat is found on gently sloping or flat land at the north-west and south-east ends of the lake.

The vegetation of the catchment consists of peatland, arable fields and meadows. The upper slopes and hilltops are mainly bare rock and scree (see Figure 4.10). There is no woodland in the catchment. Investigations in the area by Einarsson (1961, 1963), Vasari (1972) and Vasari and Vasari (1990) show that woodland (in Iceland mainly *Betula pubescens* and *Betula nana*) has fluctuated naturally with climatic changes. The greatest change, however, occurred at the time of settlement (Landnam ~AD 874) and it has been estimated that over the past 1100 years woodland coverage has been reduced from 25,000-40,000 km^2 to 1250 km^2 (Arnalds, 1992). Deforestation to provide grazing land, firewood and charcoal for iron was responsible, although the changes were exacerbated by climatic shifts to colder wetter periods through the late Holocene (Einarsson, 1963; Hallsdóttir, 1987; Bjarnason, 1974).

Few records of the early settlement of Svínadalur exist; although the history of a neighbouring valley is the basis for *Vatnsdœla Saga*, the family chronicle of Ingimundur the Old Þorsteinsson who settled in Húnavatn around AD 900 (Magnusson, 1987). He is also mentioned in some versions of "Landnámabók" in

connection with sea ice and polar bears around AD 890 (Benediktsson, 1968 cited in Ogilvie, 1990). Svínadalur may, therefore, have been inhabited early in Iceland's history, and certainly the land would have been occupied by the time pressure on land resources forced the Icelandic colonisation of Greenland around AD 1000.

On higher ground (>300m) the area is intensely cryoturbated with the remaining soil sorted into hummocks (þúfur). The removal of birch woodland cover is a possible factor explaining increased cryoturbation and solifluction processes in Svínadalur and Iceland as a whole. The birch stands played an important role in protecting soil from erosion; they gave better shelter and their root systems provided cohesion for the soils. As noted above, andisols can absorb large quantities of water intensifying freezing effects that result in solifluction, landslides, needle ice formation and the formation of hummocks (Arnalds, 1990). The tephra horizons strikingly highlight this feature since prehistoric tephra layers are reasonably horizontal whilst historic ones are uneven and lenticular as they "drape" cryoturbant þúfur (Einarsson, 1963).

Information from historical records suggests Iceland had a generally mild climate up to the late 12th century, followed by four centuries characterised by periodic short periods of harsh climate (Ogilvie, 1990). A prolonged cold spell corresponding to a "Little Ice Age" started in the mid 1700s and lasted to the 1840s (Ogilvie, 1991). Human impact and climate changes act together to make the stratigraphic record from the historic period difficult to interpret.

4.5.4 Svínavatn basin

Svínavatn is a moraine dammed lake (Thompson *et al.*, 1986), lying 125m above sea level (a.s.l.) at the junction of the Svínadalur and Stekkjardalur valleys (20°W, 65°33'N). It has an elongated shape with maximum length 11.1 km, maximum breadth of 2.1 km and a capacity of 1466 Gl (Figure 4.14 inset table). The bathymetric map was produced by the Icelandic Power Company in 1957.

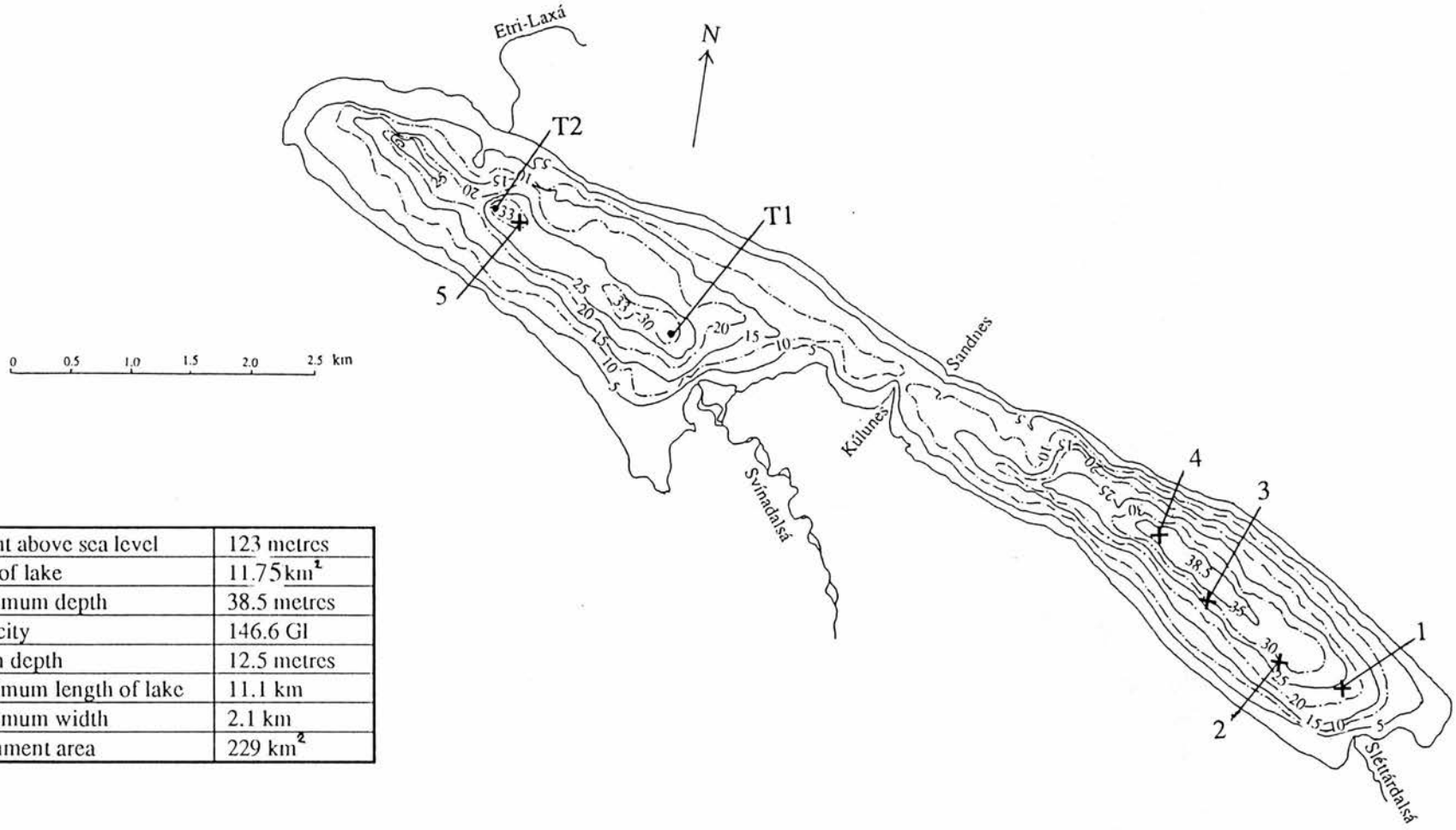

height above sea level	123 metres
area of lake	11.75 km^2
maximum depth	38.5 metres
capacity	146.6 Gl
mean depth	12.5 metres
maximum length of lake	11.1 km
maximum width	2.1 km
catchment area	229 km^2

Figure 4.14 Bathymetric map of Svínavatn with the locations of the coring sites. T1 and T2 are sites sampled by Thompson *et al*, 1986. (based on: Icelandic Power Company, unpublished bathymetric map, 1957.)

The lake is divided morphologically into two basins of very different character (Figure 4.14). The western basin has a relatively flat-bottomed topography with two deeps of 30-33m. A smaller isolated deep of 25m lies to the north-west. The largest of the main inlet rivers, the Svínadalsá, flows directly into the western basin. The underwater contours fall steeply away from the mouth of the river, suggesting that turbidity currents and underwater slumps may be important sedimentological factors in this part of the basin. The only outlet from Svínavatn (the Etri-Laxá) exits almost directly opposite the mouth of Svínadalsá. The eastern basin is separated from the western end by a ridge of material rising to within 5-10m of the surface, almost hydrologically isolating both systems. Kúlunes Point on the southern edge of the lake and Sandnes on the north mark the ends of the ridge dividing the two basins. The maximum depth of the lake in the eastern basin is 38.5m and again is flat-bottomed with a rather symmetric basin shape. The second largest inlet river, the Sléttá, feeds into the south-easternmost corner of the lake.

4.6 Field methods

4.6.1 Lake Study

4.6.1.1 Sampling System

The lacustrine record of tephra fall was obtained from cores in Svínavatn. The choice of sampling pattern depends mainly on the aim of the investigation which in this case is the areal distribution pattern of tephra. Three types of sampling programme can be distinguished: Firstly, deterministic systems based on given presuppositions, information or purposes; secondly, stochastic systems based on random sampling; thirdly, regular grid systems which can be placed randomly or deterministically on the lake. Given the time and expense involved in lake sampling, random placing of coring sites seems inefficient. In addition a purely deterministic sampling strategy would target one aspect of the objective to the exclusion of other aspects. Therefore, a regular pattern was chosen along the long axis of the basin.

The number of cores deemed sufficient to provide an even cover of the lake, and be statistically valid was calculated. According to Håkanson and Jansson (1983) about twelve factors influence the decision about the number of samples which should be taken. These include the water system, the circulation dynamics, anthropogenic factors, lake area and bottom roughness. It is impossible to account for all the factors, however, and the most commonly used parameters seem to be lake area (more samples have to be taken from large lakes), bottom roughness and shore development. More samples have to be taken from lakes with topographic irregularities.

pilot sample formula:

$n = 2.5 + 0.5 \times \sqrt{a \times F}$

where n is the number of samples; a is the lake area (km^2); F is the shore development.

F is calculated using the formula $F = \frac{l_0}{2 \times \sqrt{\pi \times A}}$ where l_0 is the normalised shoreline length in km, and A is the total lake area (i.e. the water surface, a, plus area of islands.

Substituting data for Svínavatn with a lake area of 11.75 km^2 and a normalised shoreline of 25.15 km;

therefore, F=2.07 and the number of samples needed to give good coverage of Svínavatn is 5.

Table 4.2 Statistics to determine sampling strategy for Svínavatn (*source:* Håkanson and Jansson, 1983, *Principles of sedimentology*: Springer Verlag, Berlin).

Relating these variables, Håkanson and Jansson (1983) produce simple pilot formulae to provide a rule of thumb calculation of the number of samples required for a study (see Table 4.2). For example, the parameter F, shore development, illustrates the relationship between the actual length of the shoreline and the length of the circumference of a circle of area equal to the lake area. A perfectly circular basin has an F value of 1, values of 10 are rare, the average for Nordic lakes is in the order of 2-4. Table 4.2 shows the calculated statistics for Svínavatn. The F value is 2.07,

and relating this parameter to area, it can be seen that 5 cores will provide adequate statistical coverage of Svínavatn. The spatial alignment of the sampling frame was determined by the bathymetry and the need to minimise excessive sediment input by rivers. Four cores were taken from the eastern basin along the central axis (see Figure 4.14) whilst one core was taken from the western basin. In addition, two cores from the western basin had already been sampled by Thompson *et al.* (1986).

4.6.1.2 Sampling methods

Cores 1-3 were extracted from the eastern basin in March 1992 whilst the lake surface was frozen. Cores 4 and 5 were sampled from a boat in July 1992. The coring equipment used was a gravity driven piston corer with a triggered release and 110mm diameter piping cut at regular 2m intervals. This piston corer was chosen as it was readily transportable, light to carry and easy to use.

The sampling procedure was relatively simple. The whole corer with attached tubing was lowered gently at an angle through holes cut in ice, or over the side of an anchored boat, until water had entered the coring tube. Weights (rocks, concrete blocks etc) were then placed in the container and the corer was gently lowered through the water column, taking care that the piston lever was floating free of the main apparatus. With the sample tube at the water sediment interface, a trigger mechanism released a gravity driven corer. The piston remained at the interface position permitting complete recovery of up to 1.5 metres with minimal distortion. The corer plus sample were then pulled up by attached ropes and the bottom of the core tube plugged before the equipment had fully emerged. The plastic tube was then simply detached from the corer and the upper end plugged. Each core sample was recovered in the same way and transported back to Edinburgh for analysis. No water from the sediments was lost during the interval between sampling and extrusion.

4.6.2 Catchment study: Soil and peat profiles

4.6.2.1 Sampling system

In order to obtain a terrestrial record of tephra deposition, samples were taken from the peats and soils in the catchment surrounding Svínavatn (Figure 4.15). All the sections described below were described and sampled for tephra during two periods of fieldwork in August 1991 and July 1992. The sites were mainly the cleaned faces of artificial drainage ditches around the catchment, providing open sections of at least one metre width. This method of sampling is preferable to coring due to the fact that the whole face can be examined in detail and disturbances of the peat can be recognised. The sampling pattern around the lake had two main aims; firstly to give a good areal cover, and secondly to identify areas of sediment disturbance and stability. It was possible to see major differences in stratigraphy within short distances and for this reason several areas have more than one sampled section.

4.6.2.2 Sampling methods

To aid the characterisation of the tephras, stratigraphic relations, thickness and colour changes were used to supplement the information given by analysis of the chemical composition of the glass component. The profile at each site was logged and each tephra layer sampled and placed in plastic bags, labelled and sealed. Fingerprinting of tephra deposits relies greatly on determining the sequence of eruptions and this relies on accurately identifying the initial eruption products. The original airfall of tephra from an eruption can be identified on land by considering four aspects of stratigraphy. Firstly, examining the nature of the underlying surface (composition and structure), it is possible to see whether or not the deposit drapes the underlying surface. Secondly, the stratigraphic position in relation to other tephras over a wide area will stay the same if no further disturbance has taken place. Thirdly, over a local area the apparent colour, grain size and geochemical changes within the deposit will stay constant. This factor is more important in areas near the parent volcano where all the phases of the eruption may be present. In some distal deposits distinctive geochemical trends can be identified and help to fingerprint the tephra. Fourthly,

airfall products can be identified by the homogeneity of the sample and the relative amounts of crystals, lithics and vitric components. If a sample contains a large amount of contamination from the matrix, for example clay minerals, feldspars or older tephra products, then an airfall origin can be discounted.

4.7 Laboratory methods

4.7.1 Sampling of lake cores

The cored samples retrieved from Svínavatn were opened at the British Geological Survey in Edinburgh. A jigsaw cut the plastic piping longitudinally on each side and a sharp wire cut the sediment into two halves. The face of each half was then cleaned using a sharp razor blade and the sediments were described. Following the methods of Digerfeldt *et al.*. (1975) and Koivisto and Saarnisto (1978), plastic boxes (12.5 x 8 x 2.5 cm) were pressed gently into the sediment and a fine wire was used to cut away the excess sediment. Tightly fitting lids were placed over the exposed faces and attached securely to prevent loss of moisture from the boxes. The contiguous samples were then ready for X-radiography.

X-radiography of lake sediments provides an excellent record of content and structure (Karlén, 1981; Axelsson, 1983; Saarnisto, 1986). Fine laminations, massive sediments and core disturbance are recorded by the varying degrees of light and dark banding, a useful tool especially where some structures are not readily visible by eye (Digerfeldt *et al.*, 1975; Koivisto and Saarnisto, 1978). X-radiography has been used successfully with glacial lake sediments to identify cold periods (high minerogenic content producing light banding) throughout the Holocene (Karlén and Rosqvist, 1988). Axelsson (1983) used a quantitative method of densitometry to indicate the intensity of the absorbency and this has been found to correlate well with bulk density (Rosqvist, 1992).

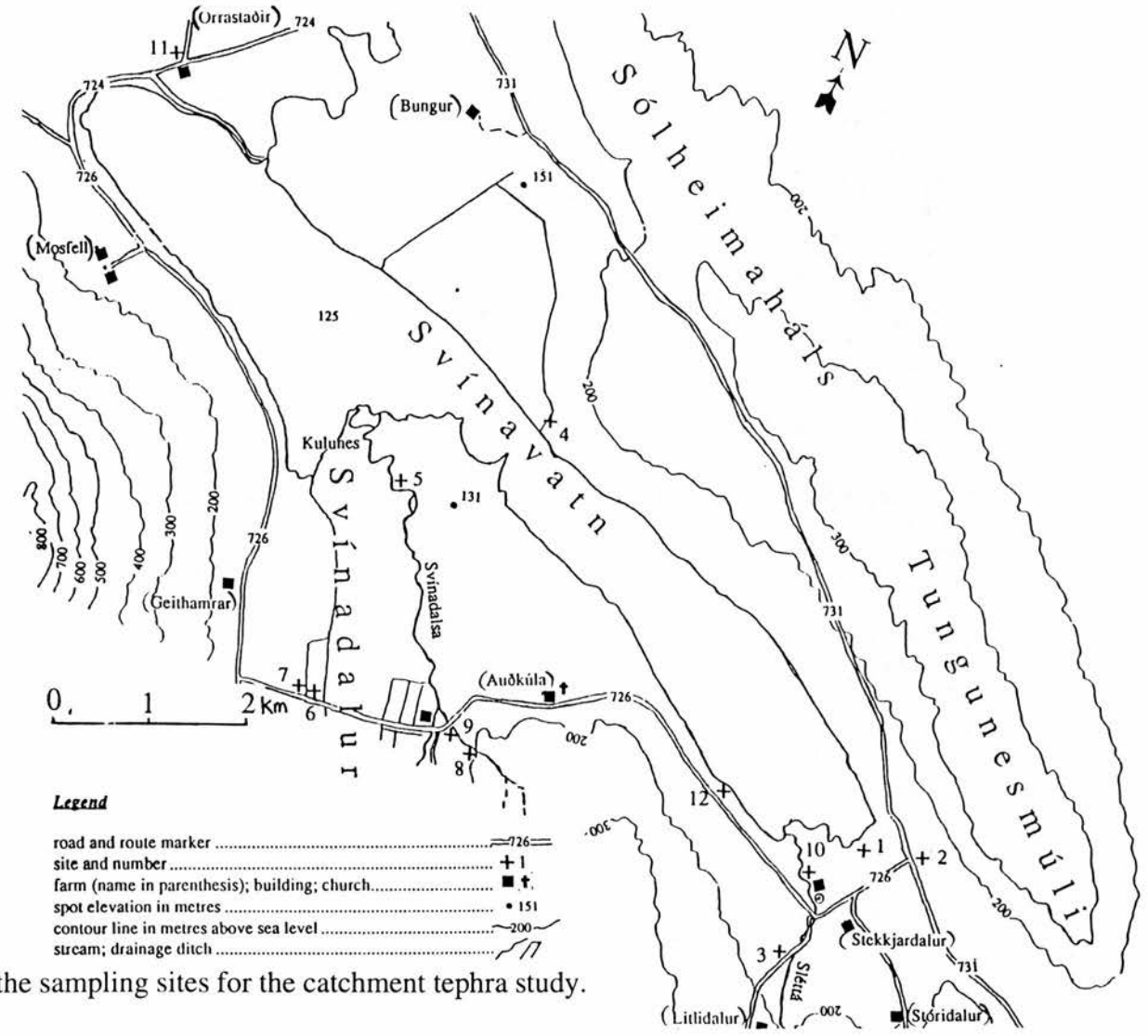

Figure 4.15 Location map showing the sampling sites for the catchment tephra study.

The cores from Svínavatn were examined using the NERC X-ray facility at BGS (Edinburgh). The optimum exposure times (2 minutes), current (5A) and voltage (44 kV) were determined experimentally for the first set of samples and then used as standard for all sections. The exposed film was processed using standard techniques. The structures apparent from the cores are described in Figure 5.1 along with the description of the colour and lithology.

Contiguous samples from two lake cores were taken for grain size analysis and loss on ignition. Loss on ignition was determined following the procedures outlined by Bengtsson and Enell (1986), firstly by oven drying samples at 105°C overnight until constant weight was attained. The samples were then ashed in a muffle furnace at 550°C for two hours. Some of the weight loss using this method may be due to loss of interstitial water (Bengtsson and Enell, 1986). However it does provide a quick, efficient indication of organic content. Tephra layers from all the cores were sampled using scalpels and spatulas. Not all tephra layers were visible; several deposits were more compact than the matrix material and could easily be detected by touch because of particle size/texture differences.

4.7.2 Acid digestion of lake and catchment samples

All samples from Svínavatn and the catchment profiles were cleaned thoroughly using acid digestion techniques (Persson, 1966; Dugmore, 1989). Forty millilitres of concentrated sulphuric acid were placed along with the sample in a conical flask and heated until no further reaction took place. Concentrated nitric acid pipetted slowly into the mixture was added until the solution was clear. This period of time was relatively short (about 30 minutes) because of the lack of contaminating organics in the lake sediments. The same method was used to separate tephra from the peat and soil samples, although the corresponding time to destroy all organic material was longer. The highly acidic solution was then neutralised with distilled water and bottled for future electron probe microanalysis following the procedures outlined in Chapter 3.

4.7.3 Particle size determinations

Grain size analysis of the tephra in the lake and catchment was made to determine the characteristics of the primary fallout layers, and to quantify any difference in the size distribution of the secondary layers. To provide an indication of the bottom dynamics operating in Svínavatn, the sediments of the two cores which contained the most detailed tephrostratigraphy were sampled. Grain size changes throughout whole cores are important to determine as particle size may also be used to infer erosional periods (Binford, 1983)

Sub-sampling of the lake cores can be made at regular, uniform intervals or according to sediment structure (Bengtsson and Enell, 1986). Examination of the X-radiographs of the lake cores showed that tephra layer and lamination thicknesses tend to range between 2.0-0.5 cm, therefore a uniform sampling interval of 0.5 cm would pick out any trends. Contiguous samples of 0.5 cm thickness were taken from lake cores 2 and 3, and oven-dried at 50°C overnight. Both dry and wet weights were measured to determine water content. Following procedures outlined by the U.K. Ministry of Agriculture Farming and Fisheries (MAFF Book 427) for the determination of particle size distribution of soil, 10 ml of ~30% m/V hydrogen peroxide solution was added to the dried sediment and allowed to stand for 30 minutes. Vigorous reactions to the acid were controlled by adding Octan-2-ol, and another 10 ml of H_2O_2 until no further reactions occurred. The samples were allowed to stand overnight at room temperature. Forty millilitres of distilled water was then added to the beakers and the mixture was heated on a thermostatically controlled hotplate at 90°C for one hour. The volume of the liquid was maintained at ~25 ml for this time and stirred frequently. Following cooling, the mixture was transferred to centrifuge tubes and centrifuged at 2000 rpm for 15 minutes. The clear supernatant liquid was decanted and discarded, and the solid residue retained for particle size analysis.

The acid treated sediment was then gently passed through a 63μm sieve using fingers to break up sediment aggregates. The sand fraction may be overestimated due to the

sieving procedure as excessive pressure was avoided to prevent glass shard disintegration. The > 63μm sand fraction was dried and weighed. The fine fraction (<63μm) remained in solution for determination of silt and clay proportions by sedigraph. The principles behind the sedigraph method of particle size analysis are outlined in Appendix 2; briefly the machine measures the sedimentation rates of particles dispersed in solution and automatically interprets these data in accordance with Stoke's Law to yield a cumulative mass % distribution in terms of Stokesian or equivalent spherical diameters (E.S.D.). To ensure standardisation of the results and minimise analytical error, the sedigraph was recalibrated each third sample and the first analyses of the day were repeated at the end to check machine drift. The percentages of silt and clay were recalculated to 100% total sample following the determination of the sand size fraction

4.7.4 Morphology of the glass shards

Sub-samples of the acid-digested tephra layers were pipetted onto microscope slides and examined using an optical microscope for shape characteristics and evidence of erosion. Each shard was placed in morphological categories based on vesicle abundance (rich/poor), vesicle shape (spherical/elongate), and shard shape (pumiceous/equant/rounded/angular). Colour was also noted during examination. The state of the shards was assessed by looking for evidence of rounded edges, presence of broken bubble walls, broken shards and anisotrophism.

5.1 Introduction

The aims of this chapter are firstly to identify geochemically and correlate tephra layers in the lake and in the catchment; secondly to identify the spatial and temporal pattern of tephra following initial fallout and during later periods of reworking and thirdly to determine the physical differences (if any) between primary and secondary tephra layers. The chapter is divided into two sections

- the tephrochronology of the lacustrine and terrestrial sites
- the grain size and morphology of the tephra layers compared to the grain size of the lake sediments

5.2 The tephrochronology of the catchment

5.2.1 Results and correlation on the basis of major element geochemistry

5.2.1.1 Description of the lake cores

Five cores were taken from Svínavatn; one from the centre of the western basin and four along the central axis and deepest section of the eastern basin (Figure 4.14). The lengths of the cores retrieved ranged from 83 cm (core 2) to 132 cm (core 3). The colour, lithology and stratigraphy of each core are shown in Figure 5.1. The main points to note are that all the cores from the eastern basin contain tephra layers and finely-banded sediments alternating with coarsely-bedded sediments. There was no tephra in core 5 from the western basin. Cores 1 and 4 comprise uniform olive brown (2.5Y 4/3) fine silt, although the x-radiographs highlight the laminations. Cores 2 and 3 are visually very different, with a yellow brown (2.5Y 7/6) matrix containing clear banding of orange (7.5YR 5/6) and brown (2.5Y 5/3) silt. Cores 1 and 4 contain only one tephra layer at the top of the section, whilst cores 2 and 3 have 10 and 9 tephras respectively.

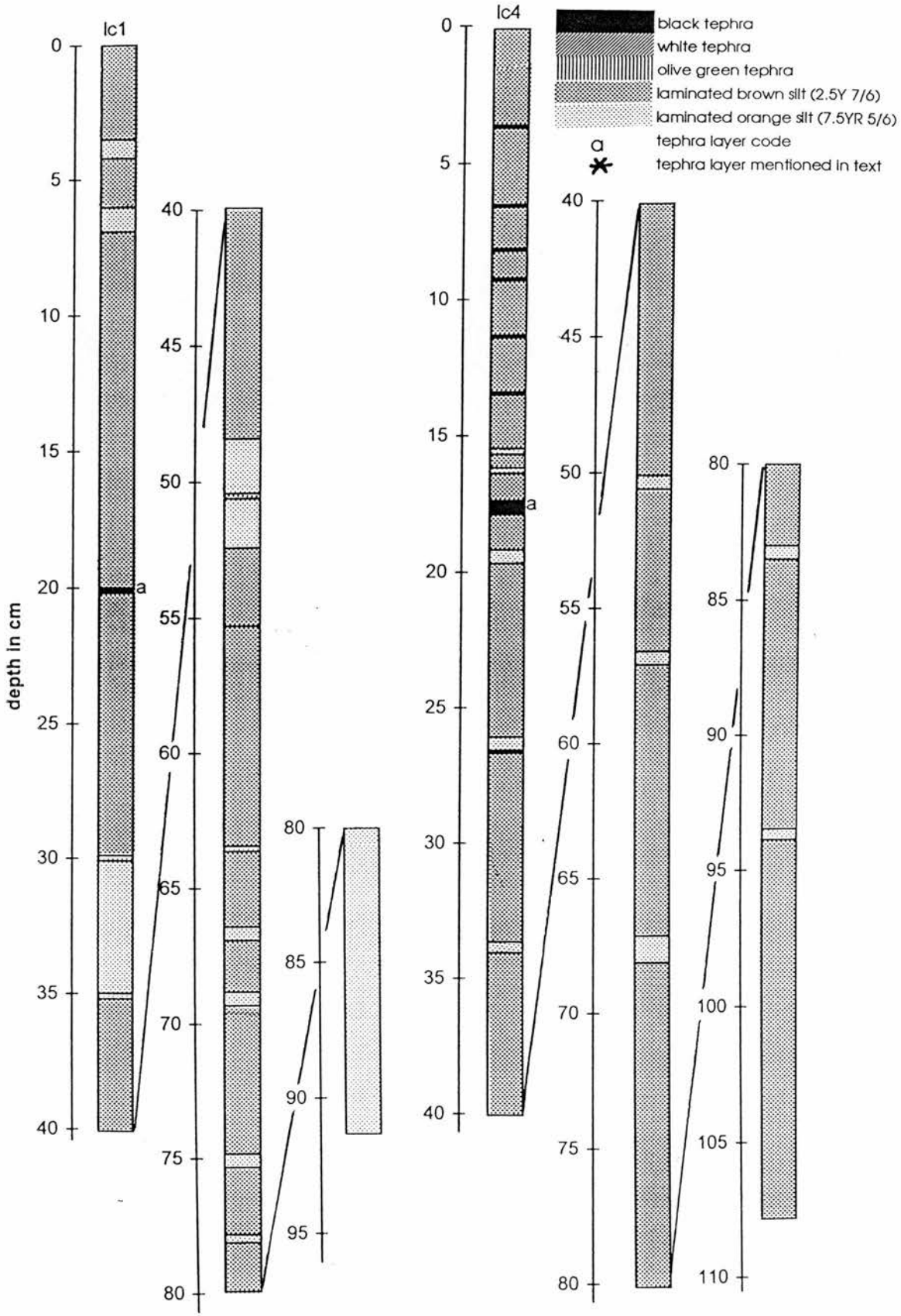

Figure 5.1 Stratigraphy of the Svínavatn lake cores showing tephra layers and sediment structure.

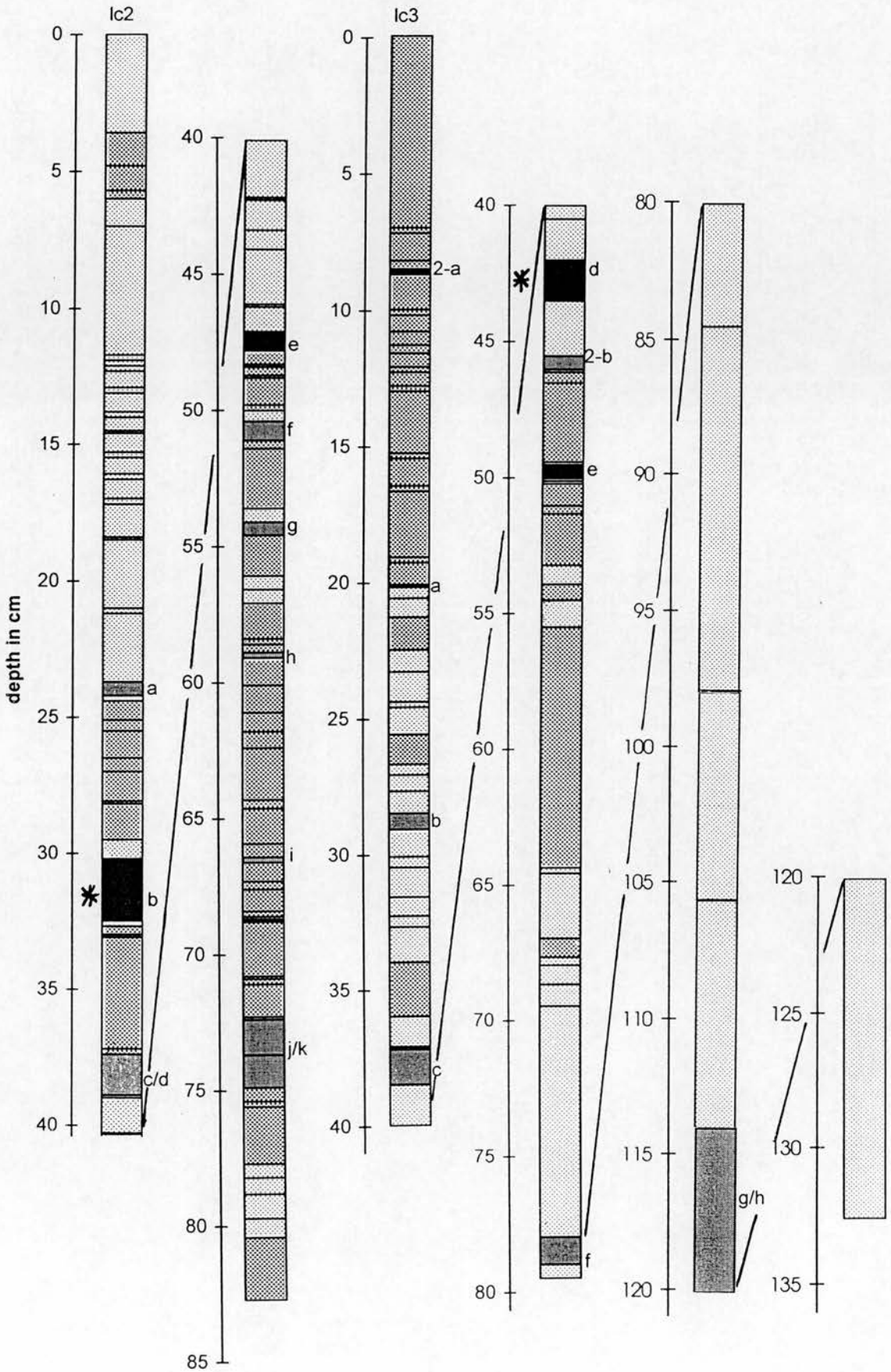
Ic2
Ic3
depth in cm
0
5
10
15
20
25
30
35
40
45
50
55
60
65
70
75
80
85
a
b
c/d
e
f
g
h
i
j/k
2-a
a
b
c
d
2-b
e
f
g/h

The tephra layers appear as dense bands in the X-radiograph negatives, usually with a sharp bottom contact and diffuse upper boundary. This can be seen clearly in core 2 where tephra b (31.6-33.1 cm) lies above unlaminated brown sediment. Other tephra layers are less clear on the x-radiographs, for example tephra d (42-43.5 cm) in core 3 is a coarse grained (>20μm) black tephra and appears dark on the negatives in comparison to other layers of minerogenic material with no apparent structure. The thickest and most visible tephra from the lake sites is a white coarse grained ash found at the bottom of cores 2 and 3 (at 71.6-73.1 cm and 114-120 cm respectively). The lower unit consists of large pumiceous grains of tephra, fining upwards and changing in colour from white to yellow grains. The structure is loose and friable. The upper unit consists of clay-size grey tephra which has consolidated into a resistant layer. In core 2 there are 3 more white tephra layers at 23-24.7 cm, 38.2-39 cm and 50-50.3 cm. In addition to the coarse white tephra, core 3 has 4 white tephra layers at 29.2-30 cm, 38.1-38.6 cm, 46-4.5 cm and 80-81 cm. All the white tephras are pale yellow/white silt size deposits. Core 2 contains 6 black tephras and core 3 has 4 black tephra layers. Cores 1 and 4 contain only one tephra each, a black layer at 20-20.5 cm and 16.3-16.8 cm respectively.

5.2.1.2 Soil and peat profiles

Twelve sites were chosen around the catchment to be representative of different landscape units. Profiles were measured in blanket peats, hillslope peaty silts, aeolian deposits, complex slope deposits and alluvial flood plain sections (Figure 4.15). The depths of the profiles ranged from 80-190cm. A large block of peat (monolith) of the top 30 cm was sampled at site 3 at Stekkjardalur. The number of tephra layers in each pit ranged from 1 to 17. In total, 73 tephra layers were sampled from catchment sites and analysed. A detailed description of the location, general stratigraphy and tephrostratigraphy of each profile is provided in Table 5.1 and Figure 5.2 a-l.

Site name and grid reference	Site description	Description of general stratigraphy	Tephrostratigraphy
pit 1 (65°30'30"N, 19°57'20"W)	North side of drainage ditch in cultivated peatland at crossroad of route 726 and Stekkjardalur farm. Ditch oriented parallel to lake shore, 131cm deep.	Horizontal topography, no frost disturbance or early cultivation. Top 10cm missing (ploughed?). Alternate layers of poorly humified light peat (68, 93, 101 cm). Red woody peat (90 cm).	Six tephra layers. Two black deposits in top 26 cm; three white tephras at 33, 49, 82 cm; one olive green tephra at 42.5 cm.
pit 2 (65°30'40"N, 19°56'45"W)	Drainage ditch running uphill, perpendicular to contours at crossroad of routes 725, 731. Peat deposit 157 cm deep overlying gravel.	Disturbed peat with several tephra layers repeated. Sloping stratigraphy. Red woody peat (77-92 cm). Well humified peat below white tephra at 114.5 cm.	Twelve white tephra layers; two black tephras; three greenish tephras. Thick white tehras at 93.5-96.5 cm and 102.5-114.5 cm, coarsening upwards.
pit 3 (65°29'45"N, 19°57'45"W)	Monolith from ditch parallel to Litlidalur farmtrack. Gently rising peatlands to west, Sletta river to east.	Horizontal topography. Thick root/turf mat above poorly humified light brown peat. Lower section red, well humified peat.	Four white tephras in monolith 30 cm long. Thick orange/white coarse layers at 16.5 and 20.5 cm; one black tephra at 10.5 cm; olive green tephra at 19 cm.
pit 4 (65°31'55"N, 20°3'20"W)	Ditch in gently sloping peatland on northern shore of Svínavatn. Running perpendicular to slope, 1.5 m deep.	Disturbed peat although layers are essentially straight. Light brown peat overlying band of brown woody peat at 66.5-73.5 cm.	Five white tephras; the youngest at 21 cm coarsening upwards, two orange mottled white layers at 49 and 64 cm. Six black tephras; one greenish layer.
pit 5 (65°31'20"N, 20°5'0"W)	Eastern bank of Svínadalsa river, exposed section in thin cover of marshy peat. High þúfa density on surface.	Silty alluvium alternating with unsorted sub-angular gravel deposits. Lower section of sandy alluvium 26.5-76.5 cm mottled from pale grey brown to heavily oxidised.	One black tephra at 10.5 cm.
pit 6 (65°30'10"N, 20°4'40"W)	Old channel of the Svínadalsa used as drainage ditch, just north of route 726.	Disturbed section of woody peat. Dense twig mat at 20 cm plus charcoal (?trackway). irregular lenses of white tephra throughout peat.	Coarse olive green tephra below twig mat at 22 cm; fine green tephra at 55 cm; coarse white tephra mixed in deposit above twig mat; two discrete layer of white tephra at 84 and 128 cm.
pit 7 (65°30'10"N, 20°4'40"W)	Opposite bank of drainage ditch to above section.	Homogenous peat deposit, 80 cm thick.	One white tephra at 40 cm.

Table 5.1 Summary descriptions of Svínavatn catchment profiles.

Site name and grid reference	Site description	Description of general stratigraphy	Tephrostratigraphy
pit 8 (65°30'10"N, 20°23'0"W)	Southern bank of gully section where tributary stream of the Svínadalsa crosses 200m contour. Further upstream gully erosion has exposed 10m thick deposit of laminated clays beneath peat.	Top section shows three generations of þúfa approx. 50 cm high with peat draping these hummocks. Layers below top black tephra are horizontal.	One black tephra at 60 cm just below þúfa; three white tephras at 70, 87.5 and 95 cm; one olive green tephra at 75 cm.
pit 9 (65°30'10"N, 20°23'0"W)	Southern bank of gully section downstream of previous profile, south of route 726 where roads bends after crossing Svínadalur.	Turf wall approx. 50 cm high above top black tephra layer with infilling on sides. Straight peat deposits. Disturbance of peat around bottom white tephra. Woody peat below this layer above greenish tephra and clay base.	One black tephra below turf wall; three white tephras at 70, 100 and 115 cm (faulting in thick bottom unit); two olive green tephras 79 and 99 cm, patchy in extent with irregular contacts.
pit 10 (65°30'20"N, 19°57'70"W)	Excavated bank of the Slétta, in marshy peatland 100m west of the community centre.	Thick root mat overlying silt deposits which are irregularly banded and mottled. Alternate units of gravel crudely banded, light grey brown and orange grey brown. Clay layer at 160 cm.	Several black tephras; discrete layers at 20, 31 and 100cm and as dispersed lenses in silt deposits. Two white layers at 70 and 135 cm, the lower is weathered; one patchy olive green tephra 105 cm.
pit 11 (65°32'50"N, 20°9'45"W)	Drainage ditch in peatland at far western point of Svínavatn. At junction of route 724 and track to Orrastaðir farm.	No disturbance of peat. Very straight stratigraphy of light brown peat overlying red woody peat.	Three white tephras at 17, 46, 65 cm, the youngest deposit coarsening upwards; two olive green tephras at 25 and 105 cm.
pit 12 (65°30'50"N, 19°59'70"W)	Drainage ditch perpendicular to slopes on southern shore of Svínavatn. Off route 726, 1km from bend at Auðkúla.	Thick deposit (122 cm) of loessial soil and silty peat. Top unit of disturbed soil with cobbles atop banded organic silts. Disturbed throughout.	Three discrete white tephras at 58, 91 and 98 cm; white pumice grains throughout.

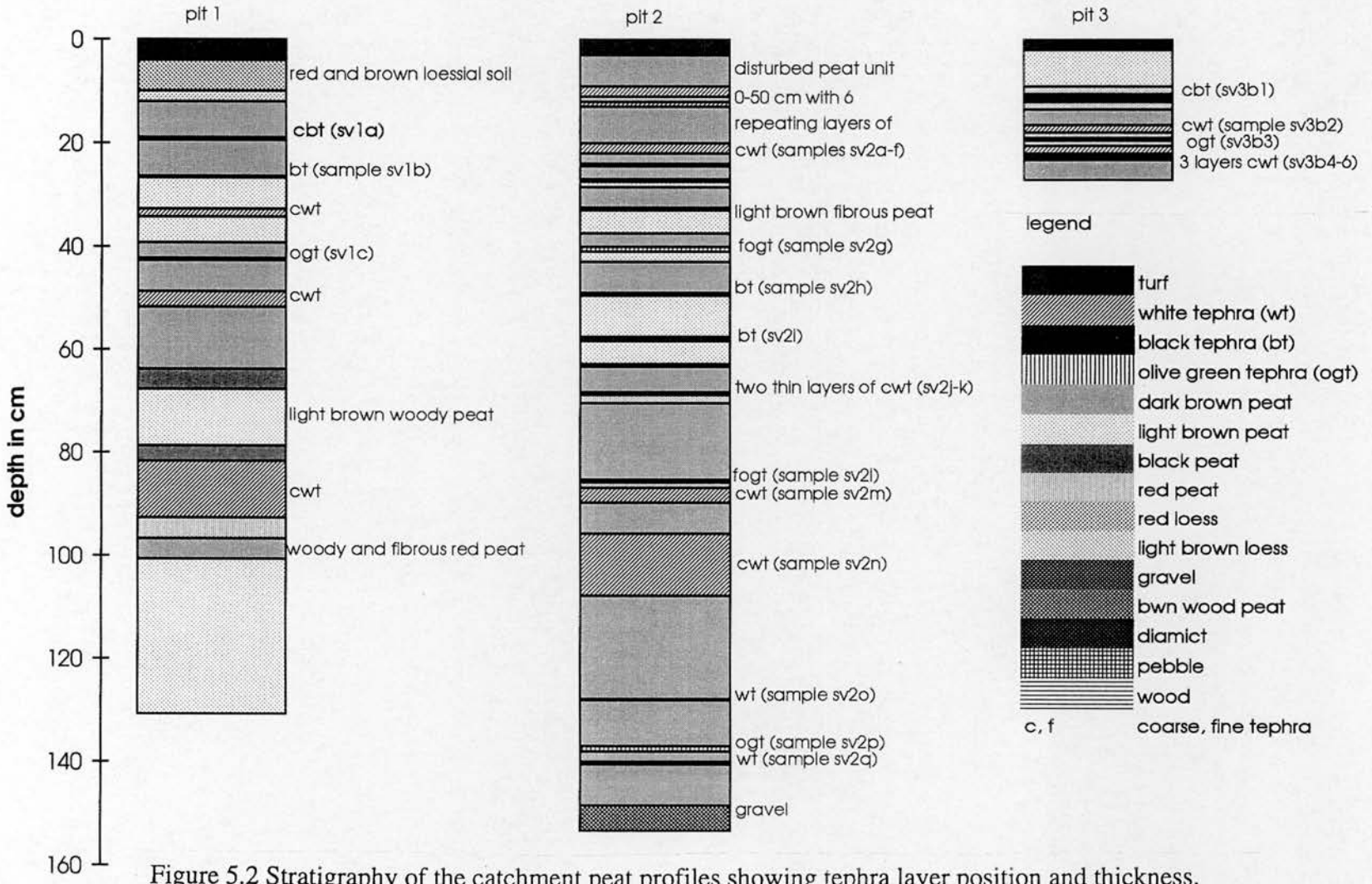

Figure 5.2 Stratigraphy of the catchment peat profiles showing tephra layer position and thickness.

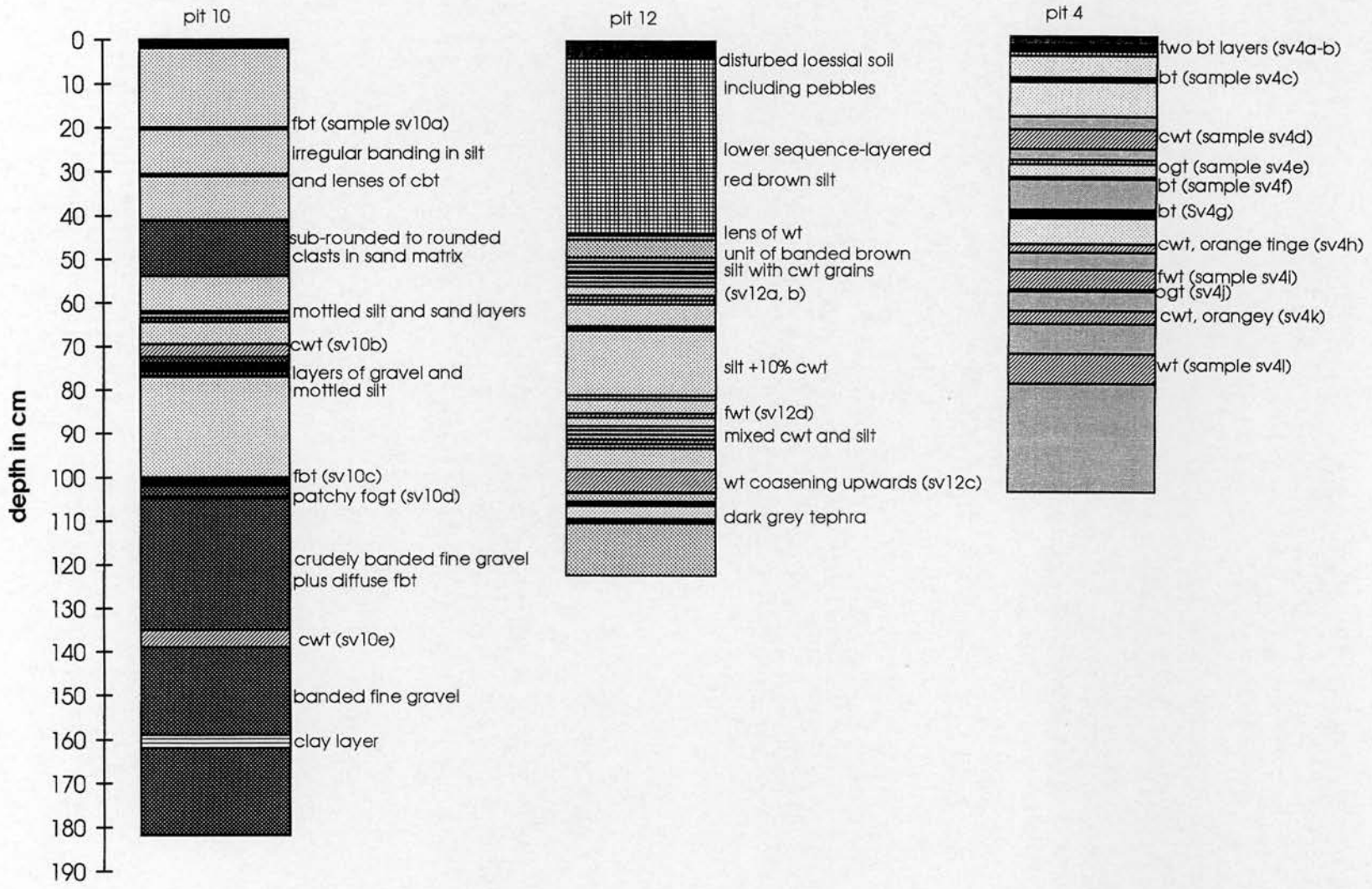
pit 10
pit 12
pit 4
depth in cm
0
10
20
30
40
50
60
70
80
90
100
110
120
130
140
150
160
170
180
190
fbt (sample sv10a)
irregular banding in silt
and lenses of cbt
sub-rounded to rounded
clasts in sand matrix
mottled silt and sand layers
cwt (sv10b)
layers of gravel and
mottled silt
fbt (sv10c)
patchy fogt (sv10d)
crudely banded fine gravel
plus diffuse fbt
cwt (sv10e)
banded fine gravel
clay layer
disturbed loessial soil
including pebbles
lower sequence-layered
red brown silt
lens of wt
unit of banded brown
silt with cwt grains
(sv12a, b)
silt +10% cwt
fwt (sv12d)
mixed cwt and silt
wt coasening upwards (sv12c)
dark grey tephra
two bt layers (sv4a-b)
bt (sample sv4c)
cwt (sample sv4d)
ogt (sample sv4e)
bt (sample sv4f)
bt (Sv4g)
cwt, orange tinge (sv4h)
fwt (sample sv4i)
ogt (sv4j)
cwt, orangey (sv4k)
wt (sample sv4l)

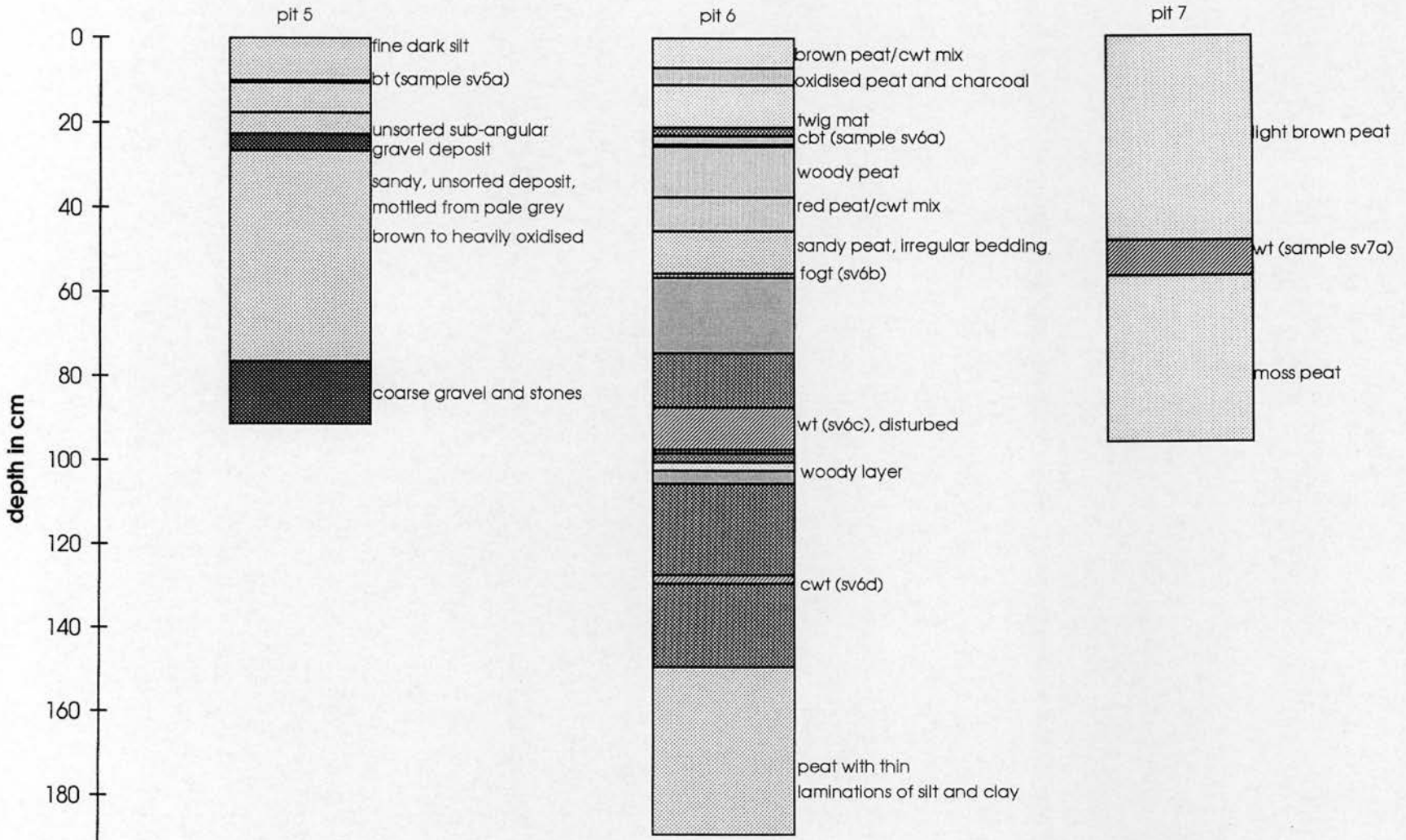
depth in cm
0
20
40
60
80
100
120
140
160
180
200
pit 5
fine dark silt
bt (sample sv5a)
unsorted sub-angular gravel deposit
sandy, unsorted deposit, mottled from pale grey brown to heavily oxidised
coarse gravel and stones
pit 6
brown peat/cwt mix
oxidised peat and charcoal
twig mat
cbt (sample sv6a)
woody peat
red peat/cwt mix
sandy peat, irregular bedding
fogt (sv6b)
wt (sv6c), disturbed
woody layer
cwt (sv6d)
peat with thin laminations of silt and clay
pit 7
light brown peat
wt (sample sv7a)
moss peat

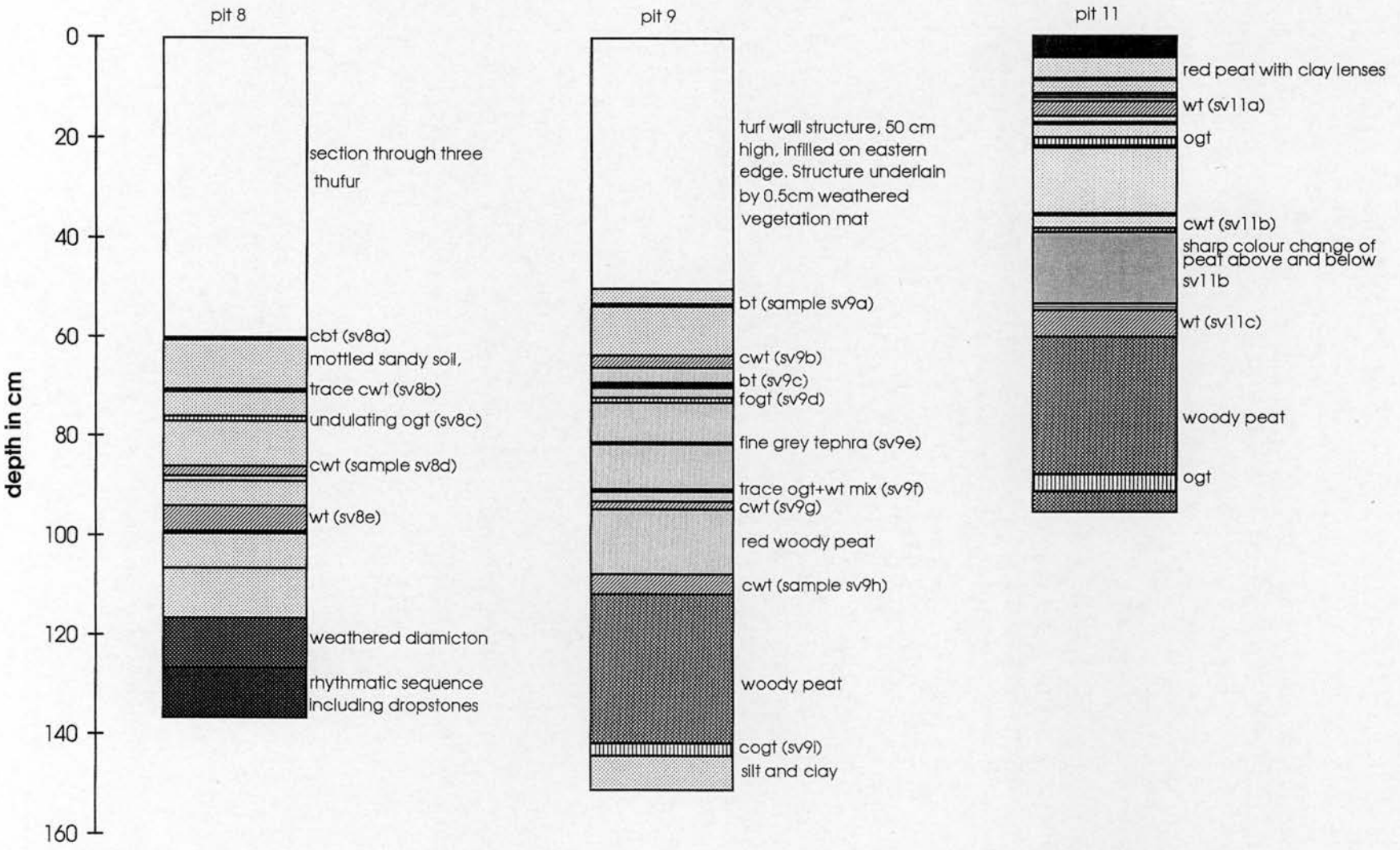
depth in cm
0
20
40
60
80
100
120
140
160
pit 8
section through three thufur
cbt (sv8a)
mottled sandy soil,
trace cwt (sv8b)
undulating ogt (sv8c)
cwt (sample sv8d)
wt (sv8e)
weathered diamicton
rhythmatic sequence including dropstones
pit 9
turf wall structure, 50 cm high, infilled on eastern edge. Structure underlain by 0.5cm weathered vegetation mat
bt (sample sv9a)
cwt (sv9b)
bt (sv9c)
fogt (sv9d)
fine grey tephra (sv9e)
trace ogt+wt mix (sv9f)
cwt (sv9g)
red woody peat
cwt (sample sv9h)
woody peat
cogt (sv9l)
silt and clay
pit 11
red peat with clay lenses
wt (sv11a)
ogt
cwt (sv11b)
sharp colour change of peat above and below sv11b
wt (sv11c)
woody peat
ogt

Pit 1 in the Stekkjardalur area of the lake contains 6 tephra layers; two black tephras in the top 26 cm, three white tephras at 33, 49, and 82 cm, and an olive green tephra at 42.5 cm depth (Figure 5.2a). The lowermost tephra at 82 cm depth is a white tephra coarsening upwards. The second lowest white tephra, the layer at 49 cm, contains white ash from the initial part of the eruption which grades upwards into darker yellow/orange and brown grains. The uppermost white tephra is coarse throughout with no grading or colour changes. In contrast to the tephrostratigraphy of pit 1, site 2 contains 12 white tephra layers, two black tephras and three greenish layers (Figure 5.2b). The thickest layer at 102.5-114.5 cm depth is a white tephra coarsening upwards, above which at 93.5 cm, lies a white tephra grading upwards into orangey coloured grains. All the remaining white tephras are coarse grained with an average thickness of layer of 1 cm. This pit is sited at the bottom of a slope and the stratigraphy slopes gently to the south. At site 3 a monolith was taken of the top 30 cm of the profile. There are four white tephras in this section, mainly orangey white and of coarse grained texture (Figure 5.2c). The monolith also contained one black and one greenish tephra.

Pit 4 contains five white tephras, the oldest of which is a thick (9cm) white tephra coarsening upwards (Figure 5.2d). Above this tephra at 64 cm is a coarse orangey white tephra layer. The white layers above this deposit alternate between predominantly fine and coarse textures; the tephra layer at 48 cm depth also has an orange tinge. There are five black tephra layers and two olive green tephras within the sloping stratigraphy. Pit 5 has a simple tephrostratigraphy with one black tephra at 40 cm depth in a deposit of alternating bands of silt and gravel (Figure 5.2e). Pit 6 consists of woody peat with a disturbed top section of twigs and lenses of white tephra (Figure 5.2f). Charcoal is present at the level of the dense twig mat (depth 20 cm) as is a layer of coarse black/green tephra. There are no distinct layers of white tephra although there are thick deposits of coarse white tephra dispersed within the peat at 88 cm, and 128 cm.

Site 7 lies on the opposite bank of the ditch from pit 6 but in contrast contains one tephra layer, a thick white tephra coarsening upwards (40 cm depth-Figure 5.2g). Pits 8 and 9 have a thick deposit of peat in the top half of each profile. Pit 8 contains hummocky peat showing the outline of þúfur within the peat (Figure 5.2h). Below this section lies one coarse black tephra, three white tephras (the lowermost coarsens upwards, the second contains darker grains, the upper appears as a trace) and one olive green tephra. Pit 9 has a turf wall structure in the top 50 cm with infilling on the eastern edge (Figure 5.2i). A coarse black tephra lies below it. This site contains three white tephras similar in appearance to pit 8 as well as two black tephras, two olive green deposits (the lower of which contains white pumice grains), a coarse green tephra and a grey tephra.

Site 10 consists mainly of banded silt and gravel deposits (Figure 5.2j). There are lenses and traces of black tephra in addition to three distinct layers. The lowest tephra deposit is a coarse white tephra. Another coarse white tephra can be found at 70 cm depth. Site 11 in peatland at the NW end of the lake contains three white tephra layers, the oldest and youngest both coarsening upwards; the middle deposit is coarse throughout, grading into orange/brown grains (Figure 5.2k). Site 12 contains two distinct white tephra layers at 60 and 98 cm depth, but white tephra grains appear throughout the loessial soil deposit and thick upper unit of cobbles (Figure 5.2l).

In summary, there are 5 sites with undisturbed deposits of peat/silt and tephra (pits 1, 6, 8, 9, 11). Stability at the sites is indicated by flat stratigraphy and non-repeating sequences of tephra. The tephrostratigraphy in these pits consists of three thick white tephra layers, one olive green tephra and one to two black tephra deposits. The lowermost white tephra is the thickest deposit at all the sites ranging from 4cm to 12 cm. The deposit is white throughout, coarsening upwards. The middle white tephra deposit is relatively thick (1-3 cm) but the deposit remains coarse throughout with a distinct colour change from white through yellow and orange to brown grains. The uppermost white tephra is white throughout, coarsening upwards. This tephra is of

greatly variable thickness and appears patchy in extent with irregular contacts in several pits.

The remaining sites (pits 2, 3, 4, 10, 12) appear to have disturbed stratigraphy and/or contain tephra in addition to the three thick white tephra layers, one olive green tephra and two black tephras described in earlier pits. Site 2 is the only profile to contain a white tephra layer below the lowermost thick white layer. Two sites (5 and 7) contain only one tephra layer. Sites 6 and 9 have evidence of disturbance of the peat by humans with a deposit of worked wood, and the presence of a turf wall respectively in the top sections.

5.2.2 Radiocarbon dating of deposits

The tephra layers in the catchment and lake were correlated on the basis of the geochemistry of the glass shards and matched with reference samples and published data. The correct identification of two of the important Hekla tephra layers (H4 and H3) was supported by radiocarbon dating of peat deposits immediately below the two tephra layers at site 9 (Auðkúla) and at site 11 (Orrastaðir at the NW of the basin). Samples for dating were taken in August 1991 and used in The International Radiocarbon Intercalibration Programme (Scott *et al..*, 1994; Hall *et al..*, 1994). The mean uncalibrated radiocarbon dates for the peat below H4 and H3 at Svínavatn are 3834±15 and 2855±24 BP (Dugmore *et al..*, submitted).

5.2.3 Geochemical correlation in lake and catchment

The geochemistry of the glass fraction of each tephra layer was determined by electron probe microanalysis, and the results plotted against data for tephras known to have fallen in northern Iceland. On the basis of published sources, the expected tephrostratigraphy in the Svínavatn area would be H5, H4, H3, Vö~900 (Landnamslag) and H1 plus several historical Hekla and Katla ashes (Þórarinsson, 1958, 1967; Einarsson, 1963; Larsen and Þórarinsson, 1977).

5.2.3.1 H5 in the catchment

The isopach map for H5 (Þórarinsson 1976) indicates a NNE wind direction for the fine grained ash and a thickness of approximately 1cm at Svínavatn (Figure 4.1). The age of H5 (~6600 BP) suggests that the layer, if present, will be close to the base of the soil/peat cover, which started forming at the end of the last glacial period. The only site in the catchment with a thin white tephra layer near the base is pit 2 on the northern edge of the lake. The geochemistry of the glass shards from this layer (Sv2q 139.5-140 cm) is listed in Appendix 3. The glass is highly silicic (SiO_2 content >71%) indicating that the tephra came from an evolved acidic centre such as Hekla or Snaefellsjökull. Sodium and potassium contents of the analysed glass are both high at around 4%, giving a Na_2O:K_2O ratio of around one. This ratio is not indicative of Hekla and the transitional alkali basalts of the Southern Volcanic Zone; therefore the lowest white tephra layer in the Svínavatn area is probably from Snaefellsjökull. Figure 5.3 shows this split clearly in a biplot of silica against alkalis for the Hekla and Snaefellsjökull volcanic systems.

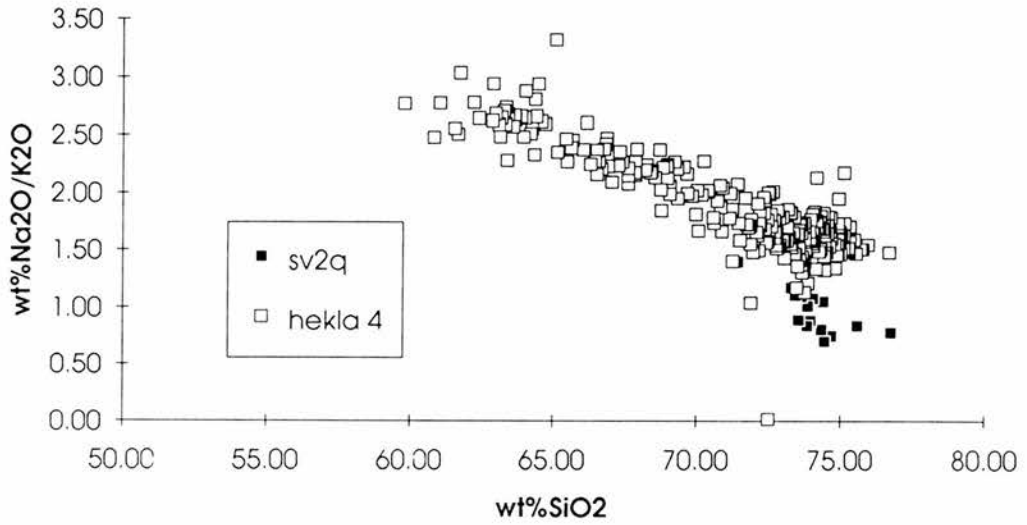

Figure 5.3 Bi-plot of silica:alkali ratios for Hekla tephras and sample Sv2q (139.5-140 cm). Sample Sv2q has alkali ratios of around 1 suggesting Snaefellsjökull volcanic system as a possible source.

The only tephra layers from Snaefellsjökull which are well mapped and dated are Sn1, Sn2, Sn3 (Figure 4.9), however the results of the geochemical analysis of these

tephras have not been published. The depth of layer Sv2q which is close to the gravel base suggests the tephra may be Sn3 with a date of 7000-9000 BP, but conclusive identification cannot be made without geochemical correlation. From the data available, the lowest white tephra layer in the catchment originates from the Snaefellsjökull volcanic system and furthermore H5 is not present at Svínavatn. This layer is termed SSn throughout the remaining chapters.

5.2.3.2 H4 deposits in Svínavatn and catchment

From the profile descriptions it is clear that at the bottom of the sections, nine profiles contain a thick (4-12 cm) deposit of white tephra coarsening upwards. The geochemistry of the glass (Appendix 3) shows it is highly silicic (>70% SiO_2). In addition the alkali ratios indicate that the tephra originates from the southern volcanic zone (transitional alkali basalts) (Imsland, 1978; Jakobsson, 1979). The data from the nine sections were plotted against the geochemical field for iron/titanium variations in H4 (Figure 5.4). It can be seen that the data fit the reference sample well. Each sample clusters around the initial part where both iron and titanium are low. There are no analyses which match the later parts of the eruption when iron and titanium appear to increase. The amount of iron and titanium in tephra is primarily a reflection of silica content, both being inversely proportional to SiO_2 abundance. As an eruption progresses, the silica content decreases and the tephra becomes more basaltic. As outlined above, the initial eruption of H4 was characterised by white tephra deposited in the north by prevailing winds (Larsen and Þórarinsson, 1977). As the eruption continued, less silicic, more iron and titanium rich tephra was produced but a change in wind direction meant that this phase was not blown north. The geochemistry, homogeneity of the sample and the stratigraphic position of these layers suggest that the layers in these nine sections are primary deposits of H4. No similar deposit was found in the lake cores. Figure 5.6 shows the location of the pits which contain this tephra.

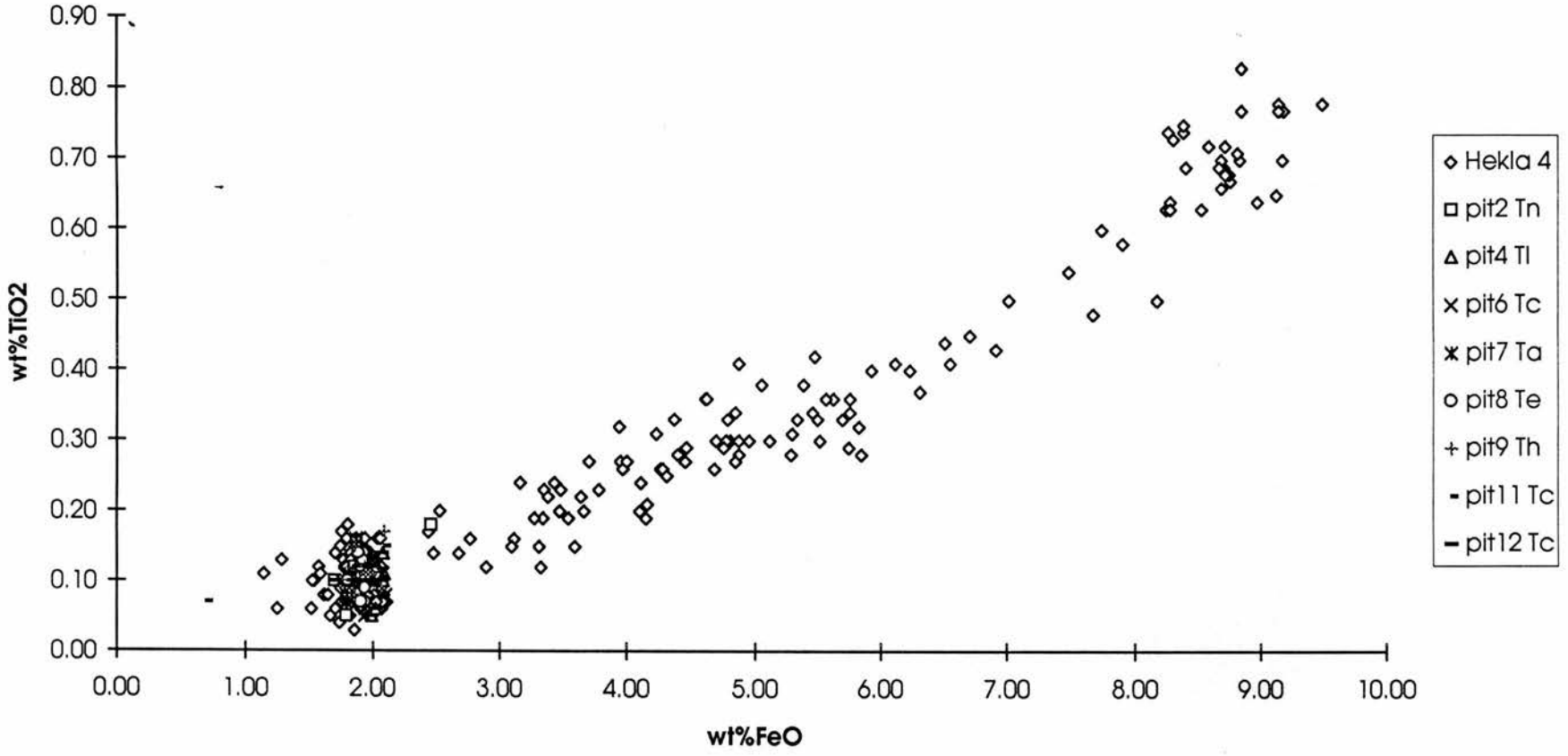

Figure 5.4 Bi-plot showing Fe-Ti variations in the geochemical analyses of the lowermost thick white tephra layers, compared with published data for H4 (source: Dugmore *et al.*, 1992).

5.2.3.3 H3 in Svínavatn and catchment

The position, thickness and colour variations of the white tephra layer found 6-30 cm above H4 in most pits and in two lake cores, indicate that it is H3. Figure 5.5 is a bi-plot of these samples compared with the reference sample for H3 supplied by Guðrún Larsen. This sample contains only the initial phase when iron and titanium are low, but it is clear from the diagram that the fallout around Svínavatn contains the full geochemical range as indicated by Þórarinsson's map and data. Therefore, the increase in iron and titanium throughout the eruption reflect the decrease in silica content of the glass. The Figure also shows that the trend for H3, although continuing in the same direction as H4 and overlapping slightly, has proportionally more titanium (and therefore less silica) throughout the course of the eruption. The colour changes in the tephra support this conclusion with the grading of white ash, which is indicative of high silica content, during the initial plinian phase of the eruption into darker yellow/orange and brown grains subsequently. The location of pits and lake cores containing H3 are found on Figure 5.6.

5.2.3.4 Hekla 1 in Svínavatn and catchment

Six sections (1 and 8-12) in the catchment contain a third white tephra layer between 13.5-62 cm above the layer identified as H3. This upper layer is white ash coarsening upwards, approximately 1-3 cm thick. This tephra is also present in the monolith taken from site 3 but is missing from profiles 5, 6, and 7. The remaining two sites (Sv2 and Sv4) contain several white tephra layers in the peat above H3. The geochemical data for the uppermost white tephra layer from all the profiles were plotted against the reference data set for H1 (Figure 5.7). The analyses cluster around the reference data where iron oxide content is approximately 3% and titanium oxide about 0.15-0.25%. There are no increases in either oxide throughout the layers and therefore no H3-like trend is produced. This cluster however overlaps with the geochemistry of H3 during the initial part of that eruption and therefore it is difficult to separate products from the start of each eruption. However the primary airfall

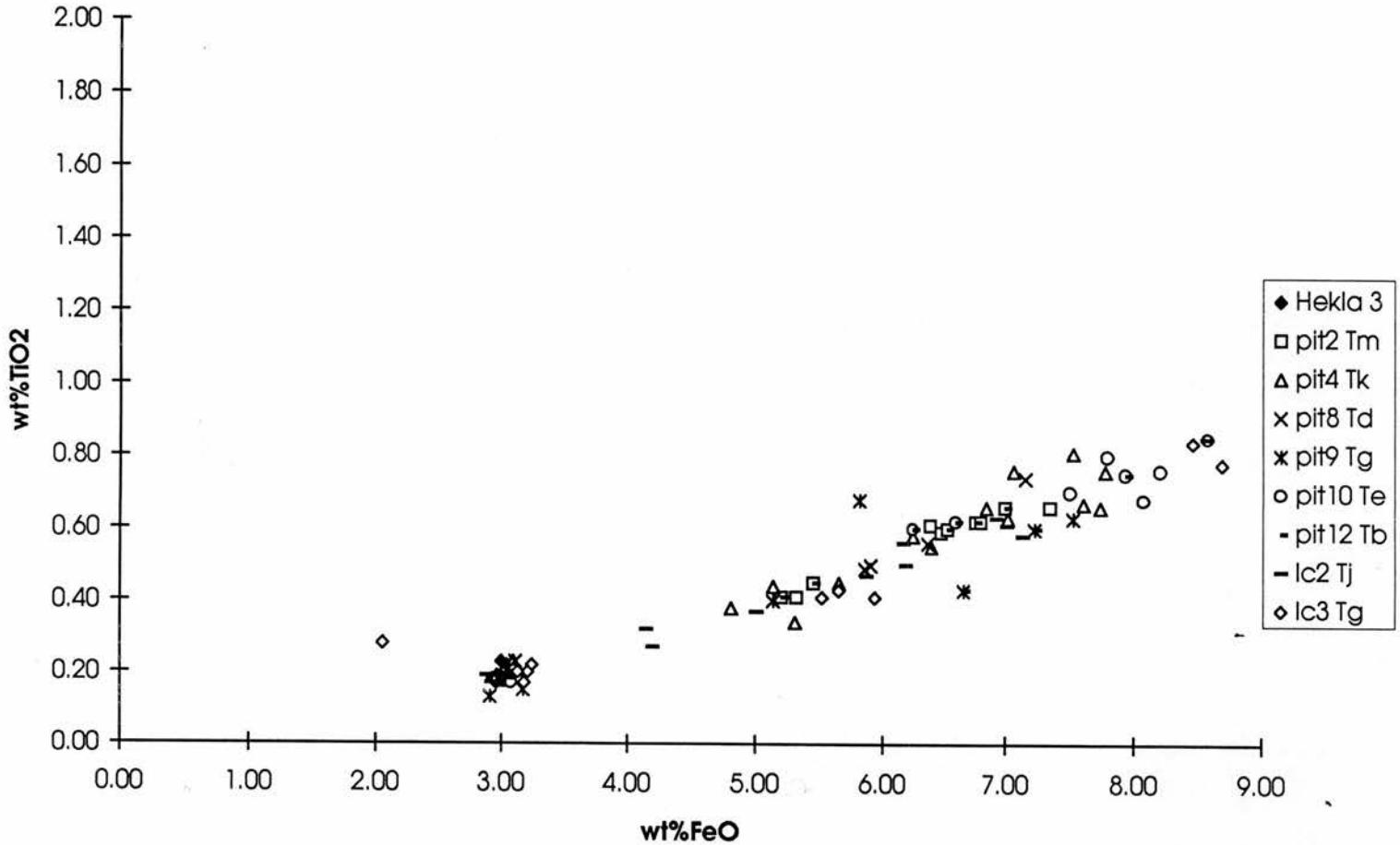

Figure 5.5 Bi-plot showing Fe-Ti variations in the geochemical analyses of the middle orange/white layer, compared with reference data for H3 (*source*: Guðrún Larsen, Volcanological Institute, Reykjavík).

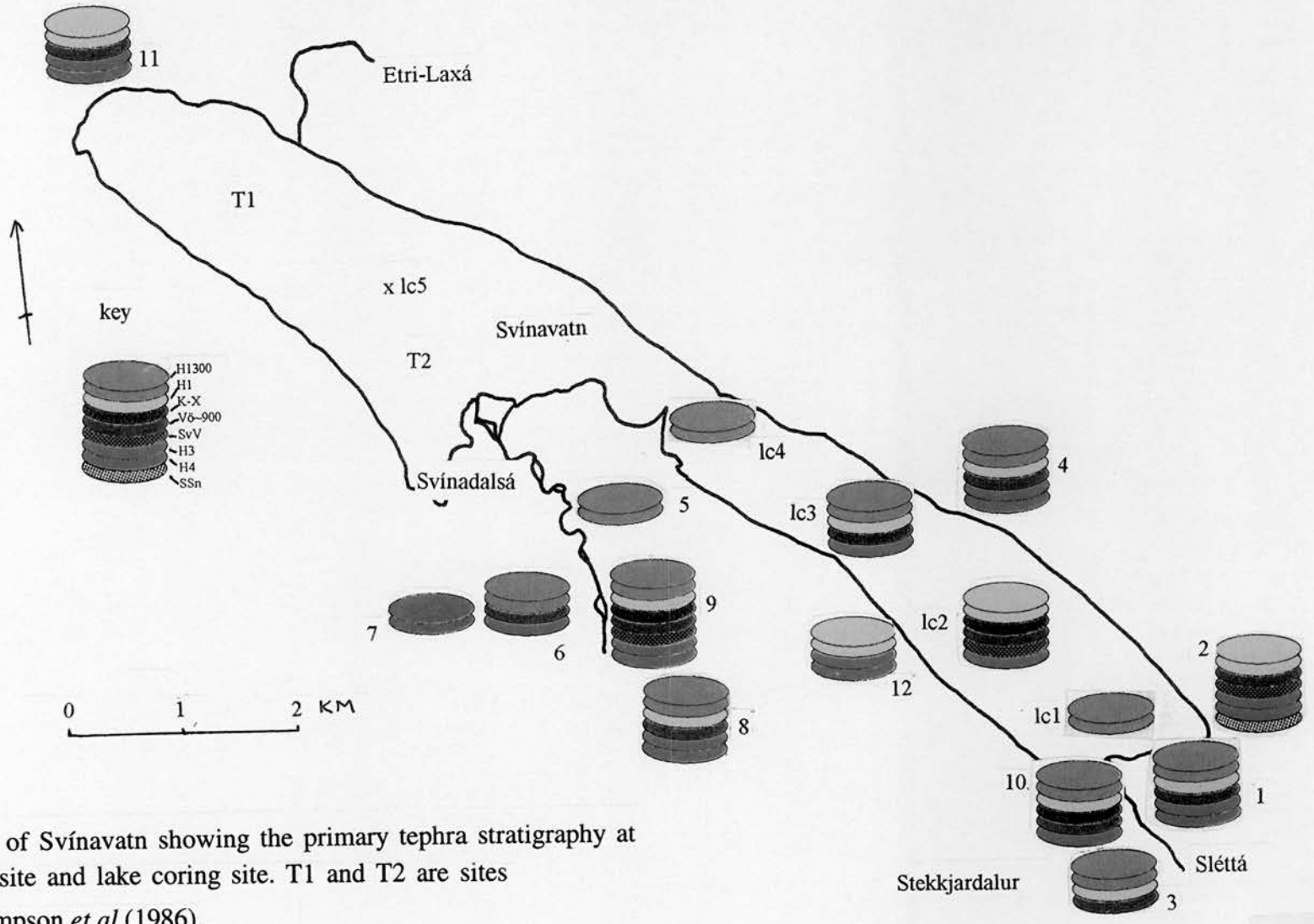

Figure 5.6 Map of Svínavatn showing the primary tephra stratigraphy at each catchment site and lake coring site. T1 and T2 are sites sampled by Thompson *et al* (1986).

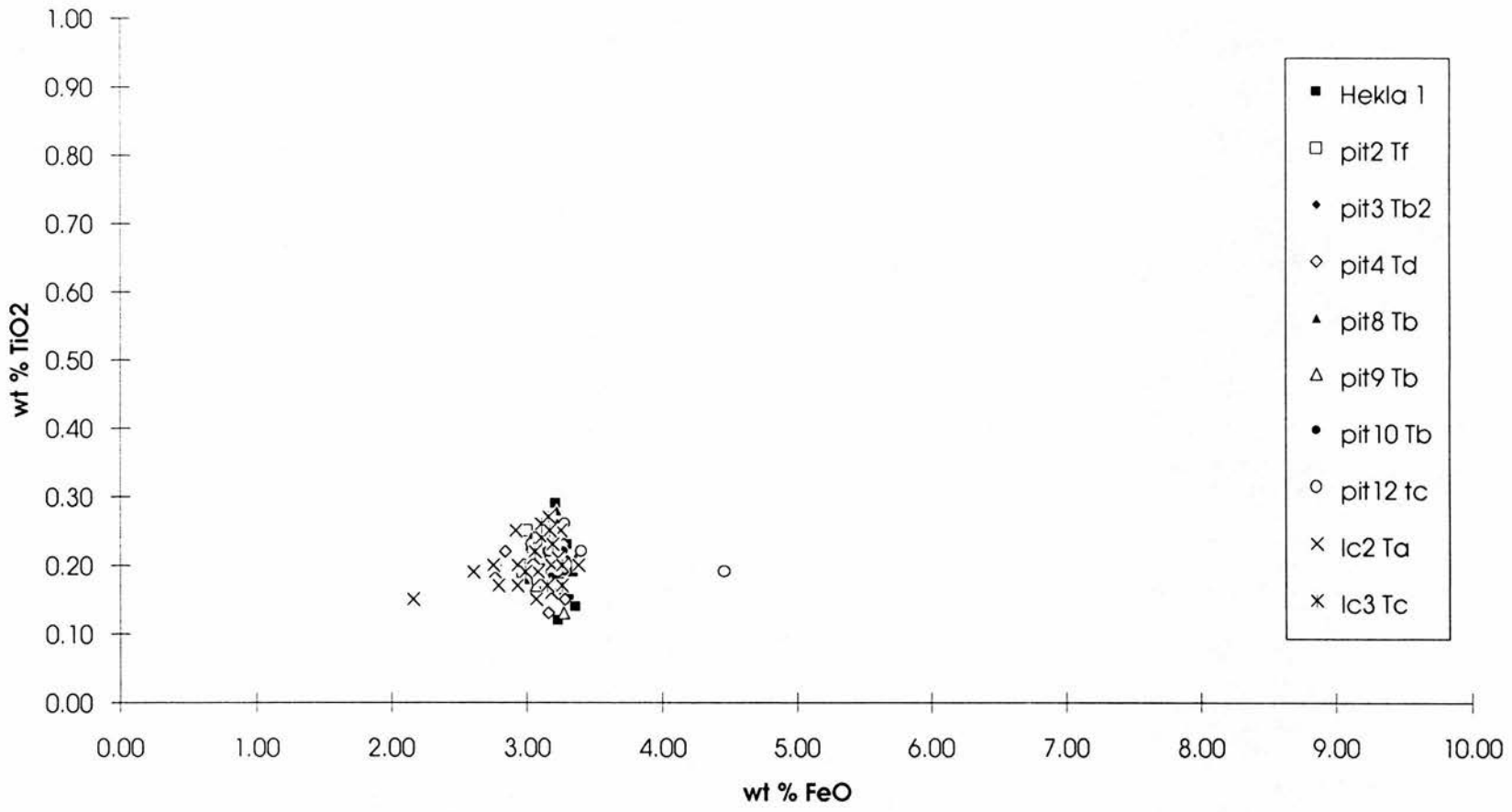

Figure 5.7 Bi-plot showing Fe-Ti variations in the geochemical analyses of the uppermost thick white tephra layer, compared with reference data for H1 (*source*: Guðrún Larsen, Volcanological Institute, Reykjavík).

from H1 can be distinguished due to the lack of a more basic fraction and the smaller size of the layer compared to H3 and H4 in the north of Iceland. For this reason deposits which correlate with the H1/H3 cluster and trendline are classified as H3, whilst analyses lying solely in the initial cluster are defined as H1.

In the lake sediments, cores 2 and 3 contain several white tephra layers in addition to H3. Layers Svin2a (23-24.5 cm) in Svínavatn lc2 and Svin3c (38.1-38.6 cm) in Svínavatn lc3 correlate exactly with the reference data for Hekla 1 (Figure 5.7). The remaining white layers are mixed products. In summary, H1 can be identified in 8 profiles in the catchment and in two lake cores (Figure 5.6).

5.2.3.5 Vatnaöldur ~AD900 (Landnamslag) in Svínavatn and catchment

Six sites on land contain one olive green tephra deposit lying between 5-32 cm below H1 and 6-30 cm above H3. Three pits have 2-3 green layers younger than H3. Svínavatn lc2 is the only lake sediment core to contain olive green tephra (2 layers). Figure 5.8 shows the geochemistry of the basaltic part of the reference sample for Veiðivötn AD 890 and the data from the field sites (15 layers in total). The data match the geochemistry of the reference sample, indicating that Veiðvötn is the source volcanic system.

Differences in the stratigraphy and in the iron/titanium ratios, however, suggest that there are two tephra layers from Veiðivötn in the catchment. Figure 5.9 is an expanded version of the previous bi-plot with the boundary of the field for the reference sample highlighted. It is clear that the layers can be divided into two groups with the group having the higher iron content matching more closely the reference data set. This group includes samples from sites which contain a single olive green tephra, and data from the top and middle green tephra layers in catchment sites Sv2, 4 and 9. In contrast, the group with lower iron content lies outside the field for Vö~900. None of the samples in this group have come from single layer sites; all the analyses come from multiple layer sections (pits 2 and 9 and Svínavatn lc2). Furthermore, all the samples in the latter group are from the lowermost olive green

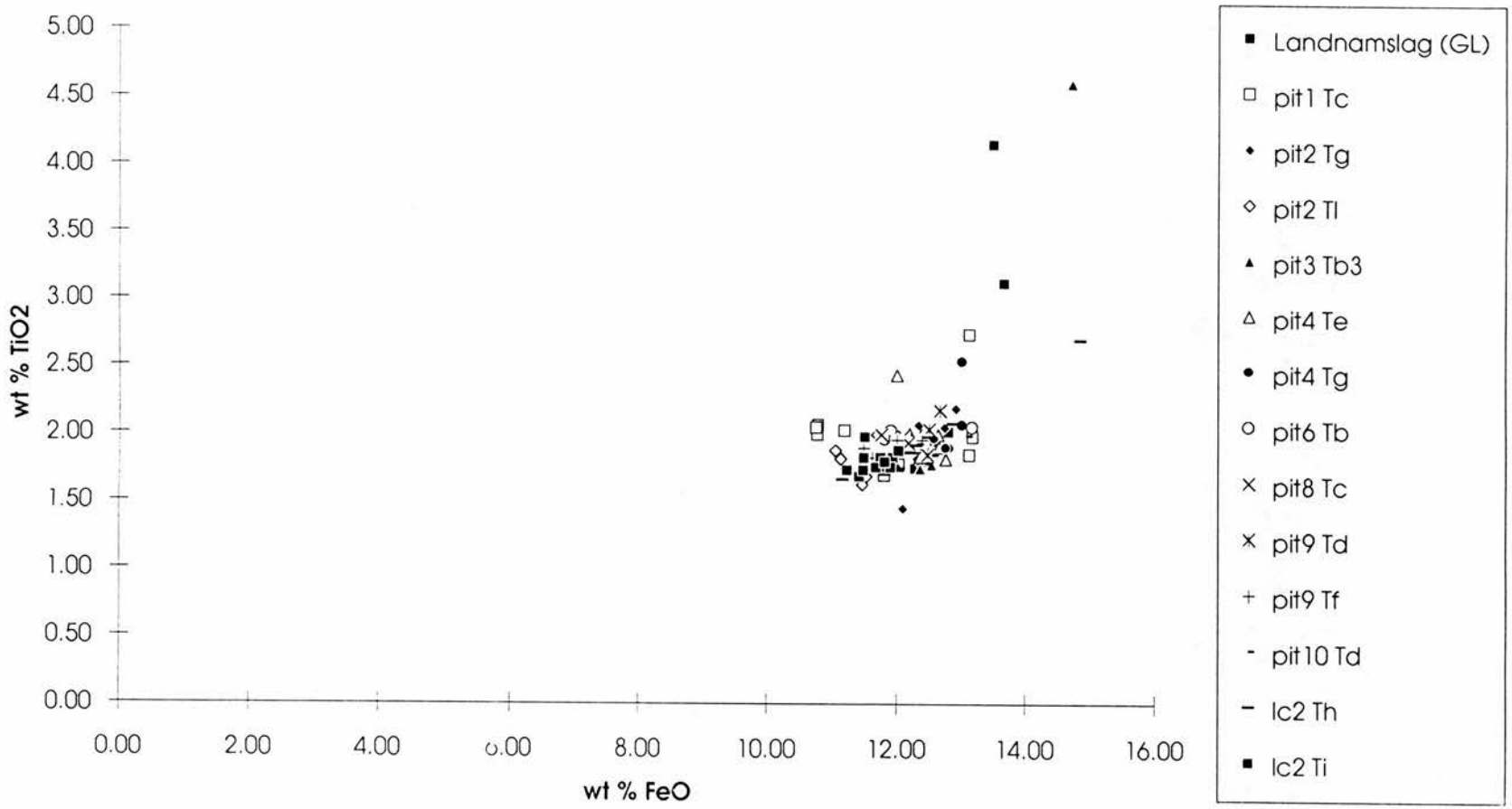

Figure 5.8 Bi-plot showing Fe-Ti variations in the geochemical analyses of the olive green tephra layers, compared with published data and reference data for the principle tephra producing systems (*sources*: Larsen and Þórarinsson, 1977, *Jökull* 27, 28-46; Dugmore *et al*, 1992, *Journal of Quaternary Science* 7, 173-183; reference samples at Edinburgh University Geography Department).

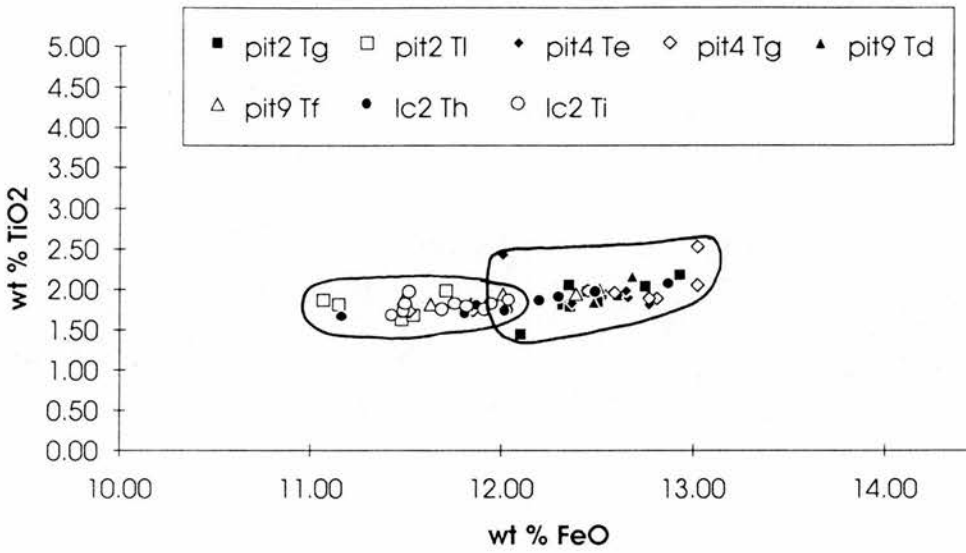

Figure 5.9 Enlarged bi-plot of the geochemical field for Veiðivötn tephra, showing the separation in the Fe-Ti abundances of the two olive green layers at Svínavatn.

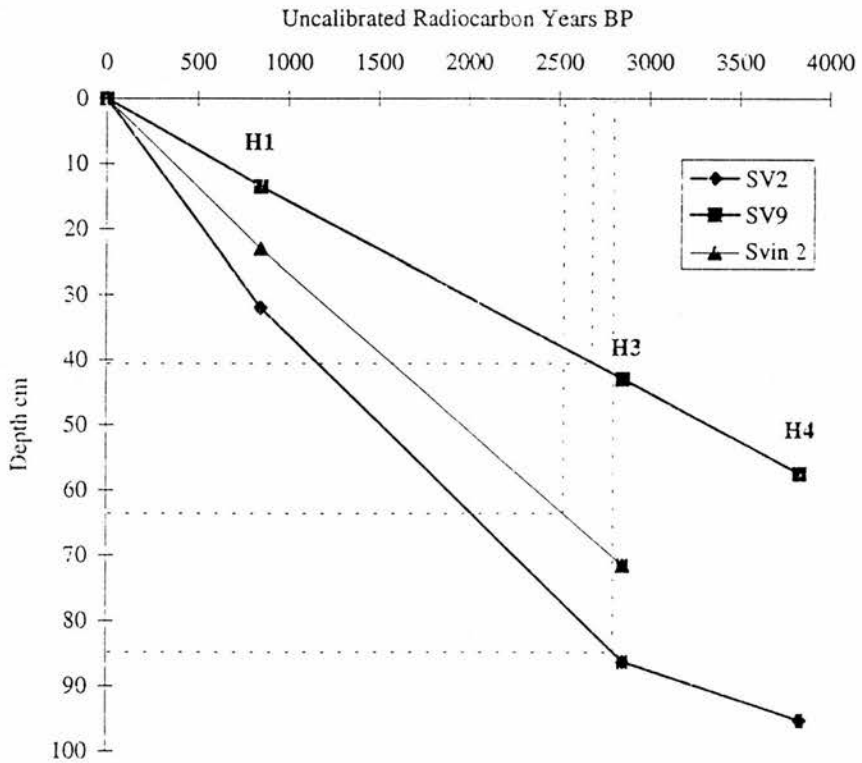

Figure 5.10 Age depth curve for the sites containing the lowermost olive green tephra layer. The dating is based on radiocarbon dating of peat immediately below H3 and H4, and the historical date of H1 (AD 1104). The errors to 1σ are indicated on the diagram. (*source of ^{14}C dates*: Dugmore *et al*, submitted).

tephra layer at these sites, lying approximately 1-3 cm above H3 in the stratigraphy. It can be concluded that there was an earlier eruption of Veiðivötn which deposited tephra in the north of Iceland around the time of H3.

To provide an estimate of the age of this tephra, Figure 5.10 shows an age depth curve for the three sites which contain the tephra. The curves were constructed using the depths for H1, H3 and H4 from each site and using the radiocarbon dates for H3 and H4 obtained from site 9 (Dugmore *et al.*, submitted). The lower olive green layer 2l (84.8 cm) from catchment site 2, yields an approximate date of 2790 BP. At site 9, the depth of 9f (40.5 cm) suggests a date of 2710 BP whilst the date from layer 2i from lake site 2 is 2520 BP.

In summary, therefore, there have been two tephra falls from Veiðivötn since H3 in the north. However only catchment sites 2 and 9 and lake core 2 contain evidence for the eruption. It is not certain if this tephra dates to the eruption of Veiðivötn in 1860+/-100 BP (Larsen, 1984). Until positive correlation can be made, this layer is referred to as SvV throughout this thesis. The remaining olive green tephra layers around the catchment and lake are identified as Vö~900 (Landnamslag). At two sites (Sv2 and Sv4) there are two deposits of Landnamslag. Additional support for the identification of Vö~900 comes from its stratigraphic relationship to H1, which has been mapped and checked throughout the north of Iceland (Larsen, 1984). Furthermore, the two tephra layers bracket the fall in birch pollen caused by settlement in the 9th and 10th centuries around Húnavatnssýsla (Einarsson, 1961, 1963).

5.2.3.6 Black tephra layers in the catchment

Four lake cores and several pits contain black tephra layers in the upper sections of the record (above H3). To determine whether all the black layers are Katla ashes, the microprobe analyses from each layer (17 in total) were plotted. Figure 5.11 shows that there are two distinct groups. The first group lies between the fields for Veiðivötn and the more basic fraction of H3. Elemental mean and standard deviation

of the latter group is shown in Table 5.2; averaging of the data is permissible in this context as it is clear from the bi-plot that there is no trend in Fe-Ti ratios in the glass. The high SiO_2 content (60%), high Na_2O and K_2O totals indicate that this group is a Hekla tephra. The historical eruptions of Hekla known to have affected the north were H1300, H1693, and H1766. There have been little published data on the geochemistry of these tephra but a comparison with Þórarinsson's (1967) analyses in Table 5.2 suggest that this Hekla tephra is H1300. Hekla AD 1300 is therefore the youngest identifiable tephra in the catchment found in the top sections of 7 profiles and 3 lake cores.

The second group in Figure 5.11 has high titanium and high iron content characteristic of Katla tephras. Whilst it is possible to distinguish Katla products from other systems, the limited compositional range makes it difficult to identify individual eruptions (Larsen, 1981). For this reason the identification and correlation of Katla tephras depend greatly on the stratigraphic relations of other tephra layers in the catchment. Although it is not essential in this study accurately to identify all the black tephra deposits, the position of the Katla tephra layer in pits Sv9 and Sv10 (19-20 cm and 96.5-98.5 cm), between Landnam and H1, suggests a date around AD 1000. As mentioned in section 4.4.2., there is some debate about this tephra so in this study it is called K-X. A stratigraphically equivalent black tephra is present in Svínavatn lake cores 2 and 3, 6.9 and 5.4 cm below H1 respectively. However definitive identification and correlation of these sites is difficult as both lake cores contain multiple black tephras in this period. In the catchment there are black tephras which cannot yet be identified geochemically. For example Sv1 in Stekkjardalur contains one black tephra but it lies 6 cm above H1 and 7 cm below H1300. No Katla eruptions in this period have been identified.

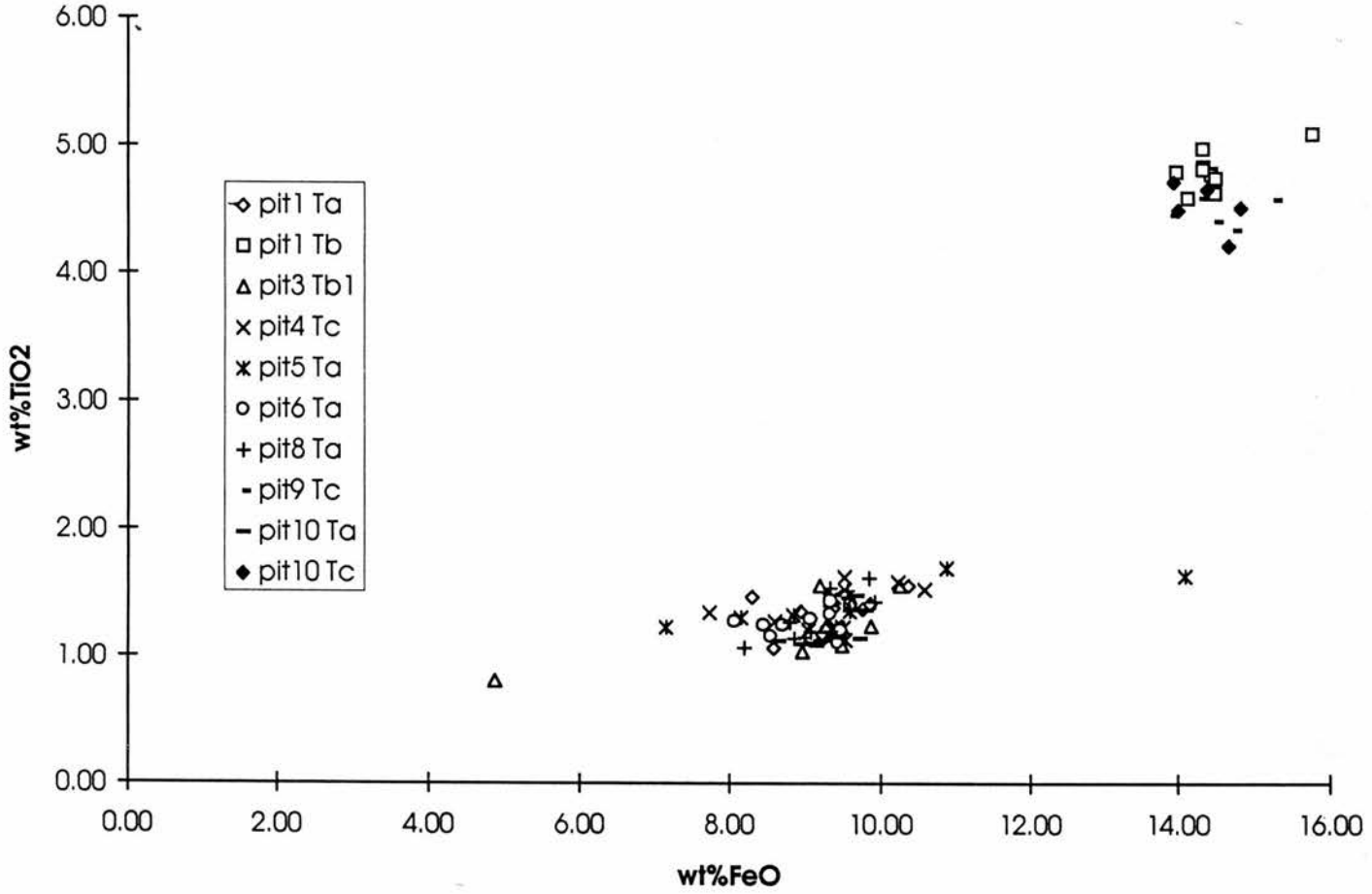

Figure 5.11 Fe-Ti variations in the geochemical analyses of the black tephra layers in and around Svínavatn. Bi-plot shows two discrete clusters separate from the known geochemical ratios for the Hekla and Veiðivötn volcanic systems.

	Svínavatn (n=70)	H1300 (Þórarinsson, 1967)
SiO_2	58.7 ± 1.1	59.25
TiO_2	1.31 ± 0.18	1.26
Al_2O_3	15.05 ± 0.91	14.9
FeO	9.27 ± 0.99	10.96
MnO	0.25 ± 0.05	0.13
MgO	1.81 ± 0.46	2.00
CaO_2	5.30 ± 0.51	5.67
NaO	4.21 ± 0.3	4.31
K_2O	1.52 ± 0.18	1.26
Total	97.44 ± 1.07	99.74

Table 5.2 Geochemical analyses of the uppermost black tephra layer compared with the published geochemical data for historical Hekla tephra (*source*: Þórarinsson, 1967).

5.2.3.7 Mixed layers

In addition to the primary airfall deposits, three catchment sites and two lake cores have multiple white layers. For example, in the section above H3, sites Sv2 and Sv4 have 6 and 3 extra white tephra layers respectively. To identify the constituents of these layers, the geochemistry of these white layers was plotted against the fields for H1, H3, H4 and the Katla and Veiðivötn systems (Figure 5.12). The lowest layers in pit 2, Sv2j (62.3-62.8 cm) and Sv2k (67.8-68.3 cm), appear to be mixed products of H4, H3 and Veiðivötn. Layers Sv2h and Sv2i correlate with H3 tail and Veiðivötn, and H4 and Veiðivötn respectively. Layers Sv2b, 2c, and 2d have analyses which match all the fields. The two lowermost layers in pit 4 (Sv4h at 48 cm and Sv4i at 54 cm) have points which match H4, H3 tail and Veiðivötn. In lake core Svínavatn 2, layer 2f (50-50.3 cm) consists of both H4 and H3 tephra, whilst Svin2c/d (38.2-39.1 cm) contains the initial products of H3, parts of the tail, Veiðivötn and Katla ashes.

Svínavatn lc3 contains 4 white tephra layers younger than H3 which have been plotted on Figure 5.12. The mixed geochemistry of these layers is shown in Table 5.3.

5.2.4 The spatial and temporal distribution of identified tephra layers in the lake and catchment

5.2.4.1 The distribution of original airfall deposits (primary layers)

To summarise the above results, there are six tephras which are known to have fallen over northern Iceland and which can be identified the profiles at Svínavatn. Figure 5.6 shows the locations of each section and the number and identity of the primary deposits. No site contains the full tephrostratigraphy. Six sites (Sv1, 2, 4, 8, 9, 11) have a near complete record. All these sites are spread around the lake basin. The sites with the least complete record are located around the Svínadal river course i.e. profiles with a single tephra (Sv5, Sv7) and Sv6 which does not have H3 or H1. The two lake cores at the extreme ends of the sample transect line contain only H1300.

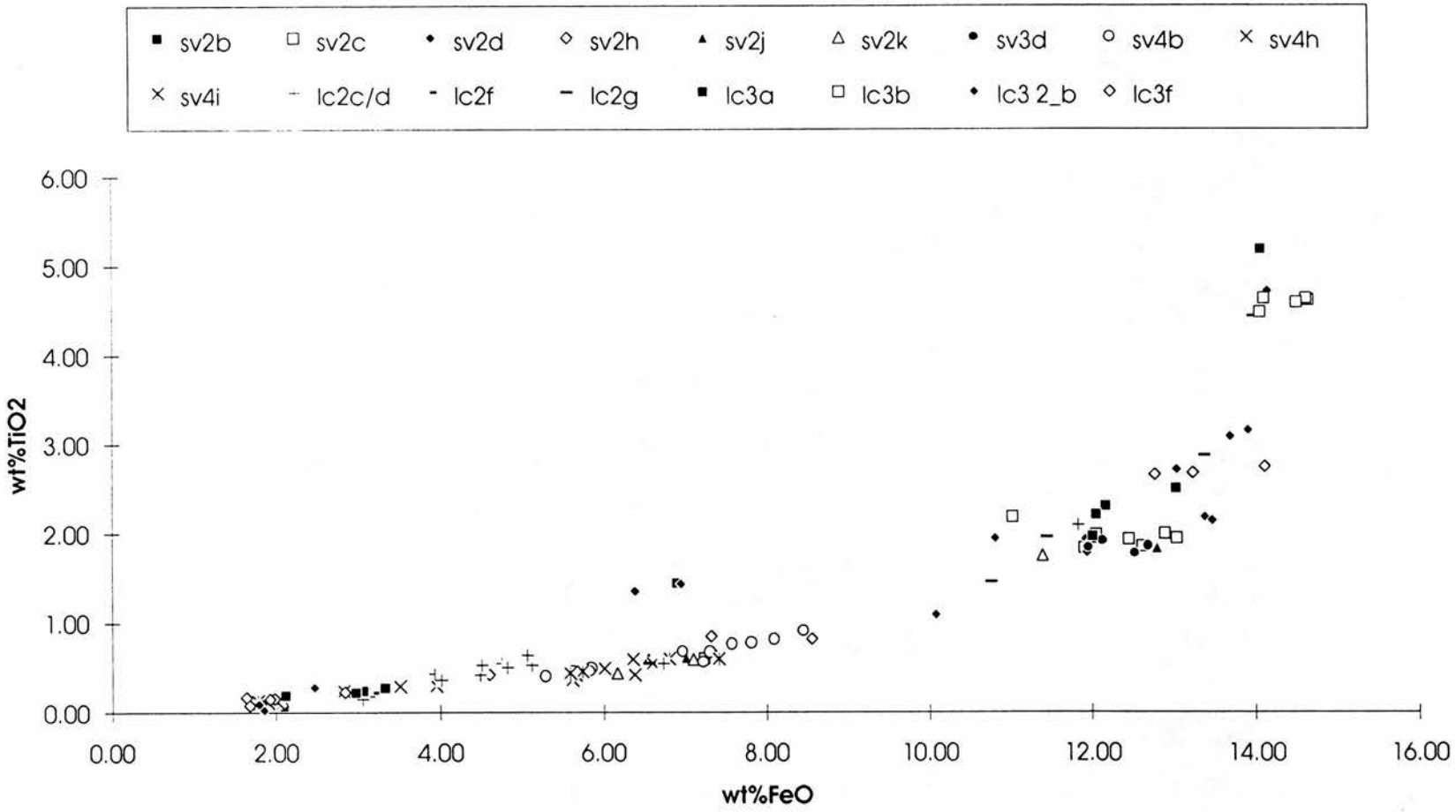

Figure 5.12 Bi-plot of Fe-Ti ratios for the mixed secondary layers at Svínavatn compared with the geochemical fields for the Hekla, Veiðivötn and Katla volcanic systems.

Sample	Sv2b	Sv2c	Sv2d	Sv2h	Sv2j	Sv2k	Sv3d	Sv4b	Sv4h	Sv4i	lc2 c/d	lc 2g	lc 3a	lc 3b	lc3 2b	lc 3f
H4	✓		✓	✓					✓		✓		✓		✓	✓
H3	✓			✓		✓		✓	✓	✓	✓					✓
H1	✓			✓									✓			
V	✓	✓	✓	✓	✓		✓				✓	✓	✓	✓	✓	✓
K		✓			✓								✓	✓		

Table 5.3 Table showing the origins of the components of the mixed secondary layers.

Lake core 2 has the most complete record and is the only lake profile to contain Veiðivötn ashes.

The correlations between the terrestrial and lacustrine records are shown in Figure 5.13 (located in the pocket at the rear of the thesis). All the correlations are based on geochemical matching of the glass and position within the stratigraphic sequence. The main points from the diagram are that;

a) there is in general the correct stratigraphic order of tephra layers,
b) the rate of accumulation at each site differs from neighbouring sites
c) the rates of peat/lake sediment accumulation varies between tephra layers.

5.2.4.2 The distribution of reworked tephra deposits (secondary layers)

Following the identification of the primary airfall layers, all further layers are by definition secondary products. Several sites have a large number of these extra layers, especially the white silicic ash from Hekla. This is most clearly seen in lake cores 1 and 2 and peat profiles 2, 3 , and 4. The previous section indicated that these layers were mixtures of several earlier tephra layers, with the deposits from H3 and H4 especially mobile in the catchment.

To give a clearer indication of where and when these extra, secondary layers were deposited, Figure 5.14 shows data from the correlation diagram with an arbitrary vertical scale. Each airfall (primary) tephra constitutes an isochronous layer and no attempt has been made to normalise the profile depths or place the sites in a specific order. Asterisks mark the secondary tephra layers which appear white in the field and have a silicic composition. The main point is that there are significant spatial and temporal differences in the tephrostratigraphy.

The terrestrial sites with repeating white tephra layers are located around Stekkjardalur and the north east edge of the lake at the foot of Sólheimaháls. These

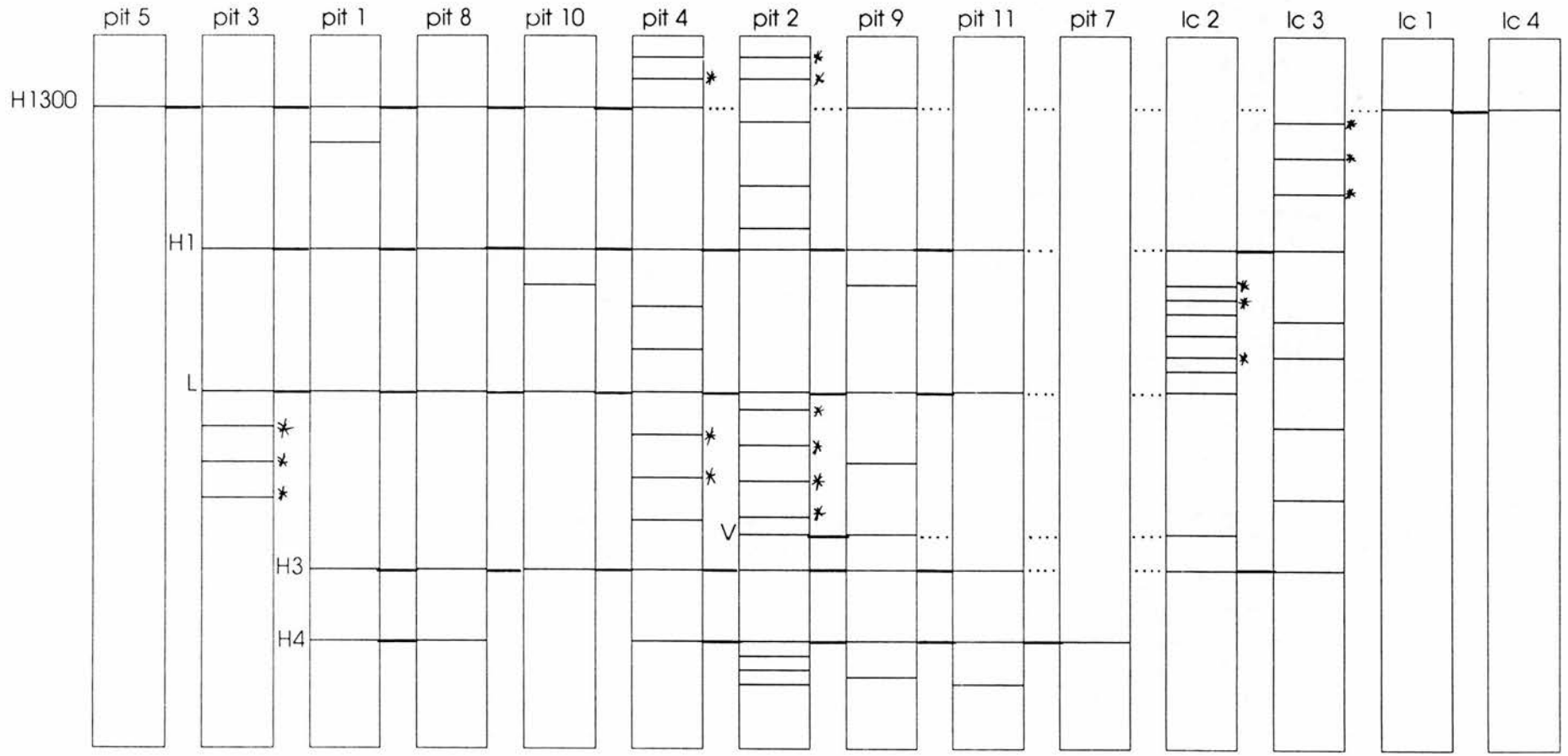

Figure 5.14 Svínavatn's tephra stratigraphy against an arbitrary timescale. Stratigraphic relationships are conserved but there is no indication of time or rate of accumulation between sites. Each primary tephra fall is depicted as an isochrone across profiles. White secondary tephra layers are marked with an *.

are sites Sv2, 3 and 4. There is some disturbance at site 12 on the southern edge of the lake where layers such as H1 and Landnam are missing from the upper sections of the profile. The main area of the catchment characterised by missing tephra layers is the Svínadalsá delta. For example, pits Sv5 and Sv7 contain one tephra layer, whilst site Sv6 has H1 and H3 missing from the tephrostratigraphy.

The temporal differences in the tephrostratigraphy are also important. There was no deposition of secondary tephra layers in the period before the eruption of H3 at any of the sites. Following the deposition of H3 up to the present, sections 2, 3, and 4 in the Stekkjardalur area and lake cores 2 and 3 have between 3-4 extra white tephra layers. At catchment site 2, two periods (H3 to Landnam and H1 to present) are characterised by secondary layers. The site was apparently stable between Landnam and H1. The record in Sv4 in similar, although there are two extra deposits of ash from Veiðivötn in the Landnam-H1 period. The secondary products in the monolith from site 3 are older than Landnam. The lake cores have contrasting histories with Svínavatn lc2 recording 4 secondary white inputs in the 214 years between Landnam and H1. Svínavatn lc3 on the other hand has two extra white layers between H3 and H1, and three distinct layers after H1. In addition there are two extra black tephra deposits in the period H3-H1, but as stated earlier it is difficult to define these layers as primary or secondary without securely identifying them.

5.2.5 Discussion of the catchment results

One of the objectives of the catchment-lake study in Iceland was to determine the eventual pattern of tephra in the landscape and the time taken to achieve this record. From the results presented above it is clear that tephra is highly mobile both at the time of original deposition and in later periods. Mobility at the time of the eruption is indicated by the fact that some catchment and lake sites do not contain a record of primary airfall. For example, H1300 is relatively widespread although absent in three terrestrial sites and one lake core, whilst K-X can only be seen in pits 9 and 10 and lake cores 2 and 3. The same is true of prehistoric tephras such as SvV, H4 (in Sv10) and H5. This phenomenon could be due to the nature of the environment at

the time of the eruption, i.e. whether snow covered, or to processes acting to disperse or concentrate deposits. This theme is examined more closely in the next chapter.

Mobility at later stages is illustrated at sites which contain multiple layers of the same tephra. As it is relatively simple to identify the secondary layers within the tightly dated framework at each site, it is possible to quantify the timescale over which tephra is still mobile. For example the top white secondary layers in pits and lake cores contain mixtures of H3 and H4 which have been redeposited after the eruption of Hekla 1 in AD 1104. This means the tephra has remained in a store or reservoir at least 3150 years (H4) or 1950 years (H3) before becoming re-mobilised and redeposited elsewhere in the catchment or lake.

It is possible therefore to define areas around the catchment as unstable or unstable at certain times over the last 4000 years. The main part of the catchment affected by instability is the Stekkjardalur area at the SE end of the lake and the lower slopes of Sólheimaháls (see Figure 4.10). Erosion of the upper slopes is reflected in the repeating secondary tephra layers downslope. The least favourable area for deposition is the Svínadalsá delta area. The least disturbed areas are the level valley peat bogs at the NW (Orrastaðir) and SE (Stekkjardalur) ends of the lake.

Is it possible to see a similar pattern reflected in the lake cores? Only Svínavatn lc2 and lc3 have a good tephrostratigraphy and they show similar patterns to the catchment profiles in that neither core is similar to the other and both have different amounts and combinations of primary and secondary deposits of tephra. These cores were taken from the central axis of the eastern basin of Svínavatn and as such should not reflect shore influences and resuspension of material.

Another important point is that the re-mobilised tephra appears in terrestrial and lacustrine records as discrete layers of material rather than decreasing volumes and concentrations over time. This implies that different processes are occurring over

time in the catchment and lake which cause pulses rather than gradual movement of material.

5.3 Physical characteristics of the tephra layers and lake sediments

5.3.1 Organic content of the lake sediments

The weight loss on ignition (LOI) of the lake cores is shown in Figure 5.15. The sediments in both lake cores are highly minerogenic with a median LOI value of 12-8%. Low amounts of organic content are recorded for layers corresponding to primary tephra input; secondary layers of tephra in each core record organic content values higher than the surrounding matrix. In Svín lc2, the greatest value for organic content is 80% (6-6.5 cm depth) and the lowest value is 1% (71.5-72 cm); the latter value is due to the tephra layer H3. The sediment below H3 has an organic content with a mean of 12%. This amount drops to an average of 10% following the deposition of H3 and doesn't recover to pre-H3 values until approximately two cm above the layer at 23.5-25 cm (H1). The loss on ignition values of the mid section of the core appear depressed due to the input of minerogenic tephra layers throughout this period. In Svín lc3, the sample with the highest organic content of 15% lies at 4-4.5 cm depth. Minerogenic layers with no organic content are found at depths of 29.5-30 cm and 49-49.5 cm, both samples corresponding to tephra layers. The lower section of the core (90-35 cm) has a mean LOI value of 6%, whereas weight loss on ignition increases steadily above 35 cm to an average of 15%. Depressed values of LOI for tephra layers are apparent throughout the core.

5.3.2 Grain size of primary and secondary tephra layers

The grain size distributions of the primary airfall tephra and the secondary reworked tephra layers are shown in Figure 5.16. The primary layers are mainly of sand and coarse silt size, with a positively skewed distribution. The secondary layers exhibit a greater spread across the size classes with greater proportions of material in the fine silt and clay size fractions.

5.3.3 Grain size changes in the lake sediments

The variations in grain size downcore are shown in Figure 5.15 with the identified tephra layers highlighted on the adjacent lithological column. The proportions of sand, grades of silt, and clay are generally constant throughout both cores, with the bulk (~75%) of the lake sediment consisting of silt-sized material. Medium and fine silt size fractions dominate lc2 whilst coarse silt increases in importance in lc3. The peaks of coarse grained material coincide with airfall tephra deposits. In addition, there are fluctuations in the relative amounts of each fraction between the sampled layers which may reflect input from the catchment or localised movement within the lake. The greatest degree of fluctuation coincides with a period of increased tephra input following several eruptions (20-45 cm in lc2 and 30-50 cm in lc3).

In more detail, Svín lc2 shows a shift in grain size distribution through time. The lower portion of the core below tephra b at 31.6 cm is of a finer texture. This section has a low percentage of fine sand (mean 8% which excludes tephra layers) and a higher percentages of the fine silt and clay fractions (mean 74% and 17.5% respectively). Above tephra b coarse silt and sand increase to a maximum of 45% at around 26 cm depth and decrease steadily in younger overlying sediments to return to previous levels. In Svín lc3, the lower portion of the core (below 50 cm) is relatively coarse with an average of 15.6% fine sand. The proportions of silt and clay remain constant during this period. Between 32-50 cm, the influence of tephra layers is apparent in the increase in the coarse fraction. In the upper half of the core (0-35 cm) the fine sand fraction decreases to a mean of 8.5% with a corresponding increase in the coarse silt fraction.

The grain size data for Svín lc2 show that the input of coarse grained tephra layers below 45 cm depth appears not to have affected the overall distribution. The sediment is dominated by silt and clay fractions, with distinct peaks caused by tephra layers. This pattern is disrupted above 45 cm following the deposition of tephra e.

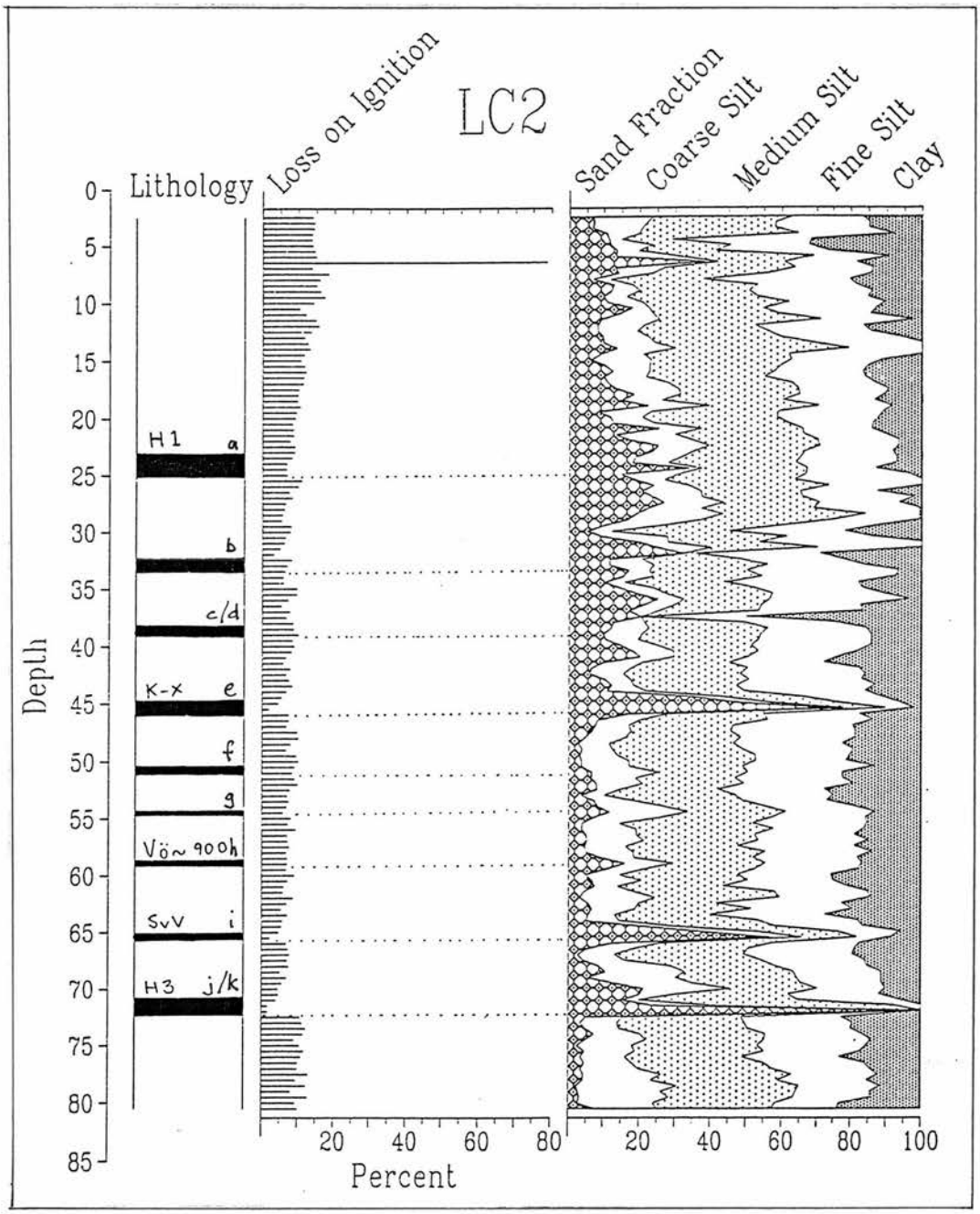

Figure 5.15 Loss-on-ignition and grain size variations in lake cores Svin lc2 and Svin lc3.

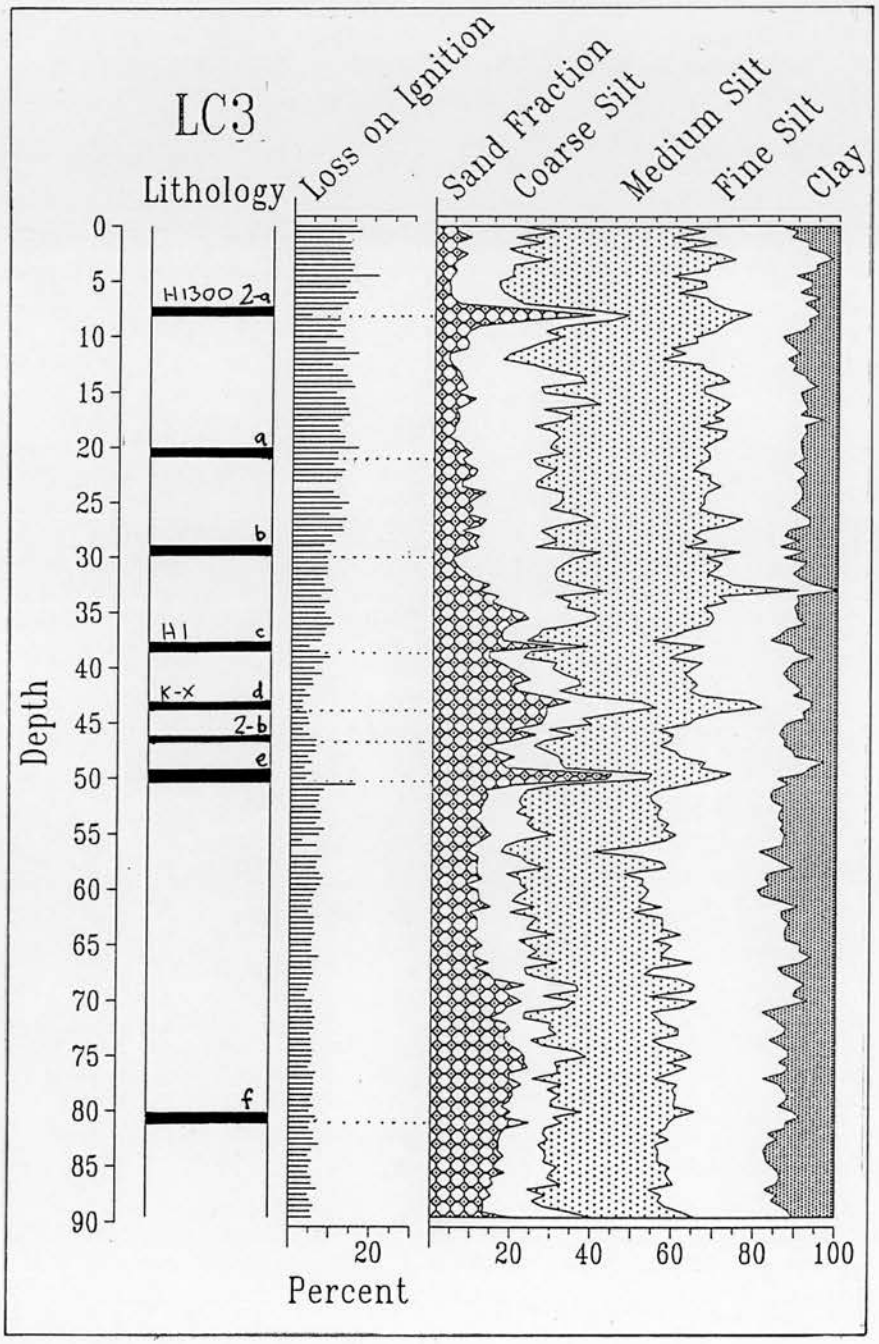
LC3
Lithology
Loss on Ignition
Sand Fraction
Coarse Silt
Medium Silt
Fine Silt
Clay
Depth
0
5
10
15
20
25
30
35
40
45
50
55
60
65
70
75
80
85
90
H1300 2-a
a
b
H1
c
K-x
d
2-b
e
f
20
20
40
60
80
100
Percent

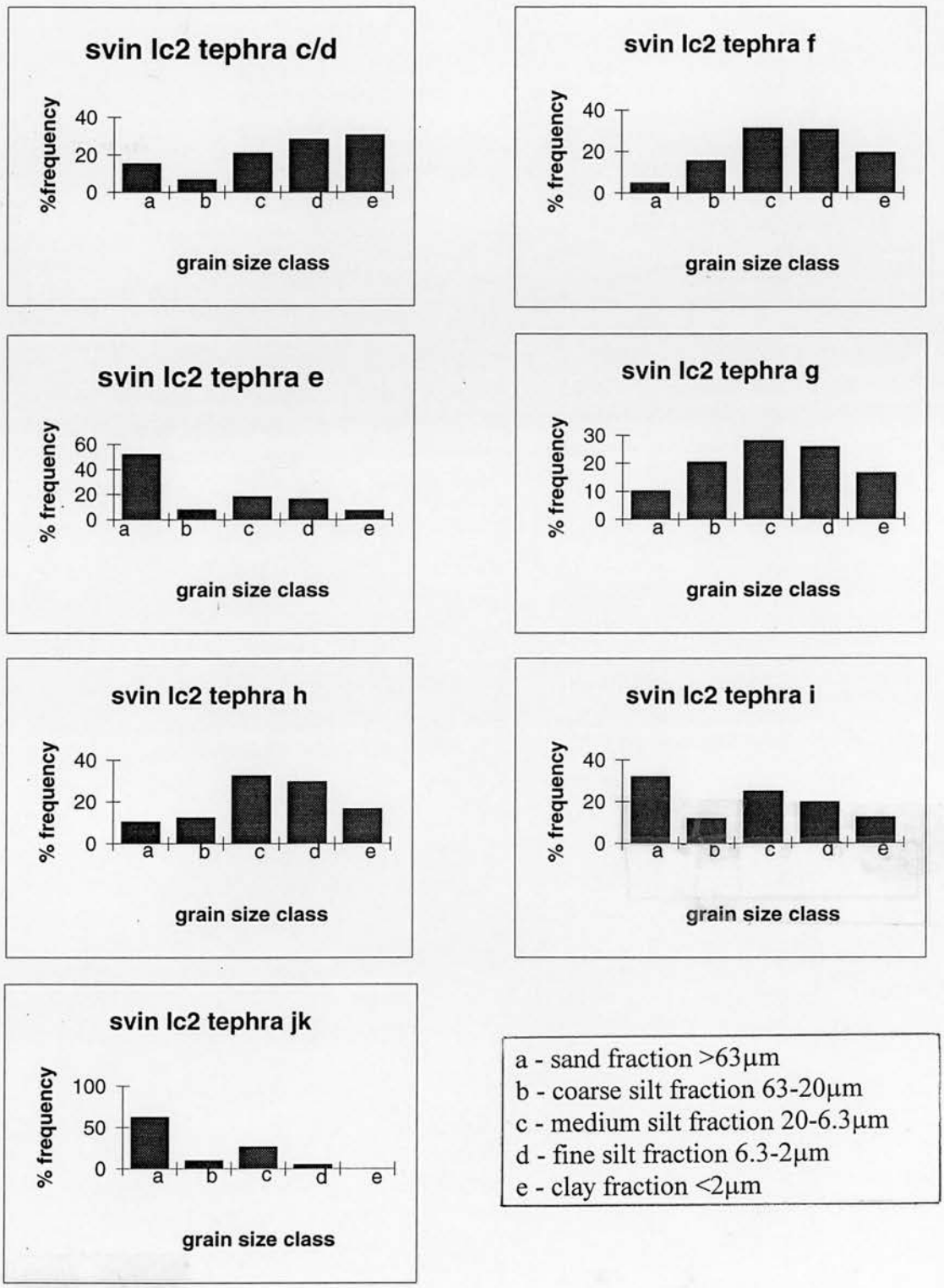

Figure 5.16 Grain size distribution of primary fallout tephra and secondary reworked tephra layers in Svínavatn lake cores.

Coarser fractions start to dominate the profile which could reflect either increased mobilisation of tephra and sand sized sediments from the catchment or lake basin slopes, or increased river action. A distinct peak of sand sized material is apparent at 6-6.5 cm depth which does not coincide with a tephra layer.

Coarse fractions dominate the period between H3 and H1 in Svín lc3, becoming finer in more recent sediments. The grain size distribution may reflect the influence of reworking and movement of slope material or river action. The opposite pattern of grain size changes in the two cores may be a factor of their location within the lake basin. Both cores are located in the deepest central axis of the eastern basin of Svínavatn; lc2 is closer to the mouth of the Sléttá and may reflect the hydrological changes of that inlet. Svín lc3, by contrast, is further from the Sléttá but nearer the large Svínadalsá delta. Although the main inlet now enters the SE corner of the western basin, there may have been channel shifts during the middle and late Holocene which would affect deposition in the eastern basin. Possible changes in the two riverine areas are shown in profiles Sv5 (Svínadalsá delta) and Sv10 (Stekkjardalur). In Sv5, shifts in the river are reflected in the change from alluvium deposits to peat development. The section here records one tephra layer in the peat at 10 cm depth (H1300). Hekla 1300 is found in lc3 at 8.5 cm depth within the period of finer sediment input. At site 10 five tephra layers have been identified; H3, Vö~900, K-X, H1, H1300. The surrounding matrix consists of fine sandy alluvium and fine gravel deposits. The age depth curve for the site shows the increase in accumulation rate after the deposition of Landnamslag. This period of increased accumulation in the Sléttá delta area coincides with the coarsening of the sediment in Svín lc2.

5.3.4 Morphology of the tephra deposits

The morphology of the glass shards in the tephra layers are shown in the photographs in Figure 5.17. The tephra shown are samples from each layer in the Svínavatn tephrostratigraphy. It can be seen that the highly silicic tephra such as SSn, H4, H3 and H1 are platy, vesicle-rich with frothy bubbles walls. The vesicle shape is both

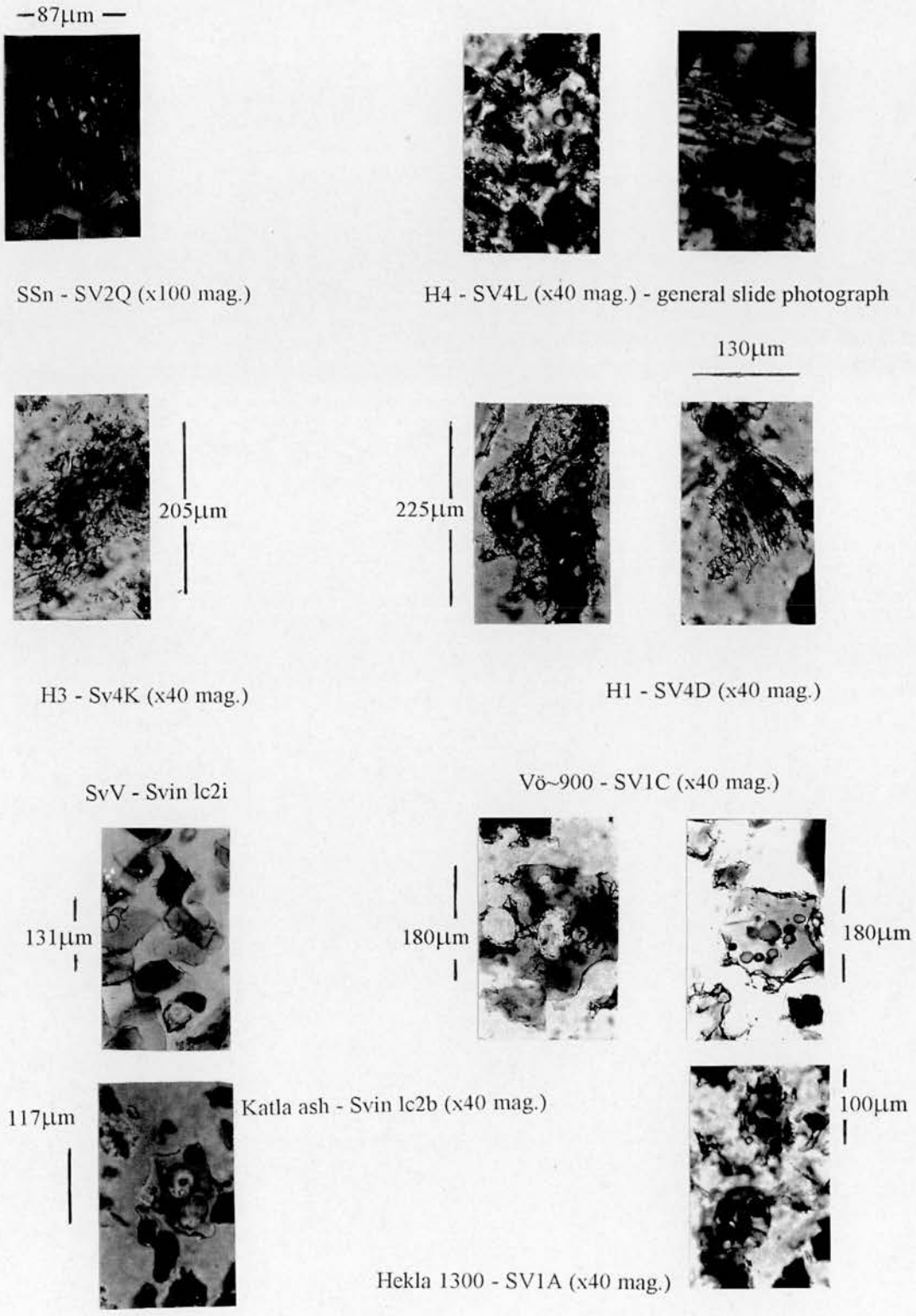

Figure 5.17 Photographs showing the morphology of glass shards from a range of geochemical compositions. Note the sharp edges and well-preserved bubble walls.

spherical or elongate (piped). The more basaltic tephra, on the other hand, is less vesicle-rich although the vesicle size is larger, appear more blocky, and have a light brown colour. The most basic of the tephra deposits (from Katla) are vesicle-poor. There is no evidence of edge abrasion or shattered vesicles in the samples.

5.4 Summary of data

This chapter has attempted firstly, to construct the tephrochronology of Svínavatn catchment and lake sedimentary records; and secondly, to determine the physical and geochemical differences between primary and secondary layers to aid differentiation in future studies.

The main points from the catchment survey are;

• The tephrochronology of Svínavatn and surrounding area has been constructed at a catchment scale using stratigraphic relationships. Published isopach maps are used as a general guideline to suggest which tephra may be present at a site. The regional tephrostratigraphy of Svínavatn consists of SSn (~7000 BP), H4 (4000 BP), H3 (2800 BP), SvV (?2600 BP), Vö~AD900, K-X, H1 (AD 1104) and H1300.

• Original airfall products can be identified stratigraphically on the basis of position, particle size, layer thickness, colour and nature of boundaries, and geochemically by correlating glass geochemistry with reference samples. The distinct geochemical ranges for each tephra allow mixed tephra deposits to be identified on the basis of their heterogenous characteristics, and therefore defined as secondary, redeposited layers.

• Several sites have an incomplete tephrostratigraphy compared with the known regional tephrostratigraphy. The tephras with the poorest areal distribution are SvV and K-X. The tephra which appear at the majority of catchment sites are H4, H3 and

H1. The catchment profiles with the least number of tephra layers (Sv5, Sv7) and the most incomplete (Sv6) are all located around the Svínadalsá delta area.

• Several sites have repeating tephra layers, i.e. secondary deposits of an earlier primary fallout. These secondary layers appear in distinct horizons and are not interpersed throughout the peat profile or lake core. These sites are found in the Stekkjardalur area of the catchment, on the lower slopes around the lake, and in the central area of the lake basin. The secondary layers in the lake sediment were deposited at the same time as the reworking in the catchment.

• The secondary reworked deposits in both the catchment and lake sites can be identified by geochemistry. There is no evidence of erosion of the glass shards to indicate vigorous reworking of material; the sharp edges and vesicle-rich appearance of the original deposits have been preserved. The grain size data indicate size-sorting of material as the secondary deposits are silt-clay size compared with sand-coarse silt size of primary airfall deposits.

6.1 Introduction

The pattern of tephra layers around the catchment is not a simple reflection of the type of depositional environment and the number of tephra falls in the area. It is spatially discontinuous; some layers are repeated in some areas, yet missing in others. Following the identification of primary airfall deposits, the construction of a regional tephrostratigraphy and the mapping of each layer, it is clear that tephra is both mobile at the time of deposition and during later periods.

This chapter assesses the possible processes which have operated on the tephra deposits, both immediately following the eruption, and in later periods. The possible causes of recurrent pulses of reworked tephra are discussed and the ideas brought together in a model of tephra deposition.

6.2 Causal mechanisms for the reworked secondary tephra layers

The tephrostratigraphy in the catchment and lake indicates periods of instability and mobilisation on the hillslopes. These may occur because thresholds are periodically exceeded and sedimentation episodes of varying magnitude are initiated. Thresholds can be both extrinsic and intrinsic to the system (Schumm, 1979). An intrinsic threshold is one where change may occur without the influence of an external forcing variable; progressive weathering may weaken aeolian slope material and the hillslope adjusts over time, or overaccumulation of peat increases the possibility of landslides. An extrinsic threshold is one that is crossed as a result of external factors such as climate or tectonics. Following the breaching of thresholds, different parts of the hillslope system will react at different rates because of differing sensitivity produced by geomorphology, climate or vegetation. This is termed complex response and can be used to consider lag times of sediment movement in a system. Three interpretations of the secondary layers in Svínavatn can be made; firstly, the layers could be the result of sporadic erosion on the catchment hillsides and immediate

deposition in the lake. Secondly, the lake record could reflect the lagged deposition from the catchment. Thirdly, the lake secondary layers could be products of internal lake processes such as slumping, turbidity currents and resuspension.

The coincidence of the major periods of slope instability and increased reworking of tephra in the lake sediments, suggests that the two records are connected. The dating of the secondary layers indicates that geomorphic slope processes may have been more effective during the period 2500 BP to the present. The upper section of the stratigraphic record confined to the post-Landnam period (~AD900AD) may increasingly reflect human influence (Hallsdóttir, 1987). Disturbance in the lower sections, however, is non-anthropogenic and may be entirely due to breaching of external and internal thresholds.

The external factor most readily invoked as the cause of partial changes in geomorphic systems and sediment yield is climatic variability. This causal mechanism is difficult to relate to a particular sediment response, unless evidence from a wider region suggests that climate did change. Acting in conjunction with natural changes within the system (e.g. vegetation succession), climatic change may exacerbate the rate and magnitude of disturbance. The literature indicates that from the time of the deposition of H3 to the present, the Holocene has been characterised by abrupt changes in temperature and precipitation. From studies throughout the northern hemisphere, it appears that climate deteriorated from around 2500 BP to ~AD1890 with expansion of mountain glaciers (Denton and Porter, 1970; Denton and Karlén, 1973; Grove, 1979) and development of upland mires (Moore, 1975).

There is evidence from palynological, glaciological and geomorphological studies in Iceland for a corresponding cold, wet period. Precision is provided by identification of isochronous tephra layers which allow correlation of the Svínavatn sites with dated pollen diagrams and environmental histories elsewhere in Iceland. A climatic regime was constructed by Einarsson (1963) to describe the vegetation changes seen in Icelandic peat bogs. Early correlations suggest that the mid-Holocene *Betula*

maximum in Iceland corresponds to the Hypsithermal (4000-2500 BP), that is, the period between the deposition of H3 and H4. The subsequent cooler and more humid climate marked the beginning of the sub-Atlantic period and reduced the birch woodland, as *Betula* pollen decreases above H3 at sites in both north and south Iceland. At the same time there were increases in sphagnum and Cyperacae pollen, indicating wetter conditions, too moist for birch growth (Einarsson, 1963; Vasari, 1972; Hallsdóttir, 1987). The work of Einarsson suggests that 50% of Iceland was covered by birch at around 2500 BP. From this time to the period of settlement (sub-Atlantic period) birch cover decreased to about 25% until it was decimated by the arrival of people and grazing mammals in the 9th Century. The human influence on vegetation is reflected in sudden rises in the concentrations of Gramineae and Cerelea type pollen, charcoal peaks and the abrupt decline in tree pollen (Einarsson, 1963; Hallsdóttir, 1987).

Further lines of evidence for climate deterioration come from tephrochronological studies of solifluction lobes in the north and south of Iceland. Sharp and Dugmore (1985) dated the onset of solifluction at Skalafellsjökull, SE Vatnajökull, to after 2820±40 BP, whilst Hirakawa (1989) reports the rate of downslope movements of solifluction lobes doubling during the period 4000-2000 BP at sites around northern Iceland. Cryoturbation processes and hummock formation (þúfur), have a maximum age of 3800 BP at Skídadalur in Trollaskagi, but the onset of periglacial conditions must have started later than this to allow sufficient time for soil development and vegetation cover (Müller *et al.*, 1984). The glacial record from both north and south Iceland indicates the onset of Neoglaciation post ca. 4000 BP. Evidence from valley glaciers in the Trollaskagi peninsula (Stötter, 1990), Halsájökull in eastern Iceland (Þórarinsson, 1964), Svínafellsjökull and Kvíarjökull off Öraefajökull (Þórarinsson, 1956) and Sólheimajökull off Mýrdalsjökull (Dugmore, 1987; Dugmore and Sugden, 1991) records extensive ice advances in the second half of the Holocene.

Several of the events recorded by the tephras could, therefore, have been caused by climatic variability. Changes from an equable climate with vegetation such as birch,

to one with deteriorating temperatures, less woodland and consequent decrease of evapotranspiration, creates conditions suitable for erosion. The climatic change may also have taken the form of increased storminess or intensity of flood and frost episodes. The following section discusses the different processes causing erosion and remobilisation of tephra following initial fallout and in subsequent periods.

6.3 Environmental processes operating in the catchment that affect the tephra stratigraphy

6.3.1 Patchy distribution of primary tephra in soils and peats

The distribution of fallout of tephra from the eruption cloud is dependent on the synoptic weather conditions at the time of the eruption. Variables include wind direction, wind speed, and the presence or absence of frontal systems and precipitation belts. Therefore, during calm dry conditions tephra would fall blanket-like over the whole landscape providing a widespread and complete cover. If, however the eruption coincides with a more vigorous weather system, then the tephra will descend with snow or rain producing a sporadic and discontinuous pattern. For example, the distribution of Hekla 1947 tephra in Finland indicates that fallout was triggered by frontal conditions in the upper atmosphere. The distribution of the tephra was most variable where the ash landed on snow (Salmi, 1948; Dugmore and McCulloch, ms).

Following deposition, the full or incomplete cover of tephra is exposed to aeolian, fluvial and slopewash processes which redistribute the layers around the catchment. The loose and friable nature makes it susceptible to wind erosion. In strong winds the tephra will move easily unless bound by vegetation which in turn reinforces the patchy nature of the distribution. The effects of wind movement are exacerbated when acting in conjunction with a deep, loose snow cover. Drifting, banking and spasmodic melting create complex distribution patterns around the catchment. Such patterns were seen following the January 1991 eruption of Hekla (Hunt, 1992) and around Snaefellsjökull (Jóhannesson *et al.*, 1981). The loss of tephra layers from

profiles due to this process is more likely when the tephra fall is a small one and of a fine grained nature.

Water action is also important following tephra deposition. During precipitation, rainsplash on exposed tephra will cause saltation of large particles downslope in much the same way as for sand particles (Arnalds, 1990). In addition, fluvial processes such as overland flow, create patchy deposits especially around gullies or natural depressions and channels where water collects and runs off. There is also the documented process of water winnowing finer particles which will change the character of the tephra deposit.

Several processes, therefore, have the potential to redistribute tephra layers around the catchment, affect their thicknesses and characteristics. Remobilisation may be both local in extent and occur over a short period of time due to meltout, overland flow and river deposition operating relatively quickly after the original deposition event. The ability of these processes to redistribute freshly fallen tephra is strongly dependent on the season in which the eruption occurs. For example, tephra deposited during the summer period when grass is growing rapidly will be less prone to movement, appearing in the record as a continuous layer The almost complete distribution of H1300 around Svínadalur may be due to the fact that the eruption took place at the start of July, just before harvest time and continued for the best part of a year (Þórarinsson, 1967).

6.3.2 Processes creating secondary tephra layers and delayed inputs in the catchment

Tephra around the catchment is subjected to gradual downslope movement until further vegetation growth affecting soil and peat accumulation binds the deposit. Over time, each tephra deposit is locked in storage in a relatively stable reservoir, forming a distinct layer. The results from the catchment survey show that this stability is disturbed in later periods when the tephra is remobilised. The following discussion focuses on erosional and depositional processes which may have resulted in the redeposition of the tephra downslope.

At the present time the Svínavatn catchment consists of hallmyri (sloping peat fed by runoff and groundwater) at the base of slopes, such as the flanks of Sólheimaháls. The tops of the ridges and the convex section of the slopes are bare of vegetation. It is likely however that these areas were once covered with birch and peat (Einarsson, 1963; Vasari, 1972). The main agents of erosion on hillsides are aeolian processes, running water, subsurface water and mass wasting.

6.3.2.1 The impact of running water on slopes

The main processes of erosion by running water are sheetwash and gullying, the effectiveness of which is limited by a full vegetation cover such as birch woodland and a cohesive cover of peat. From studies of natural erosion of hillside blanket bog in the southern Pennines, Tallis (1985) reasoned that there must be some kind of destruction of vegetation, baring of the peat surface and initial rapid incision by water. This could happen in a number of ways. Firstly, exposure of the peat surface by tree throw or natural fires increases susceptibility to erosion by precipitation and run off. The processes of grazing, trampling and deforestation are not viable interpretations in Iceland as there was no human and grazing mammal activity in the region until the Norse settlement of the 9th century. Secondly, severe climatic change could reduce the vegetation cover and leave the peat vulnerable to wetting and drying. The peatlands most susceptible to climatic change are the deposits occupying convex sites (Tallis, 1985). These areas shed water, have a lower water table and therefore are less of a buffer against precipitation changes compared to the wetter concave sites in hollows and bottom slopes. Thirdly, drying out of the bog will create desiccation cracks, enabling water to exploit holes and develop channels. These channels may develop into gullies by funnelling overland flow and cutting down into the peat, a process which is enhanced during heavy rain and snow melt. Progressive erosion occurs by lateral seepage of water from the peat to the gully, and by frost action which "puffs" up the peat during winter and leaves loose peat on the gully sides following thawing. Erosion of þúfur can occur due to severe frost when there is little protective snow cover. Once insulation is lost, needle ice formation can

occur and break up the soil, completely excavating the centre of the þúfa (Webb, 1972).

On the slopes of Sólheimaháls, therefore, there may have been localised erosion of the peat and soil by the processes described above. Precipitation and running water provide the mode of transport as well as the mechanism of erosion. Several possibilities may explain the erosion of upland areas and redeposition of tephra downslope. For example, following the opening of the forest cover by wind throw or by reduced regeneration of woodland, the surface of the adjacent peat dries out and cracks form which are later exploited by heavy rainfall to create deep channels. Successive periods of rainfall enlarge existing hollows by funnelling overland flow down these channels. Eventually tephra horizons are exposed, quickly eroded by water and wind, and transported to valley bottom peats. A similar mechanism operates in winter when the ground is frozen. Frost-heave of the surface loosens the peat which is removed following thawing, or by heavy precipitation. Again the establishment of a hollow or channel reinforces later erosion patterns.

The secondary layers of tephra at sites such as Sv2, Sv3 and Sv4 could be the result of such erosion events upslope. It is difficult, however, to determine whether the layers reflect erosion of large areas or more localised rilling and gullying. If running water was the dominant agent of erosion and transport on the hillslopes, the secondary layers should show evidence of reworking. Dependant on transport distance, the secondary tephra would have abraded and shattered glass shards (Fisher and Schmincke, 1984); the deposit would be predominantly silt sized due to selective water erosion, and would have a large amount of detrital contamination from the minerogenic peat.

6.3.2.2 Movement of tephra by subsurface water and piping

An alternative cause of erosion is removal of soil and peat by subsurface water and the creation of cavities and pipes. According to Selby (1982), factors which make soil susceptible to piping are a variable rainfall, proneness to desiccation cracking,

loss of vegetation cover, the presence of a relatively impermeable layer, an existing hydraulic gradient or dispersible soil layer. The same processes operating in peat are viable but have not been studied closely (Taylor, 1983). In Iceland, however, the presence of minerogenic, friable tephra layers within the peat mass suggests that this mechanism may be an important factor in hillslope erosion. A tephra layer provides a sharp texture change within the profile allowing lateral seepage and channel development. The characteristics of the tephra layer will determine which horizon is prone to piping as a coarse, loose tephra such as H3 will be more permeable than the surrounding peat matrix. Piping develops in most situations by the infiltration of rainwater through desiccation cracks followed by supersaturation of a more permeable layer, or by lowering of the water table. Lateral seepage removes material or causes loss of aggregation, a process which is enhanced when the water breaks the surface further downslope providing unconfined flow. Piping is important around the walls of gullies and may exacerbate earlier erosion scars.

6.3.2.3 Mass movement of soils and slopes

The main types of mass movement are soil creep, slumps and slides. Although strictly defined as wasting due to the influence of gravity, most mass movement occurs in conjunction with water and ice which reduce the strength of slope material (Selby, 1982). For example, the rate and timing of soil creep is affected by changes in temperature and moisture as particles deform and lose friction. Although creep is a relatively shallow process, soils which have high shear stresses are subject to progressive creep at depth which develops into rapid creep or failure by landsliding. The secondary pulses of eroded tephra may have been produced and transported by slumping. Slumps occur where the bottom of a slope has been undercut by river or wave action. In the Svínavatn catchment, slumps on the slopes of Svínadalsfjall can be seen at the western end of the lake, probably formed following the withdrawal of ice in the Late-glacial (Figure 6.1). Smaller scale movements possibly caused by earthquakes during the late Holocene may have triggered large-scale erosion of soil and peat as slumping disturbed soil structure and increased water content. The third

type of mass movement is landsliding which tends to occur following heavy precipitation and raising of the water table (Selby, 1982).

Peatlands are seen as inherently unstable systems which are prone to erosion by bog bursts, slides and flows (Clymo, 1984). Any hydrological changes at the surface, base or edges of the bog will instigate erosion (Taylor, 1983). For example, in a study of southern Pennine peatlands, Tallis (1985) found increased accumulation of peat towards the topographic limits of the bog during the period AD 400-1000. The rapid build-up of relatively unhumified peat on top of more decomposed peat and the prevention of further lateral expansion made an unstable peat mass liable to bog slides and bursts at the edges. This rapid drainage may have led to the formation of drainage gullies extending back into the peat bog and slumping of marginal peat downslope. The frequency with which bog bursts and slides occur in the British Isles indicates the degree of instability inherent in peatlands particularly where there is a deposit of unconsolidated, poorly humified peat overlying denser more decomposed peat (Conway, 1954; Wilson and Hegarty, 1993). These changes in texture create a potential failure plane which is exploited during intense wetting and drying cycles.

A similar process of rapid mass movement may have taken place around Svínavatn. In the peats on the lower slopes, there is a clear change in the degree of humification before, between and after H4 and H3. Before the deposition of H4 the profile consists of woody, poorly decomposed peat whilst between H4 and H3 (4000-2800 BP), the peat is dark brown and well humified. The peat which accumulated after H3 is light brown and poorly humified. In addition to the distinct changes in degree of humification, the sharp texture changes created by tephra layers may have increased the potential for landslipping. Evidence supporting the theory that mass movement, in particular peat slides, occurred on the slopes around the lake comes from the section SV9 (Figure 6.2). This profile shows that between H4 and H3 there was a

Figure 6.1 Photograph showing the large landslide on the northern flanks of Svínadalsfjall, at the NW end of Svínavatn.

Figure 6.2 Photograph of slumping within peat deposits in a profile upslope from site 9 (Auðkúla). The peat movement occurred after the deposition of H4 and before H3 which drapes the disturbance. The spade handle is 80 cm long.

slip or slump upslope from the site, which moved a thick coherent peat block. The deposition of H3 effectively mantled the fault and subsequent accumulations of peat filled the depression. Although it is not clear whether the peat slipped along the failure plane provided by the tephra or compositional changes in the peat, the site shows that the area was unstable and susceptible to mass movement.

6.4 Environmental processes affecting the lake sediment record

Allochthonous lake sediments are subject to both external and internal erosion and sedimentation processes before becoming incorporated into the lake record. Tephra is an external input to the lake system but the final tephrostratigraphy of the lake sediment record is created by both internal and external processes which affect sediment supply to the lake. The lake cores, therefore, have elements of the regional stratigraphy and also a more site-specific tephrostratigraphy. The next section examines the possible external and internal processes which produce discontinuous cover at the time of eruption and later inputs of secondary material.

6.4.1 Patchy distribution of tephra fall in a lake

Following an eruption, tephra falling over a catchment and lake surface should fall evenly through the water column. This would be the case if the eruption took place when the lake was ice-free and in calm weather conditions. Wind movement could disturb this layer in two ways. Firstly, by blowing the floating tephra along the surface as a thin film as observed during the eruption of Hekla in 1970 (Þórarinsson, 1979), and secondly by creating waves, currents and internal seiches which disturb the water column. Patchy distribution of tephra could also occur if the fallout landed on loose snow on the lake ice. Wind action would be significant in redistributing tephra throughout the winter, especially as the large expanse of the lake would have no natural wind breaks. In the most extreme case, strong winds could blow the complete tephra deposit onto one shore. Following the thaw, the tephra which had drifted with the snow would settle to the lake bottom. Redistribution of tephra by ice rafting may also be important during the thaw.

Rapid input of secondary tephra by rivers introduces another dimension to the initial pattern of airfall tephra in lakes. As well as the movement caused by incoming overcurrents and undercurrents, the river also deposits airfall tephra from elsewhere in the catchment. This means that tephra layers will be thicker near river mouth deposition areas, but may also be prone to later erosion by undercurrents. Water action in the form of slope wash could also be effective in redistributing tephra as loose tephra material is washed downhill into the lake by overland flow. Both processes suggest that tephra deposits would be thicker and more variable around the edges of lakes. This is a reasonable conclusion and it is standard practice in limnological studies to avoid sampling the shallow margins (Downing and Rath, 1988).

6.4.2 Secondary layers, stratigraphically separated from the initial tephra layer

The lake results show that tephra deposition was patchy following airfall and that there was remobilisation of tephra after an interval. As outlined in section 6.4.1. above, movement around the catchment (i.e. external to the lake system) could have produced erosion and redeposition of tephra. This extra source of allochthonous material to the lake could be readily assimilated into the record by slope wash to provide a continuous input over time or, following piping or slumping, form a discrete pulse of tephra. Dynamic processes within the lake must also affect the distribution of tephra and other sediments on the lake bed These processes include resuspension from turbidity and currents, wind/wave influences and river action. Factors such as lake topography are important also. The main sedimentological and bottom dynamic processes have been summarised by Håkanson (1982a) in Figure 6.3. The following section outlines the effects these interrelationships have on the sediment distribution and examines the applicability to the record from Svínavatn.

6.4.2.1 Resuspension and reworking of tephra within the lake system

Resuspension of material can take place through turbidity currents, which are episodic downslope movements of sediment rich water which redeposit material mainly around delta areas and slopes (Håkanson and Jansson, 1983). They can be

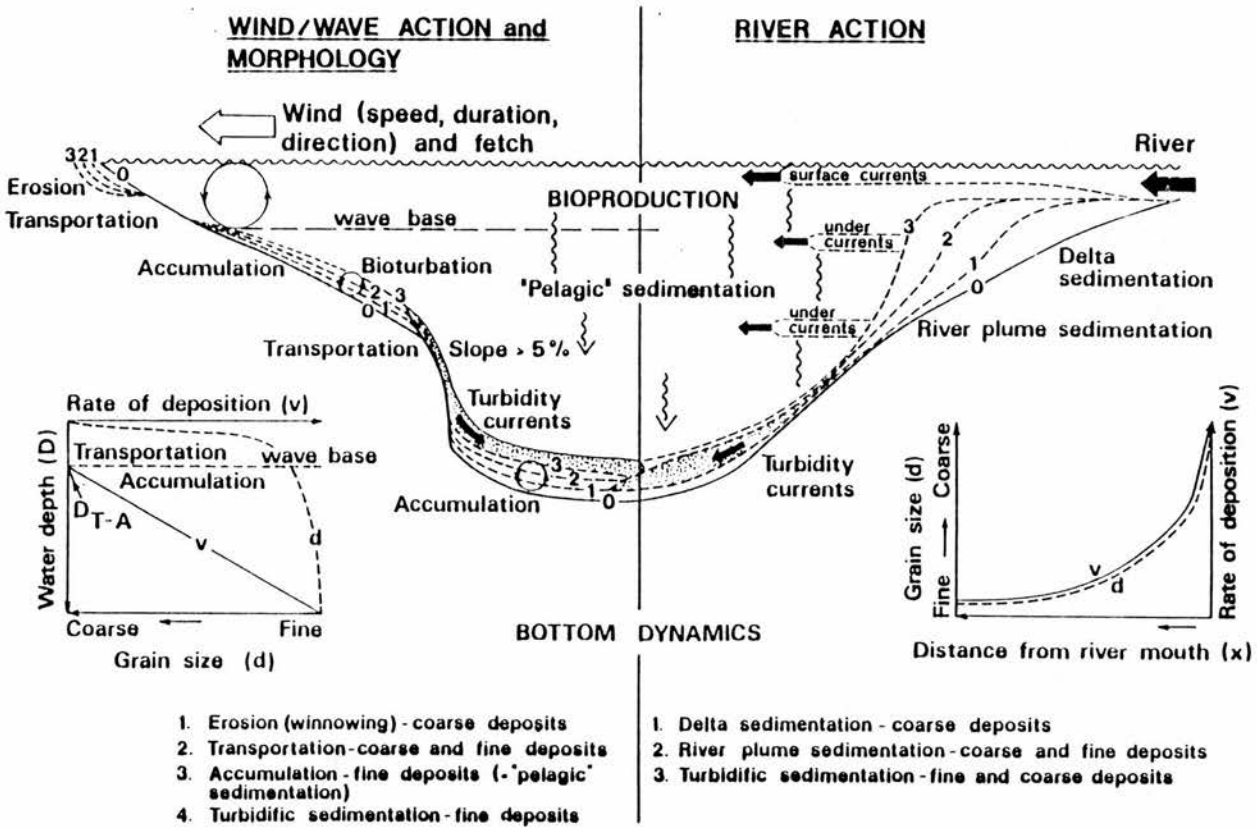

Figure 6.3 Schematic illustration of major sedimentological and bottom dynamic processes in lakes (*source*: Håkansson, 1982a).

distinguished from river-plume sedimentation by the fact that they are short lived events which redistribute older slope material rather than a more continuous process bringing in fresh sediment. Turbidites, or turbid underflows, may be caused by local slope failure on river deltas and bank collapse usually due to the steepness of the sublacustrine slopes and coarse grain size in these areas (Catto, 1987).

The effect of turbidites on the sedimentation pattern can be highly significant. For example, Sturm and Matter (1978) found that turbidity currents in Lake Brienz, Switzerland, transported material throughout the whole lake. In the sedimentological record turbidites can be recognised by sloping erosional contacts, great thickness, large grain size with little internal structure and abundant rip-up clasts. The Lake Brienz turbidites were also characterised by greater organic content due to erosion of the littoral zone. Examination of the X-radiographs and lithological diagrams for the lake cores in Svínavatn show that there are no structures resembling thick turbidites. Most of the sand-size fraction reflect input of primary tephra grains. At the top of Svínavatn lc2, however, a thin coarse-grained layer at 6-6.5 cm appears structureless on the X-radiograph and has a correspondingly high peak in loss-on-ignition (80%). The layer is not a tephra fall and may possibly represent a distal turbidite deposit originating on a slope or the Sléttá delta.

6.4.2.2 Sediment reworking by lake currents and wave action

Wind-induced waves also influence the movement and distribution of sediment in lakes. Wave action produces zones of erosion and transport which are separated from areas of accumulation by the wave base or "critical depth" (Håkanson and Jansson, 1983). The effectiveness of wave action, the depth of the wave base and the sediment response is dependent on several variables such as wind speed, effective fetch and water depth which determine wave height, period and length. The lake area affected by waves and the depth to which wave action is effective can be considerable in large lakes with strong winds.

The variables listed above determine whether wave action is a significant process in Svínavatn and is responsible for the secondary layers. It is possible to use empirically derived equations describing the relationship between energy and topography (Håkanson, 1977; Håkanson and Jansson, 1983). These theoretical models have been derived from a large data set of North American and Scandinavian lakes in the size range a=1.9 km^2 to a=3583 km^2. Determinations are based on bathymetric maps and no field data collection is required. Most of the lakes were also formed by glacial activity. Thus it is appropriate to apply these theoretical models relating to slope, form and bottom dynamics in the case of Svínavatn.

The topography of a lake affects the distribution of sediment and lake bottom dynamics, as well as the depth to which wave/wind action is important. Topographic influences can be divided into, firstly, a slope factor which reflects the fact that fine particles rarely rest permanently on slopes exceeding more than 4-5%, and secondly, a lake form factor which is related to the hypsographic curve of the lake (Håkanson 1977). The shape of the hypsographic curve indicates whether a lake has a convex profile, i.e. a large shallow bottom area influenced by wind/wave action, or a concave profile, i.e. steep sided. Håkanson (1977, 1982a, 1982b) has derived various statistical techniques to determine mean lake form and deviations from it and methods to determine the areal distribution of erosion and transportation. These formulae are all lake-specific methods based on indirect theoretical data. More site-specific models based on field observations would require detailed collection and analysis of the surficial sediments at coring sites.

Table 6.1 shows that the mean slope for Svínavatn is 5.09%. It is likely, therefore, that fine material will not remain stable on the slopes but will move to the centre of the lake under gravity. The shape, or form, of Svínavatn lake basin is expressed in terms of the relative hypsometric curve (Figure 6.4). The mean lake form, f (x bar) signifies that 50% of all lakes have relative hypsometric curves above (i.e. convex) this line and 50% are below (i.e. concave). The statistical deviations (standard deviations, f (± 0.5), etc.) are also shown. For example, a lake which has a relative

Table Svínavatn lake basin statistics

A. Variables from bathymetric map

$\overline{D}$	= mean depth (m)	= 15.73	n	= number of contours	= 7
D_{max}	= maximum depth (m)	= 38.50	l_0	= length of shoreline (km)	= 25.15
a	= lake area (km²)	= 11.75	l_t	= total length of contour lines in bathymetric map (km)	= 96.23

B. Lake specific equations to determine prevailing bottom dynamics (Håkansson and Jansson 1983)

Slope factor

$$\overline{\alpha}_p = \frac{(l_0 + 2 \bullet l_t) \bullet D_{max}}{20 \bullet n \bullet a}$$

Form factor

$$V_d = \frac{3 \bullet \overline{D}}{D_{max}}$$

Energy factor

$$DR = \sqrt{a}/\overline{D}$$

where α_p = gradient of lake slope (%)

V_d = volume development (dimensionless)

DR= dynamic ratio (dimensionless)

Energy-topography equation

$$a_{E+T} = 100 - a_A = 25 \bullet (\sqrt{a}/\overline{D}) \bullet 41^{0.061 \bullet \overline{D}/\sqrt{a}}$$

where a_{E+T}= percentage area of lake bed subjected to erosion and transportation

a_A = percentage area of lake bed subjected to accumulation

C. Model results for Svínavatn

$$\overline{\alpha}_p = \frac{[25.15 + 2(96.225)] \bullet 38.5}{20 \bullet 7 \bullet 11.75}$$

$$V_d = \frac{3 \bullet 15.73}{38.5}$$

$$DR = \sqrt{11.75}/15.73$$

$\overline{\alpha}_p = 5.09\%$ $\quad V_d = 1.2$ $\quad DR = 0.22$

Therefore, mean gradient is 5.09%, volume development 1.2, and dynamic ratio 0.22.

$$a_{E+T} = 100 - a_A = 25 \bullet (\sqrt{11.75}/15.73) \bullet 41^{0.061 \bullet 15.73/\sqrt{11.75}}$$

$a_{E+T} = 15.41\%$ $\quad a_A = 100 - a_{E+T} = 84.59\%$

Therefore the area affected by erosion and transportation is calculated to be 15.41% of the total lake area. Accumulation occurs in 84.59% of the total lake area.

Table 6.1 Table of statistics describing the factors affecting bottom dynamics in Svínavatn and the calculation of % area of erosion and transportation. (*source*: Håkansson and Jansson, 1983).

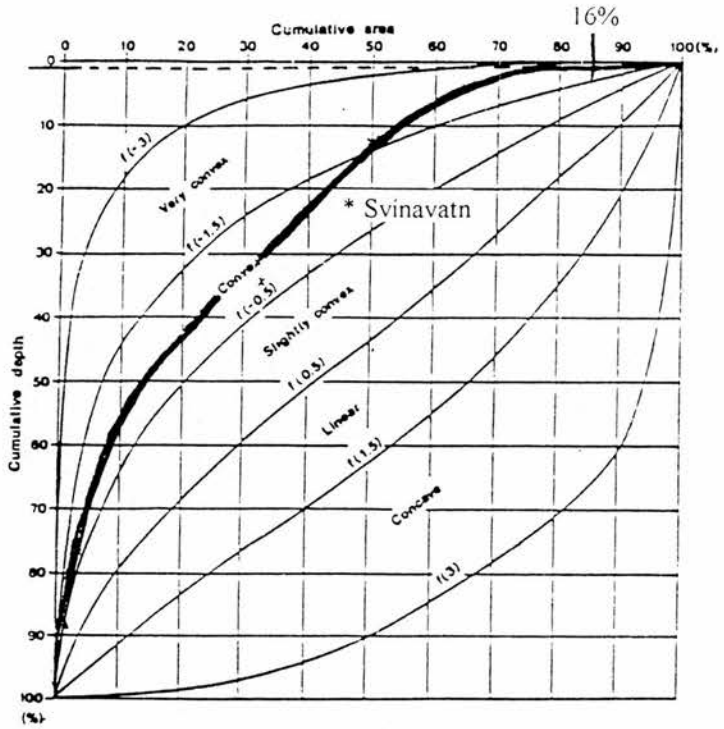

Figure 6.4 Form of a lake basin expressed as a relative hypsometric curve showing statistical deviations from the mean lake form. The relative hypsometric curve for Svínavatn is indicated on the graph. (*source*: Håkansson and Jansson, 1983).

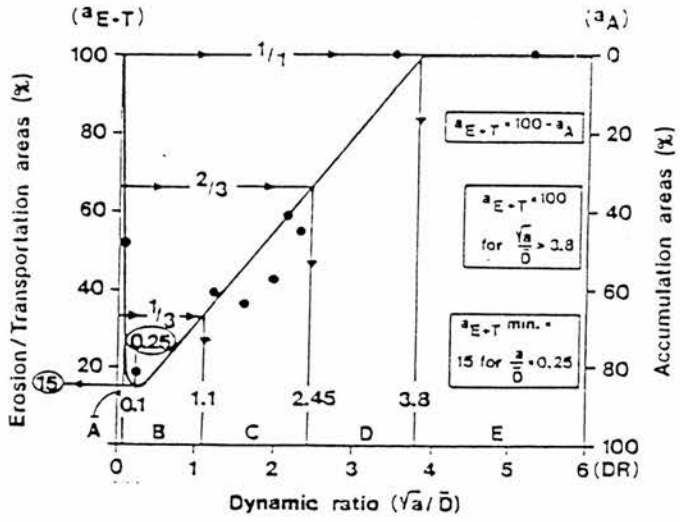

Figure 6.5 The relationship between % area of erosion and transportation (aE+T) and the dynamic ratio (*a/D). Empirical data from nine Swedish lakes illustrated with large dots. The correlation coefficient between the empirical data and the model data is 0.97. The calculated values for a_{E+T} and $\sqrt{a}/D$ for Svínavatn from Table 6.1 are marked on. (*source*: Håkansson, 1982b).

hypsometric curve of the f(+3.0) type has steep inclining walls and a large flat bottom. Converting the hypsographic data for Svínavatn, indicates that the lake is in class f(-0.5)-f(-1.5), i.e. that the lake form is convex with one (or more) deep holes and shallow edges.

The areal distribution of erosion and transportation processes on lake beds, and the critical depth, can be expressed in terms of an energy-topography equation (Håkanson and Jansson, 1983). This equation calculates the percentage area of lake bed subjected to erosion plus transport processes (a_{E+T}) and accumulation (a_A=100-a_{E+T}). Substituting the data for Svínavatn (Table 6.1), the percentage area subject to erosion and transport (and accumulation) processes is around 16% (84%).

The quotient $\sqrt{a}/D$ in the equation is called the dynamic ratio as it reflects the energy factor in the equation (Håkanson, 1982b). It means that in lakes of great area but little depth, the dynamic ratio is large and reflects the influence of waves and wind upon resuspension (the energy). When the percentage erosion/transportation area is plotted against the dynamic ratio (Figure 6.5) it appears that there is a good agreement between the model results and empirical data from Swedish lakes. The main points in the diagram are;

- firstly, in lakes with dynamic ratios greater than 3.8, the whole lake is affected by wind/wave action (a_{E+T}=100%).
- secondly, the percentage erosion/transportation area decreases to a minimum of 15% as the dynamic ratio approaches a value of 0.25. This is the point of maximum accumulation.
- thirdly, erosion and transportation area increases rapidly when the dynamic ratio is less than 0.25, up to a maximum of 100% when DR is 0.052. This means that slope processes increase in importance.

The classes marked A-E on Figure 6.5 can be used to determine which processes are the most important in lakes. For example, class A consists of lakes with steep slopes

dominated by slope processes. Class B comprises lakes with less than 33% areas of erosion and transport where there would be relatively little resuspension and effective accumulation. In classes C and D, resuspension gains in importance as the percentage area of erosion/transportation increases. In class E most limnological characteristics (e.g. transparency) are influenced by resuspension. The percentage area of erosion and transportation in Svínavatn is around 16% (84%) with a DR of 0.22. It can be seen that Svínavatn belongs to class B type lakes which are little affected by resuspension and act as effective sediment traps. The percentage area and dynamic ratio calculations (0.22<0.25 DR) indicate that slope processes are beginning to affect resuspension.

A value for the critical depth, or wave base, can also be estimated from the energy-topography formula and relative hypsographic curve. From Figure 6.4, the area of Svínavatn subject to erosion and transportation processes (16% of lake) has a depth no greater than approximately 77 cm. Below this water depth, accumulation processes dominate the bottom dynamics.

The statistics above indicate that in Svínavatn the resuspension along the shore is not great, but the mean slope is steep enough to allow movement of particles. Therefore the lake is an effective sediment trap and it is unlikely that particles are remobilised due to external factors such as wind and wave action. From these results, the formation of secondary tephra layers is not likely to be due to reworking of old tephra deposits along the shores. Any movement of material downslope from the lake shore will take place gradually over long periods of time. The expected areal and spatial sedimentation patterns in the lake would consist of tephra-rich sediment throughout lake cores extracted from the basin edges and slopes. The lake sediment between tephra horizons would exhibit the decreasing concentrations of tephra described in the mixing models of Ruddiman and Glover (1972), and Thompson *et al.*, (1986).

6.5 Post-depositional movement of tephra between the catchment and the lake sediment

Since the formation of distinct layers of reworked tephra in the deepest sections of the lake is not adequately explained by continuous erosional and depositional processes, four alternative explanations can be put forward.

1) *The source of the tephra is reworked shore material constantly stirred by wind and wave action.* The material remains at an angle of rest until thresholds such as angle or cohesiveness are exceeded. At that point the slope becomes unstable and forms either debris slumps or turbidites. Although large amounts of debris are removed, coarser fractions will be deposited rapidly near source whilst finer sediment will be transported across the lake floor. Volcanic ash is light and easily mobilised and therefore has the potential to accumulate in thick deposits large distances from the source of the slope instability. In this case there may be a grading of sediment size of both the tephra and the other lake sediment.

2) *Slope failure in the catchment contributes large amounts of peat and tephra to the lake basin.* On entering the lake the organic fraction of the peat dissolves in the water column leaving the minerogenic component (including tephra) to settle out as a layer. Again this may be reflected in differential size grading and increased organic content.

3) *Catchment slopes are eroding but the loose material lies stable on the lake edges until further erosion events exceed threshold levels and the whole mass slumps.*

4) *Reworked lake deposits reflect erosion events upstream elsewhere in the catchment.* Therefore, although erosion is obviously taking place on the immediate slopes around Svínavatn, similar events have taken place upstream. This slope erosion adds to the load of the stream (i.e. the Sléttá), which

deposits coarse material along the channel but the lighter tephra fraction forms a dense undercurrent (or overcurrent) affecting the currents and sedimentation of Svínavatn.

To assess the wider significance of the environmental record at Svínavatn the data are considered within a conceptual model of tephra movement in catchments and lakes. Figure 6.6 shows the route ways and sediment stores between lacustrine and terrestrial sites over time.

6.6 The catchment-lake model

The model focuses on the characteristics and appearance of tephra in the lake sediment core during and after initial fallout, and through time (from left to right). The upper half of the diagram represents the lake environment and the accumulation of sediment in a hypothetical lake core containing both primary and secondary tephra layers; the lower half of the figure represents the catchment; the dashed line between the two systems represents the lake-catchment interface (littoral zone or shore area). Within the catchment system there is a tephra/sediment store consisting of material such as soil, peat, snow and ice onto which tephra falls.

Restraining variables such as particle size, slope angle, vegetation and soil cover act together to prevent removal of tephra from the system. The progression of time is represented by the increase in the depth of the tephra layer in the store from left to right as more sediment accumulates. Forcing variables such as climate and disturbance at unspecified times in the future disrupt the characteristics of the restraining variables and/or the relationship between them to re-expose the catchment tephra. The pathways of the tephra to the lake system are shown by arrows.

The model distinguishes between primary deposition following initial fallout of tephra and secondary deposition through time. It examines the sedimentary

routeways between catchment and lake and corresponding characteristics of the lacustrine deposits.

6.6.1 Period I: Primary deposition

Following the production of tephra from an eruption (A), the volcanic ash falls equally on the three parts of the lake-catchment system; the lake body, the shore area or littoral zone, and the catchment.

6.6.1.1 Lake body

Figure 6.6 shows the volcanic ash falling directly onto the water surface, settling through the water column to form the original isochrone in the lake sediment. Dependant on the season when a specific eruption took place, the stability of the water column and the bed topography, this layer reflects the characteristics of the original airfall in terms of the variations in grain size, colour and geochemistry throughout the layer.

6.6.1.2 Littoral zone (the area above the wave base or critical depth)

In addition to direct atmospheric fallout, the lake system receives tephra from the edges of the lake basin. The littoral zone is a high energy environment compared to deeper waters and so the tephra is reworked continually by wind and wave action. Further deposition along the shore may occur through transport across the lake as less dense tephra lies as a thin film on the lake surface. The initial reworking and resuspension of ash in this zone will take place along the whole shoreline of the lake whereas the distribution of the floating ash will be controlled by factors such as wind fetch and wind strength. This process is site-specific and it is possible that sediments on the depositing shore will have a greater accumulation of volcanic ash and a more complex history of erosion and deposition than upwind shores. The resuspended tephra from the littoral zone eventually becomes deposited in the deeper parts of the lake. As the processes operating along the shorelines are continually eroding, resuspending and depositing sediment, the resultant signal in the hypothesised lake core will not be a pulsed discrete event but a continual input of sediment over time. The significance of the process is acknowledged in the model by the short transport

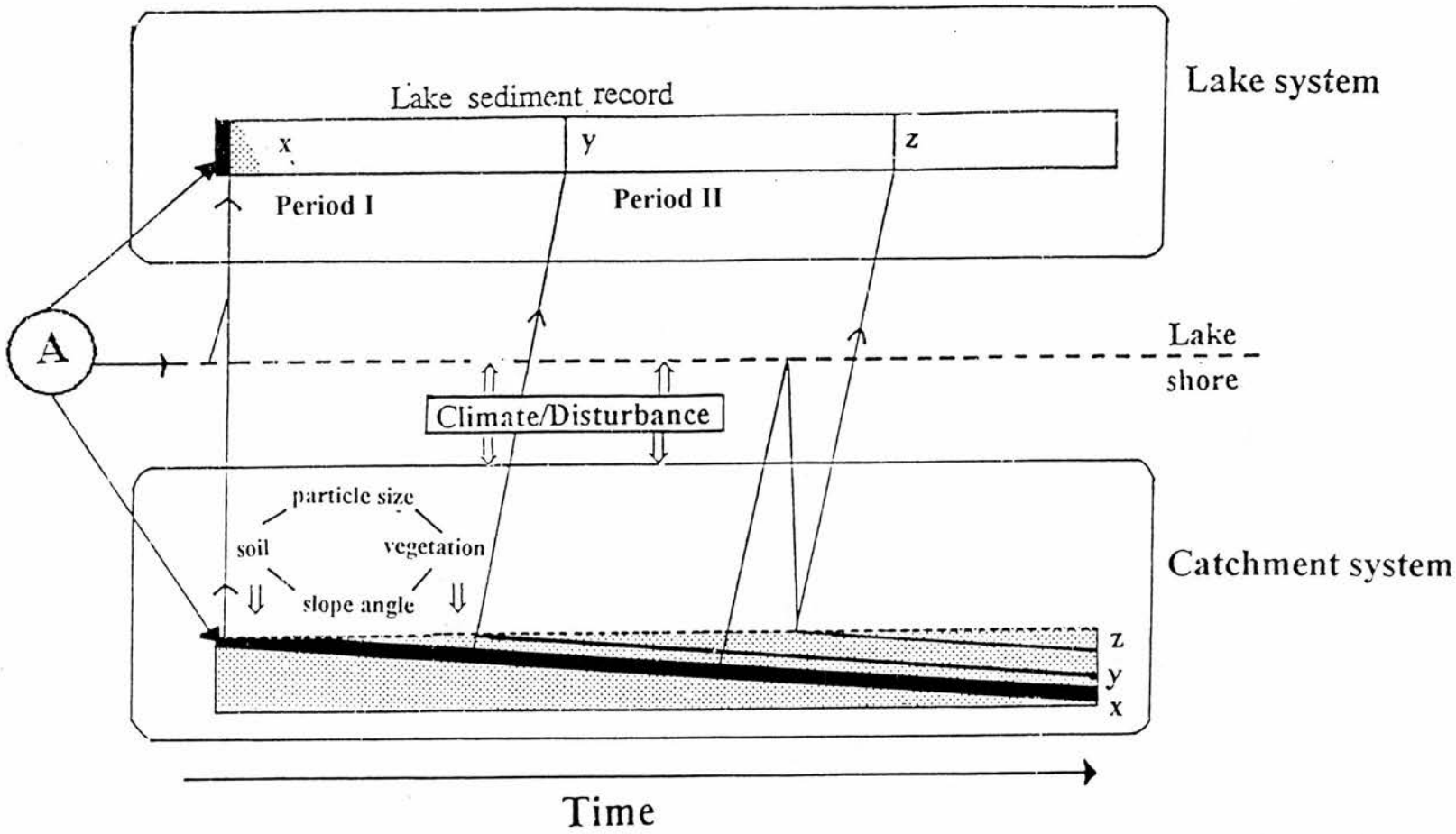

Figure 6.6 Catchment-lake model showing the routeways of tephra input into the lake system over time. The stratigraphic record in the hypothetical lake core begins following the initial tephra fall (A). The progression of time is shown by sediment accumulation in the lake, and thickening of the soil/peat deposits in the catchment.

path of tephra from the interface to the lake forming a dispersed tephra deposit covering the original airfall.

6.6.1.3 The catchment

The catchment also receives an initial input of tephra following the eruption. Until the exposed tephra is bound by vegetation or buried by subsequent development of soil, peat, vegetation or snow, the top loose layer of the tephra is reworked by the actions of wind and water. At this stage the tephra is easily mobilised as the layer is not a consolidated horizon and therefore subject to wind erosion and downslope movement by overland flow. The effect on the stratigraphic record in the catchment is that each soil profile displays variable thickness of tephra. The eroded and reworked catchment tephra eventually becomes incorporated in the lake sediments as part of the sediment delivery to the lake. In the model, this tephra forms part of the dispersed layer, physically indistinguishable from the tephra resuspended from the shore area.

6.6.2 Period I-Stratigraphic characteristics

The stratigraphy of the lake core and the catchment profiles during primary deposition reflects the balance between processes of erosion and accumulation in the systems. The catchment is characterised by rapid erosion, dispersion and relocation of tephra, the effectivenes of which is determined by the nature of the surface. For example, exposed hillsides experience more stripping than flat vegetated peatland. Certain sites are therefore better sites for load calculations and tephrostratigraphies, but provide incomplete catchment histories. The deeper parts of the lake, by contrast, are the major areas of accumulation as deposits from the catchment and shallow margins contribute to the sediment influx. For this reason, lacustrine deposits have both an initial fallout layer and a reworked dispersed layer.

The dispersed layer above the isochrone is shown in the model to be due in part to resuspension of ash within the lake and to eroded catchment tephra. Thompson *et al.*, (1986) examine this mixed layer in the sediments of the western basin of

Svínavatn to evaluate the time taken for the reworked tephra to accumulate. By measuring the variation in the concentration of 11 elements in the sediments prior to and after the deposition of the three silicic Hekla tephra, they estimate the thickness of the mixed layer to be 4.8, 1.3 and 1.9 cm for tephra layers H4, H3 and H1 respectively. Using the calculated sedimentation rates from one core, they argue that accumulation times for half the mixed layer ashes to accumulate are 36, 7 and 8 years for H4, H3 and H1 respectively. In other words, tephra is mobile around the catchment and lake edges for many years following an eruption.

Thompson *et al.*, (1986) also attempt to estimate the relative contribution of resuspension processes in the lake and catchment erosion to the mixed layer using the model in Figure 6.7.

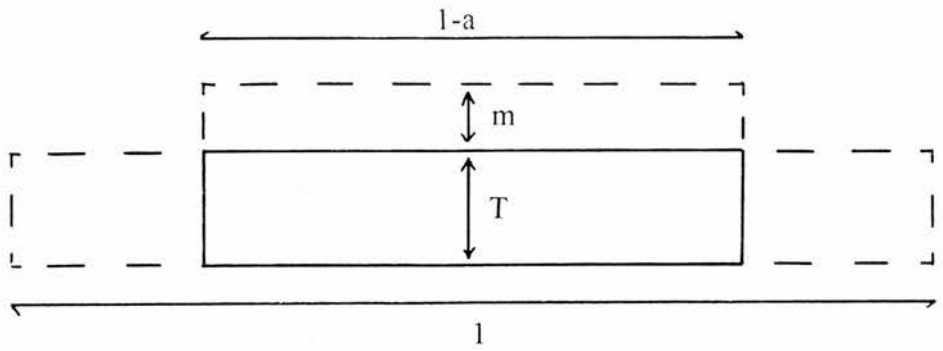

T = tephra thickness
m = exponential "decay constant"

Figure 6.7 The distribution of tephra before and after erosion and transportation of resuspended lake sediments and following catchment erosion. The dashed areas represent ash moved from its original deposition sites to new accumulation sites. The solid area represents undisturbed ash in the lake. The proportion of resuspension and stripped lake bed can be estimated from the tephra thickness, T, and the decay constant, m. The sediment delivery ratio (catchment erosion) can be estimated from T and m where a is the catchment area and 1-a the lake area. (source: Thompson *et al.*, 1986).

They assume that the mixed layer represents the accumulation of sediment from either one source or the other, but not a mixture of both. Using the equation

$$a = \frac{m}{m+T}$$

where a is the proportion of lake bed stripped of tephra and resuspended, m the thickness of the mixed layer, and T the thickness of the initial tephra layer, and solving for a with data for H3,

$$0.34 = \frac{1.3}{1.3+2.5}$$

Therefore 34% of the area of Svínavatn is estimated to have been stripped of ash following the deposition of H3. The authors state that the proportions calculated for the Hekla tephra (H4~47%, H1~40%) seem unrealistically high. Consequently they calculate the sediment delivery ratio for Svínavatn catchment after each tephra fall using the equation,

$$DR = \frac{m}{T} \times \frac{(1-a)}{a}$$

where DR is the sediment delivery rate, and $(1\text{-}a)/a$ is the lake-catchment ratio. Using a ratio for Svínavatn of 1:20, delivery rates of sediment from the catchment are 4%, 2.5% and 3% for H4, H3 and H1 respectively. On this basis Thompson *et al.*, (1986) surmise that resuspension was relatively unimportant and catchment erosion processes accounted for the depth of the mixed layer, with the caveat that the calculations of delivery ratio were overestimates if resuspension was a factor.

The results of the present study, following an examination of the morphometry of Svínavatn basin and the potential for resuspension above the wave base, indicate that approximately 16% of Svínavatn may be affected by resuspension. If this is the case,

the estimate of stripping over 34-47% of the lake area is clearly too high, as is the sediment delivery rate. It is possible to rearrange the equations and substitute the results of this study for the tephra layer H3,

$$m = \frac{aT}{1-a}$$

$$0.47 = \frac{0.16 \times 2.5}{1-0.16}$$

This means that 0.47cm of the thickness of the mixed layer can be attributable to resuspension processes in Svínavatn, whilst 0.83cm is due to catchment erosion.

6.6.3 Period II- Secondary deposition

A period of stabilisation follows the most vigorous reworking and sorting of the freshly fallen tephra in the catchment and lake edges. The restraining variables start to operate, incorporating the volcanic ash layer into the stratigraphy of the tephra store. Each variable in the model is effective over differing lengths of time. Particle size and slope angle have the strongest influence following an eruption. Transportation by water and wind selectively remove easily mobilised tephra grains and leave behind deposits more resistant to movement. Dependant on the size of the eruption, the vegetation will recover and bind the deposit further as well as accumulate organic matter. Gradually the tephra becomes a highly minerogenic horizon in the soil/peat profile; thicker in the low-lying level areas of the catchment, more variable in thickness and grain size characteristics on the slopes and interfluves.

Reworked, secondary deposits in profiles around Svínavatn indicate disturbance of the tephra store over time. The model represents this as two forcing variables, climate and disturbance; the operation of one or both affecting the balance between the restraining variables and the tephra store. For example, climatic changes during the Holocene affect vegetation cover which in turn exposes or protects the regolith

to/from erosion. In addition earthquakes and landslides affect slope angle and cause readjustments between particle size, soil and vegetation cover.

Hypotheses for the reworked layers around Svínavatn include gullying, piping and slumping in peat deposits. The disturbance may have been due to a reduction in woodland and rapid peat accumulation caused by a cooler, wetter climate, or increased incidence of storminess and heavy rain. The exposure of buried tephra layers may be a localised occurrence in a small part of the catchment where the tephra is preferentially removed, for example by piping or by cyclic erosion of peat. Alternatively, there may have been widespread disturbance throughout the landscape. The tephrochronological evidence from Svínavatn indicates extensive slope instability around 2500 BP which points to widespread erosion.

Following re-exposure, the tephra is subject to reworking and transportation. Much of the sediment will remain in the catchment as it relocates downslope to form a secondary layer in a profile. A proportion of the tephra will enter the lake as a pulse of sediment from the lake sides, or into the river for transport to the lake. The density characteristics of the eroded tephra suggest dispersal into the lake as an overcurrent of less dense material. The secondary layer thus formed will have a patchy distribution across the lake floor. For this reason, tephra stratigraphies in lake cores may be diachronous.

Different scenarios about the formation of secondary layers have been incorporated into the model. In the first case, the remobilised tephra enters the lake immediately following detachment from the slope and forms a discrete layer on the lake bottom. An alternative view of this scenario can be accommodated in the model if the secondary tephra deposition is not instantaneous but occurs as a continuous input. Dependant on the sedimentation rate in the lake the two processes may appear indistinguishable, that is, in a slowly accumulating sediment column apparently instantaneous deposits may represent several years.

A further possibility is shown in the model whereby an erosion event on the hillsides exposes the original tephra layer and it accumulates downslope but does not reach the lake system. Over time the restraining variables act to bury the secondary layer until future erosion releases the secondary tephra to the lake. An examination of the tephra stratigraphy in the lake core could make no differentiation between the two secondary layers.

6.7 Summary

The pattern of tephra within the lake-catchment system following initial fallout and during later periods is patchy and incomplete. Tephra airfall does not occur as a blanket-like deposition of ash evenly over a catchment but is related to weather conditions at the time of eruption. Immediate reworking of the freshly fallen tephra takes place through water, wind and niveo-aeolian processes, with deposition in the lake basin. The result is incomplete tephra stratigraphies around the catchment and in lake sediments. In Svínavatn catchment, the least continuous deposits of tephra are the ash layers SSn, SvV and K-X, possibly as a result of snow cover at the time of deposition.

During later periods, disturbance within the catchment and/or lake expose and redistribute early tephra layers. The characteristic which distinguishes the reworked layers in both catchment and lake is a geochemically mixed population of tephra grains. The secondary layers in the lake sediments are of a finer size grade, but have no evidence of reworking such as contamination, abraded shards and rounded edges. An important point is that the secondary layers in the lake represent discrete pulses of sediment. Several processes which could produce both continuous and discontinuous inputs of sediment are mass wasting, slope wash and internal lake processes. The freshness of the secondary tephra layers in the lake indicate short transport paths, low energy environments and selective sorting of glass shards. Possible mechanisms which explain the physical appearance of the tephra layers are peat slides and piping within peat. The input of pulses of tephra into the lake from the catchment produces discrete layers while continual movement of eroded catchment tephra down lake

basin sides would not produce such layers. Empirical models applied to Svínavatn lake basin suggest that the morphometry of the lake would provide a favourable accumulation site but sedimentation would be little affected by the action of wind and waves. The secondary layers throughout the cores do not, therefore, indicate periods of shore erosion.

CHAPTER 7

7.1 Implication of the conceptual model for lake catchments

The catchment-lake model developed in the previous chapter should apply generally as it highlights the processes affecting the deposition of volcanic ash in lake catchments both immediately following ashfall and subsequently. The emphasis and significance of different elements will change with varying intensities of fallout, catchment and lake characteristics. It should be applicable not only to the fine-grained, low-volume tephra fallout in Sweden, but also to any other mid to high latitude lake system affected by tephra fall. The results and discussion in Chapters 5 and 6 have stressed that the use of tephra as an isochrone requires an accurate assessment of what any particular deposit actually represents. For instance, is it a primary airfall, isochronous with other primary fallout from the same eruption, or is it a later deposit? If so, what is its significance? The model suggests possible route ways and sources of individual tephra layers and helps determine whether the tephra is a primary (isochronous) or secondary (diachronous) deposit. This chapter attempts to use the model framework to assess the possibility of finding tephra in Swedish varves and suggest which factors are most likely to influence tephra deposition in the Ångermanälven.

The depositional history of the tephra layer is dependant on both lake and catchment variables which control the rate and distribution of sediment around the system. These variables include the catchment characteristics of vegetation, geology, climate and morphometry, the linking processes of aeolian and fluvial inwash, and lake basin factors such as deltaic processes, water stratification, nutrient cycling, erosion and resuspension in the water body. The varve model proposed by Sturm (1979), oulined in Chapter two of this study, can be incorporated into the catchment-lake model to indicate the possibility of laminated sediments.

• the spatial pattern of tephra is not continuous across all depositional environments. This is shown by missing tephra layers in several sites in the lake and catchment at Svínavatn. Geomorphologically stable areas which would be expected to provide an accurate record of tephra fallout, such as lowland peat deposits, do not necessarily have complete tephra stratigraphies. This is probably a reflection of precipitation patterns, microclimate and exposure, and season during which the eruption took place. Only by examining several sites in different depositional environments can a full regional tephra stratigraphy be constructed.

• the geomorphic and environmental setting of profiles is of major importance when constructing local tephra stratigraphies. Processes operating on many different timescales will affect the rate and timing of sediment erosion and redistribution. It is important to view tephra not as a separate component of environmental systems, but as part of the sediment store subject to disturbance and reworking. Concepts such as complex response, intrinsic and extrinsic thresholds, and lag times can be usefully employed to examine the tephra and sediment records.

• it is not always possible to distinguish primary airfall tephra from reworked deposits on physical characteristics alone. Some erosional and depositional processes operate selectively so that there is no evidence of reworking such as abrasion or matrix contamination. Adopting a multiple core correlation strategy across different depositional areas can suggest possible mechanisms which produce pulse inputs of fresh tephra layers. The work at Svínavatn suggests an important factor is peat bog stability over time. The only secure way of identifying secondary reworked layers is by analysing the geochemistry of the individual glass shards. The presence of mixed populations of earlier tephra is firm proof of redeposition. Identification of a mixed population, however, is dependant on correct geochemical fingerprinting of tephra deposits on site and regionally. This involves distinguishing both source volcanic systems and individual eruptions. This conclusion stresses the importance of constructing secure tephrochronologies, an advantage in areas close to Iceland's volcanic system.

7.2 Application to Ångermanälven, Sweden

This section uses the conceptual model devised from the Svínavatn study to assess the key variables affecting the likelihood of tephra deposition in the Ångermanälven varves. It is important firstly, to discuss how appropriate it is to apply the Svínavatn catchment-lake model to the Ångermanälven site by examining the similarities and dissimilarities of the two sites with respect to the model.

Aspects which are similar to the sites in both Sweden and Iceland are the presence of laminated sediments, lack of bioturbation of sediments, morphometry of basin (steep sided, deep, narrow and flat-bottomed), and a vegetated catchment. The main dissimilarity is the difference in scale between Svínavatn and the Ångermanälven, both in the size of the catchments and the thickness of the tephra deposits (assuming the presence of volcanic ash in northern Sweden). The results from Svínavatn and the

resulting model highlight the relationship between catchment erosion processes and sediment transport paths into that lake. The site at Svínavatn is a small, relatively simple catchment with short sediment transport paths to the lake from either river input or direct drainage from the slopes. However, the varved sediments of the Ångermanälven are found in the non-tidal estuary of the river and are formed from the erosion of former delta deposits several kilometres upstream (see Figure 3.2). The main variables when applying the catchment-lake model to the Ångermanälven are therefore sediment supply and depositional processes.

7.2.1 The period following ashfall - primary layers in the Swedish Varve Chronology

The pattern of primary tephra layers at Svínavatn revealed the patchy distribution of relatively thick ash deposits on a small catchment scale. One implication is that tephra will be as locally variable in the Ångermanälven site because fine-grained tephra will be as subject to patchy deposition, selective erosion and variable preservation as the cm-scale layers at Svínavatn. An additional factor is determining whether or not particular tephra clouds travelled over the Ångermanälven. It is not certain that the historical tephra falls recorded by Persson (1971) in the Scandinavian peat bogs also occurred in the Ångermanälven region. However, it is clear from the Icelandic site, that even if ash was deposited, considerable variation may be introduced into both the spatial and stratigraphic record. Tephra deposition is not likely to have exceeded the levels recorded Persson (1971) in central Sweden or Bennett *et al.* (1992) in the Shetland Isles, Scotland. Fallout is likely to be in the order of 10-30 grains per 50 inorganic objects (Bennett *et al.*, 1992). With such low concentrations, reworking is likely to be hard to detect.

Assuming that tephra was deposited in the area, further controls over the pattern of initial deposition include weather patterns prevailing at the time of each tephra episode, microclimate, and the presence of snow cover/lake ice. The Svínavatn research shows the extent and importance of selective deposition and gives an indication of the types of environment which are most likely to contain isochronous deposits of tephra, although these too may have incomplete stratigraphies (e.g. flat peatlands, central deeps of lake basins).

Initial tephra deposition may not have been possible at the Ångermanälven due to the very processes which allow varve formation. Water column stratification studies in the Ångermanälven show oxygen depletion over most of the Kramfors basin (Figure

3.2) in the lower part of the estuary (Cato, 1985). The stability of the water column and the great depth of the basin (some 112 m deep) along the river allows the formation of true clastic varves. The importance of the stratification of the water column has been outlined in Chapter 2 especially in the model by Sturm (1979) which indicates that the timing of sediment input is vital to the creation of a true annual lamination. The timing of the tephra input may also affect the formation of the tephra layer. Microscopic vesicular shards, for example, entering the river during the spring floods may remain suspended in the water column until calm winter conditions allow finer particles to settle. Dependant on the density of the tephra and the state of the water column in the Ångermanälven, it may take several years for the ash to reach the lake sediments. In this case, a discrete layer will be formed but at the wrong time.

In addition, the situation at the Ångermanälven is more complicated as favourable sites for finding both tephra and varves must coincide. Varves are produced by erosion of sediment upstream and deposition downstream, that is, a lateral movement of material. The deposition of a primary tephra layer in lake sediments, on the other hand, assumes vertical settling in the water column. In a high energy riverine environment such as the Ångermanälven, tephra fallout may occur over optimal varve coring sites but deposition take place downstream. Alternately, tephra may be deposited in the higher reaches of the catchment and transported to the estuarine sites producing a dispersed primary layer which is not in situ. The importance of this possibility for the aim of linking the two chronologies is discussed below. The only method of determining whether tephra fell in the lower reaches of the Ångermanälven is to sample the peat deposits in the surrounding catchment and also further upstream. This aspect demands further research in the future before more attempts are made to find Icelandic tephra in the varves of the Ångermanälven.

7.2.2 Reworking and redeposition in the Swedish Varve Chronology

The catchment-lake model shows that secondary deposition of tephra can occur on both catchment slopes and within the lake basin. At Svínavatn, changes in the constraining variables such as slope angle and vegetation cover may have caused secondary tephra inputs to the lake system. Peat bog stability on the adjacent slopes was suggested as a possible mechanism, whilst the influence of the river input was negligible. This situation contrasts with the Ångermanälven as the river estuary lies in an area of low relief and the area is dominated by river processes.

The Ångermanälven varves are predominantly clastic, formed from estuarine clay, glacial clay and fluvial material. The varves are derived from the erosion of earlier delta deposits lying upstream. This occurs due to the continuous isostatic elevation of the land since the last glaciation which is estimated to be continuing at a rate of 1 cm/yr at the present time (Lidén, 1938). As the land is uplifted, the river incises, and deltas form in the valley downstream. As the older deltas rise above sea level, the river cuts through these old deposits to feed the younger delta downstream. The postglacial varves are therefore composed mainly of redeposited delta material and collapsed bank deposits. This has major implications for finding tephra in the varves as the original tephra fall may have occurred up river and settled in terrestrial deposits and old deltas. Later erosion mobilises the tephra deposits and they may form discrete layers within the varve sequence. The greatest concentration of glass shards within the varve chronology may reflect erosion episodes rather than airfall input, making it more difficult to distinguish peak concentrations and background inputs. However, unlike the reworked tephra at Svínavatn, it may be possible to identify reworking due to the more turbulent nature of the depositional environment, for example more mechanically degraded shards and contamination by matrix material.

The model developed for the Svínavatn lake and catchment provides a framework for examining the possible processes affecting tephra deposition in lakes. The results from Svínavatn suggest the importance of the initial airfall distribution and later erosion in the catchment on the eventual stratigraphy at that site. In contrast, potential tephra stratigraphies in the Ångermanälven will probably be more affected by the active role of varving mechanisms, than by geomorphic stability in the catchment. This has important implications for the initial aim of linking the Swedish Timescale and the Icelandic tephrochronology as it may be difficult securely to establish whether any glass shards found are primary. For example, using the model framework, any tephra layer found in the Ångermanälven varves may be interpreted in three ways;

- the layer is primary and in situ as the fallout from the eruption cloud occurred over the estuary of the Ångermanälven. Furthermore, the ash was incorporated directly into the river sediments.

- the layer is a primary deposit from a tephra fall which occurred upstream but was subsequently transported downstream to more favourable varve deposition sites. Therefore the layer is not in situ. In addition, the sediments at the airfall site upstream may contain a few dispersed shards which are the only evidence of a primary tephra fall. These shards, if found, may be dismissed as reworked, secondary deposits.

• the layer is the result of erosion of older bank deposits or former delta fronts upstream and subsequent incorporation into a new varve. Therefore, any dates for the tephra do not correspond with the age of varve formation.

The results from Iceland indicate the importance of detailed sampling in the catchment and lake to establish whether a tephra layer is primary. However, the patchy nature of relatively thick, visible tephra layers in a small catchment was also highlighted. A similar sampling strategy in the Ångermanälven catchment may establish whether tephra fell over the region, but the interpretation of any tephra deposits in the varves remains ambiguous due to the nature of clastic varve formation and the properties of microscopic, vesicular glass. Furthermore, independent checks on the age of varve sequences and tephra layers such as radiocarbon dating, are susceptible to the same reworking mechanism and may yield dates that are too old.

The formation and composition of clastic varves means that the annual nature of the Swedish Timescale (especially the recent sediments of the Ångermanälven) may be difficult to establish firmly. Any identified tephra layer may reflect simply varving mechanisms, whilst individual glass shards dispersed through sediment may or may not be the primary airfall. More profitable sites for correlating varve chronologies and tephrochronologies may be lakes which have autochthonous laminations (biogenic, calcareous or ferrigenous varves), the minimum of disturbance in the catchment and no significant inflow/outflow.

7.3 Implication for linking Icelandic tephrochronology and the Swedish varve timescale

The spatial and temporal pattern of tephra sedimentation indicates that inputs of reworked tephra into a lake basin are episodic in nature. Peaks of tephra seen in lake sedimentary sequences (cf Bennett *et al.*, 1992, Björck *et al.*, 1992) may be artefacts of geomorphic processes and not primary airfall deposits. Correct geochemical analysis of the glass shards is essential if the presence of an airfall deposit is to be established. The degree of reworking and mobilisation of tephra is revealed most clearly when multiple cores are taken from several sites in different depositional environments. Multiple site correlation allows an assessment of the distribution of favourable depositional areas and unstable areas. A complete picture cannot be formed if there is over-reliance on one or more sampling sites in the geomorphically stable areas of the catchment. For example, correlating lake cores containing multiple

reworked layers with the tephra stratigraphy in the stable areas of the catchment would have simply suggested the operation of erosional and depositional processes internal to the lake system. Instead, sampling of profiles in less stable areas reveals the important links and route ways between catchment and lake.

The probability that the reworked layers in the lacustrine site in Iceland reflect catchment disturbance is based on the coincidence in timing of events and the fresh, unweathered appearance of the secondary tephra input. Sites in the lake basin and on the slopes reflect disturbance of sediment stores after the deposition of H3, possibly due to climatic change. Alternative factors such as anthropogenic activity and the impact of grazing animals can be eliminated at sites in Iceland until the end of the 9th century AD. There is no evidence of major episodes of reworking prior to the deposition of H3 although climatic oscillations and other environmental disturbance took place. The reworked layers around the catchment and within the lake are identified on the basis of geochemistry, in that the EPMA results indicate mixed populations of tephra. Visually, there is no evidence of reworking, although the secondary layers are generally of a finer particle size compared with the original deposits. The morphology of the reworked deposits reflects the physical characteristics of the more mobile silicic tephra as vesicle-rich, frothy shards dominate the deposits. An indication of the relative ease with which silicic tephra is mobilised is that the secondary layers in lacustrine and catchment sites appear white in the stratigraphy, reflecting the concentration of silicic tephra shards compared with the bulkier basaltic products.

An important conclusion is, therefore, that it is difficult to determine whether a tephra layer is a primary or secondary deposit without a detailed tephrostratigraphic reconstruction in different depositional environments.

In summary, there are several implications for applying Icelandic tephrochronology to Swedish varves:

1) The historic tephras known to have fallen in Sweden are not obvious in the Swedish varve chronology of the Ångermanälven valley.

2) This may be because of ;

- genuine absence of tephra, i.e. the ash cloud did not reach the area; or
- mismatching of the varve chronology and the tephrochronology; the varves are not annual for most of the late Holocene sequence; or,

- the lack of knowledge about lake processes and tephra as a sediment, therefore the optimum sites for varve formation and deposition do not correlate with areas favourable to tephra input.

3) The characteristics of tephra as a sediment may be a key factor in determining response to geomorphic processes. For example, the settling velocity is dependant on degree of vesicularity of the glass shards. There is a great range of density of tephra and therefore a range of responses to internal lake processes and catchment disturbance.

4) Construction of a catchment-lake model helps highlight the possible processes and fluxes of sediment between the two systems. The model is specific to the Icelandic case study but can be modified to assess results elsewhere.

This study is possibly the first to consider the detailed spatial and temporal pattern of tephra deposition in a catchment and the implications this has for constructing regional tephrochronologies. The study in Iceland revealed that no single site or reference profile provides a definitive regional tephra stratigraphy. Several sites have to be analysed and correlated securely. It also shows that the only way of accurately identifying primary and secondary tephra layers is by geochemical analysis of the glass shards; grain size, colour and shape offer support to interpretations of reworking but these characteristics are dependant on geomorphic and sedimentological setting and the characteristics of the original eruption.

The results suggest that attempts to construct tephrochronologies in areas distant to volcanic centres, such as the British Isles, from one lake core are limited as are studies which analyse one core or site in detail without consideration of spatial variations in sediment supply. This may affect interpretation of regional histories of vegetation change based on chronologies provided by tephra layers (Bennett *et al.*, 1992: Hall *et al.*, 1994). Multiple cores and detailed analysis of tephra would enable the significance of "background" input to be assessed.

The movement of tephra around the catchment and eventual deposition in a lake may not be a unique characteristic of tephra. It is important to consider tephra as part of the sediment store, although it is an identifiable and unique deposit. In the same way, pollen may be considered as a sediment and part of a store that experiences disturbance and mobilisation through time. As reworked tephra deposits do not show physical evidence of reworking, the implication is that well-preserved pollen may not

all be primary and degraded pollen grains may not be the only evidence of redeposition. There may be some overlap between the correct palynological signal and the palaeoenvironmental "noise".

There are implications for lake studies in the future. Although a great deal of research has been undertaken examining the spatial patchiness of lake sediments (Downing and Rath, 1988; Foster *et al.*, 1988), there are few methods of differentiating the possible influx of older material into the deep parts of lake basins, identifying sediment sources, or correlating between lacustrine and terrestrial sites. Tephra has the potential to provide some solutions when lakes are used in palaeoenvironmental reconstruction studies. This research has shown the highly mobile, yet clearly identifiable, nature of tephra deposits. Future research could go beyond the use of empirical models and include monitoring limnological parameters such as currents, wind exposure and lake water column dynamics in conjunction with analysis of tephra deposits. Further research at Svínavatn would provide more secure interpretations of the sediment data and provide a test of the empirical models used in this study (Håkansson and Jansson, 1983).

REFERENCES

Almquist-Jacobson, H., Almendinger, J.E. and Hobbie, S. 1992: Influence of terrestrial vegetation on sediment forming processes in kettle lakes of West-Central Minnesota. *Quaternary Research* 38(1), 103-116.

Annertz, K., Nilsson, M., Sigvaldason, G.E. 1985: The post-glacial history of the Dyngufjoll. *Nordic Volcanological Institute Report* 8503, University of Iceland, Reykjavik.

Antevs, E. 1922: *The recession of the last ice sheet in New England.* New York: American Geographical Society, Research Series no.11.

Antevs, E. 1925: *Retreat of the last ice sheet in eastern Canada.* Geological Survey of Canada memoirs, 146, pp142.

Antevs, E. 1951: Glacial clays in Steep Rock Lake, Ontario, Canada. *Bulletin of the Geological Society of America* 62, 1223-1262.

Anthony, R.S. 1977: Iron-rich rhythmically laminated sediments in Lake of the Clouds, Minnesota. *Limnology and Oceanography* 22, 45-54.

Arnalds, O. 1990: *Characterisation and erosion of Andisols in Iceland.* Unpublished PhD Thesis, Texas A & M University.

Ashley, G.M. 1975: Rhythmic sedimentation in glacial Lake Hitchcock, Massachusetts-Connecticut. In Jopling, A.V. and McDonald, B.C., editors, *Glaciofluvial and glaciolacustrine sedimentation.* Society of Economic Palaeontologists and Minerologists Special Publication 23, 304-320.

Axelsson, V. 1983: The use of X-ray radiographic methods in studying sedimentary properties and rates of sediment accumulation. *Hydrobiologia* 103, 65-69.

Baillie, M.G.L. 1989: Hekla 3: How big was it? *Endeavour* 13, 78-81.

Baillie, M.G.L. and **Munro, M.** 1988: Irish tree rings, Santorini and volcanic dust veils. *Nature* 332, 344-346.

Benediktsson, J. 1968: *Íslendingabók I.* Íslenzk Fornrit I. Hiðslenzka Fornritafélag, Reykjavík.

Bengtsson, L. and **Enell, M.** 1986: Chemical analysis. In Berglund, B.E., editor, *Handbook of palaeoecology and palaeohydrology*, 423-451.

Bennett, K.D., Boreham, S., Sharp, M.J., and **Switsur, V.R.** 1992: Holocene history of environment, vegetation and human settlement on Catta Ness, Lunnasting, Shetland. *Journal of Ecology* 80(2) 241-273.

Bergsten, F. 1954: The land uplift in Sweden from the evidence of old water marks. *Geografiska Annaler* 36, 81-111.

Bergström, R. 1968: Stratigrafi och isrecession i sodra Västerbotten. *Sveriges Geologiska Undersökning*, Series C 634, Uppsala: SGU.

Binford, M.W. 1983: Palaeolimnology of the Peten Lake District, Guatemala. I. Erosion and deposition of inorganic sediment as inferred from granulometry. *Hydrobiologia* 103, 199-203.

Bjarnason, H. 1974: Athugasemdir við sögu Íslendinga í sambandi við eyðingu skóglendis. *Ársrit Skógræktarfélags Íslands* 1979, 30-43. (Remarks on the history of the Icelandic people in connection with the destruction of woodland).

Björck, S., Sandgren, P. and **Holmquist, B.** 1987: A magnetostratigraphic comparison between ^{14}C years and varve years during the late Weichselian, indicating significant differences between the timescales. *Journal of Quaternary Science* 2, 122-140.

Björck, S. and **Digerfeldt, G.** 1989: Lake Mullsjön- a key site for understanding the final stage of the Baltic Ice Lake east of Mt. Billingen. *Boreas* 18, 209-219.

Björck, S., Ingólfsson, O., Hafliðason, H., Hallsdóttir, M. and **Anderson, N.J.** 1992: Lake Torfadalsvatn: a high resolution record of the North Atlantic ash zone I and the last glacial-interglacial environmental changes in Iceland. *Boreas* 21, 15-22.

Blackford, J.J., Edwards, K.J., Dugmore, A.J., Cook, G.T. and **Buckland, P.C.** 1992: Icelandic volcanic ash and the mid-Holocene Scots pine (Pinus sylvestris) pollen decline in northern Scotland. *The Holocene* 2, 260-265.

v.d.Bogaard, P. and **Schmincke, H-U.** 1985: Laacher See Tephra: a widespread isochronous late Quaternary tephra in central and north Europe. *Geological Society of America Bulletin* 96, 1554-1571.

Borell, R. and **Offerberg, J.** 1955: Géokronologiska undersökningar inom Indalsälvens dalgang mellan Bergeforsen och Ragunda. *Sveriges Geologiska Undersökning*, Series Ca 31, Uppsala: SGU.

Brunnberg, L. and Miller, U. 1990: Macro-and microfossils in late Glacial clay from the Stockholm region indicating brackish environment 10,400 years ago. In Lundqvist J. and Saarnisto M., editors, *Termination of the Pleistocene*, 102-104. Geological Survey of Finland, OPAS-guide 31.

Brunskill, G.J. 1969: Fayetteville Green Lake NY III: precipitation and sedimentation of calcite in a meromictic lake with laminated sediments. *Limnology and Oceanography* 14, 830-47.

Burgess, C. 1989 Volcanoes, catastrophe and global crisis of the late Second Millennium B.C.. *Current Archaeology*, **117**, 325-329.

Caldenius, C.C. 1932: Las glaciaciones cuaternarias en La Patagonia y Tierra del Fuego. *Geografiska Annaler* 14, 1-164.

Caldenius, C.C. 1944: Baltiska issjöns sänkning till Västerhavet. En geokronologisk studie. *Geologiska Föreningens i Stockholm Fördhandlingar* 66, 366-382.

Callaghan, J. 1987: A non-toxic heavy liquid and inexpensive filters for the separation of mineral grains. *Journal of Sedimentary Petrology* 57(4) 765-766.

Carey, S.N. and **Sigurdsson, H.** 1982: Influence of particle aggregation on deposition of distal tephra from the May 18 1980 eruption of Mount St Helens volcano. *Journal of Geophysical Research* 87, 7061-7072.

Cato, I. 1985: The definitive connection of the Swedish geochronological time scale with the present, and the new date of the zero year in Döviken, northern Sweden. *Boreas* 14 117-122.

Cato, I. 1987: On the definitive connection of the Swedish time scale with the present. *Sveriges Geologiska Undersökning Series*, Ca 68, Uppsala: SGU.

Catto, N.R. 1987: Lacustrine sedimentation in a proglacial environment, Caribou River Valley, Yukon Canada. *Boreas* 16, 197-206.

Clymo, R.S. 1984: The limits to peat bog growth. *Philosophical Transactions of the Royal Society of London* B303, 605-654.

Conway, V.M. 1954: Stratigraphy and pollen analysis of southern Pennine blanket peats. *Journal of Ecology* 42, 117-147.

Cornell, W., Carey, S.N., and **Sigurdsson, H.** 1983: Computer simulation of transport and deposition of the Campanian Y-5 ash. *Journal of Volcanology and Geothermal Research* 17 89-109.

Davis, M. 1976: Pleistocene biography of the temperate deciduous forests. *Geoscience and Man* 13, 13-26.

De Geer, G. 1912: A geochronology of the last 12,000 years. *Eleventh International Geological Congress* (1910), Stockholm 1, 241-53.

De Geer, G. 1940: Geochronologia Suecica Principles. *Kungliga svenska vetenskapsakademiens handlingar* 18,6. Stockholm: Almqvist and Wiksells.

Degens, E.T. and **Kurtman, F.**, editors, 1978: *The geology of Lake van.* Ankara, Turkey: The Mineral Research and Exploration Institute of Turkey, 169.

Denton, G.H. and **Porter, S.C.** 1970: Neoglaciation. *Scientific American* 222, 101-110.

Denton, G.H. and **Karlén, W.** 1973: Holocene climatic variations: their pattern and possible cause. *Quaternary Research* 3, 155-205.

Dickman, M.D. 1979: A possible varving mechanism for meromictic lakes. *Quaternary Research* 11, 113-124.

Digerfeldt, G., Battarbee, R.W. and **Bengtsson, L.** 1975: Report on annually laminated sediment in Lake Järlasjön, Nacka, Stockholm. *Geologiska Föreningen i Stockholm Fördhandlingar* 97, 29-40.

Downing, J.A. and **Rath, L.C.** 1988: Spatial patchiness in the lacustrine sedimentary environment. *Limnology and Oceanography* 33(3), 447-458.

Drewry, D. 1986: *Glacial geological processes.* London: Edward Arnold.

Dugmore, A.J. 1987: Tephrochronological studies of Holocene glacier fluctuations in south Iceland. In Oerlemans, J., editor, *Glacier fluctuations and climatic change*, 37-55.

Dugmore, A.J. 1989: Icelandic volcanic ash in Scotland. *Scottish Geographical Magazine* 105(3), 168-172.

Dugmore, A.J., and Sugden, D.E. 1991: Do the anomalous fluctuations of Solheimajökull reflect ice-divide migration. *Boreas* 20, 105-113.

Dugmore, A.J., Larsen, G., Newton, A.J., and **Sugden, D.E.** 1992: Geochemical stability of fine-grained silicic Holocene tephra in Iceland and Scotland. *Journal of Quaternary Science* 7(2) 173-183.

Dugmore, A.J. and **McCulloch, R.D.** ms: Spatial variability of Hekla 1947 tephra fallout. *NERC Small Research Grant. Final report.*

Dugmore, A.J., Shore, J., Cook, G.T., Newton, A.J., Edwards, K.J., and **Larsen, G.** submitted: The radiocarbon dating of Icelandic tephra layers in Britain and Ireland. *Radiocarbon*, 1995.

Edwards, K.J. and **Whittington G.** 1993: Aspects of the environmental and depositional history of a rock basin lake in eastern Scotland, U.K. In McManus, J. and Duck, R.W., editors, *Geomorphology and sedimentology of lakes and reservoirs*, 155-180.

Einarsson, Á. 1982: The palaeolimnology of Lake Mývatn, northern Iceland: plant and animal microfossils in the sediment. *Freshwater Biology* 12, 63-82.

Einarsson, M.Á. 1984: The climate of Iceland. In Van Loon, H., editor, *World Survey of Climatology* Volume 15: Climates of the oceans 673-697.

Einarsson, Th. 1961: Pollenanalytische untersuchungen zur spät-und postglazialen klimageschichte Islands. *Sonder veröffentlichungen des Geologischen Institutes der Universität Köln* 6.

Einarsson, Th. 1963: Pollen-analytical studies on the vegetation and climate history of Iceland in the Late and Post-glacial times. In Löve, A. and Löve, D., editors *North Atlantic biota and their history,* 355-365.

Einarsson, Th. 1986: Tephrochronology. In Berglund, B.E., editor, *Handbook of palaeoecology and palaeohydrology*, 329-342.

Eiríksson, J. and **Wigum, B.J.** 1989: The morphometry of selected tephra samples from Icelandic volcanoes. *Jökull* 39, 57-73.

Evans, D.J.A., Butcher, C. and Kirthisingha, A. 1994: Neoglaciation and an early "Little Ice Age" in western Norway: lichenometric evidence from the Sandane area. *The Holocene* 4, 278-289.

Fisher, R.V. and **Schminke, H-U.** 1984: *Pyroclastic rocks*. Springer Verlag, Berlin, pp472.

Foster, I.D.L., Dearing, J.A. and **Grew, R.** 1988: Lake catchments: an evaluation of their contribution to studies of sediment yield and delivery processes. In *Sediment budgets (Proceedings of the Porto Alegre Symposium, December 1986)*. IAHS publication no.174, 413-424.

Fözö, I. 1980: Ådalen. Den geologiska utvecklingen vid slutet i istiden. *Länsstyrelsen i Västernorrlands län*. 64pp. Sundsvall.

Froggatt, P.C. 1992: Standardisation of the chemical analysis of tephra deposits. Report of the ICCT Working Group. *Quaternary International* 13/14, 93-96.

Fromm, E. 1964: The ice recession through southern Dalecarlia. *Geologiska Föreningens i Stockholm Fördhandlingar* 86, 173-174.

Fromm, E. 1970: An estimation of errors in the Swedish varve chronology. In Olsson, I.U., editor, *Nobel symposium 12. Radiocarbon variations and absolute chronology*. New York: Wiley Interscience Division.

Fromm, E. 1985: Chronological calculation of the varve zero. *Boreas* 14, 123-125.

Gear, A.J. and **Huntley, B.** 1991: Rapid changes in the range limits of Scots pine 4000 years ago. *Science* 251 544-547.

Gilbert, R. and Shaw, J. 1981: Sedimentation in proglacial Sunwapta Lake, Alberta. *Canadian Journal of Earth Sciences* 18, 81-93.

Gregory, M.R. and **Johnston, K.A.** 1987: A non-toxic substitute for heavy liquids - aqueous sodium polytungstate ($3Na_2WO_4.9WO_3.H_2O$) solution. *New Zealand Journal of Geology and Geophysics* 30 317-320.

Grove, J.M. 1979: The glacial history of the Holocene. *Progress in Physical Geography* 3, 1-54

Guðmundsson, Þ. 1978: *Pedological studies of Icelandic peat soils.* Unpublished PhD thesis, University of Aberdeen.

Hafliðason, H., Larsen, G. and **Ólafsson, G.** 1992: The recent sedimentation history of Þingvallavatn, Iceland. *OIKOS* 64, 80-95.

Håkanson, L. 1977: On lake form, lake volume and lake hypsographic survey. *Geografiska Annaler* 59A, 1-29.

Håkanson, L. 1982a: Bottom dynamics in lakes. In Sly, P.G., editor, *Sediment/freshwater interaction.* Junk The Hague, 1-22.

Håkanson, L. 1982b: Lake bottom dynamics and morphometry - the dynamic ratio. *Water Resources Research* 180, 1444-1450.

Håkanson, L. and **Jansson, M.** 1983: *Principles of lake sedimentology.* Springer-Verlag, Berlin, pp316.

Hall, V.A., Pilcher, J.R. and McCormack, F.G. 1994 Icelandic volcanic ash and the mid-Holocene pine (*Pinus sylvestris*) decline in the north of Ireland: No correlation. *The Holocene*, 4(1), 79-83.

Hallsdóttir, M. 1987: Pollen analytical studies of human influence on vegetation in relation to the Landnám tephra layer in southwest Iceland. LUNDQUA Thesis, 18 1-45.

Hermanns-Auðardöttir, M. 1991: The early settlement of Iceland. Results based on excavations of a Merovingian and Viking farm site at Herjólfsdalur in the Westman Islands, Iceland. *Norwegian Archaeological Review* 24(1), 1-33.

Hirakawa, K. 1989: Downslope movement of solifluction lobes in Iceland: a tephrostratigraphic approach. *Tokyo Metropolitan University Geographical Reports* Nr 26.

Hörnsten, Å. 1964: Ångermanlands kustland inder isavsmältningsskedet. Preliminärt meddelande. *Geologiska Föreningens i Stockholm Fördhandlingar* 86, 181-205.

Hunt, J. 1992: Icelandic tephras ancient and modern. *Quaternary Newsletter* 68, 4-6.

Hunt, J.B., and Hill P.G. 1993: Tephra geochemistry: a discussion of some persistent analytical problems. *The Holocene* 3, 271-278.

Huttenen, P. and Meriläinen, J. 1978: New freezing device providing large unmixed sediment samples from lakes. *Annales Botanici Fennici* 15, 128-130.

Huttenen, P. and **Tolonen, K.** 1977: Human influence in the history of Lake Lovojärvi, southern Finland. Helsinki: *Finskt Museum.*

Imsland P. 1978: *The petrology of Iceland: some general remarks.* Nordic Volcanological Institute Report 7808, 26pp.

Järnefors, B. 1963: Lervarvskronologien och isrecessionen i Östra Mellansverige. *Sveriges Geologiska Undersökning* Series Ca 68, Uppsala: SGU.

Jakobsson, S.P. 1979: Petrology of Recent basalts of the Eastern Volcanic Zone, Iceland. *Acta Naturalia Islandica* II, 26 pp100.

Jóhannesson, H., Flores, R.M., and **Jónsson, J.** 1981: A short account of the Holocene tephrochronology of Snaefellsjökull central volcano, Western Iceland. *Jökull* 31 Ár, 23-30.

Juvigne, E. and **Porter, S.C.** 1985: Micrological variations within two widespread Holocene tephra layers from the Cascade Range Volcanoes, U.S.A. *Geographie Physique et Quaternaire* 39(1) 7-12.

Karlén, W. 1981: Lacustrine sediment studies. A technique to obtain a continuous record of Holocene glacier variations. *Geografiska Annaler* 63A (3-4) 273-281.

Karlén, W. and **Rosqvist, G.** 1988: Glacier fluctuations recorded in lacustrine sediments on Mount Kenya. *National Geographic Research* 4(2) 219-232.

Kelts, K. and **Hsü, K.J.** 1978: Freshwater carbonate sedimentation. In Lerman A., editor, *Lakes: geology, chemistry, physics.* New York: Springer Verlag, 296-323.

Kjartansson, G., Þórarinsson, S., and **Einarsson, Þ.** 1964: C^{14}-aldursákvarðanir á sýnishornum varðandi íslenzka Kvarter jarðfræði. *Náttúrufræðingurinn* 34(3) 97-160. (Radiocarbon datings of samples concerning the Quaternary geology of Iceland)

Koivisto, E. and **Saarnisto, M.** 1978: Conventional radiography, xeroradiography, tomography, and contrast enhancement in the study of laminated sediments. Preliminary report. *Geografiska Annaler* 60A (1-2) 55-61.

Kristiansson, J. 1982: Varved sediments and the Swedish Timescale. *Geologiska Föreningen i Stockholm Fördhanglingar* 14, 273-275.

Kristiansson, J. 1986: The ice recession in the south-eastern part of Sweden. A varve-chronological timescale for the last part of the Weichselian. *University of Stockholm, Department of Quaternary Research Report* no.7, Stockholm.

Krukowski, S.T. 1988: Sodium metatungstate: a heavy-metal separation medium for the extraction of conodonts from insoluble residues. *Journal of Palaeontology* 62(2) 314-316.

Kuenen, P.H. 1951: Mechanics of varve formation and action of turbidity currents. *Geologiska Föreningens i Stockholm Fördhandlingar* 73, 69-84.

Kvamme, T., Mangerud, J., Furnes, H. and **Ruddiman, W.F.** 1989: Geochemistry of Pleistocene ash zones in cores from the North Atlantic. *Norsk Geologisk Tidsskrift* 69, 251-272.

Lambert, A.M. and **Hsü, K.J.** 1979: Varve-like sediments of the Walensee, Switzerland. In Schlüchter C., editor, *Moraines and varves: origin, genesis, classification.* Proceedings of an INQUA symposium on genesis and lithology of Quaternary deposits, Zurich 10-20 September 1978. Rotterdam: A.A. Balkema, 295-302.

Larsen, G. 1979: Um aldur Eldgjárhrauna. *Náttúrufræðingurinn* 49, 1-26, (Tephrochronological dating of the Eldgjá lavas in south Iceland).

Larsen, G. 1981: Tephrochronology by microprobe glass analysis. In Self, S. and Sparks, R.S.J., editors, *Tephra Studies.* D.Reidel Publishing Company, 95-102.

Larsen, G. 1984: Recent volcanic history of the Veidivötn fissure swarm, southern Iceland-an approach to volcanic risk assessment. *Journal of Volcanology and Geothermal Research* 22, 33-58.

Larsen, G. and **Þórarinsson, S.** 1977: H4 and other acid Hekla tephra layers. *Jökull* 27, 28-46.

Lemmen, D.S., Gilbert, R., Smol, J.P. and **Hall, R.I.** 1988: Holocene sedimentation in glacial lake Tasikutaaq Lake, Baffin Island. *Canadian Journal of Earth Sciences* 25, 810-823.

Lidén, R. 1913: Geokronologiska studier över det finiglacial skedet i Ångermanland. *Sveriges Geologiska Undersökning Series* Ca 9 pp39.

Lidén, R. 1938: Den senkvartära strandförskjutningens förlopp och kronologi i Ångermanland. *Geologiska Föreningens i Stockholm Fördhandlingar* 60, 397-404.

Long, D. and **Morton, A.C.** 1987: An ashfall within the Loch Lomond stadial. *Journal of Quaternary Science* 2, 97-102.

Ludlam, S. 1976: Laminated sediments in holomictic Berkshire Lakes. *Limnology and Oceanography* 21, 743-746.

Ludlam, S. 1979: Rhythmite deposition in lakes in the NE USA. In Schlüchter, Ch., editor, *Moraines and varves: origin, genesis, classification.* Proceedings of an INQUA symposium on genesis and lithology of Quaternary deposits, Zurich 10-20 September 1978. Rotterdam: A.A. Balkema, 295-302.

Lundqvist, J. 1975: Ice recession in central Sweden and the Swedish time scale. *Boreas* 4, 47-54.

Lundqvist, J. 1987: Beskrivning till jordartskarta over Västernorrlands län och förutvarande Fjällsjö k:n. *Sveriges Geologiska Undersökning Series* Ca 55, Stockholm: S.G.U.

Magnusson, M. 1987: *Iceland saga.* The Bodley Head Ltd.

Mangerud, J., Lie, S.E., Furnes, H., Kristiansen, L.L., and **Lomo, L.** 1984: A Younger Dryas ash bed in western Norway and its possible correlation with tephra in cores from the Norwegian Sea and North Atlantic. *Quaternary Research* 21(11) 85-104.

Mohn, H. 1877: Askeregnen den 29de-30te Marts 1875. *Kria. Vidensk. Selsk. Forhandlingar* 10, 1-12.

Moore, P.D. 1975: Origin of blanket mires. *Nature* 256, 267-269.

Morton, A.C. 1987 Distribution and significance of volcanic glass shards in Vibro core 59-67/276 Wyvilie-Thomson Ridge. *Stratigraphy and sedimentology Research Report No. SRG/87/15 for the Marine Earth Sciences Research Programme.*

Müller, H-N, Stötter, J., Schubert, A. and **Betzler, A.** 1984: Glacial and periglacial investigation in Skídadalur, Trollaskagi, northern Iceland. *Polarforschung* 54(2), 95-109.

Nesje, A. and Johannesson, T. 1992: What were the primary forcing mechanisms of high-frequency Holocene glacier and climatic variations? *The Holocene* 2, 79-84.

Nilsson, E. 1968: The late Quaternary history of southern Sweden. *Kungliga Sverige Vetenskapsakademiens Handlingar*, Series 4.12, 1, Stockholm: Almqvist and Wiksells.

Norðdahl, H. 1991: A review of the glaciation maximum concept and the deglaciation of Eyjafjörður, north Iceland. In Maizels, J.K. and Caseldine, C., editors, *Environmental change in Iceland: Past and Present*, 31-47.

Norðdahl, H. and **Hafliðason, H.** 1992: The Skógar Tephra, a Younger Dryas marker in north Iceland. *Boreas* 21, 23-41.

Ogilvie, A.E.J. 1990: Climatic changes in Iceland AD c.865-1598. *Acta Archaeologica* 61, 233-251.

Ogilvie, A.E.J. 1991: Documentary evidence for changes in climate in Iceland A.D. 1500 to 1800. In Bradley, R.S. and Jones, P.D., editors, *Climate since A.D. 1500*. Harper Collins, London and Boston.

Oldfield, F. 1977: Lakes and their drainage basins as units of sediment-based ecological study. *Progress in Physical Geography*, 1, 460-504.

Oldfield, F., Worsley, A.T., Appleby P.G. 1985: Evidence from lake sediments for recent erosion rates in the highlands of Papua New Guinea. In Douglas, I. and Spencer, T., editors, *Enviromental Change and Tropical Geomorphology*, Allen Unwin, London, 185-196.

O'Sullivan, P.E. 1983: Annually laminated sediments and the study of Quaternary environmental changes-a review. *Quaternary Science Reviews* 1, 245-313.

O'Sullivan, P.E., Coard, M.A. and **Pickering, D.A.** 1982: The use of annually-laminated lake sediments in the estimation and calibration of erosion. In *Recent developments in the explanation and prediction of erosion and sediment yield, Proceedings of the Exeter Symposium, July 1982*. IAHS Publication no.137, 385-396.

Palais, J.M., Taylor, K., Mayewski, P.A. and **Grootes, P.** 1991: Volcanic ash from the 1362 AD Öraefajökull eruption (Iceland) in the Greenland ice sheet. *Geophysical Research Letters* 18, 1241-1244.

Perhans, K-E. 1981: Lervarvskronologin mellan Borensberg och Vingaker. Symposium 12-13 januari 1981*: Den senaste nedisningens förlopp med särskild hänsyn till deglaciationen i Sverige*, Stockholm 66-68.

Persson, Ch. 1966: Försök till tefrokronologisk datering av några svenska torvmossar. *Geologiska Föreningen i Stockholm Fördhandlingar* 88 361-395.

Persson, Ch. 1967a: Undersökning av tre sura asklager på Island. *Geologiska Föreningen i Stockholm Fördhandlingar* 88 500-519.

Persson, Ch. 1967b: Försök till tefrokronologisk datering i tre norska myrar. *Geologiska Föreningen i Stockholm Fördhandlingar* 89 181-197.

Persson, Ch. 1971: Tephrochronological investigations of peat deposits in Scandinavia and on the Faroe Islands. *Sveriges Geologiska Undersökning* Series C 656, Uppsala: S.G.U.

Pilcher, J. and **Hall, V.A.** 1992: Towards a tephrochronology for the Holocene of the north of Ireland. *The Holocene* 2, 255-259.

Randle, K., Goles, G.G., and **Kittleman, L.R.** 1971: Geochemical and petrological characterisation of ash samples from Cascade Range volcanoes. *Quaternary Research* 1, 261-282.

Renberg, I. 1981a: Formation, structure and visual appearance of iron-rich varved lake sediments. *Verhandlungen Internationalen Vereinigung für Limnologie* 21, 94-101.

Renberg, I. 1981b: Improved methods for sampling, photography and varve counting of varved lake sediments. *Boreas* 10, 255-258..

Renberg, I. and **Segerström, U.** 1981: Applications of varved lake sediments in palaeoenvironmental studies. *Wahlenbergia* 7, 125-133.

Renberg, I., Segerström, U. and **Wallin, J.E.** 1984: Climatic reflection in varved lake sediments. In Mörner, N-A and Karlén, W., editors, *Climatic changes on a yearly to millenial basis*, Dordrecht, Boston: D.Reidel, 249-256.

Ringberg, B. 1979: Varve chronology of the glacial sediments in Blekinge and north-eastern Skåne, south-eastern Sweden. *Boreas* 8, 209-215.

Ringberg, B. 1984: Cyclic laminations in proximal varves reflecting the length of summers during the Late Weichsel in southernmost Sweden. In Mörner, N-A. and Karlén, W., editors, *Climatic changes on a yearly to millenial basis: geological, historical and instrumental records*. 57-62.

Ringberg, B. and **Rudmark, L.** 1985: Varve chronology based upon glacial sediments in the area between Karlskrona and Kalmar, southeastern Sweden. *Boreas* 14, 107-110.

Rosqvist, G. 1992: *Late Quaternary equatorial glacier fluctuations*. Department of Physical Geography Stockholm University. Doctoral dissertation nr A272.

Ruddiman, W.F. and **Glover, L.K.** 1972: Vertical mixing of ice-rafted volcanic ash in North Atlantic sediments. *Geological Society of America Bulletin* 83, 2817-2836.

Rudmark, L. 1975: The deglaciation at Kalmarsund, southeastern Sweden. *Sveriges Geologiska Undersökning* C713, pp88.

Saarnisto, M. 1986: Annually laminated sediments. In Berglund, B.E., editor, *Handbook of Holocene palaeoecology and palaeohydrology*, Chichester: John Wiley and Sons Ltd, 343-370.

Salmi, M. 1948: The Hekla ashfalls in Finland. *Suomen Geologien Seura* 21, 87-96.

Sauramo, M. 1923: Studies on the Quaternary varve sediments in southern Finland. *Communication Geologiska Finlande Bulletin* 60.

Schumm, S.A. 1979: Geomorphic thresholds: the concept and its applications. *Institute of British Geographers, Transactions* New Series 4, 485-515.

Scott, M., Harkness, D.D., Cook, G.T., Miller, B.F., Begg, E.H. and **Holton, L.** 1994: The TIRI Project: a status report. *Abstracts of the 1st International Radiocarbon Conference*. 15-19th August, 1994, Glasgow, Scotland.

Selby, M.J. 1982: *Hillslope materials and processes.* Oxford University Press, pp264.

Sharp, M. and **Dugmore, A.** 1985: Holocene glacier fluctuations in eastern Iceland. *Zeitschrift für Gletscherkunde und Glazialgeologie* 21, 341-349.

Sigurdsson, H. and **Carey, S.N.** 1989: Plinian and co-ignimbrite tephra fall from the 1815 eruption of Tambora volcano. *Bulletin of Volcanology* 51 243-270.

Simola, H. and **Tolonen, K.** 1981: Diurnal laminations in the varved sediment of Lake Lovojärvi, south Finland. *Boreas* 10, 19-26.

Sneed, E.D. and Folk, R.L. 1958: Pebbles in the Lower Colorado River, Texas, a study in particle morphogenesis. *Journal of Geology* 66, 114-150.

Sorem, R.K. 1982: Volcanic ash clusters: Tephra rafts and scavengers. *Journal of Volcanology and Geothermal Research* 16, 34-44.

Steinthórsson, S. 1967: Tvær nýjar C^{14}-aldursákvarðanir á öskulögum úr Snaefellsjöli. *Náttúrufræðingurinn* 37, 236-238.

Stevens, R. 1985: Glaciomarine varves in Late-Pleistocene clays near Göteborg, southwestern Sweden. *Boreas* 14, 127-132.

Stötter, J. 1990: Neue beobachtungen und überlegungen zur postglazialen landscaftsgeschichte Islands an beispiel des Svarfadar-Skídadals. *Münchener Geographische Abhandlungen*, Reihe B, 8.

Strömberg, B. 1985: New varve measurements in Västergotland, Sweden. *Boreas* 14, 111-115.

Strömberg, B. 1989: Late Weichselian deglaciation and clay varve chronology in east-central Sweden. *Sveriges Geologiska Undersökning Series* C 73, Uppsala:

Sturm, M. 1979: Origin and composition of clastic varves. In Schlüchter Ch., editor, *Moraines and varves: origin, genesis, classification.* Proceedings of an INQUA symposium on genesis and lithology of Quaternary deposits, Zurich 10-20 September 1978. Rotterdam: A.A. Balkema, 281-285.

Sturm, M. and **Matter, A.** 1978: Turbidites and varves in Lake Brienz (Switzerland): deposition of clastic detritus by density currents. *Special Publication International Association of Sedimentologists* 2, 147-168.

Sundborg, Å. 1992: Lake and reservoir sedimentation. Prediction and interpretation. *Geografiska Annaler* 74A, 93-100.

Swain, A. 1973: A history of fire and vegetation as recorded in lake sediments. *Quaternary Research* 3, 383-396.

Sweatman, T.R., and Long, J.V.P. 1969: Quantitative electron-probe microanalysis of rock-forming minerals. *Journal of Petrology* 10, 332-379.

Tallis, J.H. 1985: Mass movement and erosion of a southern Pennine blanket peat. *Journal of Ecology* 73, 283-315.

Tauber, H. 1970: The Scandinavian varve chronology and ^{14}C dating. In Olsson, I.U., editor, Nobel symposium 12. *Radiocarbon variations and absolute chronology*. New York: Wiley Interscience Division, 173-196.

Taylor, J.A. 1983: The peatlands of Great Britain and Ireland. In Gore, A.J.P., editor, *Ecosystems of the World. Mires: Swamp, bog, fen and moor*, 4A, General studies. Elsevier Scientific Publishers, Amsterdam, 1-21.

Thompson, R., Bradshaw, R.H.W. and **Whitley, J.E.** 1986: The distribution of ash in Icelandic lake sediments and the relative importance of mixing and erosion processes. *Journal of Quaternary Science* 1, 3-11.

Tippett, R. 1964: An investigation into the nature of the layering of deepwater sediments in two eastern Ontario lakes. *Canadian Journal of Botany* 42, 1693-1709.

Þórarinsson, S. 1944; Tefrokronologiska studier på Island. *Geografiska Annaler* 26, 1-217.

Þórarinsson, S. 1956: On the variations of Svínafellsjökull, Skaftafellsjökull and Kvíarjökull in Oraefi. *Jökull* 6, 1-15.

Þórarinsson, S. 1958: The Öraefajökull eruption of 1362. *Acta Naturalia Islandica*, Reykjavík II (2) 1-100.

Þórarinsson, S. 1964: On the age of the terminal moraines of Brúarjökull and Hálsajökull: a tephrochronological study. *Jökull* 14, 67-75.

Þórarinsson, S. 1967: The tephra fall from hekla on March 29 1947. In The Eruption of Hekla, Vol II, 3 1-65.

Þórarinsson, S. 1976: Gjóskulög. *Samvinnan* 70, 4-9.

Þórarinsson, S. 1979: On the damage caused by volcanic eruptions with special reference to tephra and gases. In Sheets, A., and Grayson, B., editors, *Volcanic activity and human ecology*. Academic Press Inc., New York, 125-159.

Þórarinsson, S. 1981: The application of tephrochronology in Iceland. In Self, S. and Sparks, R.S.J., editors, *Tephra Studies*. D.Reidel Publishing Company, 109-134.

Þórarinsson, S. and **Sigvaldason, G.E.** 1972: The Hekla eruption of 1970. *Bulletin Volcanologique* 36(2) 269-288.

Vasari, Y. 1972: The history of the vegetation of Iceland during the Holocene. *Acta Univ Ouluensis* 3(1) 239-252.

Vasari, Y. and **Vasari, A.** 1990: L'histoire Holocène des lacs Islandais. In Devers, S., editor, *Extrait de pour Jean Malaurie.* Paris, 277-293.

Waagstein, R. and Jóhansen, J. 1968: Tre vulkanske askelag fra Faerøerne. *Meddelelser fra Dansk Geologisk Forening*, Bd 18, Haefte 3-4, 8pp.

Walker, G.P.L., Wilson, L., and **Bowell, E.** 1971: Explosive volcanic eruptions I : The rate of fall of pyroclasts. *Geophysical Journal of the Royal Astronomical Society* 22 377-383.

Watkins, N.D. 1971 Geomagnetic polarity events and the problem of "The Reinforcement Syndrome". Comments on Earth Sciences, *Geophysics* 2, 39-43

Webb, R. 1972: Vegetation cover on Icelandic thúfur. *Acta Botanica Islandica* 1, 51-60.

Westgate, J.A. and Gorton M.P. 1981: Correlation techniques. In Self, S. and Sparks, R.S.J., editors. *Tephra Studies*, Dordrecht, Reidel, 73-94.

Wilson, L. and **Huang, T.C.** 1979: The influence of shape on the atmospheric settling velocity of volcanic ash particles. *Earth and Planetary Science Letters* 44 311-324.

Wilson, P. and **Hegarty, C.** 1993: Morphology and causes of recent peat slides on Skerry Hill, Co. Antrim, Northern Ireland. *Earth Surface Processes and Landforms* 18, 593-601.

Wright Jr, H.E. 1980: Cores of soft lake sediments. *Boreas* 9, 107-114.

Zingg, T. 1935: Beiträge zur Schotteranalyse. *Schweizerische Mineralogische und Petrographische Mitteilungen* 15, 39-140.

APPENDIX ONE Geochemical analyses of Öraefajökull 1362 pumice

Microprobe settings-WDS, 20kV, 15nA, 10s counting time

Density class 2.43 g/cm^3

SiO_2	TiO_2	Al_2O_3	FeO	MnO	MgO	CaO	Na_2O	K_2O	Total
73.24	0.26	13.28	3.08	0.1	0.03	0.93	5.57	3.45	99.93
72.22	0.30	13.07	3.28	0.12	0.03	1.06	5.26	3.61	98.96
72.14	0.27	13.32	2.99	0.07	0.03	0.85	5.45	3.54	98.67
71.89	0.27	12.98	3.20	0.15	0.03	0.89	5.37	3.36	98.13
71.82	0.34	12.86	3.27	0.14	0.02	1.00	5.52	3.38	98.33
71.04	0.33	12.87	3.16	0.13	0.01	0.94	5.84	3.17	97.49
70.95	0.22	12.90	3.07	0.09	0.03	1.05	5.47	3.33	97.11
70.82	0.26	13.14	3.00	0.10	0.03	0.89	5.43	3.44	97.41
70.69	0.25	13.04	3.17	0.09	0.02	0.98	5.61	3.37	97.22
70.32	0.25	13.08	3.08	0.13	0.02	0.98	5.65	3.32	96.83

Density class 2.25 g/cm^3

72.44	0.30	12.91	3.19	0.09	0.01	0.99	5.63	3.50	99.05
72.29	0.29	13.13	3.18	0.06	0.02	0.93	5.97	3.40	99.27
72.22	0.23	13.34	3.08	0.13	0.03	1.02	5.65	3.35	99.04
71.95	0.27	12.85	3.05	0.12	0.00	0.93	5.59	3.25	98.00
71.94	0.33	13.07	3.21	0.09	0.02	1.02	5.56	3.44	98.69
71.83	0.23	13.09	3.05	0.13	0.03	0.95	5.64	3.52	98.47
71.57	0.25	13.38	3.12	0.09	0.03	1.06	5.34	3.36	98.20
71.27	0.25	12.78	3.13	0.11	0.03	0.91	5.36	3.50	97.33
70.65	0.27	13.00	3.09	0.11	0.01	0.94	5.53	3.32	96.93
70.46	0.27	12.78	3.02	0.11	0.02	1.04	5.71	3.46	96.88

Density class 1.63 g/cm^3

SiO_2	TiO_2	Al_2O_3	FeO	MnO	MgO	CaO	Na_2O	K_2O	Total
73.67	0.29	12.78	3.28	0.09	0.01	0.78	5.83	2.93	99.67
72.62	0.25	13.06	3.06	0.07	0.01	1.02	5.65	3.20	98.93
71.87	0.26	13.08	3.28	0.06	0.03	1.07	5.24	3.30	98.20
71.81	0.26	12.88	3.11	0.10	0.02	0.97	4.89	3.34	97.41
71.21	0.31	12.97	3.07	0.07	0.04	1.06	5.56	3.33	97.59
71.01	0.27	12.80	3.15	0.07	0.02	1.02	5.36	3.15	96.86
70.92	0.23	12.81	3.11	0.11	0.03	0.88	5.55	3.36	96.99
70.66	0.30	13.16	3.11	0.05	0.02	0.99	5.39	3.49	97.17
70.35	0.28	12.91	3.23	0.13	0.04	0.94	5.74	3.53	97.14
69.37	0.25	12.64	3.22	0.14	0.02	1.07	5.63	3.42	95.76

Density class 1.18 g/cm^3

73.28	0.23	13.11	3.30	0.13	0.04	0.92	5.21	3.50	99.73
73.11	0.32	13.22	3.13	0.07	0.03	0.98	5.60	3.24	99.69
72.98	0.25	12.75	3.26	0.07	0.02	0.94	5.46	3.33	99.06
72.87	0.26	13.26	3.13	0.13	0.02	0.95	5.69	3.48	99.79
72.53	0.28	12.55	3.38	0.13	0.03	1.13	5.55	3.56	99.13
72.49	0.27	13.39	3.23	0.12	0.06	0.98	5.57	3.38	99.49
72.05	0.32	13.12	3.04	0.15	0.02	0.90	5.70	3.41	98.70
71.37	0.30	13.12	3.13	0.08	0.03	0.90	5.58	3.68	98.19
71.30	0.26	13.11	3.05	0.11	0.02	0.95	5.57	3.54	97.92
71.91	0.26	13.20	3.13	0.12	0.01	0.94	5.57	3.35	98.48

APPENDIX TWO Sedigraph procedure and interpretation

Sedigraph Procedure

The SediGraph 5000ET Particle Size Analyser uses soft X-radiation to detect relative particle concentration because X-ray absorption is directly proportional to particle mass. The instrument measures the sedimentation rates of particles dispersed in a liquid and automatically interprets these data in accordance with Stoke's Law to yield a cumulative mass percentage distribution in terms of Stokesian or equivalent spherical diameters (E.S.D).

The machine beam of X-rays determines the concentration of particles remaining at the decreasing sedimentation depths as a function of time. The zone of rate measurement decreases in height with time because although it may take a large particle a second to fall 25 cm, particles of the order of 0.1-0.2 μm diameter require as much as 200 hours to fall a similar distance. This decrease is automatically achieved in the SediGraph by moving the cell downward relative to the detecting X-ray beam. Therefore, the effective sedimentation depth is inversely related to elapsed time. The time function by which sedimentation distance is decreased is related to Stoke's Law. For example a particle of diameter, d, will settle a distance, h, in time, t, according to the expression

$$\Rightarrow \quad D = k\left(\frac{h}{t}\right)^{1/2}$$

where

$$k = \left[\frac{18\eta}{g\left(\rho - \rho_o\right)}\right]^{1/2}$$

where

- ρ = density of the particle
- ρ_o = density of the fluid medium
- η = viscosity of the fluid medium
- g = gravity

Substituting in the relationship

$$h_1 = \frac{B^2}{t_1}$$

where B is constant will yield the expression

$$D_1 = \frac{KB}{t_1} or \log D_1 = \log KB - \log t_1$$

Therefore cell movement according to the inverse logarithm of sedimentation time will permit direct indication of particle size on logarithmic graph paper. Consequently after a given time, t_1, all particles larger than the corresponding diameter D_1, will have fallen below a certain distance, h, from the surface of the suspension. If the initial concentration of material was C_o g/cm³ and the concentration after time, t_1, at distance h is C_1 g/cm³ then P_1 (the weight percentage of material finer than D_1) is

$$p_1 = 100\left(\frac{C_1}{C_0}\right)$$

By obtaining values of C_1 after various times, the corresponding values of P_1 and D_1 may be calculated, which when plotted yield an integral, or cumulative distribution of particle size in terms of Stoke's equivalent spherical diameter (E.S.D).

The diameter range over which analysis is desired and the time of analysis depend upon particle and liquid densities, liquid viscosity and the starting particle diameter. A preliminary "rate" calculation is made using values for these terms. Therefore for a given starting diameter, each indicated particle diameter corresponds to a definite sedimentation distance. The rate of cell movement built into the instrument to provide the proper settling distance for a given particle diameter is therefore related to the density difference divided by liquid viscosity. The digital program, base rate, gear ratio, and other functions of the instrument are such that the rate is defined by

$$rate = \frac{211.8(\rho - \rho_0)}{(50 / Dm)^2 \eta}$$

where

- Dm = maximum particle diameter
- $(\rho-\rho_0)$ = density difference in g/cm^3
- η = viscosity in millipascal seconds

Substituting this rate into the SediGraph then programmes the instrument for the specific system. For example, if the liquid viscosity is too high, sedimentation will be impeded and an unnecessarily long time will be required for analysis. The calculated rate will make the machine adjust the relevant equations so the optimum amount of time is spent on each sample.

APPENDIX THREE Geochemical data of tephra layers from Svínavatn.

Total iron expressed as FeO

Site 1 (Stekkjardalur)

Tephra a 19-19.5 cm

SiO_2	TiO_2	Al_2O_3	FeO	MnO	MgO	CaO	Na_2O	K_2O	Total
60.45	1.15	15.26	9.13	0.22	1.63	4.96	3.96	1.60	98.36
59.81	1.18	14.99	9.23	0.21	1.68	5.09	4.16	1.60	97.95
59.70	1.23	15.24	9.29	0.25	1.54	5.27	4.33	1.64	98.49
59.64	1.07	15.10	8.59	0.24	1.41	4.76	4.24	1.92	96.97
59.49	1.47	15.21	8.31	0.22	1.87	5.04	4.27	1.72	97.62
58.42	1.36	16.43	8.95	0.15	1.90	5.81	4.38	1.32	98.74
58.00	1.42	15.41	9.87	0.21	2.12	5.37	4.27	1.50	98.17
57.85	1.56	15.20	10.38	0.23	2.02	5.76	3.54	1.51	98.05
57.75	1.39	15.53	9.38	0.23	1.87	5.77	3.64	1.40	96.96
57.07	1.38	15.09	9.77	0.22	2.10	5.32	4.09	1.50	96.55

Tephra b 26.5-27 cm

46.96	4.99	12.48	14.34	0.28	4.91	9.68	3.22	0.76	97.61
46.60	4.85	12.39	14.35	0.27	5.04	9.39	3.17	0.83	96.89
46.21	4.64	12.77	14.50	0.35	5.10	9.41	3.24	0.73	96.94
45.99	4.80	12.59	14.45	0.24	5.03	9.30	3.34	0.72	96.47
45.92	4.60	12.69	14.14	0.28	4.93	9.44	3.43	0.71	96.13
45.85	4.81	12.92	13.99	0.24	4.82	9.39	3.61	0.80	96.43
45.65	4.79	13.03	14.45	0.26	5.01	9.46	3.13	0.70	96.48
45.44	4.83	12.91	14.34	0.24	4.99	9.38	3.41	0.65	96.19
44.65	5.11	11.51	15.78	0.27	5.07	9.90	3.07	0.76	96.12
44.39	4.76	12.49	14.51	0.28	5.06	9.58	3.29	0.76	95.12

Tephra c 42.5-43 cm

SiO_2	TiO_2	Al_2O_3	FeO	MnO	MgO	CaO	Na_2O	K_2O	Total
50.09	1.77	13.85	12.04	0.11	6.55	11.57	2.70	0.24	98.91
49.48	1.69	13.47	11.81	0.20	7.18	11.89	2.11	0.19	98.03
49.39	1.84	13.68	13.14	0.23	6.26	11.01	2.55	0.32	98.43
49.31	2.02	13.97	11.21	0.21	7.22	11.86	2.49	0.27	98.56
48.96	2.73	13.68	13.14	0.27	5.72	9.87	3.20	0.41	97.99
48.96	1.97	13.67	13.19	0.20	6.24	10.77	2.75	0.27	97.52
48.76	1.99	13.60	10.79	0.18	7.20	12.02	2.65	0.27	97.45
47.82	4.42	13.00	14.01	0.18	4.87	9.26	3.26	0.84	97.65
47.65	2.06	14.48	10.80	0.18	7.34	12.07	2.31	0.31	97.21
47.59	2.04	14.33	10.77	0.17	7.42	11.79	2.32	0.23	96.65

Site 2 (Stekkjardalur)

Tephra a 9-11 cm

69.02	0.78	14.50	4.16	0.12	0.72	2.04	4.87	3.12	99.32
50.90	1.82	13.83	12.08	0.23	6.60	11.02	2.56	0.27	99.30
50.72	2.04	13.67	12.45	0.17	6.42	10.74	2.75	0.28	99.23
49.86	1.85	14.07	11.76	0.20	6.66	10.99	2.66	0.27	98.31
49.07	1.99	13.74	13.01	0.22	6.31	10.65	2.93	0.30	98.22
48.35	1.85	13.53	12.57	0.17	6.54	10.78	2.42	0.22	96.44
48.12	1.83	13.32	12.54	0.19	6.35	11.48	2.73	0.24	96.70
47.39	4.76	12.50	14.70	0.22	5.39	9.72	3.37	0.80	98.85
47.21	1.81	13.35	12.78	0.20	6.41	11.04	2.50	0.20	95.51
45.27	3.12	14.95	13.95	0.21	6.07	9.87	3.03	0.52	97.00

Tephra b 12-13 cm

SiO_2	TiO_2	Al_2O_3	FeO	MnO	MgO	CaO	Na_2O	K_2O	Total
74.82	0.12	13.07	1.97	0.06	0.07	1.25	4.45	2.90	98.71
72.83	0.13	13.73	1.80	0.06	0.13	1.34	4.85	2.93	97.80
63.17	0.60	15.23	7.24	0.24	0.73	3.95	4.34	1.78	97.27
50.01	1.85	13.59	12.63	0.27	6.54	11.25	2.65	0.21	98.98
49.90	2.18	14.13	11.03	0.23	7.19	11.17	2.66	0.35	98.84
49.64	1.99	13.87	12.90	0.28	6.21	10.47	2.93	0.39	98.69
49.50	1.94	13.85	13.05	0.26	6.36	10.25	2.73	0.25	98.19
49.28	1.83	13.75	11.92	0.23	7.39	11.42	2.36	0.20	98.39
49.24	1.98	13.79	12.06	0.23	6.11	10.07	2.86	0.36	96.69
47.78	1.93	13.84	12.46	0.20	6.46	10.85	2.68	0.31	96.51

Tephra c 20-22 cm

64.13	0.65	14.92	7.38	0.23	0.77	3.98	4.07	1.86	97.99
50.41	2.18	13.72	13.39	0.21	6.32	10.51	2.55	0.23	99.52
50.02	1.93	13.40	11.93	0.25	6.95	11.55	2.30	0.21	98.54
49.99	2.71	13.45	13.05	0.25	5.72	9.91	2.84	0.39	98.31
49.73	2.14	13.57	13.48	0.29	6.05	10.32	2.35	0.27	98.19
49.44	1.78	13.56	11.95	0.25	6.75	11.48	2.50	0.22	97.94
49.43	1.86	13.41	11.95	0.24	6.60	11.31	2.50	0.24	97.55
48.90	3.15	12.61	13.92	0.19	5.82	9.83	2.67	0.45	97.51
48.65	1.94	14.14	10.81	0.22	7.36	12.27	2.37	0.25	98.01
48.16	1.09	14.62	10.08	0.16	8.16	13.11	2.18	0.06	97.62
47.81	3.08	13.21	13.70	0.31	5.68	9.98	2.67	0.50	96.93
46.40	4.71	12.59	14.16	0.24	4.93	9.41	3.05	0.70	96.19

Tephra d 24-24.5 cm

SiO_2	TiO_2	Al_2O_3	FeO	MnO	MgO	CaO	Na_2O	K_2O	Total
74.71	0.11	11.85	2.25	0.07	0.10	0.92	3.58	2.95	96.53
74.04	0.13	12.92	2.13	0.04	0.07	1.37	4.39	2.81	97.91
66.19	0.52	16.28	4.94	0.21	0.40	2.17	5.11	4.13	99.95
49.62	1.90	13.68	12.50	0.25	6.13	11.09	2.69	0.32	98.18
49.57	1.99	13.31	12.89	0.22	5.67	10.22	2.68	0.26	96.82
49.49	1.90	13.36	12.63	0.26	6.49	11.07	2.37	0.24	97.82
49.28	3.01	13.10	13.09	0.25	5.59	10.01	2.84	0.43	97.60
49.04	1.90	13.35	12.41	0.21	6.39	11.30	2.55	0.21	97.37
48.58	2.12	13.85	11.99	0.25	6.36	11.28	2.55	0.27	97.27
48.32	2.00	13.19	12.28	0.20	6.38	11.22	2.64	0.21	96.43

Tephra e 26.5-27 cm

50.00	1.91	13.86	12.89	0.19	6.51	11.48	2.41	0.19	99.42
50.00	1.84	13.63	12.72	0.24	6.59	11.55	2.40	0.16	99.13
49.82	1.89	13.34	12.48	0.24	6.53	11.29	2.29	0.17	98.05
49.73	2.88	13.36	13.42	0.27	5.38	9.54	2.77	0.43	97.77
49.66	3.23	12.63	13.96	0.28	5.51	9.76	2.90	0.48	98.42
49.39	1.78	14.00	11.87	0.19	7.19	12.17	2.45	0.16	99.20
49.27	1.56	13.66	11.68	0.22	7.23	12.35	2.44	0.17	98.58
48.65	4.58	13.01	13.93	0.22	4.69	9.19	3.11	0.77	98.16
48.64	1.93	13.62	12.03	0.16	6.74	11.53	2.27	0.17	97.08
47.07	4.62	12.60	14.23	0.24	5.09	9.51	3.17	0.73	97.26

Tephra f 32-32.5 cm

SiO_2	TiO_2	Al_2O_3	FeO	MnO	MgO	CaO	Na_2O	K_2O	Total
73.18	0.20	14.23	3.03	0.13	0.10	1.83	4.47	2.70	99.87
72.91	0.18	14.43	3.08	0.04	0.09	1.98	4.60	2.43	99.75
72.29	0.19	13.70	2.97	0.04	0.10	1.94	3.56	2.70	97.47
72.24	0.25	13.98	3.00	0.06	0.09	1.82	4.22	2.74	98.40
50.74	2.05	13.24	12.84	0.19	6.03	10.61	2.42	0.27	98.37
49.89	2.96	13.19	13.12	0.21	5.49	10.21	2.83	0.47	98.37
48.84	2.16	13.22	12.80	0.20	6.45	10.92	2.61	0.30	97.50
48.54	1.77	13.58	12.51	0.24	6.37	11.68	2.34	0.23	97.27
48.43	1.95	12.91	13.09	0.16	6.21	10.60	2.71	0.24	96.31
46.00	4.68	12.43	14.21	0.25	5.00	9.79	2.69	0.89	95.94

Tephra g 39.5-40.5 cm

50.26	1.81	13.56	12.32	0.23	6.48	11.37	2.35	0.19	98.59
49.73	2.18	13.49	12.93	0.27	6.04	11.09	2.67	0.22	98.62
49.64	1.93	13.56	12.61	0.19	6.70	11.22	2.37	0.21	98.43
49.52	1.98	13.55	12.45	0.15	6.71	11.41	2.61	0.20	98.57
49.29	1.94	13.39	12.52	0.26	6.62	11.77	2.24	0.19	98.23
49.29	2.04	13.59	12.75	0.24	6.48	11.34	2.62	0.28	98.63
49.23	1.84	13.39	12.50	0.16	6.17	11.43	2.38	0.25	97.35
48.74	1.79	13.45	12.36	0.17	6.58	11.73	2.49	0.18	97.50
48.68	1.44	13.83	12.10	0.28	5.45	11.58	2.47	0.30	96.13
46.88	2.06	13.69	12.35	0.19	6.16	10.84	2.60	0.24	95.02

Tephra h 48.5-49 cm

SiO_2	TiO_2	Al_2O_3	FeO	MnO	MgO	CaO	Na_2O	K_2O	Total
66.84	0.42	15.58	4.60	0.16	0.45	2.05	5.16	4.08	99.33
66.66	0.50	15.30	4.36	0.17	0.34	1.73	5.30	4.06	98.41
66.26	0.85	13.37	7.32	0.15	1.16	4.04	3.85	1.66	98.66
65.70	0.48	15.42	4.43	0.17	0.34	1.93	3.60	3.86	95.93
65.38	0.41	15.49	4.82	0.23	0.43	1.88	5.05	3.74	97.44
65.14	0.45	15.39	4.61	0.16	0.39	1.92	5.10	3.82	96.99
65.06	0.36	15.10	4.06	0.22	0.28	1.69	4.76	4.02	95.56
65.06	0.52	15.67	4.90	0.17	0.44	1.91	5.03	3.72	97.42
64.74	0.59	15.68	4.79	0.19	0.50	2.16	5.38	3.68	97.71
64.47	0.51	15.51	4.48	0.14	0.36	1.87	4.90	3.67	95.92
64.19	0.47	15.53	5.16	0.19	0.43	2.24	5.06	3.81	97.09
50.35	2.74	13.53	14.12	0.25	5.81	10.05	2.49	0.46	99.80
50.05	2.65	13.08	12.78	0.21	5.48	10.10	2.80	0.46	97.63
49.86	2.67	13.10	13.25	0.24	5.56	10.43	2.83	0.44	98.38
48.71	1.99	13.04	12.78	0.20	6.13	10.19	2.66	0.24	95.95

Tephra i 57-58.5 cm

74.92	0.09	12.86	2.02	0.06	0.01	1.26	4.55	2.80	98.56
71.25	0.22	14.31	3.07	0.01	0.13	2.00	4.58	2.58	98.14
63.90	0.46	15.25	4.53	0.18	0.44	2.02	4.81	4.04	95.64
62.49	0.92	15.39	6.65	0.12	1.25	4.14	4.67	1.47	97.10
49.63	2.00	13.85	10.59	0.12	7.15	11.32	2.39	0.28	97.34
49.11	2.08	13.50	12.99	0.16	6.09	10.30	2.62	0.31	97.16
49.04	2.68	13.01	13.05	0.17	5.28	9.66	2.66	0.39	95.93
49.00	2.59	12.97	12.95	0.18	5.65	9.83	2.94	0.49	96.62
48.34	3.48	12.15	14.76	0.21	4.77	8.96	2.98	0.51	96.15
46.66	4.45	12.92	14.33	0.21	4.73	9.08	3.27	0.79	96.45

Tephra j 62.3-62.8 cm

SiO_2	TiO_2	Al_2O_3	FeO	MnO	MgO	CaO	Na_2O	K_2O	Total
73.98	0.09	13.00	2.02	0.04	0.05	1.28	2.88	2.68	96.01
73.40	0.09	12.78	1.97	0.09	0.05	1.26	3.53	2.75	95.92
73.38	0.08	12.82	2.10	0.10	0.05	1.41	3.66	2.70	96.31
73.27	0.14	12.82	1.99	0.04	0.05	1.31	3.15	2.77	95.53
64.72	0.61	14.82	7.01	0.25	0.74	4.14	5.25	1.12	98.66
63.36	0.62	14.62	6.55	0.24	0.65	3.73	3.66	1.69	95.12
49.18	1.83	13.40	12.80	0.29	5.86	12.06	2.78	0.08	98.27

Tephra k 67.8-68.3 cm

74.02	0.13	12.75	2.08	0.13	0.05	1.34	4.17	2.93	97.55
72.55	0.20	14.01	3.06	0.10	0.17	1.88	4.98	2.45	99.41
71.72	0.24	14.25	3.07	0.15	0.13	1.98	4.33	2.29	98.15
65.87	0.44	15.03	6.17	0.20	0.50	3.53	4.30	1.84	97.89
63.33	0.59	14.38	7.10	0.22	0.71	3.89	4.18	1.87	96.27
48.94	1.75	13.47	11.40	0.25	7.26	11.97	2.44	0.16	97.64

Tephra l 84.8-85.3 cm

49.59	1.87	13.30	11.07	0.19	7.49	11.29	2.49	0.18	97.49
49.22	1.99	13.43	11.71	0.19	7.29	11.77	2.44	0.19	98.24
49.20	1.62	13.63	11.48	0.25	7.55	11.67	2.15	0.13	97.69
49.16	1.68	13.38	11.54	0.20	7.53	12.23	2.24	0.16	98.12
48.35	1.73	13.65	11.50	0.16	7.35	11.73	2.23	0.16	96.85
48.03	1.81	13.55	11.15	0.19	7.51	11.82	2.62	0.20	96.88

Tephra m 86.3-89.3 cm

SiO_2	TiO_2	Al_2O_3	FeO	MnO	MgO	CaO	Na_2O	K_2O	Total
69.02	0.41	14.84	5.20	0.24	0.38	3.22	4.78	1.92	100.0
68.20	0.45	14.45	5.45	0.21	0.40	3.31	4.70	2.20	99.37
68.02	0.41	14.69	5.32	0.20	0.43	3.37	4.49	2.00	98.93
66.24	0.59	15.17	6.48	0.27	0.60	3.53	4.54	2.01	99.44
66.24	0.60	15.11	6.53	0.19	0.71	3.61	4.71	2.00	99.69
65.61	0.66	14.81	7.00	0.22	0.72	3.75	4.44	1.93	99.13
65.30	0.62	14.76	6.76	0.23	0.62	3.58	4.19	1.73	97.80
65.07	0.61	14.63	6.39	0.24	0.71	3.59	4.32	1.91	97.46
63.82	0.62	14.71	6.80	0.20	0.68	3.76	4.24	1.87	96.71
63.72	0.66	14.84	7.35	0.29	0.94	4.09	4.41	1.82	98.12

Tephra n 95.3-107.3 cm

76.81	0.10	12.67	1.70	0.03	0.04	1.17	3.84	2.58	98.94
76.14	0.10	12.96	1.85	0.08	0.04	1.20	4.42	2.88	99.67
75.40	0.10	13.13	2.07	0.02	0.06	1.36	4.58	2.73	99.45
74.84	0.11	12.78	1.97	0.08	0.05	1.28	4.18	2.85	98.14
74.59	0.11	12.34	2.03	0.05	0.02	1.27	4.41	2.73	97.55
73.70	0.12	13.09	1.94	0.04	0.05	1.31	4.61	2.80	97.65
73.62	0.11	12.59	1.88	0.03	0.05	1.30	3.87	2.95	96.40
73.39	0.05	12.98	1.79	0.07	0.01	1.14	4.54	2.79	96.75
73.01	0.18	13.09	2.46	0.02	0.17	1.58	4.74	2.97	98.22
72.71	0.12	12.75	1.86	0.05	0.04	1.12	4.42	2.83	95.90

Tephra o 127.3-127.5 cm

50.93	2.22	13.28	12.12	0.16	6.58	10.85	2.89	0.25	99.29
50.48	2.77	13.14	13.11	0.22	5.00	9.59	2.63	0.45	97.39
49.54	2.25	13.81	12.08	0.21	6.68	11.38	2.68	0.24	98.88
49.16	2.58	12.87	14.12	0.20	5.49	9.76	2.86	0.42	97.45
49.10	2.16	13.21	11.95	0.21	6.92	11.55	2.72	0.20	98.02

Tephra p 136.5-137.5 cm

SiO_2	TiO_2	Al_2O_3	FeO	MnO	MgO	CaO	Na_2O	K_2O	Total
50.14	1.91	13.82	10.37	0.23	7.48	12.26	2.68	0.24	99.13
49.56	1.85	15.20	10.16	0.22	5.86	12.19	2.63	0.18	97.86
48.53	1.79	13.81	10.67	0.15	7.54	12.12	2.51	0.20	97.31
48.18	1.84	13.75	10.73	0.21	7.14	11.86	2.41	0.22	96.34
48.18	2.00	13.78	10.86	0.20	7.22	11.83	2.36	0.23	96.65
47.99	1.86	14.02	10.86	0.18	7.45	12.00	2.33	0.22	96.90
47.81	1.92	13.80	10.65	0.14	7.18	11.79	2.27	0.23	95.80

Tephra q 139.5-140 cm

76.75	0.10	12.30	1.70	0.02	0.07	0.66	3.34	4.30	99.24
75.59	0.12	12.46	1.48	0.03	0.09	0.65	3.40	4.07	97.87
74.67	0.04	12.22	1.59	0.01	0.12	0.71	2.92	3.90	96.17
74.46	0.12	12.22	1.71	0.00	0.13	0.72	3.05	4.37	96.77
74.41	0.12	12.27	1.47	0.05	0.06	0.73	3.89	3.71	96.72
74.35	0.13	12.21	1.55	0.04	0.05	0.71	3.16	3.92	96.12
74.04	0.11	12.27	1.51	0.00	0.06	0.60	4.06	3.77	96.41
73.96	0.10	12.23	1.54	0.06	0.07	0.72	3.66	4.16	96.50
73.87	0.17	11.83	1.76	0.03	0.05	0.76	3.98	3.94	96.38
73.84	0.17	12.37	1.63	0.06	0.07	0.83	3.61	4.32	96.92
73.64	0.12	12.42	1.60	0.04	0.13	0.74	4.03	3.69	96.41
73.54	0.15	12.53	1.54	0.05	0.07	0.78	3.53	3.99	96.17
73.43	0.12	12.37	1.66	0.03	0.07	0.71	4.07	3.70	96.17
73.30	0.20	11.98	1.53	0.07	0.11	0.63	4.30	3.68	95.79
71.44	0.27	13.14	3.86	0.14	0.21	1.15	4.86	3.48	98.55

Site 3 (Stekkjardalur)-monolith

Tephra 1 11-12 cm

SiO_2	TiO_2	Al_2O_3	FeO	MnO	MgO	CaO	Na_2O	K_2O	Total
60.63	1.24	15.01	9.28	0.21	1.54	5.12	4.36	1.61	98.99
60.40	1.04	15.12	8.97	0.27	1.51	4.81	4.28	1.63	98.03
60.19	1.17	15.15	9.34	0.28	1.73	5.13	4.50	1.66	99.15
59.95	1.09	14.90	9.49	0.18	1.52	5.06	4.35	1.57	98.11
58.90	1.56	14.96	9.20	0.24	2.12	5.36	4.27	1.31	97.92
58.77	1.56	14.89	10.26	0.27	2.10	5.49	3.88	1.55	98.78
58.69	0.80	18.88	4.87	0.11	1.21	7.00	4.43	0.72	96.70
58.54	1.24	14.67	9.88	0.21	1.76	5.42	4.33	1.56	97.62
57.83	1.47	14.84	9.60	0.26	2.14	5.59	3.98	1.40	97.12
57.46	1.42	14.56	9.62	0.26	2.12	5.44	3.66	1.40	95.94

Tephra 2 16.5-18 cm

73.57	0.21	13.89	3.29	0.12	0.13	1.91	4.20	2.67	99.97
72.77	0.25	13.79	3.23	0.10	0.11	1.84	4.50	2.69	99.28
72.50	0.26	13.65	3.26	0.09	0.10	1.97	4.49	2.78	99.11
72.36	0.23	13.67	3.20	0.14	0.08	1.81	4.33	2.68	98.50
72.22	0.16	14.01	3.22	0.12	0.08	1.80	4.65	2.52	98.78
71.68	0.23	13.67	3.25	0.15	0.12	1.85	4.55	2.75	98.25
71.58	0.23	13.83	3.26	0.13	0.12	1.88	4.39	2.58	97.98
71.37	0.22	13.77	3.17	0.12	0.15	1.91	4.17	2.79	97.68
71.31	0.19	13.46	4.46	0.17	0.19	2.15	4.58	2.73	99.23
70.42	0.19	14.98	2.61	0.19	0.10	2.48	4.91	2.15	98.02

Tephra 3 19-19.5 cm

SiO_2	TiO_2	Al_2O_3	FeO	MnO	MgO	CaO	Na_2O	K_2O	Total
50.17	1.79	13.29	11.99	0.14	6.23	10.77	2.37	0.21	96.96
49.98	1.77	13.46	12.54	0.24	6.40	11.16	2.38	0.25	98.19
49.76	1.84	13.52	12.47	0.17	6.55	11.53	2.56	0.22	98.62
49.37	1.90	13.34	12.40	0.23	6.49	11.21	2.49	0.19	97.63
49.24	1.92	13.46	12.40	0.22	6.48	10.95	2.68	0.26	97.61
48.88	1.85	13.37	12.38	0.20	6.60	11.23	2.50	0.21	97.21
48.69	1.89	13.49	12.34	0.20	6.23	11.49	2.42	0.20	96.95
48.08	2.02	13.46	12.20	0.23	6.61	10.94	2.52	0.15	96.21
47.97	1.74	12.93	12.37	0.19	6.48	11.08	2.47	0.18	95.41
46.88	4.59	12.52	14.72	0.22	5.03	9.82	3.25	0.76	97.80

Tephra 4 20.5-21.5 cm

73.26	0.12	12.79	1.88	0.07	0.03	1.34	4.35	2.76	96.61
49.74	1.83	13.34	11.97	0.23	6.48	10.89	2.54	0.23	97.24
49.50	1.93	13.16	12.04	0.26	6.11	10.68	2.55	0.37	96.60
49.29	1.85	13.63	12.70	0.26	6.17	10.46	2.36	0.24	96.98
49.19	1.91	13.23	12.14	0.18	6.48	10.80	2.68	0.22	96.83
49.11	1.77	13.27	12.53	0.22	6.48	11.33	2.56	0.24	97.50

Tephra 5 22-22.3 cm

49.57	1.81	13.11	12.62	0.21	6.55	11.26	2.35	0.23	97.71
48.61	1.78	12.94	12.57	0.19	6.23	10.62	2.52	0.23	95.70
48.56	1.98	13.31	12.16	0.20	6.44	11.04	2.56	0.21	96.46
48.54	1.87	13.40	12.46	0.19	6.61	11.39	2.30	0.19	96.96
48.39	1.80	13.01	12.08	0.24	6.37	10.86	2.36	0.24	95.36

Tephra 6 22.5-22.7 cm

SiO_2	TiO_2	Al_2O_3	FeO	MnO	MgO	CaO	Na_2O	K_2O	Total
67.05	0.42	15.37	4.13	0.14	0.28	1.83	4.70	4.03	97.94
66.81	0.49	15.80	4.85	0.15	0.46	2.16	4.70	3.89	99.31
66.29	0.51	15.89	4.99	0.15	0.54	2.17	4.90	3.75	99.20
64.90	0.48	15.52	4.90	0.16	0.42	2.14	5.18	3.81	97.52
63.99	0.56	15.71	4.97	0.14	0.50	2.31	4.88	3.70	96.77
49.81	2.66	13.21	13.04	0.21	5.19	9.90	2.93	0.48	97.42
49.32	2.78	13.02	12.60	0.23	5.40	9.96	2.83	0.44	96.59
49.25	1.96	13.06	12.58	0.24	6.83	11.22	2.33	0.19	97.67
48.79	1.79	13.00	12.33	0.14	6.59	10.80	2.60	0.20	96.24
48.34	2.68	12.86	12.91	0.23	5.15	9.59	2.95	0.31	95.01

Site 4 (northern shore)

Tephra a 2-2.5 cm

49.83	2.47	13.24	13.16	0.17	5.76	9.97	3.32	0.35	98.26
49.25	2.90	12.51	12.93	0.27	6.15	10.14	2.63	0.46	97.23
48.94	3.14	12.80	14.10	0.26	5.54	10.02	3.36	0.45	98.61
48.58	2.97	12.95	14.17	0.23	5.72	9.82	3.13	0.46	98.03
48.47	3.16	12.63	14.02	0.23	5.43	10.01	2.55	0.45	96.95

Tephra b 3-3.5 cm

SiO_2	TiO_2	Al_2O_3	FeO	MnO	MgO	CaO	Na_2O	K_2O	Total
66.73	0.45	14.66	5.63	0.20	0.38	3.31	3.90	2.00	97.25
66.70	0.49	14.22	5.85	0.19	0.45	3.33	3.76	1.84	97.23
66.61	0.46	15.06	5.82	0.21	0.43	3.34	3.99	2.05	97.96
65.90	0.40	14.35	5.29	0.17	0.45	3.09	3.92	2.01	95.57
64.64	0.56	14.68	7.23	0.24	0.64	3.97	4.14	1.80	97.91
64.44	0.67	14.81	7.31	0.20	0.75	4.05	4.11	1.78	98.13
63.73	0.81	15.17	8.10	0.17	0.95	4.37	3.97	1.72	98.99
62.90	0.76	15.08	7.58	0.26	0.88	4.07	4.21	1.74	97.47
62.78	0.91	15.04	8.46	0.22	1.01	4.33	3.86	1.80	98.43
62.04	0.77	14.97	7.82	0.26	1.01	4.21	4.25	1.72	97.05
60.29	0.68	15.42	6.97	0.18	0.79	3.81	5.10	1.79	95.03

Tephra c 9.5-10.5 cm

60.87	1.15	15.26	9.34	0.20	1.59	5.05	3.92	1.54	98.93
60.02	1.53	14.19	10.59	0.24	1.79	5.12	4.13	1.80	99.42
60.01	1.21	15.30	9.37	0.32	1.58	1.20	4.06	1.58	98.65
59.50	1.59	15.21	10.24	0.29	2.05	5.88	3.62	1.49	99.85
58.64	1.47	15.04	9.39	0.19	2.06	5.65	4.30	1.43	98.16
58.56	1.28	16.40	8.61	0.24	1.74	5.99	4.22	1.18	98.22
58.10	1.63	15.63	9.53	0.28	2.03	5.55	4.45	1.46	98.64
58.08	1.53	14.64	9.53	0.30	2.13	5.42	4.43	1.62	97.67
57.95	1.45	15.64	9.33	0.22	2.08	5.86	4.48	1.52	98.54
57.85	1.35	16.83	7.75	0.21	1.60	6.21	4.05	1.32	97.16

Tephra d 21.5-26 cm

SiO_2	TiO_2	Al_2O_3	FeO	MnO	MgO	CaO	Na_2O	K_2O	Total
73.01	0.22	13.84	2.84	0.11	0.12	1.97	5.00	2.84	99.94
72.71	0.23	14.16	3.27	0.07	0.13	2.01	4.48	2.69	99.75
72.51	0.15	14.19	3.28	0.10	0.13	2.05	4.77	2.68	99.84
72.05	0.23	14.26	3.14	0.10	0.13	1.97	4.26	2.84	98.97
72.04	0.22	13.62	3.10	0.13	0.12	1.78	4.53	2.88	98.42
72.02	0.13	13.35	3.16	0.11	0.13	1.77	4.63	2.87	98.19
71.99	0.20	13.74	3.21	0.11	0.11	2.03	4.40	2.64	98.44
71.97	0.21	13.94	3.24	0.13	0.13	1.98	4.56	2.67	98.84
71.86	0.22	13.98	3.08	0.08	0.14	2.05	4.65	2.47	98.54
70.59	0.23	13.88	3.06	0.11	0.12	2.02	4.40	2.76	97.17

Tephra e 28.5-29.5 cm

50.12	1.90	13.56	12.66	0.25	6.47	11.84	2.61	0.22	99.62
49.44	2.43	13.95	12.01	0.20	6.52	11.53	2.74	0.33	99.15
49.13	1.83	13.23	12.37	0.15	6.63	10.64	2.72	0.19	96.89
49.08	1.99	12.99	12.65	0.18	6.57	11.16	2.67	0.26	97.56
48.34	1.81	13.44	12.77	0.26	6.38	11.29	2.76	0.22	96.67
46.35	4.72	12.31	14.39	0.18	4.61	9.48	3.01	0.79	95.84

Tephra f 32.5-33 cm

49.78	2.06	13.42	12.88	0.20	6.14	10.60	2.73	0.30	98.11
49.43	2.09	13.18	12.83	0.25	6.01	10.77	2.82	0.28	97.66
49.40	2.34	13.23	13.39	0.31	5.81	10.70	3.07	0.19	98.44
49.28	2.21	13.52	12.38	0.27	5.82	10.97	2.93	0.31	97.67
47.83	2.09	13.79	12.42	0.24	5.90	10.90	2.90	0.25	96.33

Tephra g 40-42 cm

SiO_2	TiO_2	Al_2O_3	FeO	MnO	MgO	CaO	Na_2O	K_2O	Total
74.43	0.07	13.01	2.00	0.02	0.01	1.32	2.24	2.85	95.95
64.95	1.31	13.50	7.31	0.15	1.60	4.62	3.63	2.00	99.05
50.43	2.53	13.46	13.02	0.21	5.45	9.82	3.06	0.41	98.38
50.39	1.89	13.17	12.81	0.21	6.28	10.52	2.82	0.28	98.36
50.37	1.99	13.30	12.45	0.23	5.91	10.65	2.85	0.27	98.02
50.31	2.06	13.09	13.02	0.20	6.01	10.25	2.68	0.33	97.93
49.80	1.74	13.56	11.85	0.17	6.66	11.45	2.46	0.22	97.90
49.57	1.89	13.04	12.77	0.21	5.90	9.95	2.82	0.26	96.39
49.56	1.96	13.00	12.59	0.20	6.12	10.24	2.70	0.28	96.65
48.86	1.73	13.46	11.52	0.21	6.69	11.25	2.59	0.18	96.60

Tephra h 48-50 cm

72.80	0.24	13.67	2.83	0.07	0.18	1.90	3.78	2.64	98.10
72.13	0.18	13.68	3.08	0.13	0.13	2.00	4.11	2.61	98.06
71.77	0.20	13.71	3.07	0.10	0.11	1.96	3.26	2.77	96.96
70.63	0.29	13.63	3.52	0.12	0.24	2.00	4.55	2.47	97.46
69.81	0.30	13.95	3.95	0.16	0.18	2.41	4.28	2.33	97.38
67.43	0.36	14.49	5.62	0.16	0.44	3.19	4.68	2.04	98.41
67.00	0.55	14.95	6.60	0.17	0.69	3.81	4.11	1.89	99.77
66.42	0.42	14.58	6.38	0.16	0.56	3.45	4.35	1.97	98.29
66.24	0.49	14.91	6.01	0.15	0.40	3.36	4.40	1.86	97.81
65.67	0.59	14.67	6.36	0.18	0.47	3.38	4.72	1.95	98.00

Tephra i 54-58.5 cm

SiO_2	TiO_2	Al_2O_3	FeO	MnO	MgO	CaO	Na_2O	K_2O	Total
75.58	0.14	13.10	1.93	0.08	0.00	1.17	2.82	3.03	97.86
75.29	0.10	12.84	1.79	0.06	0.02	1.34	4.53	2.96	98.92
74.50	0.12	12.62	2.02	0.07	0.01	1.11	3.79	3.01	97.25
74.86	0.12	13.00	1.90	0.09	0.00	1.19	4.22	2.90	98.27
73.49	0.13	12.44	1.78	0.08	0.03	1.18	3.44	2.78	95.36
68.30	0.42	14.37	5.66	0.20	0.41	3.39	4.57	2.10	99.42
67.93	0.46	14.53	5.74	0.22	0.48	3.14	4.30	1.96	98.76
66.29	0.44	14.38	5.59	0.13	0.30	3.34	4.50	2.17	97.15
65.17	0.60	14.76	6.81	0.18	0.60	3.71	4.45	1.88	98.16
64.28	0.60	14.91	7.41	0.25	0.77	3.87	4.18	1.82	98.08

Tephra j 58.5-59 cm

48.38	4.50	14.60	14.33	0.28	4.69	9.10	3.00	0.83	97.70
47.54	4.69	12.34	13.70	0.22	4.72	9.35	2.98	0.92	96.45
47.16	4.55	12.23	14.08	0.20	4.55	8.97	3.21	0.76	95.70
47.13	4.42	12.70	14.18	0.26	4.64	8.86	3.37	0.93	96.50
47.11	4.43	12.36	14.07	0.27	4.86	9.11	3.23	0.85	96.29

Tephra k 63.5-66.5 cm

SiO_2	TiO_2	Al_2O_3	FeO	MnO	MgO	CaO	Na_2O	K_2O	Total
72.39	0.23	13.62	3.09	0.13	0.13	2.14	4.26	2.65	98.66
72.35	0.19	13.88	2.96	0.07	0.13	2.12	4.22	2.35	98.28
68.63	0.44	14.70	5.14	0.17	0.34	3.14	4.28	2.07	98.91
68.11	0.34	14.56	5.31	0.17	0.33	3.09	4.09	2.20	98.20
67.08	0.45	14.69	5.65	0.16	0.42	3.35	4.22	2.09	98.11
66.90	0.38	14.27	4.82	0.17	0.35	2.84	3.80	2.00	95.55
66.76	0.58	14.95	6.25	0.12	0.58	3.60	4.08	2.00	98.91
65.38	0.66	14.66	6.85	0.18	0.58	3.34	3.81	1.88	97.35
65.22	0.67	14.91	7.61	0.24	0.72	4.02	4.23	1.75	99.37
64.59	0.66	14.66	7.74	0.25	0.70	3.96	3.77	1.82	98.16
64.28	0.55	14.40	6.40	0.21	0.58	3.79	3.89	1.77	95.87
63.79	0.76	14.81	7.07	0.20	0.74	4.07	3.75	1.72	96.91
63.74	0.63	14.95	7.02	0.20	0.77	3.99	3.84	1.70	96.84
63.58	0.81	15.06	7.53	0.20	0.83	4.26	4.27	1.39	97.94
62.05	0.76	14.36	7.78	0.21	0.81	4.47	3.49	1.69	95.62

Tephra l 73.5-80.5 cm

75.85	0.11	12.94	2.09	0.05	0.04	1.36	2.23	3.00	97.67
75.65	0.10	13.02	2.08	0.08	0.05	1.38	4.06	2.90	99.32
75.25	0.06	12.86	1.95	0.04	0.00	1.32	4.15	2.88	98.53
74.47	0.05	12.13	1.99	0.06	0.04	1.37	3.67	3.13	96.91
74.39	0.10	12.94	1.97	0.06	0.03	1.29	3.53	3.12	97.44
73.96	0.06	12.84	2.02	0.08	0.02	1.43	4.11	2.98	97.50
73.95	0.14	13.15	2.08	0.05	0.04	1.24	3.98	2.96	97.59
73.87	0.11	12.74	1.94	0.10	0.06	1.39	4.14	3.07	97.42
73.22	0.12	12.53	1.94	0.07	0.08	1.41	3.21	3.09	95.67
73.04	0.12	12.73	2.02	0.13	0.04	1.38	2.46	3.10	95.02

Site 5 (Svínadalsá delta area)

Tephra a 10-10.5 cm

SiO_2	TiO_2	Al_2O_3	FeO	MnO	MgO	CaO	Na_2O	K_2O	Total
60.39	1.21	15.29	9.05	0.29	1.58	4.71	4.12	1.66	98.29
60.04	1.23	14.78	9.51	0.32	1.71	5.21	4.55	1.68	99.03
59.84	1.24	14.02	9.41	0.26	1.48	5.09	3.56	1.66	96.57
58.70	1.13	13.89	9.54	0.22	1.52	5.33	3.59	1.72	95.64
57.91	1.36	13.45	9.60	0.36	1.97	5.79	4.05	1.62	96.12
57.69	1.70	14.36	10.88	0.28	2.24	5.60	3.55	1.56	97.85
57.50	1.23	18.33	7.16	0.20	1.45	6.44	4.91	0.96	98.17
57.46	1.33	14.80	8.85	0.21	1.74	6.02	4.17	1.24	95.82
57.31	1.31	15.60	8.16	0.20	1.63	6.52	4.38	1.19	96.31
56.17	1.64	11.46	14.11	0.46	4.93	5.35	3.28	1.43	98.83

Site 6 (Svínadalur)

Tephra a 25-25.5 cm

60.71	1.28	14.70	8.08	0.28	1.28	4.30	4.56	1.74	96.94
59.96	1.25	14.74	8.71	0.27	1.60	4.87	4.38	1.74	97.52
59.94	1.11	14.93	9.43	0.28	1.60	4.99	4.43	1.38	98.09
59.91	1.16	15.02	8.55	0.26	1.55	4.77	4.28	1.72	97.24
59.04	1.34	14.91	9.33	0.26	1.62	5.06	4.31	1.60	97.47
58.79	1.30	14.60	9.07	0.27	1.62	4.91	4.06	1.57	96.19
58.47	1.21	15.36	9.47	0.27	1.58	4.88	4.38	1.55	97.16
57.42	1.44	14.98	9.34	0.30	2.02	5.25	4.18	1.48	96.41
57.42	1.15	15.01	9.09	0.24	1.44	4.75	4.53	1.76	95.38
56.97	1.25	15.59	8.46	0.20	1.60	5.73	4.76	1.41	95.97

Tephra b 55.5-56.5 cm

SiO_2	TiO_2	Al_2O_3	FeO	MnO	MgO	CaO	Na_2O	K_2O	Total
48.86	1.95	13.22	11.82	0.18	6.49	10.79	2.57	0.24	96.13
48.61	1.90	13.31	12.36	0.32	6.51	10.86	2.64	0.20	96.71
48.33	2.04	13.16	13.18	0.25	6.53	10.62	2.69	0.25	97.06
47.61	2.02	13.35	11.92	0.20	6.54	10.91	2.54	0.24	95.32
47.19	1.99	13.42	12.45	0.20	6.71	11.30	2.57	0.20	96.02

Tephra c 87.5-97.5 cm

73.32	0.10	13.14	1.76	0.11	0.05	1.30	4.53	2.77	97.07
73.15	0.07	12.80	1.89	0.13	0.01	1.27	4.51	3.01	96.83
73.11	0.10	12.88	1.98	0.10	0.04	1.42	3.65	2.77	96.05
72.70	0.07	12.99	1.84	0.12	0.05	1.15	4.65	2.87	96.45
72.50	0.09	12.66	1.94	0.15	0.04	1.35	4.34	2.83	95.89
72.00	0.07	12.65	1.88	0.09	0.03	1.24	4.48	2.70	95.14
71.97	0.13	13.10	1.99	0.15	0.04	1.29	3.91	2.82	95.40
71.87	0.05	12.68	1.94	0.09	0.03	1.34	4.61	2.84	95.45
71.69	0.08	12.77	2.10	0.11	0.03	1.38	4.03	2.89	95.07
71.42	0.14	13.09	1.93	0.09	0.02	1.47	4.79	2.90	95.83

Tephra d 127.5-129 cm

SiO_2	TiO_2	Al_2O_3	FeO	MnO	MgO	CaO	Na_2O	K_2O	Total
71.98	0.20	11.47	2.34	0.12	0.03	0.40	4.67	4.34	95.56
71.89	0.26	14.22	3.30	0.17	0.09	1.91	4.62	2.68	99.14
71.25	0.20	13.76	3.11	0.16	0.13	1.81	4.78	2.52	97.73
70.55	0.19	13.49	3.36	0.13	0.13	1.91	4.73	2.61	97.11
70.46	0.22	13.77	3.22	0.19	0.09	1.86	4.54	2.72	97.07
70.42	0.15	14.17	3.13	0.14	0.10	1.89	4.92	2.64	97.56
70.13	0.23	13.84	3.19	0.13	0.13	1.83	4.67	2.72	96.87
69.90	0.35	13.46	3.51	0.16	0.22	1.04	4.91	3.60	97.17
68.89	0.71	13.42	3.37	0.15	0.52	1.39	4.75	3.57	96.77
66.10	0.79	14.12	4.03	0.22	0.63	1.97	5.07	3.14	96.07

Site 7 (Svínadalur)

Tephra a 40-47 cm

75.57	0.11	13.36	1.81	0.13	0.03	1.38	4.49	2.79	99.67
74.66	0.11	13.47	2.08	0.10	0.06	1.23	4.58	2.78	99.08
74.39	0.16	13.13	1.87	0.12	0.03	1.23	4.30	2.76	97.99
74.26	0.09	13.27	1.82	0.07	0.03	1.32	3.82	2.83	97.52
73.81	0.10	13.37	1.95	0.11	0.04	1.38	4.62	2.76	98.15
73.74	0.11	12.91	1.78	0.06	0.07	1.26	4.41	2.85	97.19
73.21	0.07	13.20	1.79	0.15	0.03	1.28	4.78	2.95	97.46
72.96	0.12	13.10	1.97	0.11	0.02	1.27	4.78	2.90	97.23
72.82	0.10	13.07	1.90	0.11	0.05	1.20	4.60	2.86	96.72
72.78	0.06	13.39	1.94	0.13	0.01	1.42	4.62	2.84	97.19

Site 8 (Svínadalur)

Tephra a 60-60.5 cm

SiO_2	TiO_2	Al_2O_3	FeO	MnO	MgO	CaO	Na_2O	K_2O	Total
59.95	1.14	15.35	8.86	0.28	1.35	4.90	4.30	1.62	97.75
59.91	1.19	14.89	9.07	0.29	1.53	4.91	4.14	1.68	97.59
59.86	1.20	14.99	9.34	0.30	1.61	4.84	4.29	1.71	98.15
59.74	1.27	15.08	8.80	0.27	1.52	4.86	4.41	1.72	97.67
59.30	1.07	15.29	8.20	0.29	1.27	4.84	4.66	1.55	96.47
58.20	1.15	14.37	8.99	0.29	1.64	4.88	4.25	1.57	95.34
57.91	1.52	14.82	9.56	0.27	2.06	5.46	4.21	1.49	97.30
57.71	1.43	14.61	9.93	0.29	2.11	5.45	4.06	1.59	97.18
57.54	1.54	14.70	9.33	0.29	2.18	5.36	4.20	1.49	96.62
57.07	1.62	14.77	9.85	0.24	1.98	5.55	4.43	1.43	96.95

Tephra b 70.5-71 cm

72.36	0.23	13.97	3.06	0.17	0.15	1.85	4.68	2.81	99.28
71.81	0.21	13.84	3.36	0.08	0.16	1.94	4.48	2.64	98.52
71.43	0.28	14.13	3.22	0.19	0.12	1.87	4.58	2.61	98.45
71.32	0.18	14.08	2.99	0.17	0.11	1.92	4.57	2.63	97.96
71.25	0.18	13.70	3.10	0.10	0.12	1.98	4.51	2.69	97.62
70.99	0.22	13.99	3.12	0.13	0.15	1.94	4.50	2.92	97.95
70.97	0.21	13.79	3.24	0.13	0.16	1.92	4.70	2.65	97.77
70.79	0.19	14.30	3.05	0.15	0.14	1.92	4.55	2.59	97.68
70.78	0.18	13.91	3.09	0.09	0.14	1.85	4.28	2.72	97.04
70.69	0.17	14.12	3.19	0.11	0.08	1.85	4.55	2.57	97.34

Tephra c 76-77 cm

SiO_2	TiO_2	Al_2O_3	FeO	MnO	MgO	CaO	Na_2O	K_2O	Total
49.35	1.93	13.47	12.20	0.26	5.65	10.05	2.85	0.34	96.09
48.77	1.99	13.20	11.77	0.24	6.01	10.11	2.97	0.33	95.40
48.74	1.98	13.81	12.11	0.21	6.78	11.23	2.59	0.21	97.65
48.67	1.92	13.51	12.30	0.20	6.44	11.34	2.59	0.21	97.19
48.35	1.93	13.78	12.19	0.19	6.72	11.06	2.47	0.22	96.90

Tephra d 86-88 cm

72.20	0.22	13.73	3.03	0.09	0.13	2.00	4.66	2.44	98.49
72.10	0.18	13.93	3.01	0.09	0.12	2.01	4.67	2.42	98.53
71.36	0.18	13.80	3.02	0.15	0.12	2.06	4.37	2.37	97.42
70.70	0.19	13.64	3.04	0.07	0.15	1.95	4.18	2.58	96.50
70.12	0.23	14.04	3.11	0.13	0.11	1.94	4.61	2.48	96.77
69.88	0.19	14.24	3.01	0.07	0.12	1.95	4.59	2.28	96.33
64.71	0.50	14.52	5.91	0.19	0.42	3.32	4.45	2.17	96.21
63.85	0.49	14.48	5.86	0.21	0.49	3.71	4.56	1.90	95.54
63.46	0.56	15.03	6.37	0.18	0.61	3.76	4.52	1.84	96.34
60.83	0.74	16.86	7.16	0.24	0.78	5.22	5.13	1.37	98.32

Tephra e 94-99 cm

75.53	0.08	12.97	1.89	0.08	0.06	1.27	4.07	2.80	98.76
73.78	0.10	12.94	1.94	0.10	0.05	1.38	4.16	2.83	97.29
73.76	0.10	12.84	1.81	0.08	0.04	1.34	4.46	2.94	97.37
73.67	0.09	12.59	1.94	0.09	0.05	1.25	4.42	2.79	96.87
73.57	0.12	13.05	1.91	0.07	0.06	1.34	4.34	2.77	97.24
73.21	0.14	13.10	1.93	0.06	0.05	1.37	4.36	3.04	97.26
72.64	0.07	12.80	1.94	0.06	0.03	1.28	4.58	3.05	96.44
72.42	0.13	12.64	1.92	0.10	0.06	1.35	4.58	2.86	96.06
72.31	0.14	12.68	1.89	0.09	0.07	1.31	4.32	2.78	95.59
72.20	0.07	12.39	1.91	0.09	0.05	1.26	4.28	2.82	95.07

Site 9 (Svínadalur)

Tephra b 13.5-16 cm

SiO_2	TiO_2	Al_2O_3	FeO	MnO	MgO	CaO	Na_2O	K_2O	Total
73.32	0.19	14.10	3.23	0.14	0.10	1.86	4.25	2.74	99.94
73.26	0.17	13.91	3.22	0.12	0.13	2.03	4.56	2.50	99.91
72.95	0.21	14.10	3.18	0.08	0.14	1.89	4.22	2.69	99.45
72.88	0.23	14.02	3.04	0.13	0.13	2.08	4.00	2.73	99.24
72.85	0.21	13.92	3.12	0.08	0.11	2.03	4.30	2.67	99.27
72.84	0.21	14.36	3.18	0.09	0.11	1.88	4.06	2.80	99.51
72.68	0.17	14.03	3.22	0.13	0.13	1.99	4.19	2.57	99.12
72.39	0.18	14.75	3.15	0.11	0.10	2.07	4.48	2.70	99.92
72.23	0.13	13.98	3.27	0.08	0.13	1.94	4.24	2.68	98.69
71.81	0.17	14.02	3.07	0.10	0.13	1.86	4.21	2.57	97.93

Tephra c 19-20 cm

47.56	4.42	12.43	14.51	0.27	4.90	9.47	3.08	0.78	97.41
47.52	4.59	12.75	15.28	0.19	4.73	9.31	2.84	0.80	98.01
47.34	4.60	12.41	14.31	0.22	4.68	9.34	3.06	0.81	96.76
47.31	4.35	13.05	14.75	0.23	4.81	9.30	3.12	0.77	97.70
47.11	4.47	12.31	13.93	0.25	4.65	9.25	2.41	0.76	95.25

Tephra d 22-23 cm

50.65	2.17	13.39	12.68	0.25	5.97	10.27	2.82	0.36	98.57
49.54	2.03	13.32	12.51	0.18	6.37	10.84	2.72	0.19	97.69
49.27	1.94	13.00	12.40	0.21	6.67	11.30	2.41	0.30	97.49
49.16	1.84	13.76	12.48	0.19	6.47	11.22	2.52	0.25	97.90

Tephra e 31-31.5 cm

SiO_2	TiO_2	Al_2O_3	FeO	MnO	MgO	CaO	Na_2O	K_2O	Total
49.82	1.88	12.91	12.41	0.23	6.81	10.98	2.41	0.23	97.69
48.97	4.30	12.87	13.71	0.33	4.56	9.10	3.31	0.87	98.01
48.18	4.39	12.84	14.14	0.37	4.69	9.39	3.30	0.84	98.14
48.16	4.38	12.80	13.89	0.38	4.72	9.38	3.12	0.83	97.66
47.79	4.34	12.78	13.80	0.38	4.86	9.46	3.21	0.86	97.49
46.82	4.20	13.03	14.21	0.30	4.72	9.35	3.41	0.86	96.91

Tephra f 40.5-41 cm

50.30	1.95	13.36	12.39	0.18	7.17	11.79	2.37	0.19	99.68
50.30	1.95	13.36	12.39	0.18	7.17	11.79	2.37	0.19	99.68
50.30	1.95	13.36	12.39	0.18	7.17	11.79	2.37	0.19	99.68
50.30	1.95	13.36	12.39	0.18	7.17	11.79	2.37	0.19	99.68
50.28	1.95	13.81	12.01	0.22	6.79	11.98	2.27	0.20	99.51
49.34	1.89	14.11	11.49	0.20	6.82	11.40	2.41	0.18	97.85
49.31	1.82	13.32	11.84	0.17	7.17	11.84	2.30	0.22	97.98
48.87	1.82	13.81	11.63	0.20	7.36	11.78	2.18	0.17	97.83

Tephra g 43-44.5 cm

72.93	0.18	14.08	2.97	0.09	0.14	1.96	4.65	2.58	99.58
72.54	0.15	13.97	3.17	0.05	0.14	2.09	4.51	2.43	99.05
72.30	0.13	13.93	2.91	0.05	0.14	2.16	4.62	2.57	98.80
71.63	0.18	13.80	2.99	0.08	0.12	2.02	4.65	2.48	97.96
68.11	0.40	14.47	5.14	0.10	0.34	3.27	4.32	2.15	98.30
65.22	0.43	14.81	6.66	0.13	0.58	3.57	4.53	1.83	97.77
64.45	0.60	15.19	7.23	0.23	0.79	3.80	3.92	1.92	98.12
64.17	0.63	14.88	7.53	0.27	0.85	3.89	4.42	1.88	98.51
63.16	0.68	16.83	5.82	0.15	0.65	4.91	5.34	1.33	98.87

Tephra h 57.5-61.5 cm

SiO_2	TiO_2	Al_2O_3	FeO	MnO	MgO	CaO	Na_2O	K_2O	Total
75.71	0.12	12.80	1.94	0.05	0.03	1.25	4.50	3.04	99.43
75.63	0.11	13.45	1.96	0.09	0.02	1.28	4.50	2.92	99.96
75.27	0.11	12.77	1.94	0.08	0.02	1.28	4.77	2.93	99.16
75.08	0.09	12.88	2.06	0.08	0.02	1.34	4.51	2.92	98.99
75.08	0.08	13.04	1.82	0.05	0.03	1.27	4.59	2.91	98.86
74.85	0.15	12.98	1.86	0.12	0.01	1.19	4.36	2.85	98.37
74.57	0.17	12.98	2.09	0.02	0.01	1.36	4.56	2.82	98.58
74.19	0.10	12.95	1.75	0.06	0.02	1.27	4.45	2.78	97.57
73.87	0.11	13.06	1.97	0.08	0.02	1.22	4.35	2.90	97.58
72.77	0.08	13.08	1.86	0.08	0.04	1.25	4.34	2.83	96.33

Tephra i 91.5-94 cm

49.52	3.73	15.84	11.49	0.17	4.07	10.39	3.29	0.65	99.13
48.53	4.23	13.12	14.26	0.18	5.36	9.72	3.52	0.80	99.71
48.41	4.16	13.59	14.11	0.19	5.48	9.94	3.08	1.44	100.0
48.32	4.32	13.65	13.80	0.24	5.09	9.46	3.27	0.67	98.83
47.76	4.20	12.79	14.50	0.18	5.28	9.95	3.40	0.92	98.99
47.66	4.39	13.48	13.65	0.20	4.90	9.90	3.17	0.80	98.16
47.24	4.02	13.16	14.21	0.21	5.10	9.57	3.17	0.80	97.48
46.95	4.21	13.11	13.97	0.20	5.14	9.47	3.31	0.86	97.21
46.94	4.14	13.25	14.38	0.28	4.92	9.50	3.47	0.78	97.68
46.67	4.18	13.34	14.17	0.19	5.34	9.71	3.26	0.77	97.65
46.38	4.11	12.47	15.32	0.15	5.23	8.31	2.82	0.93	95.72

Site 10 (Stekkjardalur)

Tephra a 18-18.5 cm

SiO_2	TiO_2	Al_2O_3	FeO	MnO	MgO	CaO	Na_2O	K_2O	Total
59.85	1.12	14.87	9.20	0.25	1.63	4.85	4.29	1.42	97.47
58.93	1.37	14.61	9.81	0.21	2.07	5.49	4.32	1.52	98.34
58.77	1.14	14.53	9.73	0.26	2.11	4.72	4.24	1.54	97.04
58.69	1.09	15.00	9.15	0.24	1.57	5.08	4.42	1.59	96.83
58.68	1.15	15.33	9.42	0.20	1.62	4.91	4.27	1.58	97.16
58.60	1.10	14.75	8.98	0.25	1.69	4.94	4.33	1.54	96.18
57.77	1.12	15.23	8.65	0.25	1.44	4.84	4.50	1.61	95.41
57.43	1.37	15.36	9.60	0.24	2.16	6.03	4.34	1.33	97.85
56.75	1.48	14.40	9.69	0.24	2.15	5.60	4.12	1.49	95.91
56.45	1.46	14.35	9.57	0.24	2.15	5.60	4.24	1.43	95.49

Tephra b 67-69 cm

72.39	0.22	13.51	3.40	0.11	0.16	1.89	4.01	2.57	98.25
72.04	0.23	14.03	3.04	0.11	0.17	1.88	4.61	2.60	98.71
71.30	0.20	13.74	3.30	0.12	0.17	1.86	4.64	2.61	97.95
71.24	0.26	13.74	3.28	0.12	0.16	1.95	4.62	2.64	98.00
71.01	0.22	13.88	3.27	0.09	0.13	1.91	4.57	2.65	97.75
70.82	0.26	13.60	3.21	0.11	0.15	1.90	4.76	2.65	97.46
70.72	0.22	13.79	3.21	0.14	0.19	1.96	4.45	2.58	97.26
70.65	0.24	13.73	3.06	0.12	0.12	1.85	4.87	2.73	97.37
70.36	0.19	13.58	3.02	0.13	0.13	1.82	4.58	2.68	96.49
70.23	0.19	13.86	3.28	0.03	0.17	1.84	4.59	2.71	96.90

Tephra c 96.5-98.5 cm

SiO_2	TiO_2	Al_2O_3	FeO	MnO	MgO	CaO	Na_2O	K_2O	Total
46.20	4.23	12.57	14.68	0.19	4.85	9.47	3.21	0.75	96.15
46.79	4.67	12.35	14.40	0.29	4.81	9.41	3.24	0.77	96.74
46.14	4.51	12.50	14.02	0.26	5.00	9.30	3.32	0.83	95.87
46.03	4.53	12.91	14.84	0.16	4.91	9.33	3.36	0.82	96.89
45.80	4.73	12.75	13.96	0.20	4.89	9.60	3.45	0.79	96.16

Tephra d 101-101.5 cm

47.95	1.78	13.31	12.47	0.22	6.49	11.18	2.55	0.21	96.16
47.91	1.84	13.38	12.56	0.17	6.52	11.08	2.68	0.24	96.39
49.78	1.98	13.17	13.09	0.19	6.21	10.66	2.55	0.25	97.89
48.67	1.89	13.46	11.99	0.16	6.64	10.98	2.70	0.21	96.69
48.58	1.92	13.38	12.33	0.20	6.53	11.13	2.58	0.26	96.91

Tephra e 131.5-135.5 cm

70.55	0.20	14.06	3.11	0.16	0.12	2.03	4.17	2.53	96.92
69.89	0.17	13.90	3.08	0.11	0.19	2.05	4.09	2.60	96.08
64.14	0.62	14.65	6.60	0.20	0.64	3.67	4.47	1.79	96.78
63.82	0.60	14.72	6.25	0.25	0.60	3.52	4.19	1.80	95.77
63.10	0.75	14.89	7.94	0.24	0.99	4.40	4.85	1.49	98.65
62.03	0.76	14.99	8.21	0.25	0.96	4.19	4.48	1.75	97.62
61.91	0.70	14.92	7.51	0.23	0.81	4.02	4.30	1.83	96.24
61.78	0.68	14.43	8.08	0.23	0.92	4.23	4.24	1.69	96.28
61.10	0.85	14.96	8.58	0.19	1.11	4.47	4.29	1.68	97.23
61.09	0.80	14.77	7.80	0.20	0.98	4.24	3.95	1.71	95.53

Site 11 (Orrastaðir)

Tephra a 22-24.5 cm

SiO_2	TiO_2	Al_2O_3	FeO	MnO	MgO	CaO	Na_2O	K_2O	Total
72.88	0.23	13.63	3.33	0.10	0.14	1.79	5.02	2.87	99.99
72.29	0.27	13.75	3.13	0.08	0.10	1.97	4.70	2.76	99.06
71.91	0.24	13.47	3.21	0.12	0.14	1.90	4.57	2.70	98.26
71.75	0.26	13.36	3.23	0.10	0.18	1.72	4.75	2.92	98.26
71.74	0.19	14.22	3.15	0.11	0.15	1.93	4.75	2.66	98.89
71.71	0.22	14.54	2.92	0.13	0.14	2.15	5.01	2.52	99.33
71.51	0.22	13.81	3.11	0.09	0.12	2.05	4.94	2.71	98.57
71.49	0.25	13.64	3.20	0.09	0.14	1.78	4.39	2.78	97.76
71.47	0.21	13.80	3.31	0.15	0.14	1.74	4.92	2.61	98.34
71.27	0.17	13.41	3.26	0.10	0.13	1.91	4.54	2.73	97.51

Tephra b 46.5-49.5 cm

73.38	0.14	14.07	3.13	0.10	0.16	2.01	4.26	2.68	99.93
73.25	0.15	14.21	3.08	0.07	0.11	2.10	4.14	2.70	99.82
72.95	0.20	14.08	3.23	0.12	0.20	2.08	4.39	2.61	99.88
71.92	0.19	14.23	3.05	0.15	0.14	2.12	4.30	2.82	98.92
71.61	0.18	14.07	3.08	0.08	0.14	2.02	4.41	2.66	98.25
71.55	0.20	13.93	4.61	0.10	0.23	2.21	3.89	2.62	99.34
71.44	0.12	14.08	2.91	0.14	0.14	1.96	4.50	2.49	97.78
71.41	0.16	13.85	2.85	0.12	0.14	2.02	4.39	2.82	97.76
70.92	0.18	13.79	3.03	0.09	0.16	2.01	4.23	2.38	96.81
69.77	0.15	13.96	3.09	0.06	0.08	1.86	3.92	2.66	95.56
68.03	0.54	14.83	5.68	0.16	0.43	3.65	4.63	1.71	99.67
67.71	0.37	14.58	5.40	0.18	0.41	3.51	4.07	2.29	98.53
67.14	0.47	14.96	5.86	0.16	0.47	3.46	4.24	1.84	98.63
66.99	0.35	14.77	5.81	0.22	0.44	3.18	4.27	2.17	98.20
66.82	0.51	14.94	6.58	0.19	0.60	3.73	3.89	1.91	99.17
66.50	0.56	15.01	6.75	0.22	0.66	3.81	4.24	2.14	99.90

SiO_2	TiO_2	Al_2O_3	FeO	MnO	MgO	CaO	Na_2O	K_2O	Total
66.22	0.42	14.67	6.11	0.17	0.55	3.81	4.02	1.91	97.88
65.99	0.49	14.96	6.32	0.19	0.60	3.74	4.54	2.02	98.87
65.97	0.68	15.44	6.83	0.16	0.62	3.84	3.91	1.91	99.35
65.61	0.46	14.94	6.19	0.19	0.47	3.46	4.33	2.09	97.74
65.01	0.62	14.98	7.22	0.14	0.67	4.03	4.21	1.89	98.78
64.38	0.50	14.71	6.23	0.18	0.63	3.48	4.20	1.87	96.20
64.38	0.47	14.86	6.57	0.25	0.63	3.63	4.28	2.07	97.13
63.93	0.65	15.16	6.64	0.17	0.73	4.10	4.08	1.88	97.34
63.60	0.67	15.09	7.94	0.27	0.93	4.26	4.15	1.79	98.72
63.35	0.76	15.15	7.97	0.23	0.98	4.55	4.14	1.80	98.93
63.09	0.89	15.22	8.36	0.19	1.05	4.65	3.93	1.76	99.15
63.07	0.63	15.29	7.62	0.23	0.86	4.52	4.03	1.99	98.24
62.84	0.74	14.89	7.64	0.21	0.86	4.28	4.02	1.76	97.25
56.82	1.89	13.28	10.99	0.23	2.56	6.24	3.76	1.51	97.28
56.18	1.23	16.81	8.68	0.24	2.62	7.22	4.88	1.81	99.67
Tephra c 70-75 cm									
74.59	0.15	13.37	2.09	0.13	0.00	1.41	4.23	2.92	98.91
74.34	0.14	13.01	2.07	0.11	0.02	1.30	4.55	2.89	98.45
74.21	0.07	12.61	0.69	0.01	0.01	0.86	4.36	3.06	95.87
74.05	0.14	13.42	2.02	0.12	0.05	1.39	4.10	2.89	98.19
73.94	0.12	13.10	1.84	0.11	0.04	1.25	4.15	2.81	97.35
73.89	0.13	12.81	2.02	0.09	0.04	1.41	3.91	2.65	96.95
73.72	0.11	13.14	1.82	0.06	0.02	1.29	3.91	2.68	96.76
59.46	1.59	14.74	9.89	0.24	2.50	5.91	3.89	1.38	99.61
57.80	1.49	14.46	9.24	0.27	2.27	5.97	4.10	1.22	97.53
56.77	1.65	14.52	10.39	0.27	2.41	5.86	3.90	1.39	97.18
56.63	1.49	14.76	9.93	0.22	2.33	5.67	4.10	1.29	96.40

Site 12 (Stekkjardalur)

Tephra a 58-60 cm

SiO_2	TiO_2	Al_2O_3	FeO	MnO	MgO	CaO	Na_2O	K_2O	Total
73.32	0.19	14.10	3.23	0.14	0.10	1.86	4.25	2.74	99.94
73.26	0.17	13.91	3.22	0.12	0.13	2.03	4.56	2.50	99.91
72.95	0.21	14.10	3.18	0.08	0.14	1.89	4.22	2.69	99.45
72.39	0.22	13.51	3.40	0.11	0.16	1.89	4.01	2.57	98.25
72.04	0.23	14.03	3.04	0.11	0.17	1.88	4.61	2.60	98.71
71.30	0.20	13.74	3.30	0.12	0.17	1.86	4.64	2.61	97.95
71.24	0.26	13.74	3.28	0.12	0.16	1.95	4.62	2.64	98.00
71.37	0.22	13.77	3.17	0.12	0.15	1.91	4.17	2.79	97.68
71.31	0.19	13.46	4.46	0.17	0.19	2.15	4.58	2.73	99.23
70.42	0.19	14.98	2.61	0.19	0.10	2.48	4.91	2.15	98.02

Tephra b 91-92 cm

69.02	0.41	14.84	5.20	0.24	0.38	3.22	4.78	1.92	100.0
68.20	0.45	14.45	5.45	0.21	0.40	3.31	4.70	2.20	99.37
66.24	0.60	15.11	6.53	0.19	0.71	3.61	4.71	2.00	99.69
65.61	0.66	14.81	7.00	0.22	0.72	3.75	4.44	1.93	99.13
65.30	0.62	14.76	6.76	0.23	0.62	3.58	4.19	1.73	97.80
65.22	0.43	14.81	6.66	0.13	0.58	3.57	4.53	1.83	97.77
64.45	0.60	15.19	7.23	0.23	0.79	3.80	3.92	1.92	98.12
64.14	0.62	14.65	6.60	0.20	0.64	3.67	4.47	1.79	96.78
63.82	0.60	14.72	6.25	0.25	0.60	3.52	4.19	1.80	95.77
63.10	0.75	14.89	7.94	0.24	0.99	4.40	4.85	1.49	98.65

Tephra c 98-103 cm

SiO_2	TiO_2	Al_2O_3	FeO	MnO	MgO	CaO	Na_2O	K_2O	Total
76.81	0.10	12.67	1.70	0.03	0.04	1.17	3.84	2.58	98.94
76.14	0.10	12.96	1.85	0.08	0.04	1.20	4.42	2.88	99.67
75.40	0.10	13.13	2.07	0.02	0.06	1.36	4.58	2.73	99.45
74.47	0.05	12.13	1.99	0.06	0.04	1.37	3.67	3.13	96.91
74.36	0.10	12.94	1.97	0.06	0.03	1.29	3.53	3.12	97.44
73.96	0.06	12.84	2.02	0.08	0.02	1.43	4.11	2.98	97.50
73.72	0.11	13.14	1.82	0.06	0.02	1.29	3.91	2.68	96.76
73.21	0.07	13.20	1.79	0.15	0.03	1.28	4.78	2.95	97.46
72.96	0.12	13.10	1.97	0.11	0.02	1.27	4.78	2.90	97.23
72.82	0.10	13.07	1.90	0.11	0.05	1.20	4.60	2.86	96.72

Svínavatn lake core 1

Tephra a 20-20.5 cm

61.33	1.30	13.98	8.63	0.21	1.42	4.96	3.23	1.40	96.46
59.73	1.11	14.51	9.30	0.25	1.65	5.08	4.05	1.51	97.20
58.51	1.51	14.38	9.87	0.22	2.03	5.28	3.84	1.51	97.15
58.06	1.36	15.24	9.34	0.30	1.93	5.71	4.03	1.63	97.61
57.95	1.49	14.86	9.99	0.32	2.20	5.73	4.04	1.46	98.04
57.89	1.41	14.70	10.08	0.22	2.11	5.59	4.19	1.43	97.62
57.85	1.17	16.09	9.28	0.30	2.65	6.17	4.84	1.28	99.61
57.79	1.60	15.00	9.37	0.22	2.02	5.67	4.23	1.50	97.60
57.71	1.58	14.90	10.17	0.31	2.11	5.58	3.65	1.62	97.62
56.38	1.41	15.42	10.18	0.28	2.14	6.08	4.27	1.48	97.64
48.47	2.97	12.87	13.28	0.22	5.84	9.96	2.96	0.42	97.39

Svínavatn lake core 2

Tephra a 24.6-24.7 cm

SiO_2	TiO_2	Al_2O_3	FeO	MnO	MgO	CaO	Na_2O	K_2O	Total
72.77	0.25	14.42	3.18	0.11	0.12	1.93	3.81	2.75	99.34
71.72	0.19	14.03	2.76	0.12	0.11	1.94	4.37	2.46	97.69
71.62	0.18	12.99	3.10	0.12	0.15	1.91	4.43	2.58	97.09
71.63	0.20	14.06	3.18	0.09	0.09	2.05	4.49	2.61	98.40
71.58	0.19	13.92	3.03	0.13	0.13	1.90	4.53	2.64	98.05
71.42	0.26	13.97	3.10	0.09	0.13	1.82	4.68	2.67	98.14
71.14	0.21	13.79	3.23	0.13	0.13	1.95	4.21	2.56	97.34
70.57	0.15	13.70	3.07	0.10	0.13	1.68	4.39	2.86	96.65
70.51	0.25	13.92	2.92	0.09	0.15	1.91	4.43	2.79	96.97
69.16	0.17	13.94	2.93	0.09	0.11	2.04	4.26	2.75	95.46

Tephra b 31.6-33.1 cm

47.03	4.61	12.65	14.66	0.23	4.92	9.68	3.22	0.76	97.75
47.00	4.63	13.03	14.63	0.25	4.93	9.69	2.90	0.74	97.82
46.92	4.58	12.83	14.51	0.26	5.09	9.29	3.49	0.82	97.78
46.48	4.47	12.41	14.07	0.29	5.09	9.51	3.39	0.72	96.43
46.33	4.63	12.65	14.12	0.24	4.89	9.66	3.08	0.76	96.36

Tephra c 38.2-39 cm

SiO_2	TiO_2	Al_2O_3	FeO	MnO	MgO	CaO	Na_2O	K_2O	Total
72.72	0.18	13.73	3.13	0.10	0.16	1.85	4.00	2.59	98.48
71.20	0.15	13.47	3.06	0.08	0.12	1.82	3.47	2.13	95.50
68.00	0.43	15.44	3.93	0.20	0.27	1.66	4.92	3.96	98.81
67.28	0.55	15.24	4.75	0.19	0.40	2.14	3.11	2.83	96.47
66.64	0.53	15.83	5.12	0.20	0.51	2.16	4.77	3.66	99.40
66.33	0.42	16.93	4.48	0.14	0.35	2.61	5.30	3.46	100.0
66.27	0.64	15.94	5.08	0.19	0.56	2.20	4.60	3.78	99.25
66.11	0.36	15.15	4.01	0.17	0.34	1.82	4.74	4.05	96.75
65.82	0.64	15.69	5.07	0.17	0.50	2.22	4.61	3.67	98.40
64.69	0.55	14.77	6.73	0.20	0.52	3.54	3.99	1.88	96.85
64.34	0.53	14.96	4.50	0.17	0.41	2.26	4.77	3.80	95.74
64.12	0.50	15.26	4.82	0.14	0.43	2.12	3.98	3.75	95.12
49.95	2.09	16.97	11.84	0.23	4.69	9.83	3.29	0.33	99.21

Tephra d 39-39.1 cm

66.41	0.38	15.78	4.81	0.17	0.38	1.98	5.22	4.17	99.30
62.22	0.70	15.41	7.28	0.20	0.81	4.18	5.03	1.52	97.33
62.74	0.63	14.48	8.26	0.16	0.91	4.62	5.15	1.26	98.23
49.97	2.65	13.32	13.59	0.21	5.67	10.23	3.18	0.41	99.23
49.80	2.86	13.27	13.53	0.17	5.57	9.77	3.10	0.35	98.43
49.59	2.76	13.20	13.18	0.17	5.39	10.17	2.85	0.41	97.72
49.31	1.74	13.57	11.81	0.23	6.77	11.34	2.39	0.21	97.38
48.88	2.61	13.14	13.06	0.20	5.48	10.02	3.04	0.40	96.83
48.71	2.00	12.89	12.59	0.20	5.91	10.01	2.84	0.33	95.48
48.22	4.69	12.80	14.38	0.21	4.96	9.43	3.31	0.90	98.90

Tephra e 46-46.7 cm

SiO_2	TiO_2	Al_2O_3	FeO	MnO	MgO	CaO	Na_2O	K_2O	Total
47.78	4.37	12.97	14.06	0.27	4.60	9.06	3.51	0.82	97.44
47.44	4.60	12.63	14.19	0.21	4.72	9.10	3.34	0.87	97.12
47.00	4.55	12.50	14.35	0.24	4.80	9.31	3.45	0.84	97.03
46.91	4.68	12.48	14.53	0.23	4.53	8.81	3.17	0.83	96.18
46.74	4.66	12.37	14.12	0.27	4.70	8.99	3.45	0.92	96.22
46.68	4.91	13.12	14.07	0.24	4.98	9.55	3.38	0.79	97.72
46.64	4.48	12.63	14.62	0.20	4.70	9.27	3.28	0.88	96.70
46.47	4.44	12.62	14.42	0.17	4.81	8.99	3.52	0.86	96.29
46.38	4.75	12.86	14.06	0.23	4.66	9.03	3.29	0.82	96.09
46.33	4.94	12.57	14.64	0.17	4.69	8.81	3.24	0.82	96.21

Tephra f 50-50.3 cm

73.72	0.10	13.11	1.67	0.07	0.01	1.42	4.41	2.84	97.34
73.60	0.22	13.99	3.20	0.08	0.14	1.99	3.98	2.31	99.50
71.72	0.17	14.00	2.97	0.12	0.12	2.00	4.23	2.39	97.73

Tephra g 53.6-53.8 cm

63.70	0.55	14.85	6.56	0.17	0.61	3.82	4.30	1.79	96.35
48.66	2.87	12.90	13.39	0.28	5.34	9.61	2.82	0.53	96.39
48.40	1.95	13.45	11.45	0.16	7.20	11.85	2.31	0.19	97.18
48.19	1.45	14.00	10.76	0.19	7.72	12.35	2.23	0.14	97.02
45.87	4.43	12.54	13.99	0.20	5.03	9.69	3.54	0.86	96.15

Tephra h 57.2-58.5 cm

SiO_2	TiO_2	Al_2O_3	FeO	MnO	MgO	CaO	Na_2O	K_2O	Total
51.37	1.66	13.12	11.17	0.19	5.49	9.61	3.06	0.43	96.09
49.20	1.74	13.39	12.04	0.21	7.06	11.40	2.63	0.23	97.89
49.00	1.80	13.35	11.87	0.18	6.96	11.64	2.37	0.22	97.39
48.97	2.07	13.02	12.87	0.26	6.31	11.27	2.46	0.21	97.44
48.73	1.97	13.18	12.49	0.15	6.73	11.39	2.62	0.25	97.50
48.62	1.91	13.51	12.30	0.21	6.65	11.17	2.58	0.23	97.17
48.54	1.70	13.50	11.81	0.15	7.08	11.49	2.36	0.19	96.83
48.48	2.69	12.32	14.86	0.26	5.10	9.73	2.72	0.37	96.54
48.36	1.86	13.79	12.20	0.18	6.78	11.76	2.26	0.19	97.38
47.58	1.73	13.59	12.02	0.15	6.89	11.44	2.48	0.25	96.14

Tephra i 65.3-65.5 cm

49.05	1.82	13.78	11.95	0.18	7.23	11.78	2.61	0.24	98.65
49.02	1.97	13.54	11.52	0.22	6.68	11.25	2.60	0.25	97.05
48.82	1.75	13.54	11.91	0.24	7.21	12.02	2.26	0.16	97.92
48.79	1.68	13.44	11.43	0.24	6.93	12.09	2.34	0.17	97.09
48.60	1.87	13.63	12.04	0.23	7.18	11.75	2.43	0.21	97.93
48.53	1.82	13.70	11.76	0.31	7.41	11.63	2.28	0.18	97.62
48.15	1.75	13.52	11.69	0.13	7.04	11.93	2.50	0.18	96.90
48.08	1.73	13.73	11.49	0.18	7.13	12.61	2.27	0.18	97.40
47.99	1.82	13.40	11.50	0.24	6.94	11.94	2.25	1.19	96.29
47.79	1.79	13.58	11.82	0.18	7.31	11.98	2.30	0.19	96.95

Tephra j 71.6-73.1 cm

SiO_2	TiO_2	Al_2O_3	FeO	MnO	MgO	CaO	Na_2O	K_2O	Total
72.93	0.16	14.28	2.98	0.07	0.13	2.00	4.46	2.55	99.56
68.52	0.37	14.69	5.01	0.14	0.38	3.10	4.50	2.25	98.96
66.47	0.50	14.96	6.19	0.15	0.61	3.40	4.20	1.88	98.35
66.22	0.47	14.82	5.87	0.16	0.42	3.23	4.54	2.15	97.88
65.55	0.56	14.78	6.17	0.21	0.58	3.58	4.68	2.02	98.12
64.69	0.63	15.29	6.93	0.20	0.65	3.68	4.73	1.95	98.75
64.18	0.58	14.86	7.14	0.24	0.67	4.11	4.37	1.93	98.08
63.51	0.61	14.64	7.01	0.23	0.63	3.73	4.52	1.84	96.73
61.94	0.85	14.92	8.57	0.22	0.92	4.17	4.95	1.85	98.38

Tephra k 73.1-73.6 cm

72.79	0.20	14.29	3.15	0.14	0.14	1.93	4.18	2.44	99.26
72.48	0.19	14.18	3.09	0.12	0.10	1.20	4.36	2.47	99.00
72.38	0.18	14.28	3.05	0.14	0.17	1.98	4.48	2.60	99.25
72.28	0.19	14.30	3.13	0.11	0.14	1.85	4.86	2.59	99.46
71.92	0.20	13.93	3.11	0.10	0.09	1.84	4.66	2.49	98.34
71.61	0.17	13.78	2.92	0.09	0.09	1.89	4.79	2.65	97.98
71.45	0.19	13.98	2.88	0.10	0.11	1.95	4.15	2.61	97.41
71.32	0.18	14.29	3.06	0.10	0.15	1.99	4.30	2.44	97.81
70.92	0.27	14.75	4.20	0.14	0.23	2.38	4.70	2.36	99.95
68.78	0.32	14.43	4.15	0.16	0.18	2.37	4.36	2.45	97.20

Svinavatn lc2 tephra stone 375cm

69.93	0.24	13.54	3.10	0.13	0.16	1.96	4.27	2.41	95.75
66.90	0.45	15.32	4.08	0.16	0.37	1.73	5.09	3.87	97.96
64.95	0.49	15.42	4.65	0.19	0.47	2.08	4.52	3.95	96.72
64.88	0.65	14.91	7.20	0.27	0.80	3.92	4.34	1.76	98.74
48.20	2.81	12.92	13.12	0.29	5.52	9.98	3.03	0.43	96.29

Tephra clump 26.5-27 cm

73.23	0.30	13.42	3.20	0.18	0.15	1.86	4.59	3.02	99.95
73.02	0.18	13.96	3.23	0.12	0.14	1.94	4.33	2.62	99.54
72.83	0.21	13.85	3.16	0.12	0.11	1.90	4.58	2.69	99.46
72.59	0.19	13.66	3.39	0.08	0.17	1.98	4.29	2.61	98.97
72.30	0.21	13.36	3.09	0.10	0.12	1.74	3.89	2.59	97.40
71.64	0.22	13.23	3.16	0.14	0.15	1.85	4.15	2.78	97.32
71.57	0.21	13.21	3.32	0.10	0.14	1.98	4.59	2.91	98.03
71.44	0.21	13.63	3.11	0.07	0.10	1.88	4.40	2.58	97.41
70.66	0.27	13.34	2.96	0.10	0.09	1.89	4.56	2.79	96.67
69.47	0.20	13.38	2.96	0.07	0.14	1.78	4.47	2.79	95.25

Tephra b 23-23.5cm

72.65	0.24	13.75	3.09	0.08	0.12	1.77	4.40	2.99	99.10
71.09	0.15	16.12	2.16	0.10	0.09	2.45	5.48	1.99	99.63
70.84	0.21	13.75	3.05	0.10	0.14	1.77	4.64	2.69	97.18
70.61	0.16	13.89	3.18	0.12	0.09	1.91	4.36	2.52	96.84
70.42	0.20	13.49	2.93	0.09	0.12	1.68	3.75	2.46	95.13

Tephra b 23.5-24cm

73.43	0.19	14.02	3.08	0.11	0.13	1.86	4.48	2.67	99.97
72.52	0.25	14.43	3.25	0.12	0.10	1.90	4.51	2.70	99.77
71.01	0.20	14.14	2.75	0.13	0.12	1.95	4.55	2.44	97.30
70.86	0.17	14.77	2.79	0.08	0.15	2.41	5.13	2.38	98.74
65.99	0.75	14.51	6.83	0.21	0.68	3.78	4.46	2.03	99.25
61.11	0.88	15.54	6.06	0.17	1.19	4.54	4.43	1.41	95.34

Tephra b 24-24.5cm

SiO_2	TiO_2	Al_2O_3	FeO	MnO	MgO	CaO	Na_2O	K_2O	Total
72.69	0.20	13.78	3.38	0.13	0.07	1.85	3.08	2.51	97.69
71.60	0.23	13.92	3.19	0.17	0.14	1.90	4.52	2.55	98.23
71.22	0.23	13.87	3.20	0.11	0.14	2.03	4.43	2.68	97.92
69.08	0.19	14.65	2.60	0.12	0.09	2.26	4.92	2.17	96.09

Svínavatn lake core 3

Tephra a 21.1-21.4 cm

73.44	0.19	11.65	2.12	0.03	0.08	1.00	3.93	2.99	95.43
73.06	0.09	12.65	1.83	0.06	0.05	1.14	4.54	2.91	96.34
71.62	0.24	14.15	3.07	0.12	0.13	2.05	4.93	2.56	98.87
70.79	0.22	13.88	2.98	0.04	0.14	2.03	4.41	2.61	97.10
70.10	0.27	13.30	3.34	0.06	0.09	1.85	4.03	2.78	95.81
64.22	1.44	13.82	6.91	0.21	1.21	3.47	4.38	2.67	98.34
50.06	2.50	13.37	13.04	0.23	5.97	10.57	2.97	0.37	99.08
49.80	2.30	13.27	12.18	0.16	6.39	11.03	2.48	0.23	97.86
49.38	2.20	13.12	12.06	0.22	5.52	10.42	3.01	0.33	96.27
49.20	1.96	13.42	12.02	0.11	6.41	10.83	2.59	0.26	96.78
46.14	5.18	12.44	14.08	0.21	4.62	9.43	2.82	0.81	95.72

Tephra b 29.2-30.0 cm

SiO_2	TiO_2	Al_2O_3	FeO	MnO	MgO	CaO	Na_2O	K_2O	Total
73.53	0.05	12.68	1.87	0.00	0.03	1.26	4.69	2.68	96.78
73.41	0.07	14.41	1.42	0.02	0.02	1.94	5.24	2.24	98.77
73.07	0.04	12.56	1.89	0.04	0.01	1.30	4.98	2.60	96.49
72.81	0.05	12.59	2.00	0.01	0.06	1.25	4.71	2.60	96.09
72.18	0.15	14.18	3.13	0.09	0.11	1.88	4.76	2.82	99.29
71.98	0.03	13.20	1.99	0.06	0.02	1.24	4.56	2.68	95.76
71.75	0.22	13.78	3.23	0.08	0.09	2.07	4.89	2.35	98.45
71.68	0.16	13.72	3.33	0.07	0.11	1.98	4.94	2.49	98.49
71.30	0.14	14.35	3.19	0.10	0.14	1.93	4.79	2.68	98.61
49.71	2.30	13.56	13.06	0.20	6.30	11.03	2.93	0.18	99.25

Tephra c 38.1-38.6 cm

SiO_2	TiO_2	Al_2O_3	FeO	MnO	MgO	CaO	Na_2O	K_2O	Total
71.92	0.20	14.02	3.26	0.15	0.14	2.00	5.05	2.63	99.38
71.76	0.24	14.02	3.11	0.15	0.11	1.96	4.91	2.59	98.86
71.76	0.26	13.69	3.11	0.11	0.14	1.93	4.62	2.80	98.41
71.22	0.27	13.90	3.16	0.08	0.15	1.93	4.73	2.66	98.09
71.19	0.23	14.06	3.19	0.03	0.10	2.08	4.72	2.82	98.40
71.00	0.17	13.73	3.26	0.11	0.10	1.97	4.81	2.68	97.84
70.53	0.25	13.74	3.17	0.10	0.10	2.03	4.95	2.54	97.41
70.47	0.19	13.83	2.99	0.11	0.17	1.99	4.58	2.69	97.04
70.43	0.17	14.07	3.15	0.11	0.11	1.83	5.14	2.79	97.79
69.71	0.22	13.93	3.06	0.09	0.13	1.97	5.05	2.58	96.74

Tephra d 44-44.5 cm

SiO_2	TiO_2	Al_2O_3	FeO	MnO	MgO	CaO	Na_2O	K_2O	Total
48.03	2.00	12.93	12.43	0.24	6.34	11.22	2.47	0.21	95.88
46.22	5.21	12.10	14.64	0.24	4.82	9.71	3.28	0.83	97.04
46.01	5.17	12.22	14.57	0.28	4.85	9.83	2.83	0.76	96.59
45.81	4.94	12.41	14.56	0.28	4.62	9.73	3.04	0.78	96.17
45.73	5.33	12.35	15.02	0.30	4.66	9.47	3.13	0.74	96.73
45.60	5.07	12.33	14.93	0.25	4.67	9.57	3.06	0.72	96.20
45.60	5.22	12.26	14.63	0.25	4.81	9.40	3.23	0.75	96.14
45.31	5.06	12.20	14.78	0.24	4.85	9.68	3.22	0.69	96.01
45.11	5.22	12.25	14.34	0.28	4.83	9.22	3.54	0.87	95.66
44.81	5.14	12.48	14.73	0.25	4.62	9.70	3.41	0.86	96.01

Tephra e 50.4-52 cm

49.62	4.18	12.69	12.27	0.26	4.75	10.13	2.70	0.63	97.23
47.43	5.18	12.79	14.53	0.30	5.03	9.51	3.82	0.78	99.37
47.33	5.03	12.42	14.07	0.25	4.73	9.51	3.53	0.95	97.83
47.23	5.10	13.27	14.01	0.29	5.24	9.43	4.06	0.85	99.48
47.22	5.24	12.86	14.35	0.31	4.86	8.85	3.10	0.87	97.66
47.13	5.11	12.35	14.00	0.29	4.53	9.71	3.47	0.80	97.38
47.09	4.97	13.14	14.86	0.26	5.29	9.89	2.91	0.87	99.27
46.52	5.32	12.67	14.32	0.26	4.68	9.78	3.16	0.88	97.59
46.05	4.68	12.97	14.03	0.25	5.14	9.48	3.95	0.87	97.43
44.76	5.20	12.82	13.55	0.26	4.89	9.33	3.62	0.72	95.17

Tephra f 80-81 cm

SiO_2	TiO_2	Al_2O_3	FeO	MnO	MgO	CaO	Na_2O	K_2O	Total
75.22	0.16	13.31	1.98	0.09	0.02	1.26	3.50	2.97	98.51
74.15	0.15	12.91	1.93	0.02	0.01	1.32	4.50	2.96	97.94
73.09	0.08	12.51	1.68	0.09	0.02	1.27	3.74	2.71	95.19
73.01	0.17	12.57	1.64	0.08	0.00	1.35	4.95	2.78	96.56
72.73	0.23	13.70	2.84	0.07	0.16	1.92	4.22	2.50	98.36
60.66	0.82	14.45	8.56	0.31	1.07	4.18	5.05	1.30	96.42

Tephra g/h 122cm

66.73	0.41	14.78	5.52	0.21	0.37	3.15	4.63	2.16	97.96
66.35	0.41	14.51	5.94	0.21	0.44	3.33	4.33	2.19	97.72
65.98	0.43	14.25	5.65	0.21	0.43	3.39	4.07	1.99	96.39
62.42	0.78	14.82	8.69	0.22	1.05	4.58	3.99	1.64	98.19
61.57	0.84	14.96	8.46	0.33	1.12	4.46	3.90	1.68	97.32
72.56	0.22	13.83	3.24	0.10	0.14	1.91	4.39	2.46	98.86
72.10	0.17	13.59	3.18	0.15	0.11	2.09	4.43	2.56	98.38
71.62	0.20	13.54	3.21	0.12	0.17	1.90	4.39	2.63	97.78
70.28	0.20	13.71	3.13	0.13	0.12	2.08	4.38	2.43	96.45
68.02	0.28	14.49	2.06	0.18	0.28	3.00	4.31	2.30	97.92

Tephra 2b 46-46.5 cm

75.29	0.03	12.93	1.85	0.06	0.07	1.47	4.57	2.97	99.25
74.84	0.28	11.98	2.47	0.04	0.28	1.60	4.08	2.41	97.98
72.66	0.09	12.65	1.79	0.03	0.05	1.32	4.10	2.74	95.42
64.69	1.43	13.67	6.95	0.18	1.53	3.64	4.59	2.38	99.07
64.66	1.35	14.29	6.39	0.20	1.34	3.46	4.44	2.46	98.59

Tephra 3c 49.4cm

SiO_2	TiO_2	Al_2O_3	FeO	MnO	MgO	CaO	Na_2O	K_2O	Total
48.59	4.53	12.69	14.30	0.23	5.04	9.19	3.15	0.80	98.51
48.57	4.65	12.54	13.87	0.20	5.00	9.32	3.09	0.81	98.05
47.83	4.54	12.59	14.33	0.20	5.05	9.29	3.31	0.86	97.99
47.58	4.71	12.88	14.00	0.15	5.02	9.17	3.29	0.82	97.62
47.51	4.58	12.81	14.31	0.21	4.88	9.17	3.21	0.91	97.59

Svínavatn lake core 4

Tephra a 16.3-16.8 cm

60.11	1.19	14.87	9.30	0.24	1.49	5.13	4.16	1.69	98.18
59.79	1.16	14.5	9.08	0.33	1.56	4.85	4.30	1.60	97.15
59.31	1.13	14.86	9.04	0.22	1.53	4.87	4.13	1.61	96.71
59.26	1.18	15.28	9.18	0.22	1.55	4.90	4.27	1.69	97.54
58.89	1.14	14.62	9.60	0.29	1.54	4.97	4.47	1.50	97.02
58.81	1.15	14.47	8.60	0.21	1.48	4.80	4.55	1.76	95.82
58.29	1.22	14.63	9.28	0.25	1.48	4.83	4.29	1.61	95.88
58.29	1.25	14.57	9.17	0.27	1.55	5.41	4.38	1.72	96.62
58.10	1.46	15.08	8.68	0.26	2.01	4.82	4.67	1.66	96.72
56.80	1.55	14.60	9.64	0.26	2.07	5.86	4.06	1.42	96.25

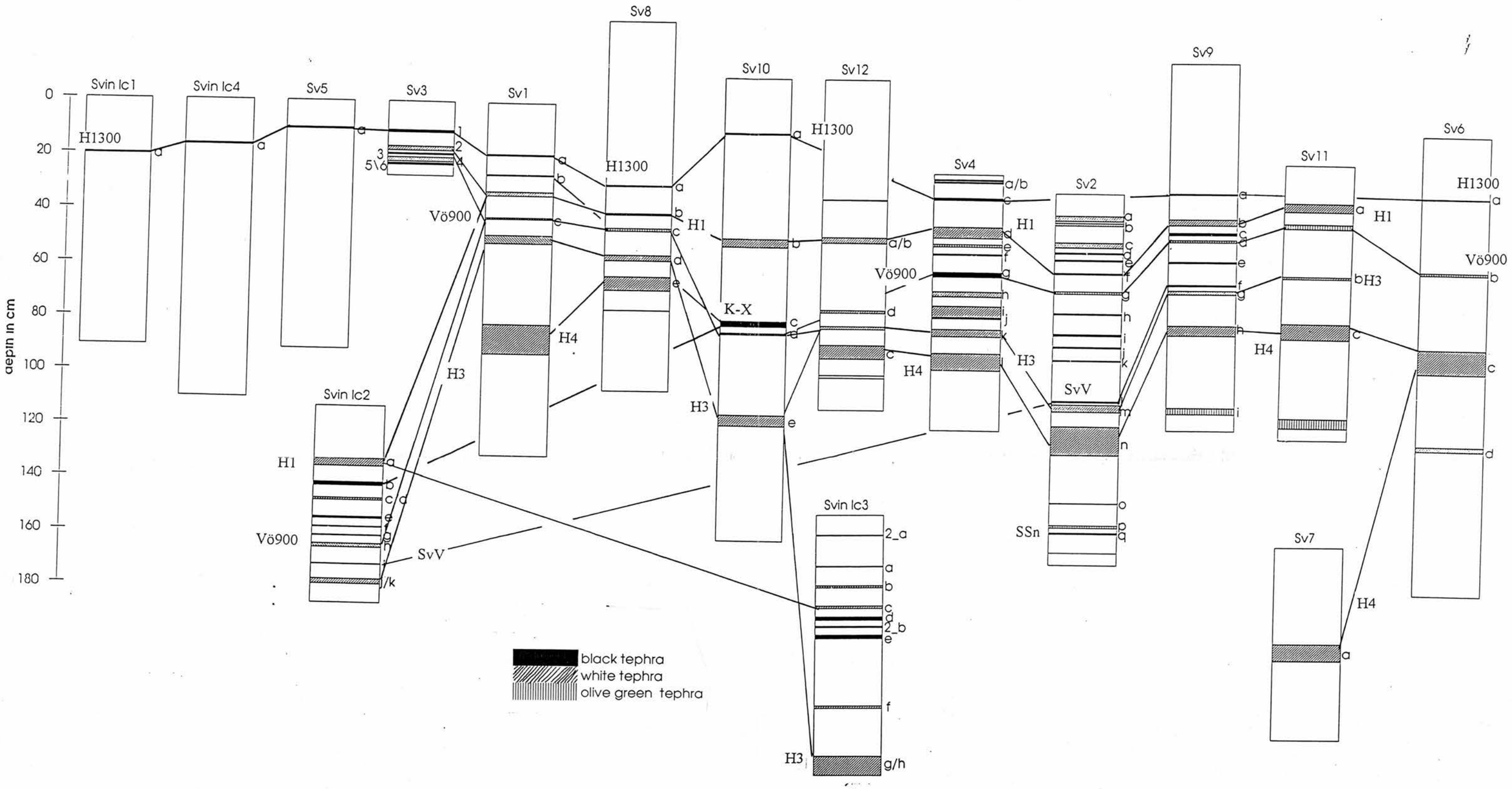

Figure 5.13 The tephra stratigraphy of Svínavatn catchment and lake profiles. The correlations are based on geochemical analyses of glass shards and stratigraphy.